U.S. DEPARTMENT OF COMMERCE
National Technical Information Service

PB-297 500

Test of Fabric Filtration Materials

Institute of Industry of Cement Building Materials (Poland)

Prepared for

Industrial Environmental Research Lab, Research Triangle Park, NC

Mar 79

TECHNICAL REPORT DATA

(Please read Instructions on the reverse before completing)

1. REPORT NO. EPA-600/7-79-087

2.

3. RECIPIENT'S ACCESSION NO. PB297500

4. TITLE AND SUBTITLE Test of Fabric Filtration Materials

5. REPORT DATE March 1979

6. PERFORMING ORGANIZATION CODE

7. AUTHOR(S) Jan R. Koscianowski, Lidia Koscianowska, and Maria Szablewicz

8. PERFORMING ORGANIZATION REPORT NO.

9. PERFORMING ORGANIZATION NAME AND ADDRESS
Institute of Industry of Cement Building Materials
45-641 Opole
21 Oswiecimska Str., POLAND

10. PROGRAM ELEMENT NO. EHE624; ROAP 21ADJ-094

11. CONTRACT/GRANT NO.
Public Law 480
Project P-5-533-4

12. SPONSORING AGENCY NAME AND ADDRESS
EPA, Office of Research and Development
Industrial Environmental Research Laboratory
Research Triangle Park, NC 27711

13. TYPE OF REPORT AND PERIOD COVERED Project Final; 6/73 - 12/78

14. SPONSORING AGENCY CODE EPA/600/13

15. SUPPLEMENTARY NOTES IERL-RTP project officer is James H. Turner, MD-61, 919/541-2925. EPA-600/7-78-056 is an earlier related report.

16. ABSTRACT
The report describes pilot scale and laboratory tests of U.S. and Polish woven baghouse fabrics. Cotton, polyester, aramid, and glass fabrics were tested using cement, flyash, coal, and talc dusts at loadings of about 10 g/cu m, filtration velocities of 60 and 80 cu m/sq m, and ambient temperature and humidity. General conclusions reached were: (1) air permeability is a poor predictor of fabric performance, (2) fabric construction parameters do not correlate well with the resistance coefficient for fabrics K1, (3) a critical value of pressure drop exists above which fissures are formed in the dust cake, (4), there is a maximum in the efficiency versus air-to-cloth-ratio curve which is related to fissure formation, and (5) cleaning properties of the fabric depend primarily on its chemical composition, the dust being filtered, and the superficial structure of the dust cake and fabric (they do not depend on air-to-cloth ratio).

17. KEY WORDS AND DOCUMENT ANALYSIS

a. DESCRIPTORS		b. IDENTIFIERS/OPEN ENDED TERMS	c. COSATI Field/Group	
Pollution	Glass Fibers	Pollution Control	13B	11B
Air Filters	Cements	Stationary Sources	13K	13C
Woven Fabrics	Fly Ash	Baghouses	11E	21B
Caking	Coal Dust	Fabric Filters	07A,13H	21D
Cotton Fabrics	Talc	Poland		08G
Polyester Fibers		Aramid		

18. DISTRIBUTION STATEMENT Unlimited

19. SECURITY CLASS *(This Report)* Unclassified

20. SECURITY CLASS *(This page)* Unclassified

21. NO. OF PAGES 268

22. PRICE PC A12 A01

EPA Form 2220-1 (9-73)

United States
Environmental Protection
Agency

Industrial Environmental Research
Laboratory
Research Triangle Park NC 27711

EPA-600/7-79-087
March 1979

Test of Fabric Filtration Materials

PB 297500

Interagency Energy/Environment R&D Program Report

JUN 18 1979

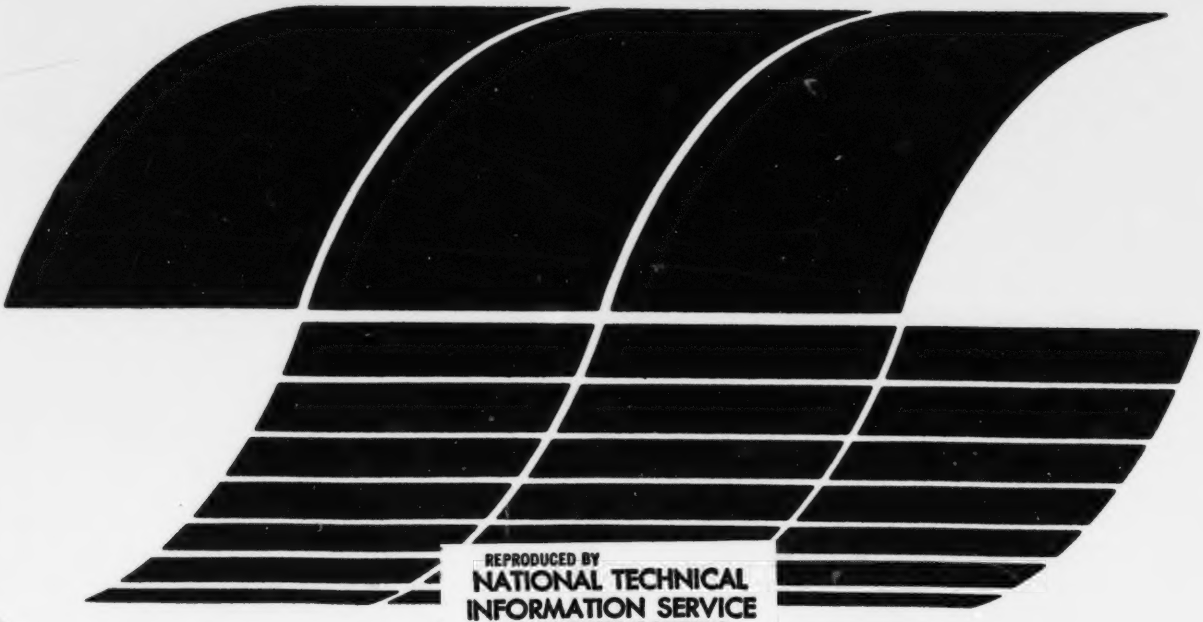

REPRODUCED BY
NATIONAL TECHNICAL
INFORMATION SERVICE
U. S. DEPARTMENT OF COMMERCE
SPRINGFIELD, VA. 22161

RESEARCH REPORTING SERIES

Research reports of the Office of Research and Development, U.S. Environmental Protection Agency, have been grouped into nine series. These nine broad categories were established to facilitate further development and application of environmental technology. Elimination of traditional grouping was consciously planned to foster technology transfer and a maximum interface in related fields. The nine series are:

1. Environmental Health Effects Research
2. Environmental Protection Technology
3. Ecological Research
4. Environmental Monitoring
5. Socioeconomic Environmental Studies
6. Scientific and Technical Assessment Reports (STAR)
7. Interagency Energy-Environment Research and Development
8. "Special" Reports
9. Miscellaneous Reports

This report has been assigned to the INTERAGENCY ENERGY-ENVIRONMENT RESEARCH AND DEVELOPMENT series. Reports in this series result from the effort funded under the 17-agency Federal Energy/Environment Research and Development Program. These studies relate to EPA's mission to protect the public health and welfare from adverse effects of pollutants associated with energy systems. The goal of the Program is to assure the rapid development of domestic energy supplies in an environmentally-compatible manner by providing the necessary environmental data and control technology. Investigations include analyses of the transport of energy-related pollutants and their health and ecological effects; assessments of, and development of, control technologies for energy systems; and integrated assessments of a wide range of energy-related environmental issues.

EPA REVIEW NOTICE

This report has been reviewed by the participating Federal Agencies, and approved for publication. Approval does not signify that the contents necessarily reflect the views and policies of the Government, nor does mention of trade names or commercial products constitute endorsement or recommendation for use.

This document is available to the public through the National Technical Information Service, Springfield, Virginia 22161.

EPA-600/7-79-087
March 1979

Test of Fabric Filtration Materials

by

Jan R. Koscianowski, Lidia Koscianowska, and Maria Szablewicz

Institute of Industry of Cement Building Materials
45-641 Opole
21 Oswiecimska Str., Poland

Public Law 480
Project P-5-533-4
Program Element No. EHE624
ROAP 21ADJ-094

EPA Project Officer: James H. Turner

Industrial Environmental Research Laboratory
Office of Energy, Minerals, and Industry
Research Triangle Park, NC 27711

Prepared for

U.S. ENVIRONMENTAL PROTECTION AGENCY
Office of Research and Development
Washington, DC 20460

1a

EPA-600/7-79-087

March 1979

Test of Fabric Filtration Materials

by

Jan R. Koscianowski, Lidia Koscianowska, and Maria Szablewicz

Institute of Industry of Cement Building Materials
45-641 Opole
21 Oswiecimska Str., Poland

Public Law 480
Project P-5-533-4
Program Element No. EHE624
ROAP 21ADJ-094

EPA Project Officer: James H. Turner

Industrial Environmental Research Laboratory
Office of Energy, Minerals, and Industry
Research Triangle Park, NC 27711

Prepared for

U.S. ENVIRONMENTAL PROTECTION AGENCY
Office of Research and Development
Washington, DC 20460

ACKNOWLEDGEMENT

The authors would like to thank each employee of the United States Environmental Protection Agency who participated in this endeavor for their contribution and help. Special thanks for help and support throughout the program are extended to our Project Officer, Dr. James H. Turner.

CONTENTS

Page

Acknowledgement ii
Figures v
Tables x
SECTION I CONCLUSIONS 1
SECTION II RECOMMENDATIONS 4
SECTION III INTRODUCTION 5
  Testing of Woven Textile Filtration Materials 5
  Research Objectives 8
  General Program 8
    Laboratory Testing 8
    Large Scale Testing 9
    Comparative Analysis 9
  Detailed Program 9
    Laboratory Tests 9
    Large Scale Testing 10
    Auxiliary Studies 10
  Fabric and Dust Selection 10
SECTION IV LABORATORY TESTING OF FILTRATION 18
  Introduction 18
  Equipment and Procedures 24
  Results and Discussion 27
    Air Flow Through Clean Filtration Fabrics 27
    Laboratory Testing of Filtration Fabrics 46
    Cotton and Nylon Fabrics 58
    Polyester Fabrics 60
    Nomex Fabrics 62
    Glass Fabrics 62

CONTENTS (continued)

Page

Testing of Duct/Canal Formation Mechanism 65

Filtration Resistance Variation in Laboratory Testing 75

Conclusions 75

SECTION V LARGE SCALE TESTING OF FILTRATION 79

Introduction 79

Equipment and Procedures 80

Results and Discussion 91

Basic Test 91

The Influence of Hopper Efficiency on Conducted Experiments . . 104

Fractional Efficiency of Fabrics 112

Filtration Resistance 122

Conclusions 133

SECTION VI STUDY OF THE REGENERATION PROPERTIES OF FABRICS 135

Introduction 135

Results and Discussion 139

Conclusions 151

SECTION VII COMPARISON OF THE FILTRATION PROPERTIES OF POLISH AND U.S. FABRICS 154

Introduction 154

Analysis of Filtration Properties 155

Natural Fiber Fabrics 155

Polyester Fabrics 155

Polyamide Fabrics 170

Glass Fabrics 170

Conclusions 170

REFERENCES 171

APPENDIX A 173

B 208

C 237

D 248

E 251

FIGURES

No.		Page
1	Dust Filtration Type I.	21
2	Increase of pressure drop in time during Dust Filtration Type 1	22
3	Illustration of laboratory stand.	25
4	Diagram of the laboratory test stand.	26
5	Hydraulic characteristic of polyester fabrics	28
6	Hydraulic characteristic of glass, cotton, and nylon fabrics	29
7	Hydraulic characteristic of Nomex fabrics	29
8	Specific hydraulic resistance of polyester fabrics	33
9	Variation of specific hydraulic resistance of glass, cotton, and nylon fabrics	34
10	Variation of specific hydraulic resistance of Nomex fabrics	34
11	Resistance coefficient, K_1', of a woven fabric	35
12	Dependence of resistance coefficient K_1 on free area.	38
13	Dependence of resistance coefficient K_1 on fabric porosity.	41
14	Dependence of resistance coefficient K_1 on porosity function.	42
15	Dependence of resistance coefficient K_1 on fabric weight.	44
16	Dependence of resistance coefficient K_1 on air permeability.	45
17	Superficial structure of fabrics.	59
18	Ducts/canals distribution on polyester fabric covered with talc (style no. 865B).	61
19	Comparison of surface structure of staple and continuous filament Nomex fiber fabrics.	63
20	Relationship between duct/number and: 1) A/C, and 2) final pressure drop.	67

FIGURES (continued)

No.		Page
21	Histogram showing the size distribution of duct/canal equivalent diameter (exp 1, series 2)	69
22	Histogram showing size distribution of duct/canal equivalent diameter (exp. 2, series 2)	70
23	Superficial structure of model fabric	72
24	Kinds of free areas in woven structure (Q53-878)	73
25	Duct/canal shape	74
26	Illustration of large-scale stand	81
27	Diagram of the large-scale test stand	83
28	Construction of bags	85
29	Diagram of regeneration cycles	86
30	Diagram of cascade impactor measurement system	88
31	Photography of cascade impactor measurement system	89
32	Velocity distribution in duct	90
33	Time variation of filtration resistance for fabric C866B (dust: separated talc)	93
34	Time variation of filtration resistance for fabric C866B (dust: unseparated coal)	94
35	Correlation between measurement efficiency and dust balance efficiency for experiments for fabric C890B dusted with cement at $q_g = 60$ m^3/m^2 hr	111
36	Fractional efficiency of polyester and cotton fabrics (cement dust at $q_g = 80$ m^3/m^2 hr, $L_o = 400$ g/m^2, and $c_i = 10$ g/m^3)	116
37	Fractional efficiency of Nomex, glass, and polyamide fabrics (cement dust at $q_g = 80$ m^3/m^2 hr, $L_o = 400$ g/m^2, and $c_i = 10$ g/m^3)	117
38	Fractional efficiency of polyester fabrics (fly ash at $L_o = 400$ g/m^2 and $c_i = 10$ g/m^3)	118
39	Fractional efficiency of Nomex and glass fabrics (fly ash at $L_o = 400$ g/m^2 and $c_i = 10$ g/m^3)	119
40	Fractional efficiency of cotton and polyamide fabrics (fly ash at $L_o = 400$ g/m^2 and $c_i = 10$ g/m^3)	120
41	Variation of filtration resistance in time for fabric style no. 862B (cement dust at $q_g = 60$ m^3/m^2 hr)	127
42	Variation of filtration resistance in time for fabric style no. C890B (cement dust at $q_g = 60$ m^3/m^2 hr)	128

FIGURES (continued)

No. Page

43 Variation of filtration resistance in time for fabric style no. C892B (cement dust at $q_g = 60\ m^3/m^2\ hr$) 129

44 Variation of filtration resistance in time for fabric style no. Q53-875 (cement dust at $q_g = 60\ m^3/m^2\ hr$) 130

45 Variation of filtration resistance in time for fabric style no. Q53-870 (cement dust at $q_g = 60\ m^3/m^2\ hr$) 131

46 Variation of filtration resistance in time for fabric style no. Q53-878 (cement dust at $q_g = 60\ m^3/m^2\ hr$) 132

47 Theoretical plot of filtration and regeneration process 137

48 Realistic behavior of filtration and regeneration process . . . 138

49 Theoretical plot of susceptibility for regeneration vs. time 140

50 Empirical time dependence of susceptibility for regeneration (cement dust, $q_g = 60\ m^3/m^2\ hr$) 146

51 Microscopic pictures of testing dusts (a-cement, b-coal, c-fly ash, d-talc) 152

52 Comparison of filtration properties of Polish and U.S. fabrics (wool, cotton) 156

53 Comparison of regeneration properties of Polish and U.S. fabrics (wool, cotton) 157

54 Comparison of filtration properties of Polish and U.S. polyester fabrics 158

55 Comparison of regeneration properties of Polish and U.S. polyester fabrics 159

56 Comparison of filtration properties of Polish and U.S. polyester fabrics 160

57 Comparison of regeneration properties of Polish and U.S. polyester fabrics 161

58 Comparison of filtration properties of Polish and U.S. polyester fabrics 162

59 Comparison of regeneration properties of Polish and U.S. polyester fabrics 163

60 Comparison of filtration properties of Polish and U.S. polyester fabrics 164

61 Comparison of regeneration properties of Polish and U.S. polyester fabrics 165

62 Comparison of filtration properties of Polish and U.S. polyamide fabrics 166

FIGURES (continued)

No.		Page
63	Comparison of regeneration properties of Polish and U.S. polyamide fabrics	167
64	Comparison of filtration properties of Polish and U.S. glass fabrics	168
65	Comparison of regeneration properties of Polish and U.S. glass fabrics	169
A-1	Particle size distribution of cement test dusts: 1 - for laboratory testing; 2 - for large scale testing	174
A-2	Particle size distribution of coal test dusts: 1 - for laboratory testing; 2 - for large scale testing	175
A-3	Particle size distribution of talc test dust	176
A-4	Particle size distribution of fly ash test dust	177
A-5	Filtration resistance vs. filtration time for fabric style no. 960	178
A-6	Filtration resistance vs. filtration time for fabric style no. 960	179
A-7	Filtration resistance vs. filtration time for fabric style no. 862B	180
A-8	Filtration resistance vs. filtration time for fabric style no. 862B	181
A-9	Filtration resistance vs. filtration time for fabric style no. C866B	182
A-10	Filtration resistance vs. filtration time for fabric style no. C866B	183
A-11	Filtration resistance vs. filtration time for fabric style no. C868B	184
A-12	Filtration resistance vs. filtration time for fabric style no. C868B	185
A-13	Filtration resistance vs. filtration time for fabric style no. 865B	186
A-14	Filtration resistance vs. filtration time for fabric style no. 865B	187
A-15	Filtration resistance vs. filtration time for fabric style no. C890B	188
A-16	Filtration resistance vs. filtration time for fabric style no. C890B	189
A-17	Filtration resistance vs. filtration time for fabric style no. C892B	190
A-18	Filtration resistance vs. filtration time for fabric style no. C892B	191

FIGURES (continued)

No.		Page
A-19	Filtration resistance vs. filtration time for fabric style no. 852	192
A-20	Filtration resistance vs. filtration time for fabric style no. 852	193
A-21	Filtration resistance vs. filtration time for fabric style no. 853	194
A-22	Filtration resistance vs. filtration time for fabric style no. 853	195
A-23	Filtration resistance vs. filtration time for fabric style no. 190R	196
A-24	Filtration resistance vs. filtration time for fabric style no. 190R	197
A-25	Filtration resistance vs. filtration time for fabric style no. 850B	198
A-26	Filtration resistance vs. filtration time for fabric style no. 850B	199
A-27	Filtration resistance vs. filtration time for fabric style no. 802B	200
A-28	Filtration resistance vs. filtration time for fabric style no. 802B	201
A-29	Filtration resistance vs. filtration time for fabric style no. Q53-875	202
A-30	Filtration resistance vs. filtration time for fabric style no. Q53-875	203
A-31	Filtration resistance vs. filtration time for fabric style no. Q53-870	204
A-32	Filtration resistance vs. filtration time for fabric style no. Q53-870	205
A-33	Filtration resistance vs. filtration time for fabric style no. Q53-878	206
A-34	Filtration resistance vs. filtration time	207

TABLES

No.		Page
1	Fabric Parameters	12
2	Physical Properties of Testing Dusts	13
3	Particle Size Distribution of Cement Dust	14
4	Particle Size Distribution of Coal Dust	15
5	Particle Size Distribution of Talc	16
6	Particle Size Distribution of Fly Ash	16
7	Chemical Properties of Testing Dusts	17
8	Empirical Functions of Hydraulic Resistances of Filtration Fabrics	30
9	Empirical Functions of Specific Hydraulic Resistances of Filtration Fabrics	32
10	Resistance Coefficients of Woven Fabrics	37
11	Additional Energy Losses	39
12	Porosities ε_1 and ε_2 of Filtration Fabrics	40
13	Air Permeability of Dust Filtration Polyester Fabrics Manufactured in Poland	46
14	Air Permeability of U.S. Filtration Fabrics	47
15	Laboratory Efficiencies (in percent) of Tested Filtration Fabrics	48
16	Filtration Resistances at Laboratory Testing	54
17	Classification of Fabrics According to Obtained Outlet Concentration	56
18	Number of Ducts/Canals Observed in Laboratory Testing	64
19	Number of Ducts/Canals Observed During Testing of Fabric Style Q53-878 - Series 1	65
20	Number of Ducts/Canals Observed During Testing of Fabric Style Q53-878 - Series 2	66
21	Average Equivalent Diameter for Experiments of Series 2	71
22	Effective Drag S_E and Specific Resistance Coefficient K_2 in Laboratory Tests	76

TABLES (continued)

No. Page

23 Large-Scale Efficiency (in percent) of Tested Filtration Fabrics 95

24 Classification of Fabrics According to Outlet Concentration. 101

25 Efficiencies E_{T2}, E_H, and E_B Calculated By Dust Balance. . 105

26 MMD For Feed Dust, Bag Dust, and Hopper Dust 110

27 Fractional Efficiency of Fabrics Tested With Cement. . . . 112

28 Fractional Efficiency of Fabrics Tested with Fly Ash . . . 114

29 MMD of Outlet Dust - Cascade Impactor Measurements 121

30 S_E and Specific Resistance Coefficient in Large Scale Tests. 123

31 Rate of Increase of Filtration Resistance. 125

32 Susceptibility for Regeneration (in percent) of Fabrics Tested with Cement at q_g = 60 m^3/m^2hr. 141

33 Susceptibility for Regeneration (in percent) of Fabrics Tested with Cement at q_g = 80 m^3/m^2hr. 142

34 Susceptibility for Regeneration (in percent) of Fabrics Tested with Coal at q_g = 60 m^3/m^2hr. 142

35 Susceptibility for Regeneration (in percent) of Fabrics Tested with Coal at q_g = 80 m^3/m^2hr. 143

36 Susceptibility for Regeneration (in percent) of Fabrics Tested with Talc at q_g = 60 m^3/m^2hr. 143

37 Susceptibility for Regeneration (in percent) of Fabrics Tested with Talc at q_g = 80 m^3/m^2hr. 144

38 Susceptibility for Regeneration (in percent) of Fabrics Tested with Fly Ash at q_g = 60 m^3/m^2hr 144

39 Susceptibility for Regeneration (in percent) of Fabrics Tested with Fly Ash at q_g = 80 m^3/m^2hr 145

40 Regeneration Properties of Tested Fabrics. 148

SECTION I

CONCLUSIONS

Results obtained from laboratory and large scale tests on fifteen kinds of filtration fabrics manufactured in the United States confirmed some of the observations made during previous tests conducted on Polish filtration fabrics. The tests contributed to the enlargement of knowledge about the dust filtration process, especially concerning the effect of filter structure on dust collection efficiency. Because of the fixed testing program, some observations that warranted further investigation could not be pursued and were deferred to further tests.

It is important to notice that apart from the general purpose of the program, i.e., the determination of the filtration and regeneration properties of the tested fabrics, the completion of this program made available a lot of general information concerning the dust filtration process.

Detailed conclusions about each section are enclosed at the end of the respective sections. Following here are general conclusions resulting from the total research program.

- Examination of the hydraulic properties of fabrics under clean air flow show that air permeability is too weak and imprecise a parameter for classifying filtration fabrics. Any comparison of effects of changing fabric technological parameters upon the hydraulic properties of fabric should be carried out at constant air flow: one of the statistical methods can be used. The structural parameter previously proposed to characterize the woven structure of a filtration material--Free Area (FA)--cannot be used for continuous filament fabrics because of structural deformations during the weaving process and/or air flow.
- Air flows through clean woven structures in the range of $q_g = 50$ - 180 m^3/m^2hr are placed in the transition region between laminar and turbulent flow.

- Because of the complicated character of flow due to the periodicity of the woven structure, there are additional energy losses proportional to the ratio b/q_g, where b is a constant coefficient for certain structures and q_g is the gas loading of the filtration area (the air-to-cloth ratio).
- The ratio b/q_g reaches the lowest value for turbulent flow after which the flow resistances depend upon the resistance coefficient K_1 and the square of the gas loading of the filtration area (the air-to-cloth ratio).
- The structural parameters of a woven fabric--free area, porosity, fabric weight, and air permeability--are not correlated with K_1.
- Both the laboratory and the large scale tests confirmed the good filtration properties of the U.S. as well as the Polish fabrics. The observed influence of air-to-cloth (A/C) ratio on filtration efficiency and on filtration resistance confirms the test results obtained previously. Some unexpected dependencies (the ocassional increase of dust collection efficiency with air-to-cloth [A/C] ratio) are probably caused by electrostatic effects.
- The existence of a definite critical value of pressure drop, causing duct/canal formation, was proven during laboratory testing. More careful microscopic and structural examinations of the fabrics led to the conclusion that the ducts/canals form in the voids created by the interlacing warp and fill yarns where the dust cake has the lowest mechanical strength. This newly discovered effect was called the "basket effect." It is characteristic of all woven materials. The magnitude of the basket effect depends upon the kind of fiber, the method of yarn production, and the production conditions of the fabric.
- Each kind of filtration material has a specific A/C ratio at which it achieves the highest level of filtration efficiency. The testing conditions for glass fabrics were already beyond the optimium A/C ratio so these fabrics displayed the lowest filtration efficiencies of the fabrics tested. The decrease of efficiency was caused by the basket effect, leading to duct/canal formation at all A/C ratios investigated.

- Examination of the regeneration properties confirm that they depend mainly upon the kind of raw textile materials, the kind of dust, and the superficial structure of the dust cake and fabric. The regeneration properties do not depend upon the A/C ratio during the filtration process.

SECTION II

RECOMMENDATIONS

This project made possible the compilation of very valuable empirical data concerning Dust Filtration Process Type I, as well as Dust Filtration Process Type III. The obtained experimental data should now be used to mathematically model dust filtration processes.

Besides the major objective of the project, the flow of clean air through woven structures and also the mechanism of dust cake defect formation were examined. The suggestion is made that further investigations should concentrate mainly on physical descriptions of the woven fabric structure and the dust cake.

The knowledge gained from the research performed during this project is of itself not sufficient for complete process understanding. The necessity of the further investigations suggested above results from a preliminary probabilistic mathematical model of dust filtration as previously described.

SECTION III

INTRODUCTION

TESTING OF WOVEN TEXTILE FILTRATION MATERIALS

In the most general sense, filtration is defined as a process for the removal of dispersed solid particles from a fluid stream (dispersed medium) during flow through a porous medium (ref. 1).

Depending on the state of the dispersion medium, the type of the dispersed and porous mediums, and the conditions of the process, the following characteristic kinds of filtration processes can be distinguished (ref. 2):

- High efficiency air filtration,
- Air filtration, and
- Dust filtration.

In dust filtration processes, it is generally assumed that:

- The process operates in the range of superheated steams (dry steam) and the thermodynamic state of the dispersion medium is above the dewpoint temperature at all times,
- The aerosol is regarded as a 2-phase system (solid/gas), which, under certain conditions, is quasi-stable,
- The particles of the dispersed solid state have definite physical/ chemical properties characteristic of certain materials,
- Precipitated particles in or on the structure of the filtration medium can displace each other in the filtration structure; they do not become permanent elements of the structure,
- Filtration media are characterized by certain physical properties, depending on fiber raw material and method of fabric formation.

Furthermore, it is worthwhile to notice that initial aerosol parameters (temperature, humdity, dust concentration, etc.) and also filtration parameters (A/C ratio, dust loading of filtration area, etc.) are not constant during a true dust filtration process but are changing randomly. It therefore follows that the final parameters of the aerosol and the qualitative/

quantitative parameters of the process vary as a function of time and are never stable. So, a description of the filtration process by functional dependencies is very difficult and even in some cases impossible because these dependencies are of a stochastic, not functional, character (ref. 3). From a mathematical point of view, the dust filtration process is a multiparameter stochastic process. The above statement is based on statistical analysis of rich empirical material (ref. 3).

This situation forces the use of specific testing methods and specific data processing techniques so as to be compatible with probabilistic modelling of the dust filtration process. Work on this problem continues and there is hope that a complete probabilistic model of dust filtration, adequate for optimization of filtration structures and parameters and also able to specify test methods and interpretation, will eventually be developed. Because the probabilistic model of the dust filtration process is empirical, its development and verification require extensive, coordinated test data.

At present there is no theoretical base, so tests are carried out under conditions thought to best simulate true dust filtration. In many cases, these tests help solve existing problems; nevertheless, the results always have local character and cannot be generalized.

Depending on the application, the testing can be carried out in laboratory scale, large scale, pilot scale, or industrial scale. So, testing of filtration materials, depending upon the purpose of their testing, can have utilitarian and scientific character.

The laboratory and large scale tests always have scientific character. The values of the initial aerosol parameters and filtration parameters selected depend on the research program. Because of costs, the examining or the testing of filtration materials are seldom carried out in pilot and industrial scale. In addition, initial values of aerosol and filtration parameters are forced by local conditions and are not representative.

The obtained data can be put in series according to definite dependencies:

- Efficiency vs. A/C ratio, $E = f(q_g)$,
- Efficiency vs. covered with dust structure, $E = f(L_o)$,
- Increase in filtration resistance vs. A/C ratio, $\Delta P = f(q_g)$, etc.

In this way we can obtain cross sections of the dust filtration process expressed as functional dependencies and which represent mathematical models for the mean values of the examined parameters.

Based on the comparative analysis of the same filtration process cross section, but for different examined parameters (different fabrics), we can draw qualitative and quantitative conclusions.

The purpose of testing filtration fabrics manufactured in the United States was to define their filtration properties and to compare them with filtration fabrics of Polish production. According to the general program, the testing of U.S. fabrics was conducted at one level of initial concentration, one level of dust cover, and two A/C ratios. The conditions were the same for laboratory and large scale.

It is important to notice that from both a mathematical and a physical viewpoint, the dust filtration process is different in the laboratory and at large scale because of the vastly different dust fills that characterize the two filtration mediums. In a previous report of this project, we proposed to distinguish three main kinds of dust filtration processes: Dust Filtration Process Types I, II, and III (ref. 4). Dust Filtration Process Type I is characteristic of laboratory scale tests and Dust Filtration Process Type III is characteristic of large scale tests. The correlation between these two types of dust filtration processes is outside the scope of this work. Such a correlation would require much parametric variation.

In this program, study of filtration effects is based on a comparative analysis of fabric filters from a qualitative and quantitative point of view. In the opinion of the researchers, all fabrics selected for tests meet the definition of a good filtration fabric.

The assumed criteria are:

- Final concentration,
- Average value of efficiency, and
- Final filtration resistance.

By establishing acceptable limits for these variables, it is possible to classify the examined filtration fabrics.

RESEARCH OBJECTIVES

The basic research objectives of this program, which was financed by the EPA and conducted by the Institute of Cement Building Materials in Opole, were established as:

- Determination of the dust removal efficiency of the fabrics manufactured in the United States (supplied by EPA),
- Determination of the hydraulic characteristics of both the clean fabrics and of dusty fabrics during the filtration process,
- Compilation and comparative analysis of the results for the determination of the qualitative parameters of the tested fabrics,
- Evaluation of the regeneration properties of the fabrics, and
- Comparison of the filtration properties of Polish and U.S. fabrics.

The total research program will include laboratory testing, large scale testing, and auxiliary studies.

GENERAL PROGRAM

Laboratory Testing

Laboratory testing was accomplished on 15 kinds of filtration fabrics and 4 types of dust and was measured under the following conditions:

- Dust concentration in the air at the inlet of the test chamber:
  $10\ g/m^3 \pm 10\%$.
- Dust covering of the filtration structure:
  $400\ g/m^2$
  with $\Delta P < 250$ mm of water.
- A/C ratio:
  $60\ m^3/m^2/hr$
  $80\ m^3/m^2/hr$.
- Humidity of the dispersion medium (not adjustable):
  RH = 55% ± 10.
- Temperature of the dispersion medium: 20 to 30° C.
- Dispersion medium: atmospheric air.
- Pressure: atmospheric.

Large Scale Testing

Large scale tests were scheduled using filtration bags with an operating length of 3,300 mm and the same dusts as used in the laboratory testing. Test conditions were:

- Dust concentration in the air at the inlet of the test chamber:
  $10 \text{ g/m}^3 \pm 10\%$.
- Dust covering of the filtration structure:
  400 g/m^2
  with $\Delta P < 250$ mm of water.
- A/C ratios:
  $60 \text{ m}^3/\text{m}^2/\text{hr}$
  $80 \text{ m}^3/\text{m}^2/\text{hr}$.
- Humidity of the dispersion medium (not adjustable):
  RH = 65% ± 10.
- Temperature of the dispersion medium: 20 to 30° C.
- Dispersion medium: atmospheric air.
- Pressure: atmospheric.

Comparative Analysis

The purpose of the comparative analysis was to determine, qualitatively, the dust filtration performance of the fabrics based on tests using four types of dust. The obtained test results will be used for further investigations of the probabilistic model of the dust filtration process (Project P-5-533-3).

DETAILED PROGRAM

Laboratory Tests

- Preparation of the separated dusts (cement, coal, talc, and fly ash) using the ALPINE separator,
- Determination of the physical-chemical properties of the separated and unseparated dusts,
- Testing of the filtration fabrics received from the United States (15 kinds) using the following dusts: cement, coal, talc, and fly ash; and

- Compilation and analysis of the results.

Large Scale Testing

- Separation, by the subcontractor, of test dusts (cement, talc, and fly ash),
- Determination of the physical-chemical properties of the separated and unseparated dusts,
- Testing of 15 kinds of filtration fabrics received from the United States and 4 types of dust (cement, coal, talc, and fly ash),
- Estimation of the fractional efficiency of the filtration fabrics using the cascade impactor, and
- Compilation and analysis of the results.

Auxiliary Studies

- Testing of hydraulic properties of filtration fabrics during clean air flow,
- Determination of filtration fabric parameters according to Polish standards,
- Special testing of filtration fabrics concerning structural parameters, using a scanning microscope,
- Determination of the regeneration properties of the fabrics, and
- Comparison of fabric properties of both Polish and U.S. production.

FABRIC AND DUST SELECTION

Fifteen types of filtration fabrics, manufactured in the United States and supplied by EPA, were selected for use in the major part of the testing under Project P-5-533-4. These selected fabrics are produced from the following raw materials:

- Cotton (staple fiber):
    - No. 960
- Dacron® polyester (staple fiber):
    - No. 862B
    - No. C866B
    - No. C868B

- Dacron® polyester (continuous filament):
    - No. 865B (staple fill)
    - No. C890B
    - No. C892B
- Nomex® aromatic nylon (staple fiber):
    - No. 852
    - No. 853
    - No. 190R
- Nomex® aromatic nylon (continuous filament):
    - No. 850B
- Nylon polyamide (staple fiber):
    - No. 802B
- Glass (staple fiber):
    - No. Q53-875
- Glass (continuous filament):
    - No. Q53-870
    - No. Q53-878 (texturized fill).

Technical characteristics of these fabrics are shown in Table 1.

Cement dust, coal dust, talc, and fly ash were selected as test dusts. These industrial dusts were taken from appropriate points of the production processing line so as to preserve realistic physical-chemical properties. According to contractor wishes, separated dusts were used. Test dusts for laboratory testing were separated by the ALPINE separator. For large scale tests, the dusts were separated by subcontractors.

In accordance with suggestions from Dr. James H. Turner, the EPA Project Officer, testing under this project was of only those dust samples containing no more than 10 percent, by weight, of particles with a diameter greater than 20 μm. Because of the explosive properties of coal dusts, the subcontractor would not accept the responsibility of separating the dusts for large scale tests. So, it was approved by the Project Officer to conduct laboratory tests on separated and unseparated coal dust, but large scale tests only on unseparated coal dusts.

The physical and chemical properties of the test dusts are shown in Tables 2 through 7 and Figures A-1 through A-4.

TABLE 1. FABRIC PARAMETERS

Parameter	Unit	Fabrics														
		960	862B	C866B	C868B	865B	C890B	C892B	852	853	190R	850	802B	Q53-875	Q53-870	Q53-878
Fabric weight	g/m²	337	330	379	438	337	168	151	292	350	510	155	401	281	282	451
Thread count 10 cm:																
warp		384	138	164	164	302	292	254	122	154	-	380	140	210	210	176
fill		238	110	138	158	178	262	232	100	144	-	288	136	204	204	96
Thickness (pressure 20 g/cm²)	mm	0.74	0.87	0.92	0.96	0.63	0.24	0.24	0.92	1.08	1.79	0.24	1.08	0.31	0.30	0.56
Tensile strength:																
warp	kg/5cm	99	162	212	210	330	170	162	148	175	67.4	188	173	176	188	475
fill	kg/5cm	103	125	162	221	135	136	122	120	148	108	151	179	160	196	248
Elongation during tension:																
warp	%	15	35	34	34	41	20	29	30	28	19	40	41	3.9	3.5	6
fill	%	14	42	44	42	37	34	33	23	28	56	35	44	4.1	4.1	6
Bursting strength (ball diameter 10 mm)	kg	41.5	69.5	97.5	113.0	92.5	58.5	71.5	75.0	92.0	82.0	82.0	91.0	†	†	†
Abrasion resistance ‡	Number of strokes for rubbing through	275	615	890	960	640	160	215	450	920	1100§ 1760	180	1330	70	55	225
Permeability	dm³/m²/s at 10 mm of water	45	382	240	163	166	107	70	457	187	97	148	140	226	58	219
Weave		$\frac{4}{1}$	$\frac{1}{1}$	$\frac{2}{2}Z$	$\frac{2}{2}S$	$\frac{3}{1}X$	$\frac{3}{1}Z$	$\frac{3}{1}Z$	$\frac{1}{1}$	$\frac{2}{2}S$	-	$\frac{3}{1}Z$	$\frac{2}{2}Z$	$\frac{1}{3}S$	$\frac{3}{1}X$	$\frac{3}{1}S$

*All the values have been determined according to Polish standards.
†Under the pressure of the ball, the threads displace, but do not break.
‡Conditions of testing: Measuring instrument type STOLL, loading 0.907 kG, grinder-abrasive paper No. 600.
§Rubbing to interlayer.

TABLE 2. PHYSICAL PROPERTIES OF TESTING DUSTS*

Kind of dust	Parameter			
	Angle of repose dust (on glass surface)	Poured dust weight of 1 liter (in g/dm³)	Cone angle of heaped dust	Jogged dust weight (in g/cm³)
Cement				
After separation	41°50'	898.33	47°17'	1.40
Before separation	55°20'	736.67	48°09'	1.13
Coal				
After separation	44°40'	571.67	41°49'	0.77
Before separation	62°	406.67	49°56'	0.62
Talc				
After separation	90°	498.30	40°01'	0.87
Before separation	90°	446.70	61°45'	0.77
Fly ash				
After separation	61°67'	610.00	46°15'	1.03
Before separation	57°33'	560.00	45°56'	0.858-1.018

*All the values have been determined according to Polish standards.

TABLE 3. PARTICLE SIZE DISTRIBUTION OF CEMENT DUST

Separated (for laboratory scale)		Separated (for large scale)		Separated (for large scale)	
Density: 2.86 g/cm^3		Density: 2.78 g/cm^3		Density: 2.857 g/cm^3	
Range of particle size in μm	Percent by weight	Range of particle size in μm	Percent by weight	Range of particle size in μm	Percent by weight
< 2.13	6.70	< 2.15	11.91	< 2.17	9.85
2.13- 3.91	10.80	2.15- 3.95	18.90	2.17- 3.97	17.90
3.91- 5.92	16.80	3.95- 5.99	30.19	3.97- 6.02	34.06
5.92- 9.17	23.10	5.99- 9.28	24.89	6.02- 9.34	25.52
9.17-14.20	24.10	9.28-14.37	10.46	9.34-14.46	10.08
14.20-23.67	16.30	14.37-23.95	3.02	14.46-24.09	2.82
23.67-28.99	2.10	23.95-29.34	0.43	24.09-29.52	0.33
28.99-32.54	0.10	29.34-32.93	0.07	29.52-33.13	0.21
>32.54	-	32.93-60.00	0.13	>33.13	-
		>60.00	-		

TABLE 4. PARTICLE SIZE DISTRIBUTION OF COAL DUST

Separated (for laboratory scale)		Unseparated (for large scale)		Unseparated (for large scale)	
Density: 1.55 g/cm³		Density: 1.48 g/cm³		Density: 1.50 g/cm³	
Range of particle size in μm	Percent by weight	Range of particle size in μm	Percent by weight	Range of particle size in μm	Percent by weight
< 2.38	7.15	< 2.95	4.70	< 2.42	2.72
2.38- 4.11	13.86	2.95- 5.41	6.89	2.42- 4.18	4.68
4.11- 8.31	30.20	5.41- 8.19	9.90	4.18- 8.44	6.06
8.31-12.10	21.51	8.19-12.70	11.28	8.44-12.29	12.52
12.10-20.72	23.88	12.70-19.67	10.86	12.29-21.06	12.80
20.72-36.13	3.21	19.67-32.78	12.07	21.06-36.72	12.51
36.13-45.08	0.09	32.78-40.16	4.26	36.72-45.82	5.85
45.08-51.77	0.02	40.16-45.08	2.25	45.82-52.62	3.23
51.77-60.00	0.01	45.08-60.00	8.56	52.62-60.00	7.02
> 60.00	0.07	69-88	10.95	60-88	9.70
		88-150	12.98	88-150	14.00
		150-200	3.50	150-200	4.56
		>200	2.80	>200	4.35

TABLE 5. PARTICLE SIZE DISTRIBUTION OF TALC

Separated (for laboratory and large scale)		Separated (for large scale)	
Density: 2.80 g/cm^3		Density: 2.78 g/cm^3	
Range of particle size in μm	Percent by weight	Range of particle size in μm	Percent by weight
< 2.15	6.86	< 1.77	4.93
2.15- 3.95	14.00	1.77- 3.05	11.39
3.95- 5.99	20.52	3.05- 6.17	17.14
5.99- 9.28	25.61	6.17- 8.98	41.37
9.28-14.37	18.96	8.98-15.39	22.45
14.37-23.95	11.49	15.39-26.83	2.72
23.95-29.34	2.04	26.83-33.47	-
29.34-32.93	0.52		
>32.93	-		

TABLE 6. PARTICLE SIZE DISTRIBUTION OF FLY ASH

Separated (for laboratory and large scale)	
Density: 2.27 g/cm^3	
Range of particle size in μm	Percent by weight
< 2.38	11.06
2.38- 4.37	20.72
4.37- 6.62	33.61
6.62-10.26	25.81
10.26-15.89	8.20
15.89-26.49	0.58
26.49-32.45	0.02
>32.45	-

TABLE 7. CHEMICAL PROPERTIES OF TESTING DUSTS

Component	Unit	Kind of test dust			
		Separated cement test dust	Unseparated coal test dust	Separated coal test dust	Separated fly ash test dust
Loss of roasting	Percent by weight	6.93	25.51	24.14	7.84
SiO_2		21.32	51.13	46.75	50.05
TiO_2		-	0.92	1.04	1.22
Fe_2O_3		2.37	8.58	10.46	7.08
Al_2O_3		6.73	22.96	22.78	22.39
CaO		54.36	6.91	8.25	4.97
MgO		1.99	2.62	3.34	2.50
SO_3		5.63	3.21	4.42	0.48
Na_2O		0.23	0.88	0.85	0.64
K_2O		0.61	2.35	1.81	3.00
TOTAL		100.17	99.56	99.70	100.17

SECTION IV

LABORATORY TESTING OF FILTRATION

INTRODUCTION

Laboratory testing of filtration fabrics is conducted mainly to determine the time dependence of the efficiency and the pressure drop during a single dust cycle--from a given initial state to a predetermined final state using a non-varying aerosol.

Usually laboratory testing is completed by measuring the hydraulic characteristics of the test materials, i.e., the determination of resistance variations as a function of A/C ratio. The hydraulic resistance of clean air flow through filtration structures depends upon the structural parameters of the filtration structure. Generally, two kinds of structural parameters can be distinguished:

1. Physical parameters of structure (porosity, density of packing, etc.), and
2. Technological parameters of structure (diameter of fiber, diameter of thread, the kind of weave, etc.).

Correlations between the physical and the technological parameters of woven filtration materials have not previously been made nor has the effect of technological parameters on chosen physical parameters characterizing the material been examined during both clean air flow and flow during the dust filtration process. Because of the extremely complicated composition of the fabric structure, the comparison of certain types of woven material structures is conducted by comparing their hydraulic properties during clean air flow only.

Permeability is a commonly used parameter describing the value of air flow through a unit area at a definite pressure drop. Pressure drop has been standardized as:

- 0.5 in. of water - United States,
- 20 mm of water (sometimes 10 mm of water) - Poland.

Based on the results of testing different fabrics, it can be said that the permeability of certain fabrics (manufactured under the same technological conditions) from different series can vary greatly. It is caused by the heterogeneity and quality of the raw materials, by specification of the spinning and weaving processes, and also by finishing operations.

From a mathematical viewpoint, permeability is not a representative enough parameter for comparing woven filtration fabrics. It is better to compare hydraulic characteristics as defined in the following equation:

$$\Delta P = f(q_g). \tag{1}$$

In order to characterize woven filtration fabrics, the parameter called "free area," FA, calculated from technological parameters, was introduced (refs. 5, 6).

$$FA = 100 - (n_o d_o 10 + n_w d_w 10 - n_o n_w d_o d_w) \tag{2}$$

where FA = free area, in percent,
n_o = number of warp threads/10 cm,
n_w = number of fill threads/10 cm,
d_o = diameter of warp yarn, in cm, and
d_w = diameter of fill yarn, in cm.

In the phase I report of this project, it was proven that because of thread deformation in continuous filament polyester, nylon, and glass fabrics the calculation of FA does not correspond to the pressure drop obtained during clean air flow. Staple fiber threads also show the deformation, but it is very small. Moreover, FA does not consider the presence of "free fiber" in spaces not filled by yarn, which also influences the flow resistance and filtration effects.

To apply FA as a technological structural parameter, it is necessary to define the method of determining the diameter of the warp and fill yarns (ref. 5).

The diameter of the yarns can be calculated from the metrical numbers of the yarn or can be measured using a microscope, taking deformation into consideration. In the second case, the analytical size is either the long or the short projected dimension. Sometimes, the diameter of the yarn is calculated as the average of the lengthwise projected dimensions of the yarn.

So, we can obtain three different diameters, resulting in three values of FA. It should be added that FA does not concern the spatial structure of fabrics. The laboratory filtration process is not the same as the industrial fabric collector process where the filtration medium has reached a definite state-of-balance. The laboratory process has been defined as Dust Filtration Type I (refs. 2, 3).

Dust Filtration Type I is the initial phase of the complete process, when the fabric first begins operation as a filtration medium. This phase ends when the pressure drop across the fabric reaches a predetermined level for a given A/C ratio.

Dust Filtration Type I is presented in Figure 1. The initial state is described by ΔP_o (pressure drop of the pure clean fabric structure) at q_g = constant and $q_p = 0$, so that $L = 0$. The final state of the process is described by ΔP_K (final pressure drop) at q_g = constant, q_p = constant, and $L = L_o = L_N + L_P$. (L_P represents the dust in the dust cake that will be removed during regeneration; L_N represents the dust not removed during regeneration.) On both laboratory and industrial scale the dust filling of the structure (L_N) is determined by weighing after a specific regeneration cycle.

Because of the long time required to reach a constant quantity of residual dust remaining in the fabric, the dust filling of the structure in laboratory conditions is very small and is only an auxiliary parameter for interpretation of results.

Described by initial and final pressure drop, dust filtration is characterized by a certain effectiveness, the measurement of which is the average efficiency of dust collection, E_I. Subscript "I" indicates that efficiency concerns Dust Filtration Type I.

The filtration pressure drop in time is shown in Figure 2. During the first phase of the process, the increase of filtration resistance is very fast and has a parabolic character of the general form $y = ax^2 + bx + c$ with $a<0$ to point A, the point of inflexion. Beyond point A, the increase also has parabolic character but with $a>0$.

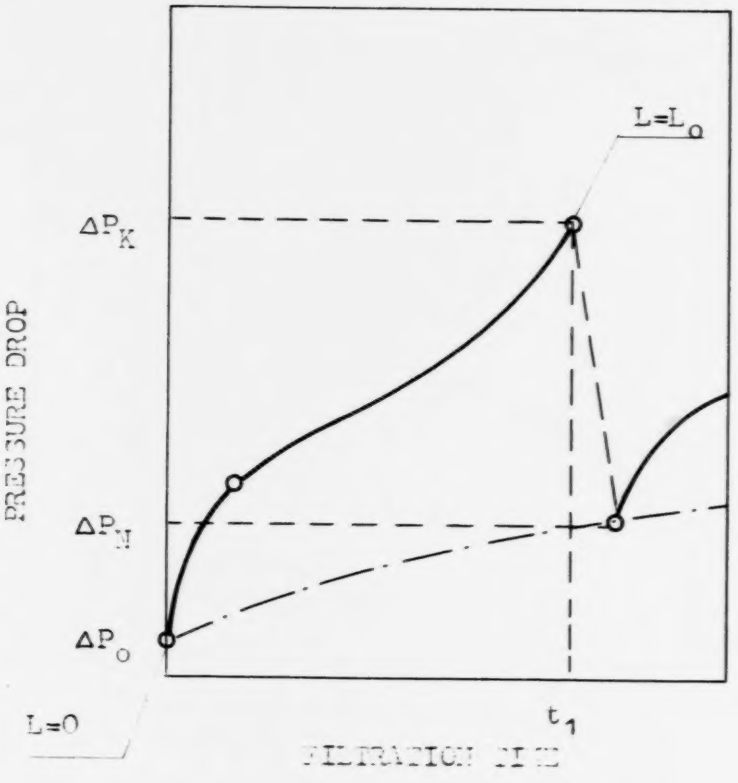

Figure 1. Dust Filtration Type I.

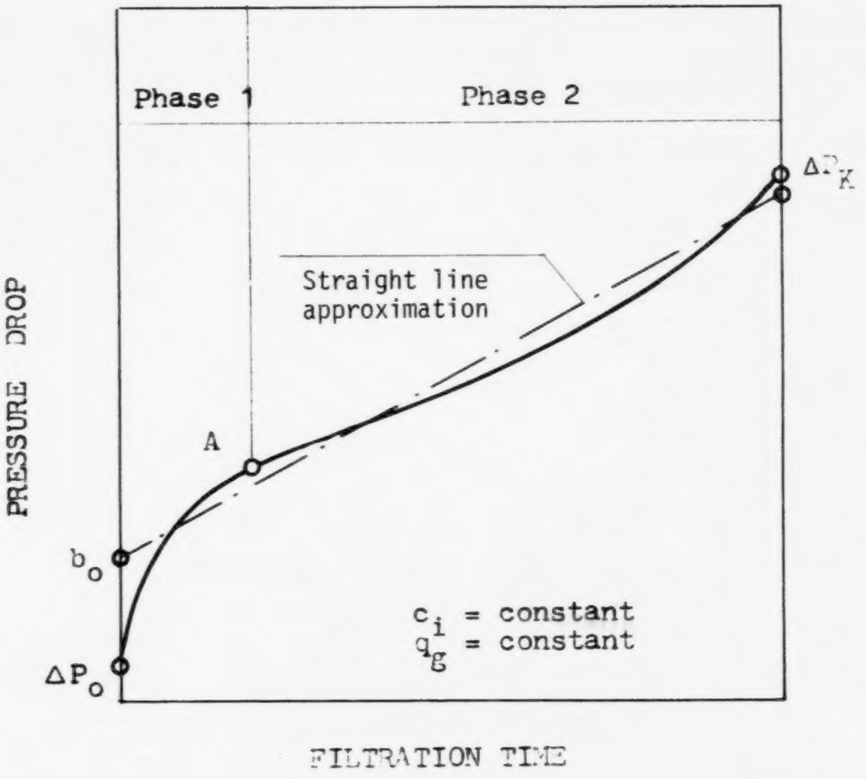

Figure 2. Increase of pressure drop in time during Dust Filtration Type I.

The length of phase 1 and 2 depends on the kind of filtration material, the kind of dust, and its particle size distribution. The rate of increase of resistance depends on the above variables and also on the A/C ratio (ref. 7).

For some dust-fabric systems the dependence $\Delta P = f(t_F)$ or $\Delta P = f(L_o)$ can be approximated by a straight line. The hypothesis can be made that during phase 1 there is filling of the free spaces of the filtration medium and from the point of inflexion on the dust cake starts to build (ref. 8).

Because there is no theory interpreting the results of laboratory testing of filtration fabrics, comparative analysis is widely applied. To facilitate the comparative analysis, a systematic format can be applied.

Concerning the efficiency of dust collection, the test results can be classified by levels of analytically estimated final concentrations. Concerning the pressure drop with filtration time, the results are usually approximated to the following dependence using linear regression:

$$\Delta P = f(t_F) = b_o + b_1 t_F. \tag{3}$$

Regarding this dependence as the first approximation of a process that really has parabolic character, it is possible to compare the filtration resistances between different dust-fabric systems.

According to Stephan, Walsh, and Herrick (ref. 9), the value b_o from equation (3) is proportional to S_E, the effective drag.

$$S_E = b_o/q_g \tag{4}$$

where S_E = effective drag, in $mmH_2O/m/hr$,
b_o = effective pressure drop, in mmH_2O,
q_g = A/C ratio, in m^3/m^2hr.

The value b_1 is proportional to K_2, the specific dust-fabric resistivity according to the following dependence:

$$K_2 = b_1 \frac{1}{c_i q_g^2} \tag{5}$$

where K_2 = specific dust-fabric resistivity, in $(mmH_2O/m/hr)/(g/m^2)$,
b_1 = coefficient, in mmH_2O/hr,

c_i = initial concentration, in g/m^3,
q_g = A/C ratio, in m^3/m^2hr.

The rate of increase of filtration resistance during the filtration process can be described by the following dependence:

$$V_{\Delta P} = \frac{d(\Delta P)}{dt_F} = b_1 \quad (6)$$

where $V_{\Delta P}$ = rate of increase of filtration resistance, in mmH_2O/hr,
ΔP = pressure drop, in mmH_2O,
t_F = filtration time, in hours.

It depends on the properties of the filtration medium (dust-fabric system) and also on filtration parameters.

EQUIPMENT AND PROCEDURES

Laboratory testing of selected filtration fabrics was conducted on a stand, illustrated in Figure 3, specially designed by the IPWMB and adapted for the testing of flat fabric specimens under ambient air conditions.

This stand includes a test chamber, a rotameter for measuring flow intensity, a needle valve to control flow intensity, a vibrating-injecting dust feeder, a micromanometer to measure pressure drop, and a vacuum pump (see Figure 4). The testing chamber, the main part of the stand, is equipped with a diffuser at the inlet end, a fabric specimen table, and a control filter table at the outlet end. A round fabric specimen with a 100 cm^2 test area is positioned in the middle of the table, supported by wire net screening 4 cm along one side.

In testing, dusty air flows through the fabric, from the top downward, with the inlet diffuser providing a uniform flow throughout the entire test area of the fabric. After passing through the fabric specimen, the air then passes through a control filter of soft batting and paper (a disc with a 200 cm^2 test area). The control filter is positioned on the table at the outlet end, supported by wire net screening 1 cm along one side.

Average dust collection efficiency was determined by weighing the fabric specimen and the control filter and then applying the following equation:

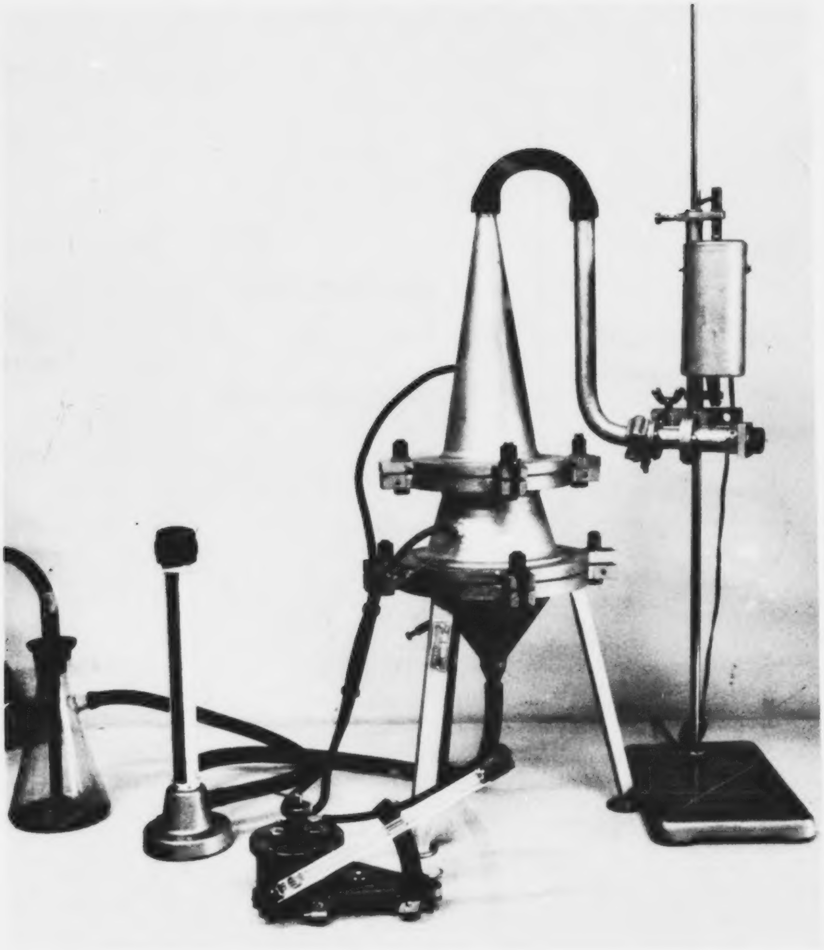

Figure 3. Illustration of laboratory stand.

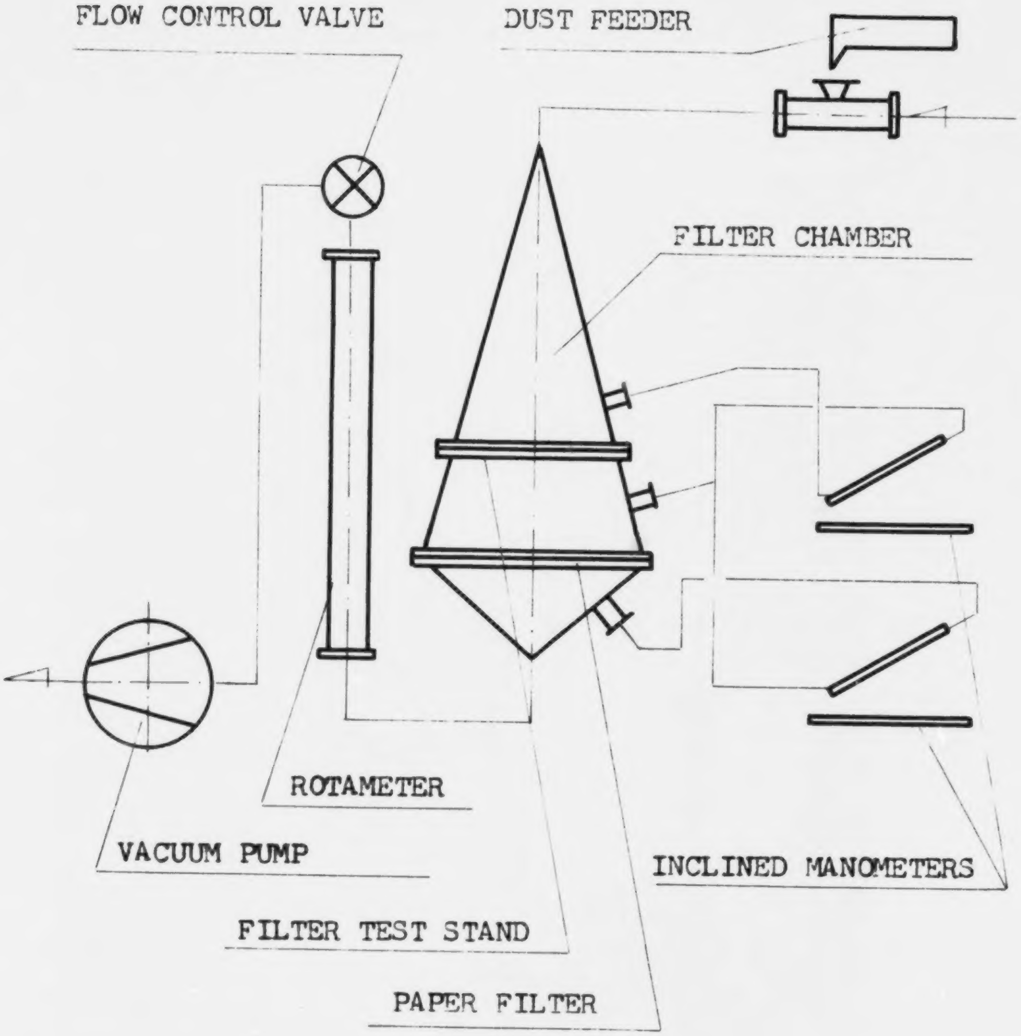
FLOW CONTROL VALVE
DUST FEEDER
FILTER CHAMBER
ROTAMETER
VACUUM PUMP
INCLINED MANOMETERS
FILTER TEST STAND
PAPER FILTER

Figure 4. Diagram of the laboratory test stand.

$$\frac{E}{100} = \frac{G_z}{G_c} = \frac{G_c - G_o}{G_c} = \frac{G_z}{G_z + G_o} \qquad (7)$$

where E = dust collection efficiency in percent,

G_z = weight in grams of dust collected on the fabric,

G_o = weight in grams of dust collected on the control filter, and

G_c = weight in grams of dust fed into the testing chamber.

During testing the temperature and humidity of the ambient air were recorded. The fabric samples and control filters were conditioned in ambient air for 72 hours.

Using the laboratory test stand, the following data can be obtained:

- Mean filtration efficiency,
- Hydraulic characteristics of filtration materials during clean air flow,
- Increases in hydraulic resistance during dusty air flow,
- Degree of filling of filtration materials.

Although specially designed for the laboratory testing of woven filtration fabrics, this stand can also be used for laboratory testing of other filtration materials, e.g., felt.

RESULTS AND DISCUSSION

Air Flow Through Clean Filtration Fabrics

The testing of hydraulic resistances of clean filtration fabrics during air flow was conducted for A/C's in the range of 50 - 180 m^3/m^2 hr. Five series of measurements were done on all fabrics to determine the average values of hydraulic resistance. The results are shown in Table B-1.

Based on the average values of hydraulic resistance for certain A/C's, the curves of hydraulic resistance, as a function of A/C ratio, were drawn. They are shown on Figures 5 through 7.

The dependences $\Delta P = f/(q_g)$ for each kind of fabric were determined using the least squares method. It appeared that the empirical data best approximated the parabolas. The results of the calculations, in the form of empirical dependences, are shown in Table 8.

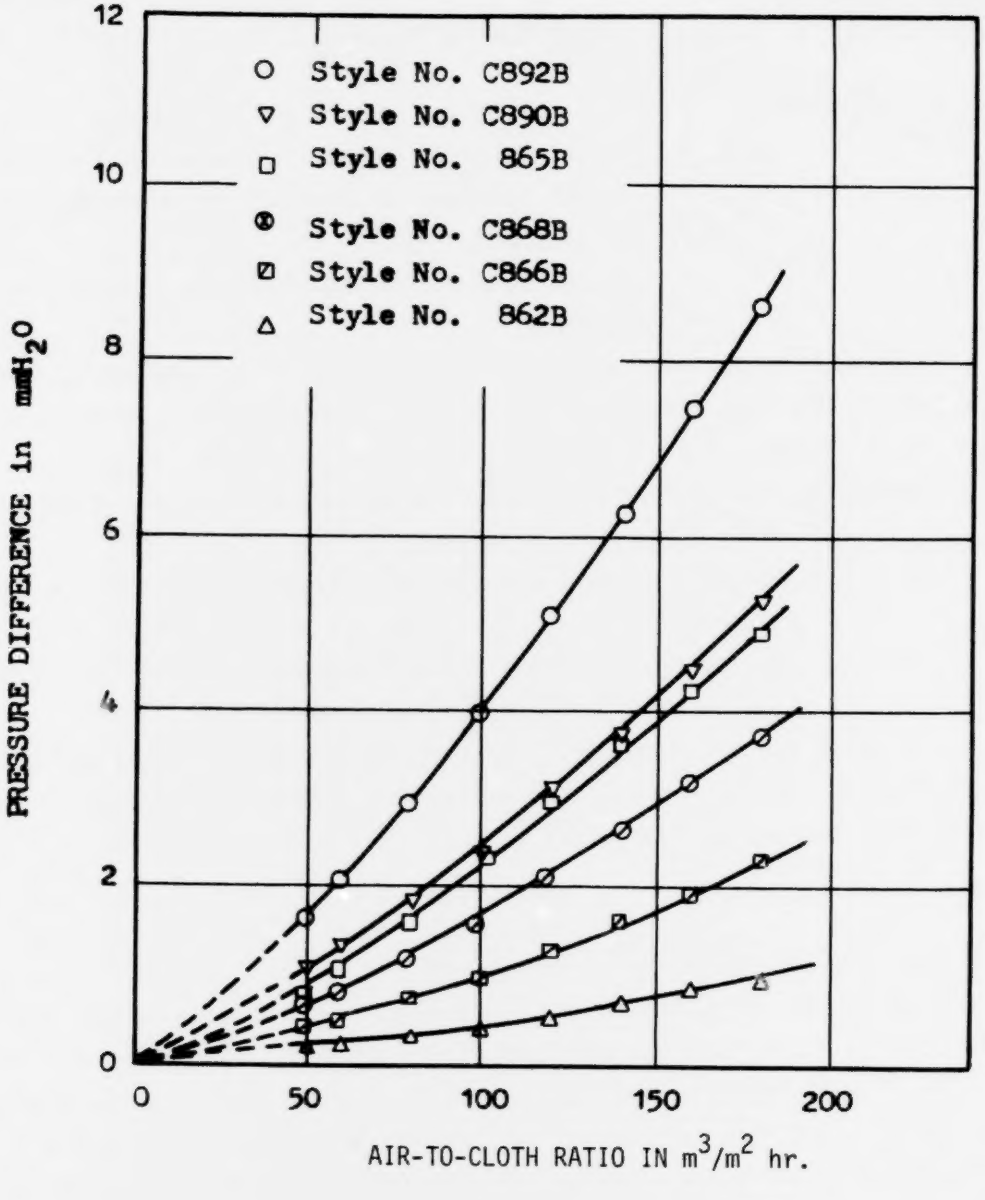

Figure 5. Hydraulic characteristic of polyester fabrics.

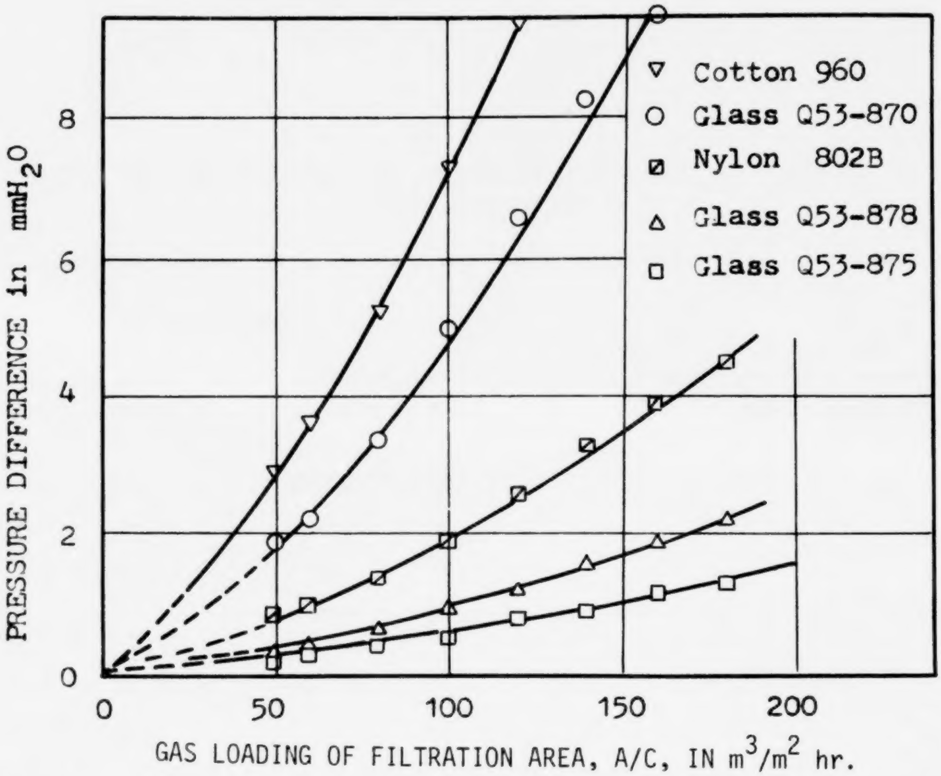

Figure 6. Hydraulic characteristic of glass, cotton, and nylon fabrics.

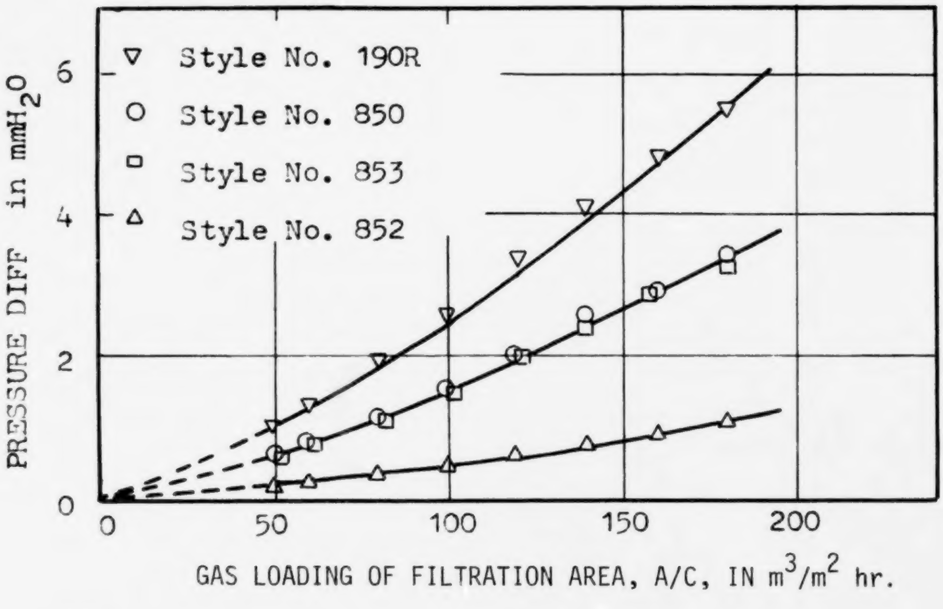

Figure 7. Hydraulic characteristic of Nomex fabrics.

TABLE 8. EMPIRICAL FUNCTIONS OF HYDRAULIC RESISTANCES OF FILTRATION FABRICS

Type of fabric		Function*
Cotton	960	$\Delta P = 0.6533q_g^2 + 3.3369q - 0.1475$
Dacron®	862B	$\Delta P = 0.0674q_g^2 + 0.1292q_g + 0.0022$
	C866B	$\Delta P = 0.1450q_g^2 + 0.3403q_g - 0.0030$
	C868B	$\Delta P = 0.2104q_g^2 + 0.6380q_g - 0.0080$
Dacron®	865B	$\Delta P = 0.2227q_g^2 + 1.0278q_g - 0.0770$
	C890B	$\Delta P = 0.2315q_g^2 + 1.0679q_g + 0.0190$
	C892B	$\Delta P = 0.3905q_g^2 + 1.7511q_g - 0.0300$
Nomex®	852	$\Delta P = 0.0595q_g^2 + 0.1880q_g - 0.0035$
	853	$\Delta P = 0.1509q_g^2 + 0.6922q_g - 0.0140$
	190R	$\Delta P = 0.2261q_g^2 + 1.2202q_g - 0.0350$
Nomex®	850B	$\Delta P = 0.1705q_g^2 + 0.6549q_g + 0.0174$
Nylon	802B	$\Delta P = 0.2401q_g^2 + 0.8076q_g - 0.0110$
Glass	Q53-875	$\Delta P = 0.0736q_g^2 + 0.2258q_g - 0.0110$
Glass	Q53-879	$\Delta P = 0.5629q_g^2 + 2.1110q_g - 0.1871$
	Q53-878	$\Delta P = 0.1471q_g^2 + 0.3326q_g - 0.0140$

*q_g in m^3/m^2 min.

The specific hydraulic resistance of the porous layer, according to the Darcy equation for turbulent flow (ref. 10), is:

$$\Delta P_i = \Delta P/b = K_1' (q_g)^2 \tag{8}$$

where ΔP_i = specific hydraulic resistance of porous layer in mmH_2O/mm,
ΔP = hydraulic resistance in mmH_2O,
b = thickness of porous layer in mm,
K_1' = resistance coefficient, and
q_g = A/C ratio in m^3/m^2min.

The dependence of the specific hydraulic resistance of the tested fabrics as a function of A/C ratio, in the form of equations, is presented in Table 9. The above equations are shown in the form of curves in Figures 8 through 10. Neglecting the free terms of the equations in Tables 8 and 9 (the parabola must cross the point of coordinates 0,0) and taking into consideration equation (8), we get:

$$\Delta P_i = \Delta P/b = K_1' (q_g)^2 = aq_g^2 + bq_g$$

$$= q_q^2 \left(a + \frac{b}{q_g}\right), \tag{9}$$

so
$$K_1' = a + \frac{b}{q_g}. \tag{10}$$

The resistance coefficient K_1' of the Darcy equation (equation. 10) is not a stable value characterizing the filtration structure, but is a function of A/C ratio. Its functional dependence is presented in Figure 11. The function is a hyperbola with asymptotes, $q_g=0$ and $K_1'=a$.

Because of the absence of physical and also mathematical descriptions of woven filtration structures, it is very difficult to define the kind of flow through the clean structure over the range of A/C ratio studied. It was only ascertained that the flow is between laminar and turbulent flow. Assuming the above, the discussion of dependence (10) was carried out. The following are conclusions of the discussion:

TABLE 9. EMPIRICAL FUNCTIONS OF SPECIFIC HYDRAULIC RESISTANCES OF FILTRATION FABRICS

Type of fabric		Function*
Cotton	960	$\Delta P_i = 0.8828q_g^2 + 4.5093q_g - 0.1993$
Dacron®	862B	$\Delta P_i = 0.0775q_g^2 + 0.1485q_g + 0.0025$
	C866B	$\Delta P_i = 0.1576q_g^2 + 0.3699q_g - 0.0033$
	C868B	$\Delta P_i = 0.2192q_g^2 + 0.6646q_g - 0.0083$
Dacron®	865B	$\Delta P_i = 0.3535q_g^2 + 1.6314q_g - 0.1222$
	C890B	$\Delta P_i = 0.9645q_g^2 + 4.4496q_g + 0.0792$
	C892B	$\Delta P_i = 1.6271q_g^2 + 7.2962q_g - 0.1250$
Nomex®	852	$\Delta P_i = 0.0647q_g^2 + 0.2043q_g - 0.0038$
	853	$\Delta P_i = 0.1397q_g^2 + 0.6409q_g - 0.0129$
	190R	$\Delta P_i = 0.1263q_g^2 + 0.6817q_g - 0.0195$
Nomex®	850B	$\Delta P_i = 0.7104q_g^2 + 0.7478q_g - 0.0725$
Nylon	802B	$\Delta P_i = 0.2223q_g^2 + 0.7478q_g - 0.0100$
Glass	Q53-875	$\Delta P_i = 0.2374q_g^2 + 0.7284q_g - 0.0355$
Glass	Q53-870	$\Delta P_i = 1.8763q_g^2 + 7.0367q_g - 0.6236$
	Q53-878	$\Delta P_i = 0.2627q_g^2 + 0.5939q_g - 0.0250$

*q_g in m^3/m^2 min.

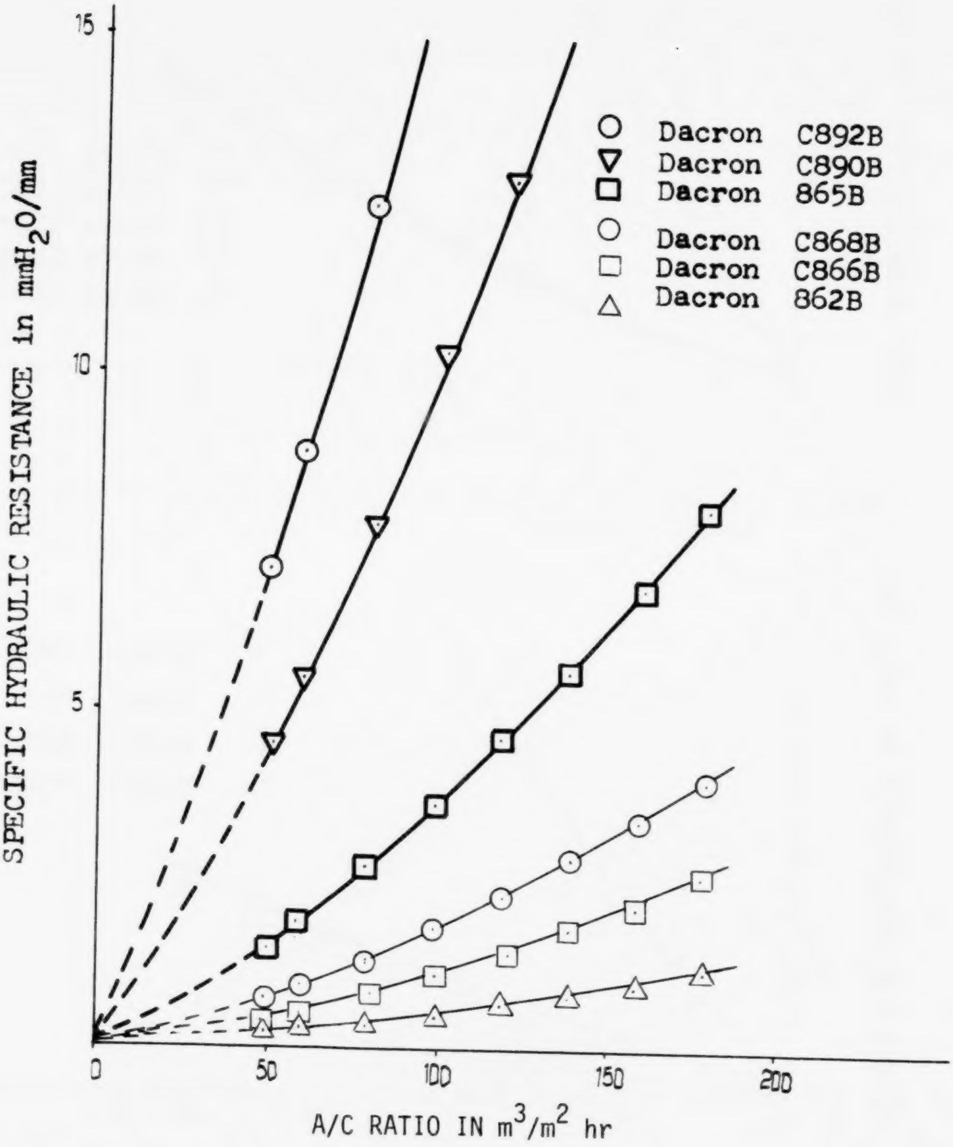

Figure 8. Specific hydraulic resistance of polyester fabrics.

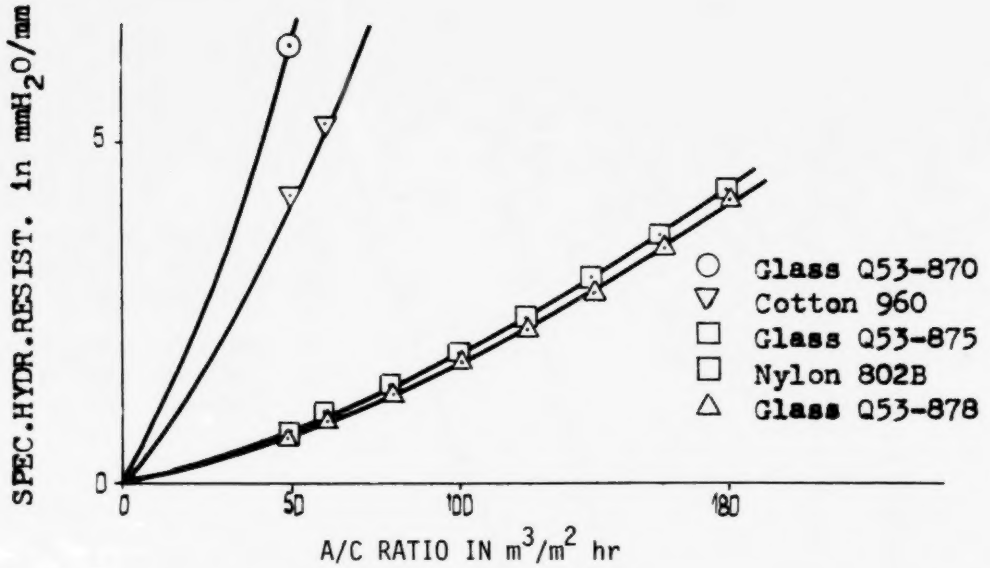

Figure 9. Variation of specific hydraulic resistance of glass, cotton, and nylon fabrics.

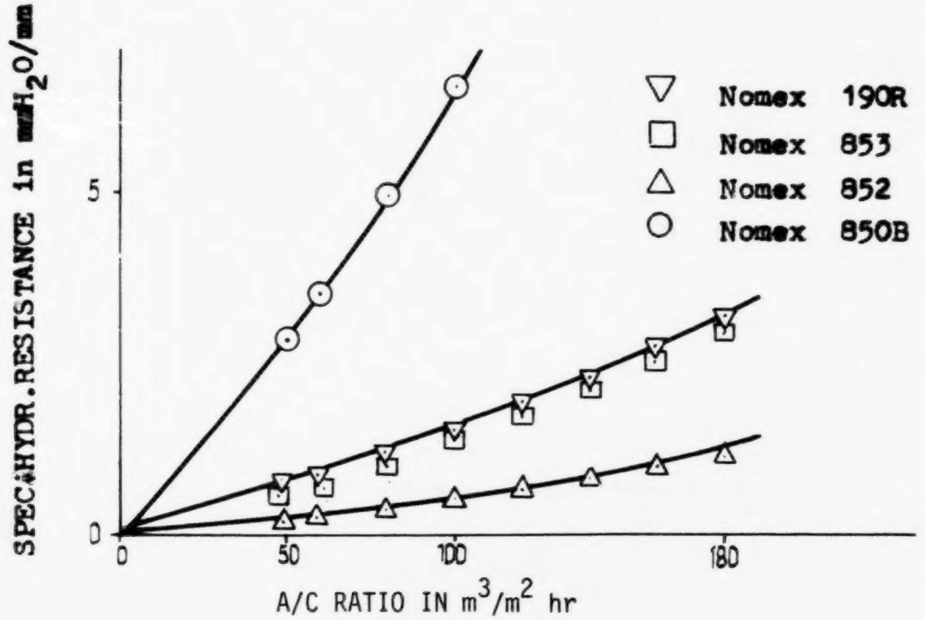

Figure 10. Variation of specific hydraulic resistance of Nomex fabrics.

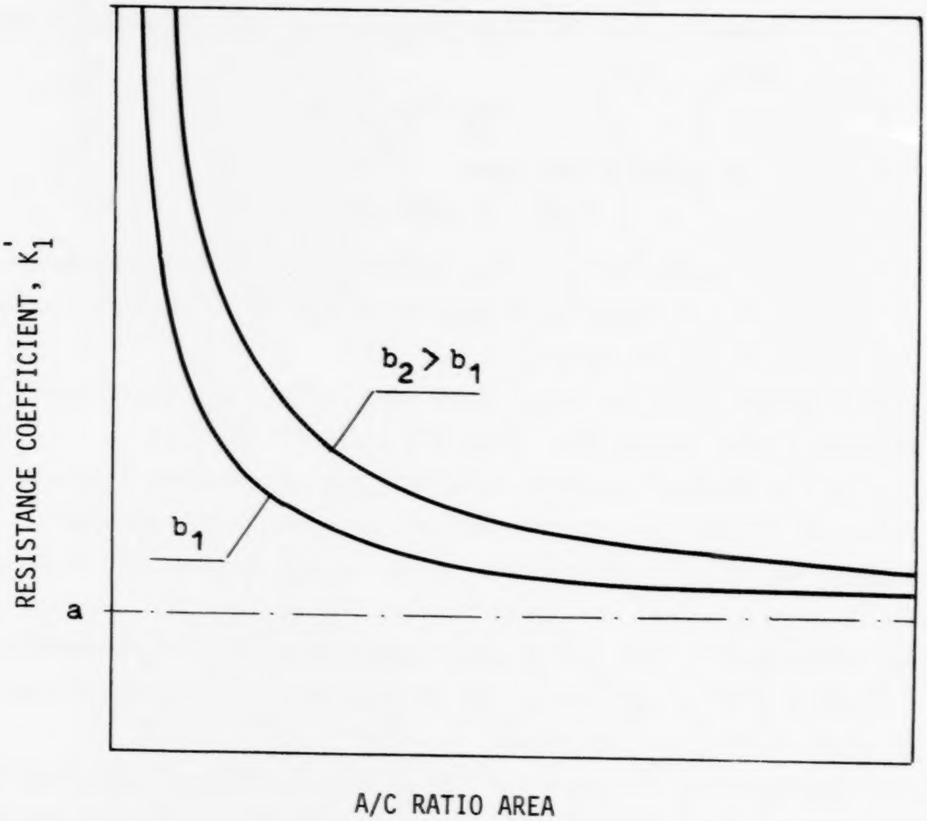

Figure 11. Resistance coefficient, K_1', of a woven fabric.

- Value K_1 = a statistical parameter characterizing the woven structure. It is the so-called resistance coefficient of a woven fabric,
- Because of the complicated character of flow, due to periodicity of the woven structure, there are additional energy losses proportional to the ratio b/q_g.
- The ratio b/q_g reaches the lowest values, tending towards "a", at increasing A/C ratio--that means at increasing values of Reynolds number. Thus for high values of q_g, the dependence (10) is of the form:

$$K_1' = a = K_1.$$

From equation (9) then:

$$\Delta P_i = \Delta P/b = K_1 (q_g)^2.$$

We propose to call K_1', which is dependent on the woven material structure and the character of the air flow, the function of woven fabric resistance.

From equation (10), the resistance coefficients for individual filtration materials were determined. They are shown in Table 10.

As can be seen from the compiled data, continuous filament fabrics, (also cotton fabrics) independent of the kind of raw material, have the highest values of coefficient K_1. It is very interesting that the additional energy losses for these fabrics, as measured by the coefficient b/q_g, are the highest. The preliminary explanation of this phenomenon was made in Project P-5-533-3 concerning the determination of the structural parameters of woven filtration materials.

Accordingly, to correlate the values of the resistance coefficient of the woven filtration material, K_1, with some technological and structural parameters, the effect of these parameters on the value of the resistance coefficient was examined. Considered were the structural parameters of free area, calculated porosity, fabric weight, and air permeability. The correlation between free area, determined according to the metrical number of the yarn (Table B-2), and the resistance coefficient of the fabrics is presented in Figure 12.

TABLE 10. RESISTANCE COEFFICIENTS OF WOVEN FABRICS

Type of fabric		Fabric number in Figures 12 through 16	Resistance coefficient K_1
Cotton	960	1	0.8828
Dacron®	862B	2	0.0775
	C866B	3	0.1576
	C868B	4	0.2192
Dacron®	865B	5	0.3535
	C890B	6	0.9645
	C892B	7	1.6271
Nomex®	852	8	0.0647
	853	9	0.1397
	190R	10	0.1263
Nomex®	850B	11	0.7104
Nylon	802B	12	0.2223
Glass	Q53-875	13	0.2374
Glass	Q53-870	14	1.8763
	Q53-878	15	0.2627

The staple filament fabrics, or fabrics having a staple warp or a staple fill, show the correct correlation. But continuous filament fabrics show behavior in disagreement with hydraulic principles, increasing in resistance coefficient with increase of free area. The above disagreement was observed during the examination of the dependence between the fabric hydraulic resistance at a constant A/C (q_g = constant), and the value FA as reported in the first phase of this project. The hypothesized deformation of continuous filament yarn, looking to errors between the calculated (the yarn cross section was assumed to be circular) and true value of FA, was ascertained by microscope examination.

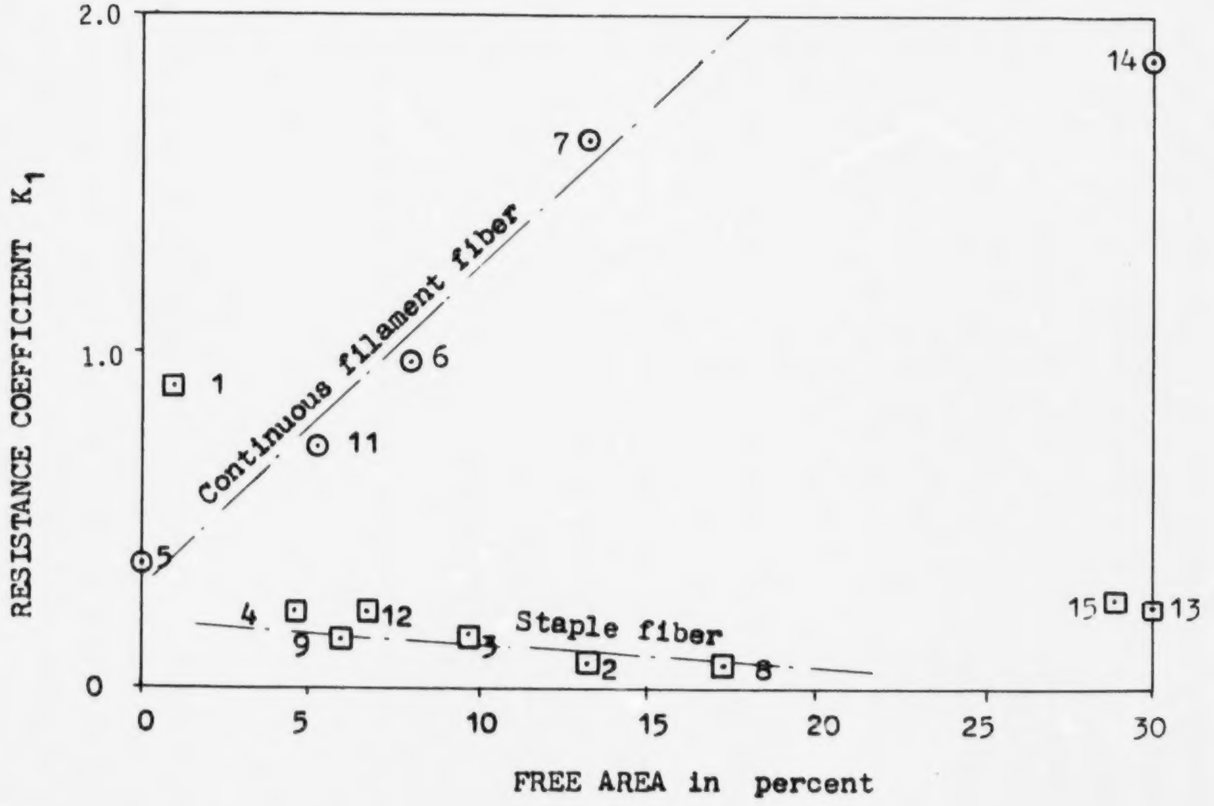

Figure 12. Dependence of resistance coefficient K_1 on free area.

TABLE 11. ADDITIONAL ENERGY LOSSES

Type of fabric		Value of ratio b/q_g from equation 10
Cotton	960	4.5093
Dacron®	862B C866B C868B	0.1485 0.3699 0.6646
Dacron®	865B C890B C892B	1.6314 4.4496 7.2962
Nomex®	852 853 190R	0.2043 0.6409 0.6817
Nomex®	850B	2.7287
Nylon	802B	2.7478
Glass	Q53-875	0.7284
Glass	Q53-870 Q53-878	7.0367 0.5939

Considering the above deformation, in the second phase of this project, FA was also determined by projected sizes. Projected sizes take account of the deformation of yarns. It appeared that FA calculated in this way took on negative values, so for further discussion of these structures, the FA should be assumed to be zero. Thus we come to the conclusion that, for continuous filament fabrics, FA is not a very selective structural parameter, especially for fabrics with high yarn count.

Because of the porosity effect on the fabric resistance coefficient, K_1, two porosities were defined. The first was based on the thickness of the fabric measured under the load (see Table 11) and the second, the thick-

TABLE 12. POROSITIES ε_1 AND ε_2 OF FILTRATION FABRICS

Type of fabric		Calculated porosity ε_1	Calculated porosity ε_2
Cotton	960	0.71	0.52
Dacron®	862B	0.73	0.70
	C866B	0.57	0.63
	C868B	0.67	0.78
Dacron®	865B	0.62	0.58
	C890B	0.49	0.66
	C892B	0.54	0.69
Nomex®	852	0.72	0.74
	853	0.72	0.60
	190R	0.75	-
Nomex®	850B	0.43	0.57
Nylon	802B	0.68	0.60
Glass	Q53-875	0.66	0.67
Glass	Q53-870	0.65	0.65
	Q53-878	0.70	0.66

Note: The following specific densities were assumed for calculation: glass fiber = 2.65 g/cm^3, polyester fiber = 1.38 g/cm^3, polyamide fiber = 1.14 g/cm^3, and cotton fiber = 1.55 g/cm^3.

ness of the fabric calculated from technological parameters. The obtained values of ε_1 and ε_2 and are shown in Table 12.

In the diagrams presented in Figure 13 (K_1 vs. ε), the points for individual fabrics are marked. As seen in the figure, a clear dependency was not obtained; but the points for the continuous filament fabrics were particularly dispersed. The correct trend was obtained for the staple fiber fabrics--the porosity increases with decreasing values of resistance coefficient K_1. Additionally, the influence of the porosity function $(1-\varepsilon)/\varepsilon$ on K_1 was examined. The obtained dependencies were similar as in the case of porosity (see Figure 14).

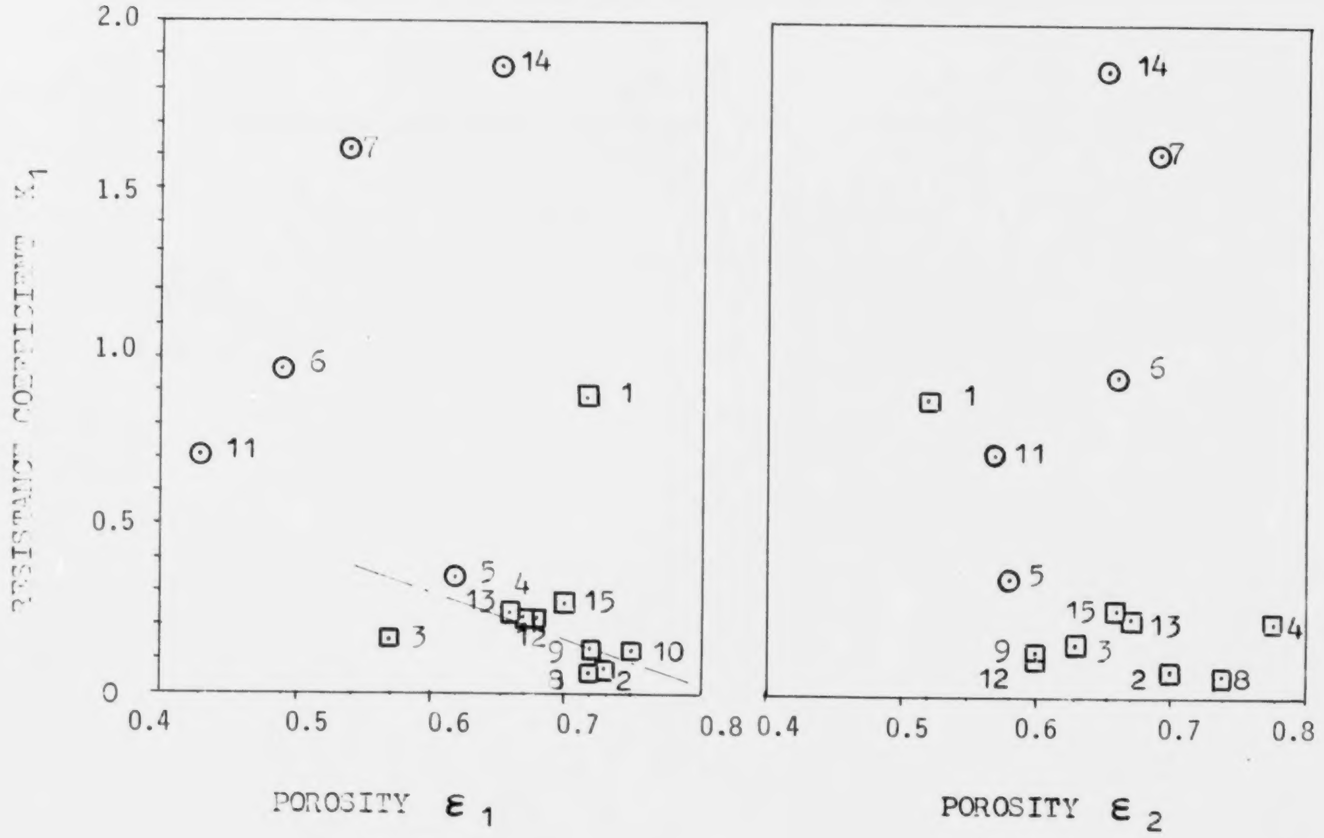

Figure 13. Dependence of resistance coefficient K_1 on fabric porosity.

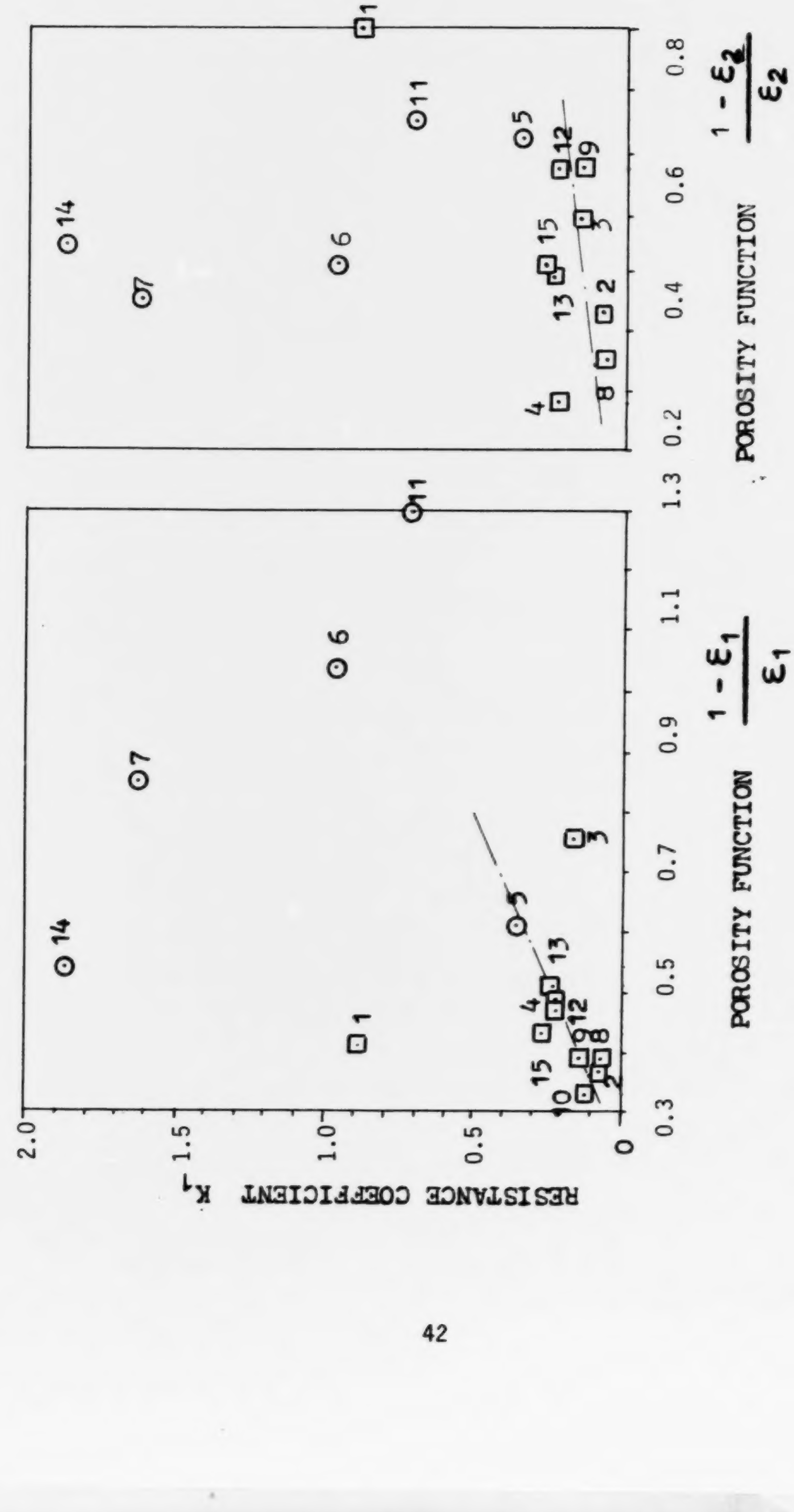

Figure 14. Dependence of resistance coefficient K_1 on porosity function.

Concluding, the above analysis of the effect of porosity on the resistance coefficient K_1 confirmed the existence of flow peculiarities during clean air flow through woven structures. It can be assumed that the periodicity of the woven structures causes the specific flow, and that porosity, which describes flow through homogenous structures, cannot be regarded as a structural parameter.

Figure 15 shows the correlation between the resistance coefficient K_1 and fabric weight, which is an important technological parameter. Despite the fact that the points are quite dispersed, the dependence is clear. The conclusion is that increase in fabric weight causes an increase in the resistance coefficient. An especially quick increase of the curve is observed for continuous filament fabrics. Small changes in fabric weight lead to considerable increase of the resistance coefficient.

The big difference between continuous filament and staple fiber fabrics can be observed in the correlation between K_1 and air permeability. Air permeability, which is still one of the most important technological parameters and simultaneously is a qualitative parameter used for the estimation of fabric homogeneity, has a noteable relationship with both the resistance coefficient and filtration resistance.

From the curves presented in Figure 16 an important conclusion, concerning the permissible tolerance of air permeability for woven filtration fabrics, follows. A wide range of air permeability for staple fiber fabrics (also texturized) is permissible as long as it does not cause significant changes in the resistance coefficient, thus lowering the dust collection efficiency.

But for continuous filament fabrics [very quick increase of value $K_1 =$ f(air permeability)] a wide variation in air permeability tolerance causes considerable variations in filtration resistance.

In Poland, the tolerance in air permeability is determined by so-called branch standards concerning the technological requirements that must be met by fabrics. Table 13 illustrates the air permeability for polyester fabrics. As seen in Table 13, the range of permissible air permeability is quite wide and reaches, on the average, 50 percent of the extreme values.

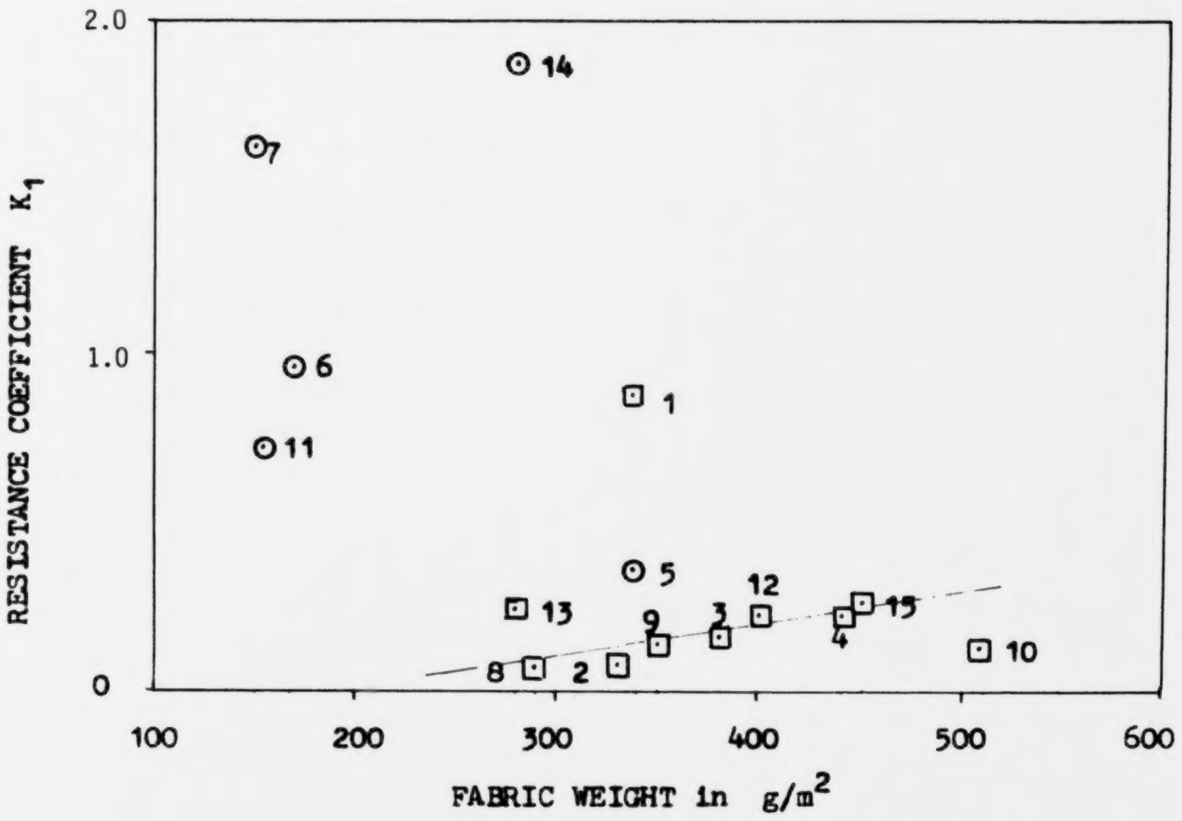

Figure 15. Dependence of resistance coefficient K_1 on fabric weight.

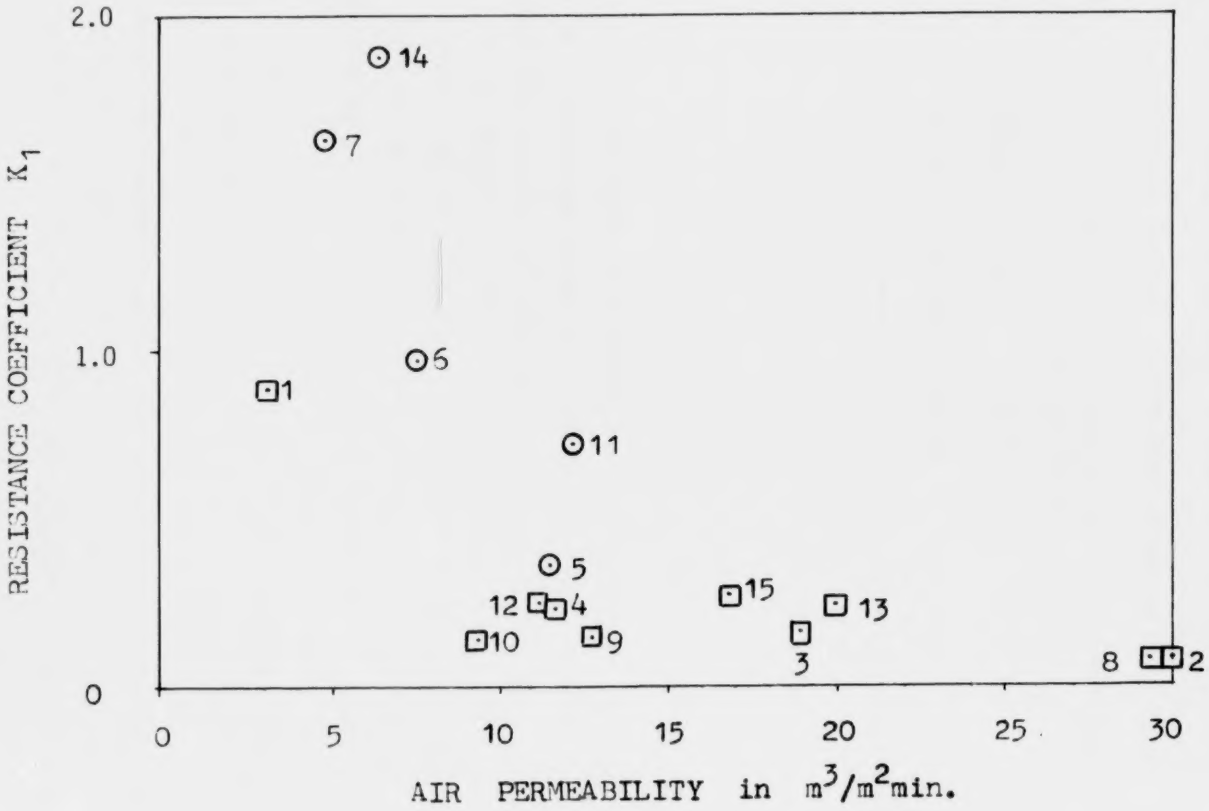

Figure 16. Dependence of resistance coefficient K_1 on air permeability.

TABLE 13. AIR PERMEABILITY OF DUST FILTRATION POLYESTER FABRICS MANUFACTURED IN POLAND (According to NB-70/7547-05)

Parameter	Kind of fabric			
	ET-1	ET-3	ET-4	ET-30
Air permeability in m^3/m^2min at $\Delta P = 20\ mmH_2O$	11-17	15-22	12-18	12-18

Concerning U.S. fabrics, there was not enough technological data for a full analysis of the effect of air permeability on their resistance coefficient. It was noted, however, that the air permeability for two shipments of fabric Q53-878 differed very much and were for the first part 16.78 m^3/m^2min, and for the second part 22.23 m^3/m^2min (see Table 14). This observation leads to the assumption that U.S. standards also have quite large ranges of tolerance in air permeability for woven filtration materials.

In conclusion, it can be said that:

- Air flows through clean woven structures in the range of q_g = 50 - 180 $m^3/m^2/hr$ are placed in the transition region of flow,
- The differences concerning the hydraulic properties between the continuous filament and staple fiber fabrics probably result from the differences in the character of flow (additional energy losses),
- The complicated character of air flow provides for additional energy losses, which decrease with increasing q_g,
- Structural parameters used today, concerning the woven structures, are not correlated with K_1.

Laboratory Testing of Filtration Fabrics

The results of laboratory testing conducted during this project are shown in Tables 15 and 16. Figures A-5 through A-34 illustrate differences

TABLE 14. AIR PERMEABILITY OF U.S. FILTRATION FABRICS

Type of fabric		Air permeability in m^3/m^2 min		
		According to producer at ΔP = 0.5 in	According to measurements at ΔP = 0.5 in	According to measurements at ΔP = 20 mm
Cotton	960	--	3.14	4.72
Dacron®	862B	21.34	29.95	37.36
	C866B	12.19	18.90	23.60
	C892B	9.14	11.58	14.98
Dacron®	865B	10.67	11.50	16.60
	C890B	5.49	7.55	10.36
	C892B	3.05	4.93	7.07
Nomex®	852	22.86	29.31	40.13
	853	10.67	12.74	15.63
	190R	9.14	9.43	12.12
Nomex®	850B	6.71	12.23	14.64
Nylon	802B	12.80	11.11	13.36
Glass	Q53-875	15.85	20.04	22.83
Glass	Q53-870	4.27	6.48	7.84
	Q53-878	14.63	16.78*	19.59*
			22.23†	29.16†

* First delivery.
† Second delivery.

of filtration resistances as a function of filtration time. To evaluate the filtration materials, a comparative analysis was applied. It included all fabrics in the same raw material group. The two main criteria used for comparison were the average obtained efficiency of dust collection and its variation as a function of A/C ratio; and the obtained filtration resistances at certain values of A/C ratio. Table 17 gives a better presentation

TABLE 15. LABORATORY EFFICIENCIES (in percent) OF TESTED FILTRATION FABRICS (c_i = 10 g/m^3, L_o = 400 g/m^2)

Type of filtration fabric	q_g area in m^3/m^2 hr)	Efficiency (in percent)	Outlet concentration (in g/m^3)
		Testing with cement	
Cotton Style No. 960	60	99.962	0.0039
	80	99.980	0.0020
Dacron® polyester Style No. 862B	60	99.830	0.0173
	80	99.744	0.0261
Style No. C866B	60	99.933	0.0068
	80	99.928	0.0070
Style No. C868B	60	99.943	0.0058
	80	99.953	0.0046
Dacron® polyester Style No. 865B	60	99.949	0.0050
	80	99.935	0.0063
Style No. C890B	60	99.588	0.0413
	80	98.179	0.1789
Style No. C892B	60	99.871	0.0125
	80	99.454	0.0549
Nomex® aromatic nylon Style No. 852	60	99.771	0.0231
	80	99.867	0.0130
Style No. 853	60	99.945	0.0053
	80	99.896	0.0106
Style No. 190R	60	99.948	0.0053
	80	99.937	0.0060
Nomex® aromatic nylon Style No. 850B	60	99.352	0.0658
	80	98.642	0.1379

(continued)

TABLE 15. (continued)

Type of filtration fabric	q_g area in m³/m² hr)	Efficiency (in percent)	Outlet concentration (in g/m³)
Nylon polyamide Style No. 802B	60	99.962	0.0038
	80	99.964	0.0036
Glass Style No. Q53-875	60	97.540	0.2550
	80	84.633	1.5163
Glass Style No. Q53-870	60	95.026	0.5083
	80	86.384	1.3127
Style No. Q53-878	60	94.513	0.5530
	80	85.104	1.4682
		Testing with separated coal	
Cotton Style No. 960	60	99.959	0.0043
	80	99.966	0.0034
Dacron® polyester Style No. 862B	60	99.894	0.0110
	80	98.388	0.1646
Style No. C866B	60	99.928	0.0075
	80	99.928	0.0075
Style No. C868B	60	99.921	0.0080
	80	99.936	0.0065
Dacron® polyester Style No. 865B	60	99.949	0.0050
	80	99.867	0.0133
Style No. C890B	60	99.793	0.0210
	80	98.644	0.1367
Style No. C892B	60	99.755	0.0250
	80	99.117	0.0866

(continued)

TABLE 15. (continued)

Type of filtration fabric	q_g area in m^3/m^2 hr)	Efficiency (in percent)	Outlet concentration (in g/m^3)
Nomex® aromatic nylon			
Style No. 852	60	99.906	0.0095
	80	99.906	0.0095
Style No. 853	60	99.946	0.0055
	80	99.960	0.0041
Style No. 190R	60	99.975	0.0025
	80	99.982	0.0019
Nomex® aromatic nylon			
Style No. 850B	60	99.687	0.0318
	80	99.087	0.1829
Nylon polyamide			
Style No. 802B	60	99.954	0.0045
	80	99.984	0.0015
Glass			
Style No. Q53-875	60	98.597	0.1413
	80	82.179	1.7613
Glass			
Style No. Q53-870	60	93.032	0.7088
	80	82.054	1.4801
Style No. Q53-878	60	96.036	0.4041
	80	78.321	2.2051
		Testing with unseparated coal	
Dacron® polyester			
Style No. 862B	60	99.678	0.0323
	80	98.743	0.1273
Style No. C866B	60	99.934	0.0065
	80	99.915	0.0085
Style No. C868B	60	99.945	0.0053
	80	99.921	0.0080

(continued)

TABLE 15. (continued)

Type of filtration fabric	q_g area in m^3/m^2 hr)	Efficiency (in percent)	Outlet concentration (in g/m^3)
Dacron® polyester			
Style No. 865B	60	99.874	0.0123
	80	99.879	0.0119
Style No. C890B	60	99.634	0.0375
	80	98.763	0.1244
Style No. C892B	60	99.690	0.0305
	80	99.189	0.0782
Testing with talc			
Cotton			
Style No. 960	60	99.988	0.0012
	80	99.992	0.0007
Dacron® polyester			
Style No. 862B	60	99.869	0.0133
	80	98.970	0.1060
Style No. C866B	60	99.943	0.0058
	80	99.943	0.0058
Style No. C868B	60	99.956	0.0045
	80	99.968	0.0031
Dacron® polyester			
Style No. 865B	60	99.970	0.0030
	80	99.949	0.0051
Style No. C890B	60	99.766	0.0243
	80	99.376	0.0612
Style No. C892B	60	99.764	0.0245
	80	99.550	0.0448
Nomex® aromatic nylon			
Style No. 852	60	99.957	0.0043
	80	99.944	0.0057

(continued)

TABLE 15. (continued)

Type of filtration fabric	q_g area in m^3/m^2 hr)	Efficiency (in percent)	Outlet concentration (in g/m^3)
Style No. 853	60	99.944	0.0057
	80	99.919	0.0082
Style No. 190R	60	99.965	0.0035
	80	99.973	0.0027
Nomex® aromatic nylon			
Style No. 850B	60	98.996	0.1013
	80	87.416	0.2645
Nylon polyamide			
Style No. 802B	60	99.970	0.0030
	80	99.972	0.0029
Glass			
Style No. Q53-875	60	88.647	1.2048
	80	70.319	2.9567
Glass			
Style No. Q53-870	60	93.647	0.6648
	80	85.974	1.4140
Style No. Q53-878	60	91.743	0.8363
	80	80.808	1.8464
		Testing with fly ash	
Cotton Style No. 960	60	99.980	0.0023
	80	99.989	0.0011
Dacron® polyester			
Style No. 862B	60	99.741	0.0260
	80	99.760	0.0440
Style No. C866B	60	99.845	0.0158
	80	99.795	0.0206
Style No. C868B	60	99.887	0.0114
	80	99.895	0.0107
Dacron® polyester			
Style No. 865B	60	99.895	0.0109
	80	99.781	0.0220

(continued)

TABLE 15. (continued)

Type of filtration fabric	q_g area in m^3/m^2 hr)	Efficiency (in percent)	Outlet concentration (in g/m^3)
Style No. C890B	60	99.905	0.0094
	80	99.589	0.0409
Style NO. C892B	60	99.947	0.0058
	80	99.468	0.0510
Nomex® aromatic nylon Style No. 852	60	99.850	0.0155
	80	99.771	0.0223
Style No. 853	60	99.907	0.0093
	80	99.844	0.0151
Style No. 190R	60	99.869	0.0133
	80	99.954	0.0048
Nomex® aromatic nylon Style No. 850B	60	99.675	0.0328
	80	99.575	0.0416
Nylon polyamide Style No. 802B	60	99.897	0.0105
	80	99.831	0.0172
Glass Style No. Q53-875	60	99.195	0.0081
	80	97.841	0.2132
Glass Style No. Q53-870	60	99.135	0.0877
	80	98.044	0.2007
Style No. Q53-878	60	99.184	0.0838
	80	97.321	0.2710

TABLE 16. FILTRATION RESISTANCES AT LABORATORY TESTING (in mmH$_2$O)

Type of filtration fabrics	q_g (in m^3/m^2 hr)	Kind of dust				
		Separated cement	Separated coal	Unseparated coal	Separated talc	Separated fly ash
Cotton						
Style No. 960	60	31.60	39.97	--	36.28	17.03
	80	48.35	77.58	--	68.41	38.87
Dacron® polyester						
Style No. 862B	60	22.51	28.44	18.87	28.52	12.64
	80	37.45	59.09*	41.00*	38.63	26.07
Style No. C866B	60	22.21	35.63	20.35	22.83	13.37
	80	36.42	67.31	46.05	41.23	26.62
Style No. C868B	60	23.70	31.60	21.27	25.09	12.64
	80	38.24	65.57	48.82	44.16	24.88
Dacron® polyester						
Style No. 865B	60	32.31	40.93	25.15	35.15	20.16
	80	60.99	77.42	65.41	71.73	41.87
Style No. C890B	60	43.06	63.60	42.58	54.11	23.04
	80	66.05	107.76	43.38	95.43	48.90
Style No. C892B	60	58.86	66.99	45.35	60.91	26.70
	80	99.22	126.56	100.01	113.60	65.57
Nomex® aromatic nylon						
Style No. 852	60	20.22	31.44	--	23.46	10.90
	80	38.71	59.72	--	47.80	21.05
Style No. 853	60	18.80	30.89	--	26.23	11.75
	80	38.24	65.65	--	47.87	23.13

(continued)

TABLE 16. (continued)

Type of filtration fabrics	q_g (in m^3/m^2 hr)	Kind of dust				
		Separated cement	Separated coal	Unseparated coal	Separated talc	Separated fly ash
Style No. 190R	60	20.29	29.48	--	27.34	11.44
	80	37.32	66.36	--	50.09	27.77
Nomex® aromatic nylon Style No. 850B	60	44.64	53.56	--	47.40	23.96
	80	73.79	99.86*	--	92.75	48.43
Nylon polyamide Style No. 802B	60	21.68	29.15	--	20.79	13.21
	80	36.18	59.33	--	46.61	25.99
Glass Style No. Q53-875	60	43.45*	54.04	--	34.13	33.49
	80	63.04*	64.46*	--	39.50	60.75
Glass Style No. Q53-870	60	59.09*	58.46*	--	58.70	39.34
	80	88.32*	92.43*	--	79.95	84.37
Glass Style No. Q53-878	60	33.58*	45.51*	--	30.18	28.75
	80	44.71*	49.53*	--	40.61	53.01*

*Observed ducts/canals formation.

TABLE 17. CLASSIFICATION OF FABRICS ACCORDING TO OBTAINED OUTLET CONCENTRATION

Kind of dust	q_g (in m^3/m^2hr)	Outlet concentration in g/m^3							
		Below 0.0025	0.0025-0.0050	0.0050-0.01	0.01-0.05	0.05-0.1	0.1-0.5	0.5-1.0	Above 1.0
Sep. cement	60		960 865B 802B	C866B C868B 853 190R	862B C890B C892B 852	850B	Q53-875	Q53-870 Q53-878	
	80	960	C868B 802B	C866B 865B 190R	862B 852 853	C892B	C890B 850B		Q53-875 Q53-870 Q53-878
Sep. coal	60	190R	960 865B 802B	C866B C868B 852 853	862B C890B C892B 850B		Q53-875 Q53-878	Q53-870	
	80	190R 802B	960 853	C866B C868B 852	865B	C892B	862B C890B 850B		Q53-875 Q53-870 Q53-878
Unsep. coal	60			C866B C868B	862B 865B C890B C892B				
	80			C866B C868B	865B	C892B	862B C890B		
Sep. talc	60	960	C868B 865B 852 190R 802B	C866B 853	862B C890B C892B		850B	Q53-870 Q53-878	Q53-875

(continued)

TABLE 17. (continued)

Kind of dust	q_g (in m^3/m^2hr)	Outlet concentration in g/m^3							
		Below 0.0025	0.0025- 0.0050	0.0050- 0.01	0.01- 0.05	0.05- 0.1	0.1- 0.5	0.5- 1.0	Above 1.0
	80	960	C868B 190R 802B	C866B 865B 852 853	C892B	C890B	862B 850B		Q53-875 Q53-870
Sep. fly ash	60	960		C890B C892B 853	862B C866B C868B 865B 852 190R 850B 802B	Q53-875 Q53-870 Q53-878			
	80	960	190R		862B C866B C868B 865B C890B C892B 852 853 850B 802B		Q53-875 Q53-870 Q53-878		

of the obtained results. It classifies the individual types of fabrics according to calculated final concentrations following specific filtration cycles.

Cotton and Nylon Fabrics

Because cotton and nylon fabrics were represented by only Cotton 960 and Nylon 802B, they will be discussed in one chapter, in spite of the fact that they are two different kinds of fabrics.

These two fabrics appeared to have the highest dust collection efficiency among all fabrics tested. It is very interesting to notice that fabric Nylon 802B, independent of the test dust (except fly ash) and the A/C ratio always showed a dust collection efficiency, E = 99.96 percent. With fly ash, dust collection efficiency decreased considerably to the value E = 99.89 percent at $q_g = 60\ m^3/m^2hr$, and decreased even more to E = 99.83 percent at $q_g = 80\ m^3/m^2hr$.

Both fabrics showed the tendency to increase dust collection efficiency at increasing A/C ratio. This tendency is probably caused by electrostatic effects.

It was found that such high dust collection efficiency results from staple fibers used for fabric production (cotton fiber has definite sizes) and from good filling of spatial and superficial structure by fibers. Staple fibers tend to fill partly free areas in the fabric with "free fibers." The effect of "free fibers" on fabric structure is illustrated in Figure 17.

Filtration resistances measured by static pressure gradient at q_g = constant at the end of the filtration cycle (see Table 16), are different for these fabrics. Fabric Cotton 960 shows higher filtration resistances, which is characteristic for this group of fabrics. Fabric Nylon 802B is characterized by low values of filtration resistances. It was observed that fly ash produces the lowest values of filtration resistances for both fabrics and these values are similar. This is interesting because the degree of pulverization for all the test dusts is the same or similar, so the spatial structure of the dust cake built on the fabrics should be similar, giving comparable hydraulic effects. To explain this phenomenon the following hypothesis was made: the fly ash particles differ from particles of all the other test dusts. This hypothesis was proven by microscopic examination of the dusts.

Photo credit: SEM by K. Skudlanski, Electronic Microscopy Laboratory of Wrocław Polytechnic.

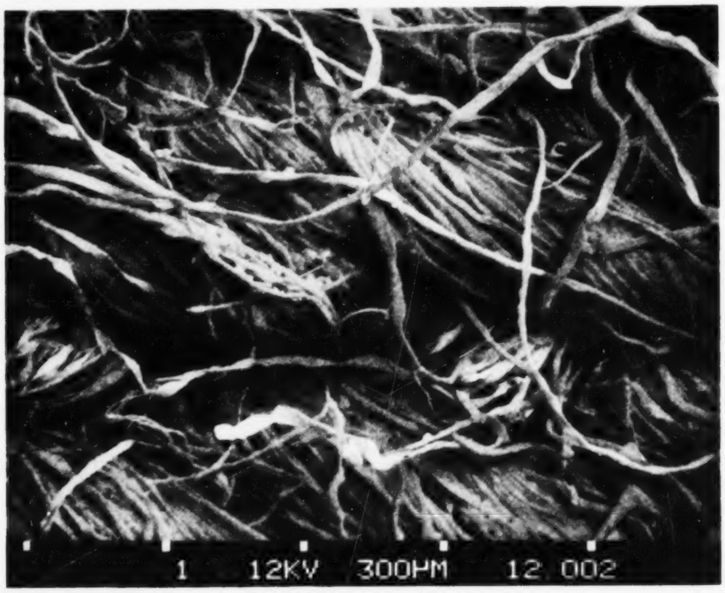
1 12KV 300PM 12 002

a. Cotton style no. 960

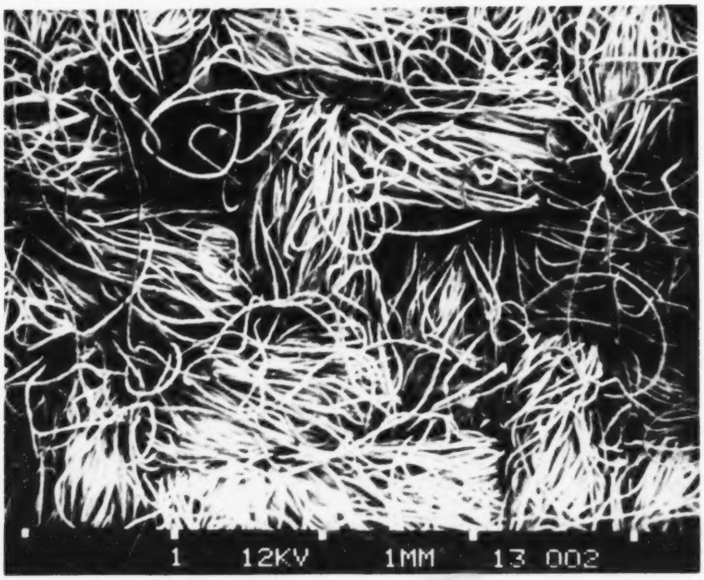
1 12KV 1MM 13 002

b. Nylon polyamide style no. 802B

Figure 17. Superficial structure of fabrics.

Polyester Fabrics

Polyester fabrics make up the largest group of test fabrics but the fibers, as well as technological parameters, that make up this fabric group differ very much. The effect of staple fibers vs continuous filament fibers on filtration efficiency and on hydraulic resistance are very apparent.

The lowest value of efficiency in the group of polyester fabrics was recorded for fabrics C890B and C892B manufactured with polyester continuous filament fiber--values a little lower than those for fabric 862B manufactured with polyester staple fiber. Fabric 862B has a much more porous structure than the other fabrics.

The big decrease of filtration efficiency below 99 percent, when testing with coal and talc dusts, and at an A/C ratio of 80 m^3/m^2hr, was caused by dust cake cracking and the formation of ducts/canals. The distribution of ducts/canals on the dust cake surface is shown on Figure 18. The mechanism of duct/canal formation is caused by dust cake structural defects and is a result of the static pressure gradient. The ducts/canals are observed in the areas of the structure not filled with fibers (areas between threads). The formation of ducts/canals was also observed during the testing of fabric C890B with cement and separated coal dust.

Staple fiber fabrics C866B and C868B have the best filtration properties, taking laboratory filtration efficiency as a criterion. The obtained filtration efficiencies were 99.9+ percent for all types of dusts and two levels of A/C ratio. Slightly poorer properties were shown by continuous filament fabric 865B and staple fiber fabric 862B. Filtration resistances of these three types of polyester continuous filament fabrics are two times higher than those of the polyester staple fiber fabrics.

The additional testings were conducted for polyester fabrics using unseparated coal dust to obtain more results necessary for analysis on a large scale. Large scale tests were conducted only on unseparated coal dust because of the explosive hazard associated with preparing and handling a size-separated coal dust sample.

The difference in the particle size distribution of the separated and unseparated dusts is quite large. Average particle size is:

- Unseparated dust d_{50} = 28 μm (MMD)
- Separated dust d_{50} = 7.5 μm (MMD).

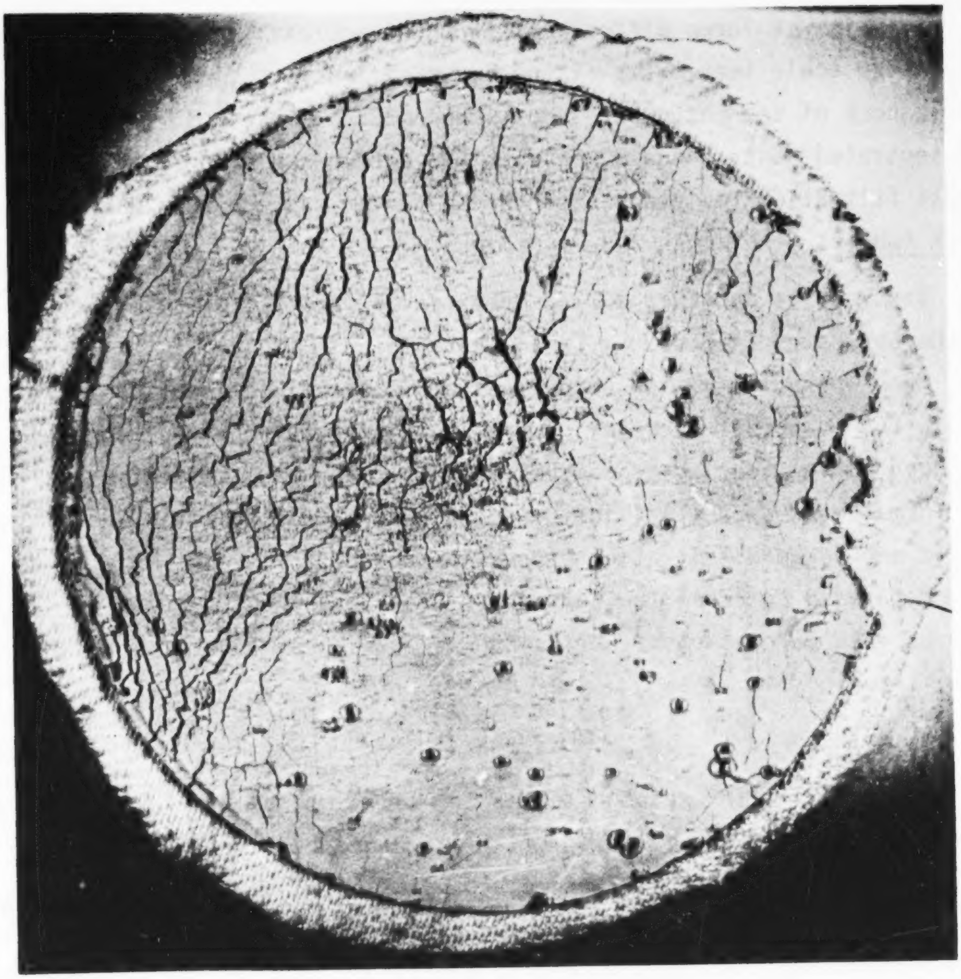

Figure 18. Ducts/canals distribution on polyester fabric covered with talc (style no. 865B).

In spite of large differences in the fractional composition of the laboratory scale test dusts filtration efficiency is similar. Filtration resistances of the unseparated dusts were 30-45 percent lower than those of the separated dusts. Again, as with the cotton and nylon fabrics, the lowest filtration resistances of the polyester fabrics were with fly ash.

Nomex Fabrics

The results obtained during Nomex fabric testing are similar to those of the polyester fabrics.

Much worse filtration properties are observed for continuous filament fabric 850 than for the other fabrics. The formation of ducts/canals was observed during testing of fabric 850 with cement and separated coal dust. The formations had a great influence on the filtration efficiency. The fabric showed good filtration properties only for fly ash.

Figure 19 compares the surface structure of the two types of Nomex fabrics. As before Nomex fabrics showed the lowest filtration resistances when filtering fly ash.

Glass Fabrics

Among the efficiencies obtained for all kinds of fabrics and types of dusts used, the lowest values of filtration efficiency were observed for glass fabrics tested at laboratory scale.

The low values of efficiency are caused by duct/canal formation, which favors the process of dust particle penetration through the fabric/dust structure. Duct/canal formation is characteristic of glass fabrics. Glass fibers have a very small coefficient of friction, which is why threads and fibers displace during the production process, creating "free areas" not filled with fabric material.

These free areas can increase their surface area during air flow and thereby increase their effect on the average dust collection efficiency. Comparing the calculated final concentration determined from experimental data, very apparent effects of structural parameters on filtration properties can be observed. They are included in Table 17. (In this table, the final concentrations were placed in classes that enable the analysis of fabric behavior under the different kinds of dust and A/C ratios. Concerning the glass fabrics, the considerable increase of final concentration with increasing q_g was observed. It is explained by duct/canal formation.)

Photo credit: SEM by K. Skudlanski, Electronic Microscopy Laboratory of Wrocław Polytechnic.

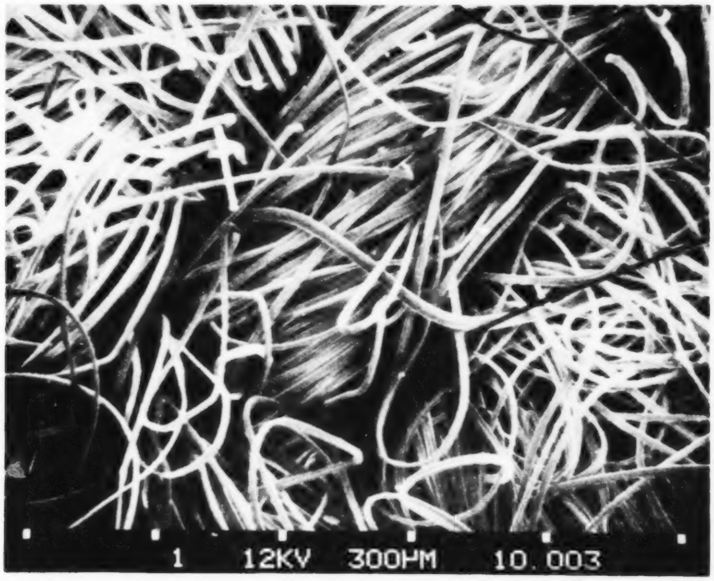
1 12KV 300µM 10.003

a. Staple fibers (style no. 853)

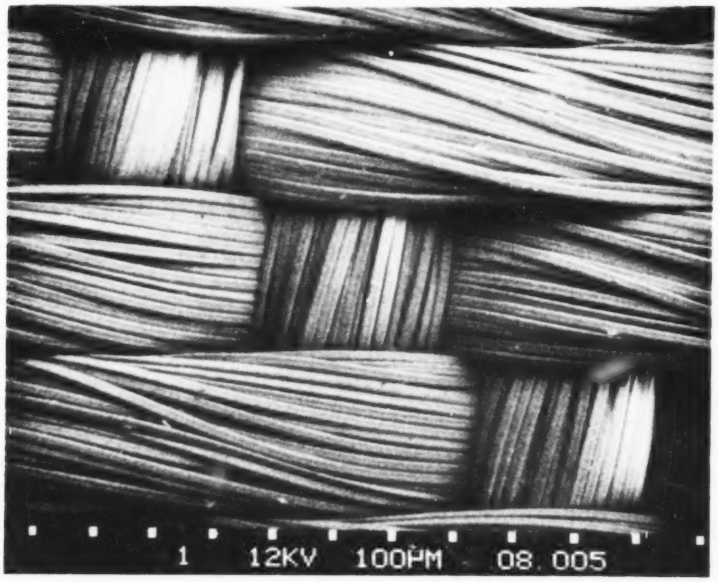
1 12KV 100µM 08.005

b. Continuous filament fibers (style no. 850B)

Figure 19. Comparison of surface structure of staple and continuous filament Nomex fiber fabrics.

TABLE 18. NUMBER OF DUCTS/CANALS OBSERVED IN LABORATORY TESTING
(Testing of glass fabrics with separated coal dust)

Kind of Fabric	A/C(m^3/m^2hr)	Number of ducts/canals
Q53-875	60	--
	80	102
Q53-870	60	16
	80	42
Q53-878	60	7
	80	69

The number of ducts/canals is quite large, as presented in Table 18 which gives the number per 100 cm^2 for separated coal dust (laboratory scale). There is a correlation between the number of formed ducts/canals and the filtration efficiency.

The operating conditions of the laboratory tests are too severe to be practical for field use of the glass fabrics. The formation of canals during the filtration process is an undesirable situation.

By relating duct/canal formation to an upset of force balance in the dust cake structure (and which depends upon the dust properties and the superficial structure of fabric), the hypothesis can be made that there is a certain value of static pressure gradient for each fabric/dust cake system which results in static balance. It is possible to estimate this value experimentally, determining simultaneously the highest permissible A/C. The formation of ducts/canals was confirmed by Holland's examination (ref. 11). The problem of defects formation in dust cake structure should be verified in Dust Filtration Process Type III--conditions characteristic of industrial dust collectors.

Filtration resistances in glass fabrics are higher than those for polyester and Nomex fabrics. The highest values of resistance are reached by glass fabrics made of continuous filament fabric Q53-870. It is interesting that the application of texturized yarn in the fill of fabric Q53-878 did not cause an increase in efficiency, compared to continuous filament fabric Q53-870, but caused only a decrease in filtration resistance. A similar effect of yarn texturization on the filtration properties of glass fabric was observed during the testing of Polish prototype glass fabrics.

Testing of Duct/Canal Formation Mechanism

Taking into consideration the importance of the effect of duct/canal formation on the most representative qualitative parameter of filtration--dust collection efficiency--additional testing and structural examination were conducted to learn more about the mechanism of duct/canal formation.

Tests--

Tests were carried out on a laboratory stand according to the method prescribed in a previous report. Glass fabric Q53-878 and separated cement dust were used for the testing.

Two series of test were made over an A/C range of 50 - 200 m^3/m^2hr. The first series, the results of which are presented in Table 19, was to determine the dependence of canal number density upon A/C. The second

TABLE 19. NUMBER OF DUCTS/CANALS OBSERVED DURING TESTING OF FABRIC STYLE Q53-878 - SERIES 1 (TEMPERATURE: 20-22° C, RH = 61-64%, B = 740 mmHg)

Gas loading of filtration area (A/C) m^3/m^2hr	Final pressure drop mmH_2O	Dust loading of filtration area g/m^2hr	Dust covering of filtration area g/m^2	Number of ducts/canals
50	29.62	465.5	195.5	--
60	33.97	698.4	230.5	1
80	51.35	870.4	217.6	21
100	61.62	1,075.0	215.0	96
120	72.68	1,093.2	185.8	140
150	79.00	1,296.0	168.5	200
200	96.38	1,804.0	180.4	260

series was conducted twice (experiments 1 and 2) and was to determine the size as well the number of canals as a function of A/C ratio. The results are shown in Table 20 and Table B-3. The main reason for the testing was to obtain the dusty fabric samples for the counting and measurement of the canals; a similar dust cover was used in both the first and the second series.

The dependence of the number of canals upon A/C ratio and final pressure drop is presented in Figure 20. The correlation can be seen, but because of the small number of measurements, this correlation cannot be expressed analytically.

TABLE 20. NUMBER OF DUCTS/CANALS OBSERVED DURING TESTING OF FABRIC STYLE Q53-878 - SERIES 2 (TEMPERATURE: 20-22° C, RH = 61-64%, B = 740 mmHg)

Gas loading of filtration area (A/C) m^3/m^2hr	Final pressure drop mmH_2O	Dust loading of filtration area g/m^2hr	Dust covering of filtration area g/m^2	Number of ducts/ canals
50	17.40	500	85	--
60	26.81	600	102	3 2
80	63.20	800	200	39 43
100	79.00	1,000	200	66 48
120	88.48	1,200	216	90 100
150	106.70	1,500	195	180 160
200	158.00	2,000	400	210

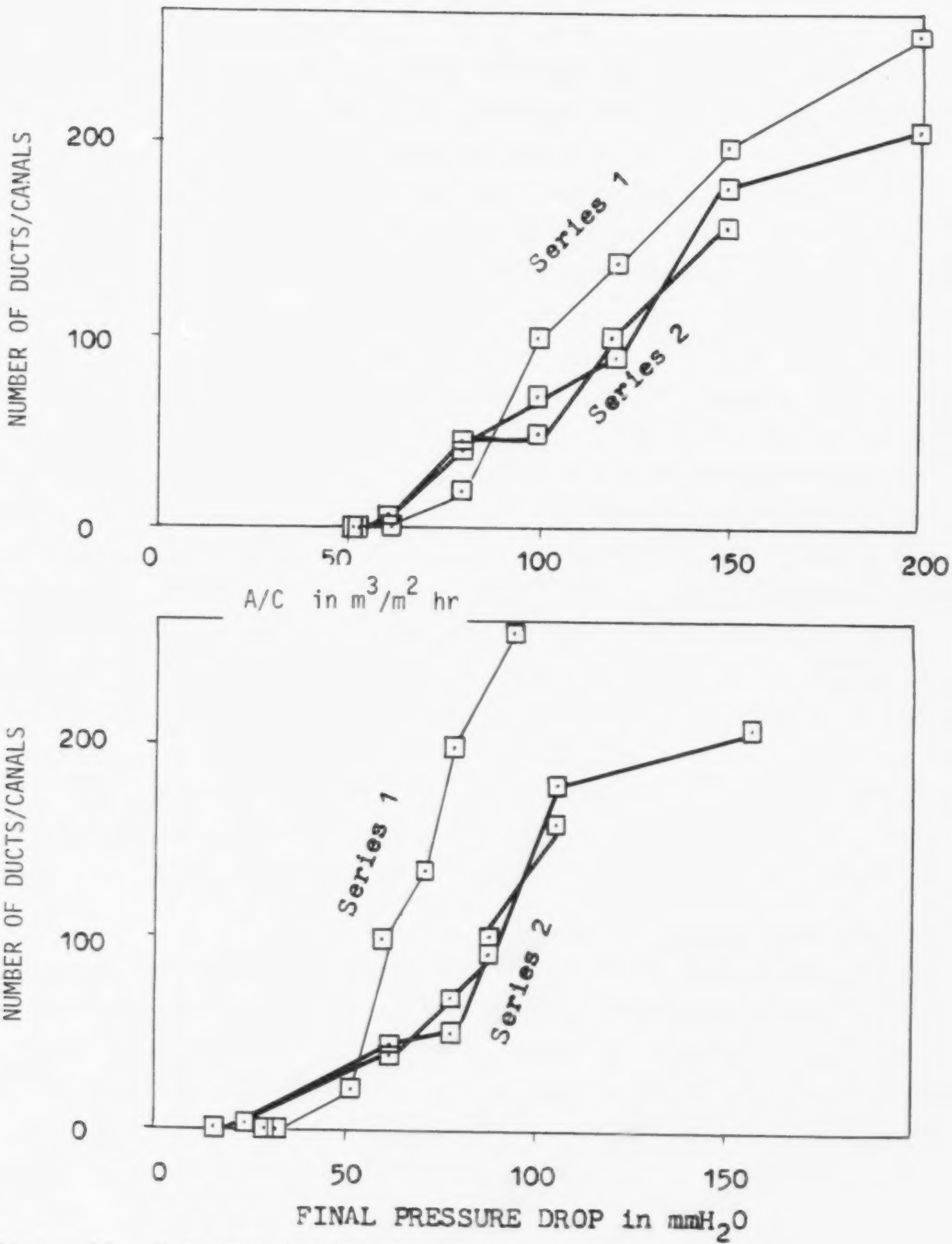

Figure 20. Relationship between number of ducts/canals and: 1) A/C, and 2) final pressure drop.

Based on the data from Table B-3 (the results of measurements of the geometrical size of the ducts/canals), verification of canals of equivalent diameter size distribution was done by applying the Kolmogorov λ criterion.

The equivalent diameter was considered a characteristic value because of the kind of hydraulic phenomena occurring during duct/canal formation. Figures 21 and 22 show the equivalent diameter distribution for experiments 1 and 2, the second series of testing. The hypothesis of a normal distribution was confirmed in 50 percent of the cases at a significance level of α = 0.05. It is presumed that by increasing the number of experiments, there would be no basis for rejecting the hypothesis of a normal distribution.

The confirmation of the normal distribution hypothesis was very important because during the development of the probabilistic model of the dust filtration process (Project 5-533-3) it was ascertained that the structural properties of fabrics have a normal distribution.

Table 21 includes the sizes and standard deviations of the mean equivalent diameter. From these values the average equivalent diameter, independent of A/C ratio, is in the range of 80-85 μm. Despite the large standard deviation, the data lead to the conclusion that the woven structure has a large surface area, a characteristic that influences dust cake defects. As a result of this conclusion, additional microscopic examinations of the clean fabric structure and of the dust cake surface were made.

Structural examination of fabrics - "basket effect"--

Microscopic examination of the model fabric (hemp cord of weave 3/1) was made in order to obtain information about free area formation between the fill and warp yarns. It appeared (Figure 23) that the model fabric, which did not show the free areas in a vertical (normal) direction to the surface, has characteristic right triangles of not-filled areas between the fill and warp yarns, oriented, askew to fabric surface, but normally (vertically) to fill years (Figure 23b).

The decision was made to carry out structural microscopic examination of all test fabrics. The examinations were done by the Electronic Microscopy Laboratory of Wrocław Polytechnic, directed by Dr. Krzysztof Skudlarski. A scanning microscope Stereoscan 180, manufactured by Cambridge Instruments in England, was used for the examinations.

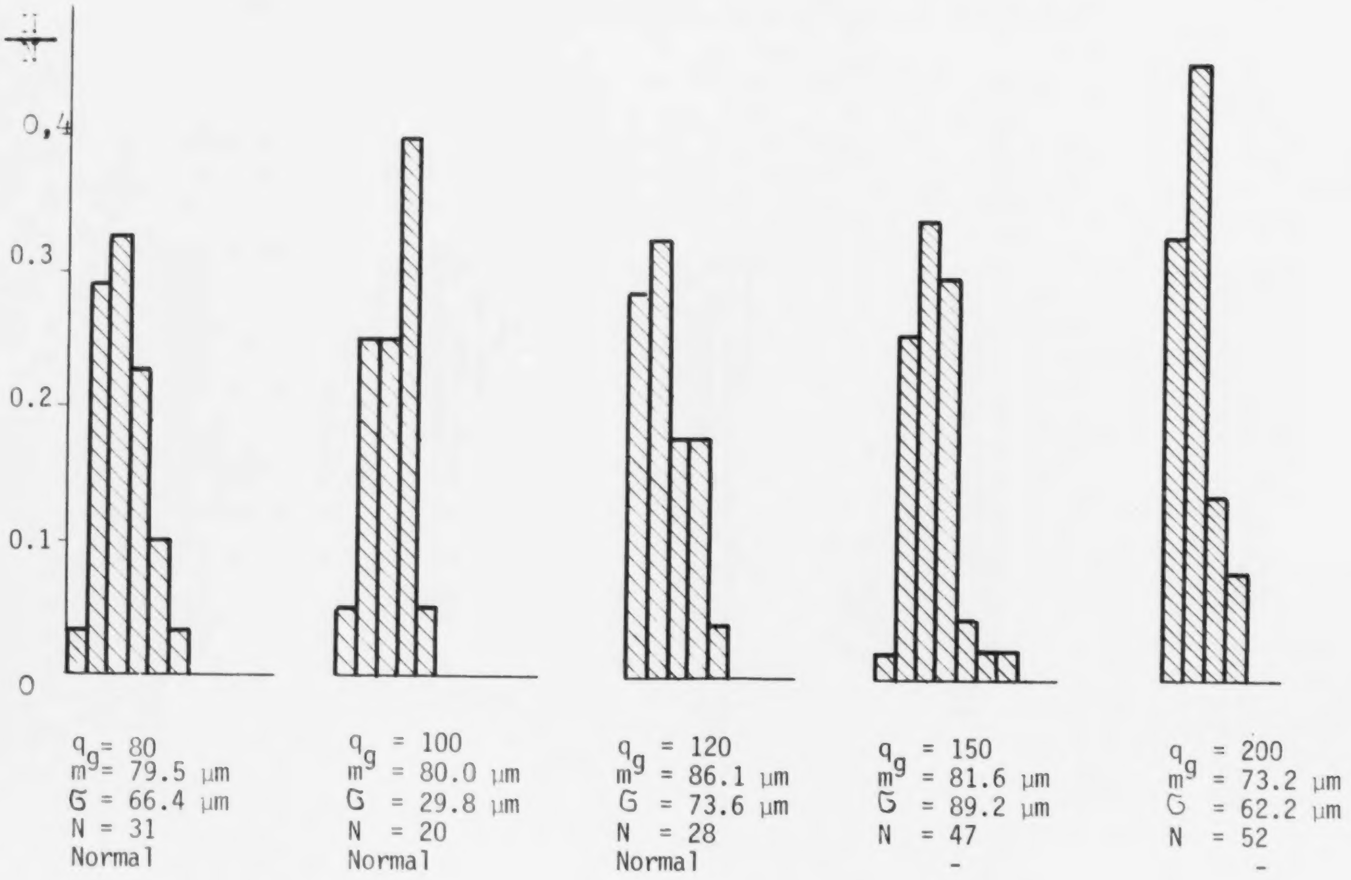

Figure 21. Histogram showing the size distribution of duct/canal equivalent diameter (exp. 1, series 2).

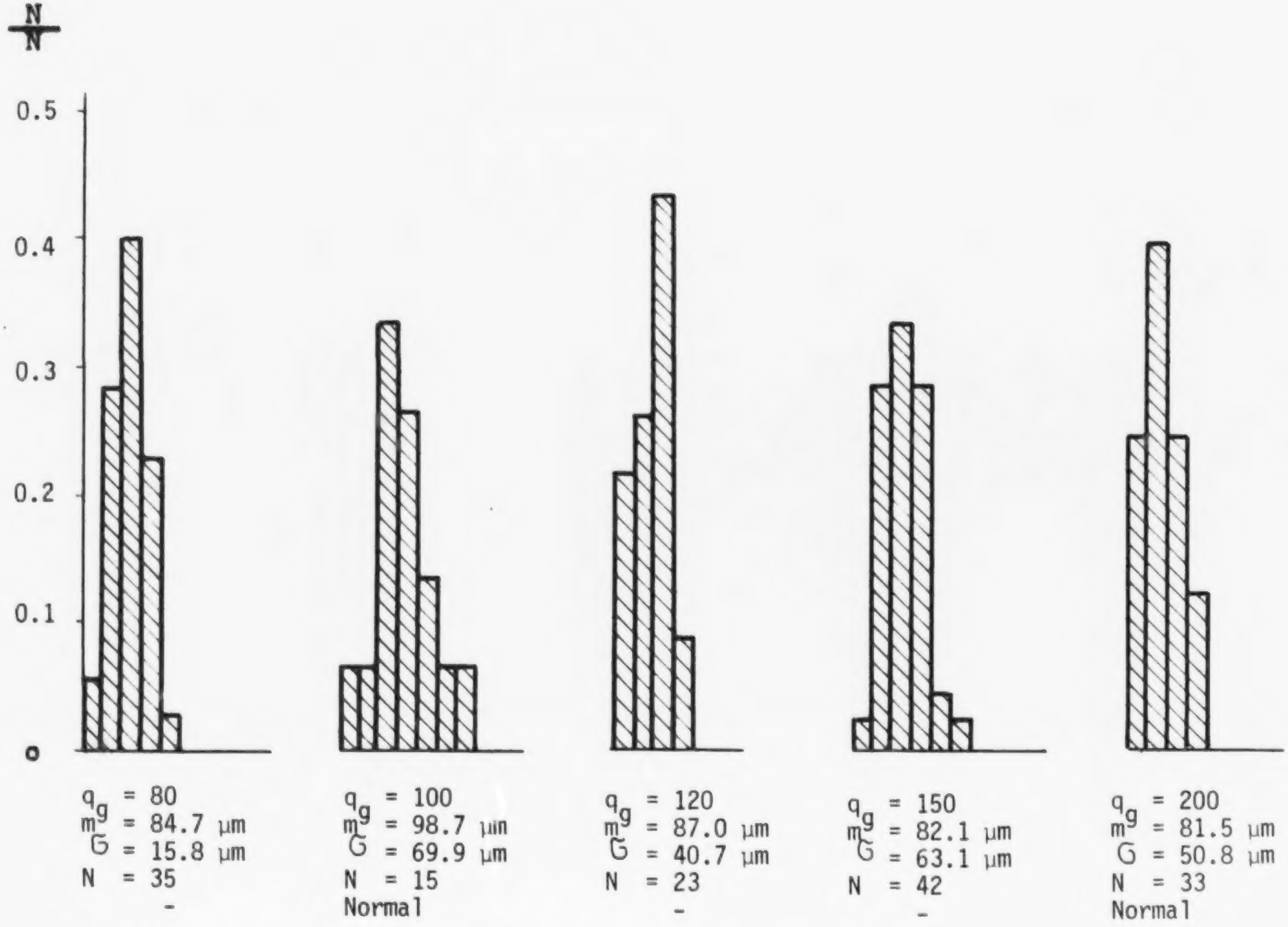

Figure 22. Histogram showing size distribution of duct/canal equivalent diameter (exp. 2, series 2).

TABLE 21. AVERAGE EQUIVALENT DIAMETER FOR EXPERIMENTS OF SERIES 2

Gas loading of filtration area (A/C) m^3/m^2hr	Mean equivalent diameter μm	Standard deviation μm
1	2	3
80	79.59	66.4
	84.70	15.8
100	80.80	29.8
	98.70	69.9
120	86.10	73.6
	87.00	40.7
150	81.60	89.2
	82.15	63.1
200	73.20	62.2
	81.50	50.8

Figure 24 shows two characteristic types of free area appearing in the fabric structure. The first type, already taken into consideration and characterized by FA, is in the fabric plane. The second type, related to the canal formation phenomenon and not included in the FA value, occurs in a plane askew to the fabric surface. The average size of the equivalent diameter (based on photographs) for the free areas viewed in an askew plane is 100 - 150 μm. Considering the very poor and not representative photographical material, it can be said preliminarily, that structural examination confirms the experiments in which the statistical equivalent diameter of the canals was calculated to be 80-85 μm. More careful photographic examination of canal shapes and their spatial composition confirms their askew direction to the fabric plane (Figure 25) and is consistent with askew placement of free areas in the fabric.

Because of their characteristic shape and similarity to the spatial structure of wicker products, the newly recognized existence of askew free areas and their relationship to dust cake defects was called the "basket

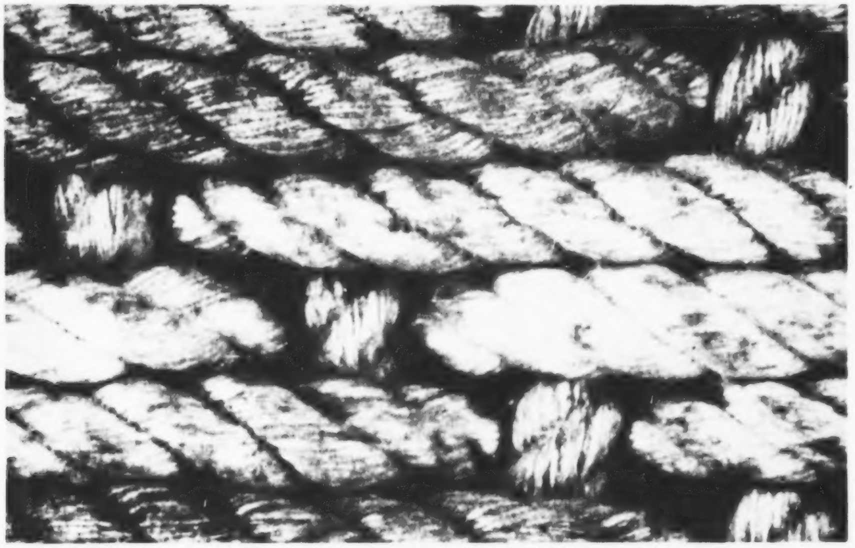

a. Vertical view

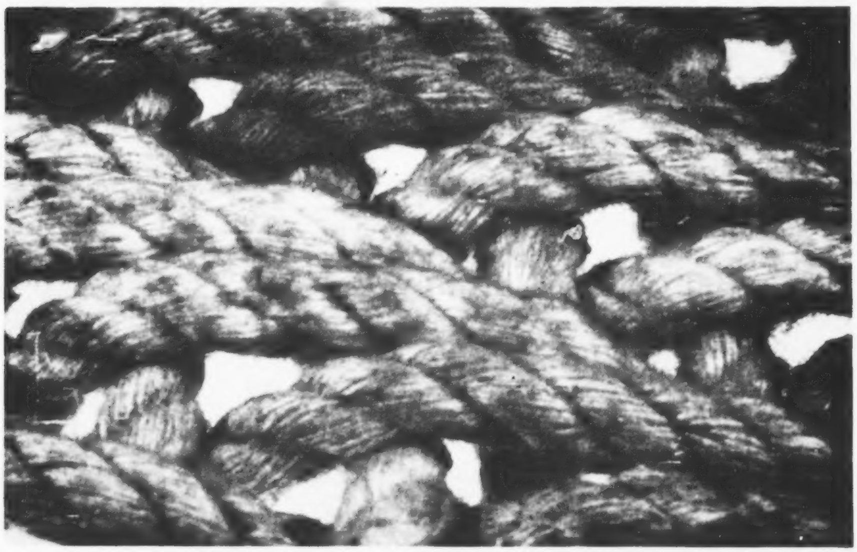

b. Askew view

Figure 23. Superficial structure of model fabric.

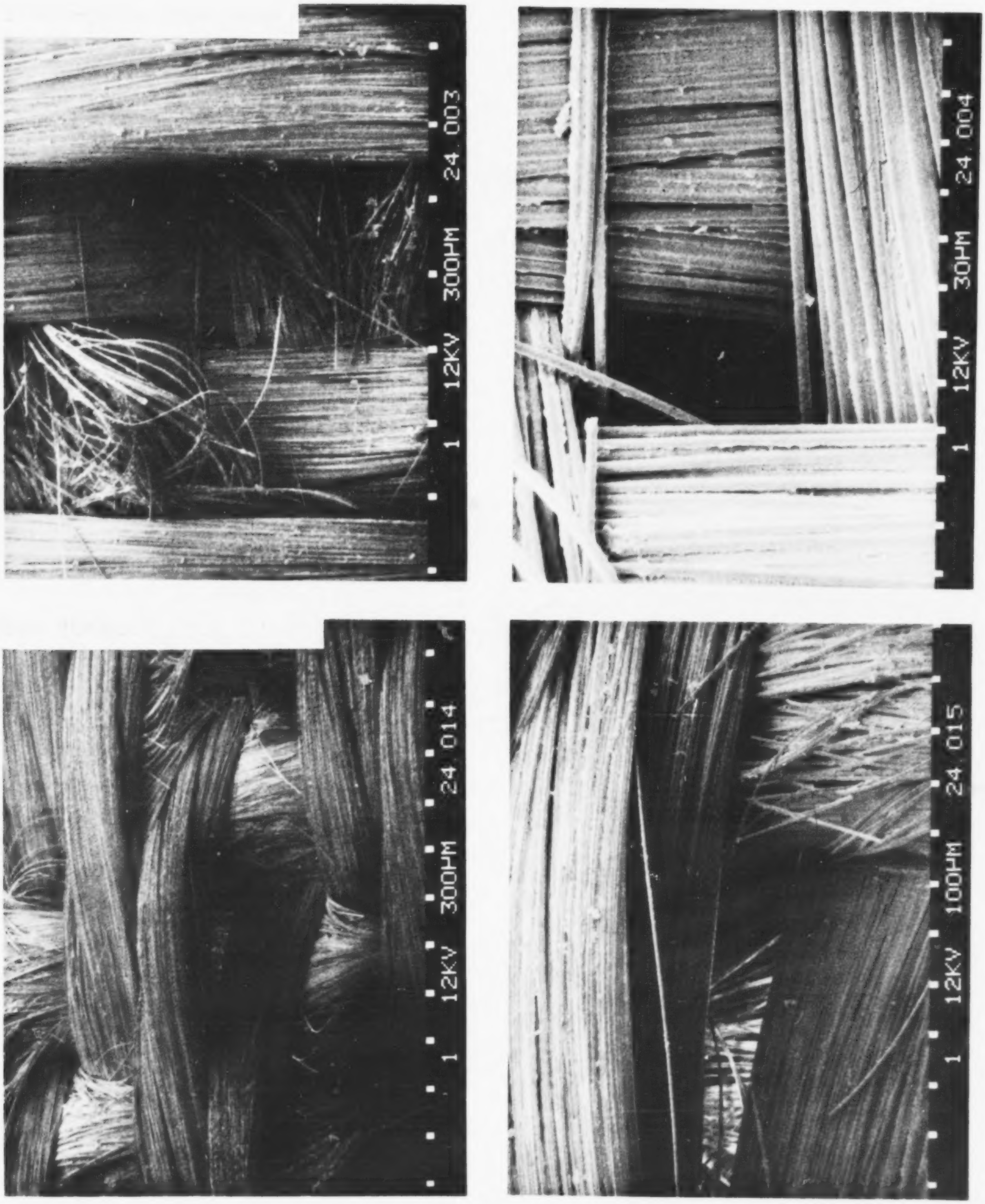
1 12KV 300HM 24 003
1 12KV 30HM 24 004
1 12KV 300HM 24 014
1 12KV 100HM 24 015

Figure 24. Kinds of free areas in woven structure (Q53-878).

Photo credit: SEM by K. Skudlanski, Electronic Microscopy Laboratory of Wrocław Polytechnic.

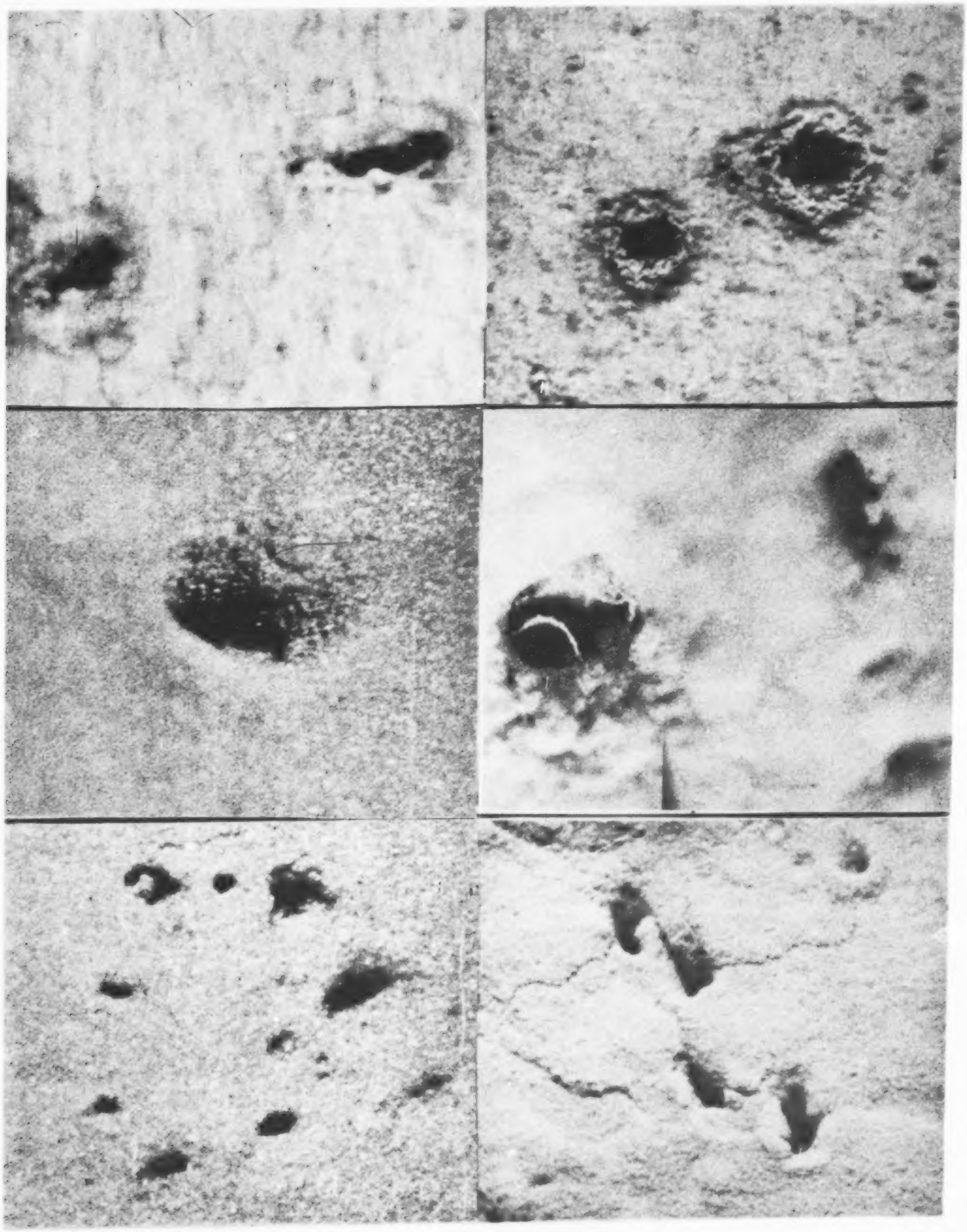

Figure 25. Duct/canal shape.

effect." It can be preliminarily said that the basket effect depends mainly on the kind of weave, the kind of fiber and its raw material, and also on yarn diameter and take-up degree of warp and fill. Continuous filament yarns of high elasticity favor large free area formation, so the basket effect is very apparent on such fibers (glass fabric). Staple fiber yarns of lower elasticity show smaller basket effects. More detailed discussion of this problem will be included in the final report of Project 5-533-3.

Filtration Resistance Variation in Laboratory Testing

The linear regression method was used for calculating laboratory and large scale filtration resistances. The data were obtained from measurement reports that are enclosed in this report or are in the archives of IPWMB. Equations approximating the time increase of filtration resistance by straight lines were obtained. The effective drag and the fabric-dust resistivity were calculated from these equations with the help of dependencies (4) and (5). The results are compiled in Table 22.

Table 22 is also auxiliary material for the discussion of increase of filtration resistance in time, discussed in the next section of this document.

CONCLUSIONS

- Under test conditions, i.e., at a specific A/C ratio and its dust cover and for the separated dusts of cement, coal, talc, and fly ash, the following fabrics can be regarded as satisfactory from a qualitative point of view:
    - cotton fabrics: style 960;
    - polyamide fabrics: style 802B
    - polyester fabrics: styles 865B, 862B, C866B, and C868B;
    - Nomex fabrics: styles 190R, 852, and 853;
    - glass fabrics: style Q53-875.
- Polyester and Nomex fabrics made with continuous filament and polyamid fabric 802B achieve good filtration properties at lower A/C, $q_g = 60\ m^3/m^2hr$.
- Test conditions were too rigid for the glass fabrics because of their structural and mechanical parameters; the consequent formation of dust cake defects in the form of ducts/canals considerably decreased their filtration efficiency.

TABLE 22. EFFECTIVE DRAG S_E [in (mmH_2O/m/hr)] AND SPECIFIC RESISTANCE COEFFICIENT K_2[in (mmH_2O/m/hr)/(g/m^2)] IN LABORATORY TESTS

Type of fabric	q_g in m^3/m^2hr	Effective drag S_E					Specific resistance coefficient K_2				
		Sep. cement	Sep. coal	Unsep. coal	Sep. talc	Sep. fly ash	Sep. cement	Sep. coal	Unsep. coal	Sep. talc	Sep. fly ash
Cotton 960	60	4.6	1.5	--	0.7	5.1	0.07	0.09	--	0.09	0.03
	80	6.3	1.3	--	0.3	6.6	0.07	0.14	--	0.12	0.05
Dacron® 862B	60	0.5	-4.4	-0.9	-3.2	1.1	0.05	0.08	0.05	0.08	0.03
	80	0.7	-5.7	-3.3	-2.0	0.8	0.07	0.12	0.08	0.07	0.04
C866B	60	-0.9	-3.4	-0.3	-2.7	0.9	0.06	0.10	0.05	0.06	0.03
	80	1.8	-4.7	-2.5	-0.3	1.1	0.06	0.13	0.09	0.06	0.04
C868B	60	1.5	-2.4	-1.1	10.2	1.5	0.05	0.08	0.05	0.02	0.03
	80	2.1	0.7	-2.8	-1.9	2.1	0.06	0.12	0.09	0.08	0.05
Dacron® 865B	60	5.4	1.4	2.0	0.4	6.1	0.07	0.10	0.06	0.09	0.04
	80	13.9	0.4	4.2	3.3	10.1	0.08	0.13	0.11	0.12	0.05
C890B	60	17.5	14.8	11.2	11.5	11.9	0.06	0.12	0.08	0.10	0.03
	80	21.8	17.3	19.1	15.1	18.9	0.07	0.15	0.12	0.13	0.04
C892B	60	25.2	22.1	17.2	18.8	17.7	0.08	0.11	0.07	0.10	0.02
	80	40.0	31.9	31.9	28.7	32.1	0.08	0.16	0.10	0.13	0.04

(continued)

TABLE 22. (continued)

Type of fabric	q_g in m^3/m^2hr	Effective drag S_E					Specific resistance coefficient K_2				
		Sep. cement	Sep. coal	Unsep. coal	Sep. talc	Sep. fly ash	Sep. cement	Sep. coal	Unsep. coal	Sep. talc	Sep. fly ash
Nomex®											
852	60	-0.3	-4.0	--	-2.0	1.4	0.05	0.08	--	0.06	0.02
	80	2.5	-7.2	--	-3.8	0.6	0.06	0.12	--	0.09	0.03
853	60	0.7	2.5	--	-1.8	0.3	0.04	0.08	--	0.07	0.03
	80	15.4	-3.6	--	-4.3	0.7	0.07	0.13	--	0.09	0.04
190R	60	-2.2	-3.3	--	-2.2	0.4	0.05	0.08	--	0.07	0.03
	80	-3.7	-6.8	--	-3.1	-0.6	0.07	0.13	--	0.10	0.05
Nomex®											
850	60	20.6	12.7	--	13.7	12.6	0.06	0.10	--	0.08	0.03
	80	20.2	18.6	--	11.5	17.0	0.08	0.14	--	0.14	0.05
Nylon											
802B	60	-0.3	-0.9	--	-0.9	1.2	0.05	0.08	--	0.05	0.03
	80	-0.2	-1.4	--	-2.4	0.7	0.12	0.11	--	0.09	0.04
Glass											
Q53-875	60	6.7	12.3	--	6.7	11.6	0.07	0.10	--	0.07	0.05
	80	18.1	15.6	--	4.3	20.9	0.07	0.08	--	0.06	0.06
Glass											
Q53-870	60	25.0	21.0	--	18.1	22.5	0.08	0.09	--	0.10	0.04
	80	28.1	24.7	--	20.8	34.4	0.08	0.11	--	0.10	0.07
Q53-878	60	8.3	7.7	--	7.1	11.3	0.06	0.09	--	0.06	0.04
	80	4.8	12.1	--	-0.6	17.0	0.08	0.06	--	0.09	0.06

- Observed and documented large ranges of final concentrations (varying with the fabric type and depending upon the type of dust and the A/C) are characteristic of Dust Filtration Process Type I--when the structure has not yet reached the state-of-balance.
- Duct/canal formation during dust filtration through woven filtration materials was explained.
- The effect of fabric structure on dust cake defects via the basket effect was ascertained. Basket effect is connected with the presence of not-filled-by-yarn areas askew to the fabric surface. The degree of the effect depends upon the technological parameters of the materials.

SECTION V

LARGE SCALE TESTING OF FILTRATION

INTRODUCTION

Large scale testing is a main phase of the qualitative testing of the filtration materials. The dust collection efficiency and the filtration resistance as a function of A/C are estimated.

Because the filtration process in large scale (Dust Filtration Type III) is equivalent to the processes taking place in an industrial fabric dust collector, the experience obtained during large scale experimentation can be applied directly to engineering research and practice.

The basic objective of the large scale experiments is the determination of all relevant dependencies among the process parameters after the filtration test material has reached a state-of-balance under a specific set of test conditions. The state-of-balance is characterized by a constant gradient of static pressure after regeneration (ΔP_{NK}) and, corresponding to it, a constant amount of dust (L_{NK}) remaining in the spatial structure of the filtration material.

Because large scale testing is very labor-consuming, the basic test experiments, determining the total efficiency and filtration resistance, usually include measurements of fractional efficiency regeneration susceptibility, etc. so that test results are enriched.

As with the laboratory scale tests, the absence of a theoretical base for the process favors a comparative analysis of test results. For constant fabric test conditions, the quality of the filtration fabrics is very often estimated from the outlet dust concentrations.

According to Stephan, Walsh, and Herrick, filtration resistance depends on the filtration material and dust and can be easily analyzed and compared after the determination of the empirical effective drag and permeability of a dust-fabric system. However, this interpretation is not entirely accurate since unequal dust cake often exists on different filtration material surfaces, both before and after regeneration. The calcuated factors, based on mean measurement values, reveal specific fabric properties that depend on the type of dust and the filtration parameters.

The determination of the true value of the dust cover on the filter is an important element of large scale testing. Usually with test stands the dust is introduced to the hopper and then to the filtration bag. The mechanical efficiency of the hopper depends on the kind of dust and its pulverization, and also on the gas velocity. So, basing the examination only on the measurement of dust fed to the test stand, we obtain an effective drag and permeability of the dust-fabric system, but they cannot be compared to other tests.

The big disadvantage of large scale testing is that there is no chance to observe the surface of the filtration test material after contact with the dust. Defects in dust cake structure and also the appearance of other effects, e.g., basket effect, can be deduced only from the obtained measurement values.

EQUIPMENT AND PROCEDURES

Large scale testing of EPA-selected filtration fabrics was conducted on an apparatus specially designed by IPWMB (single compartment baghouse). The apparatus is illustrated in Figure 26 and includes a filter chamber, collection hopper, dust feeder, fans, pipelines and valves, and a control and measurement system.

The filter chamber, of cylindrical form, (diameter 700 mm and length 3,520 mm) is composed of four separate sections tightly connected together. This type of construction permits the filter bags to be of various lengths. The last section of the filter chamber is the head, on which an arbitrary mechanical regeneration system can be installed. The filter chamber is thermally insulated. There is a collection hopper in the lower part of the filter chamber. The filter bag, 710 to 3,250 mm in length and 200 mm in diameter, is installed off center from the filter chamber axis because of the presence of an isotopic probe used for the measurement of dust cake thickness deposited on the filter bag. The total filtration area is 2.01 m^2

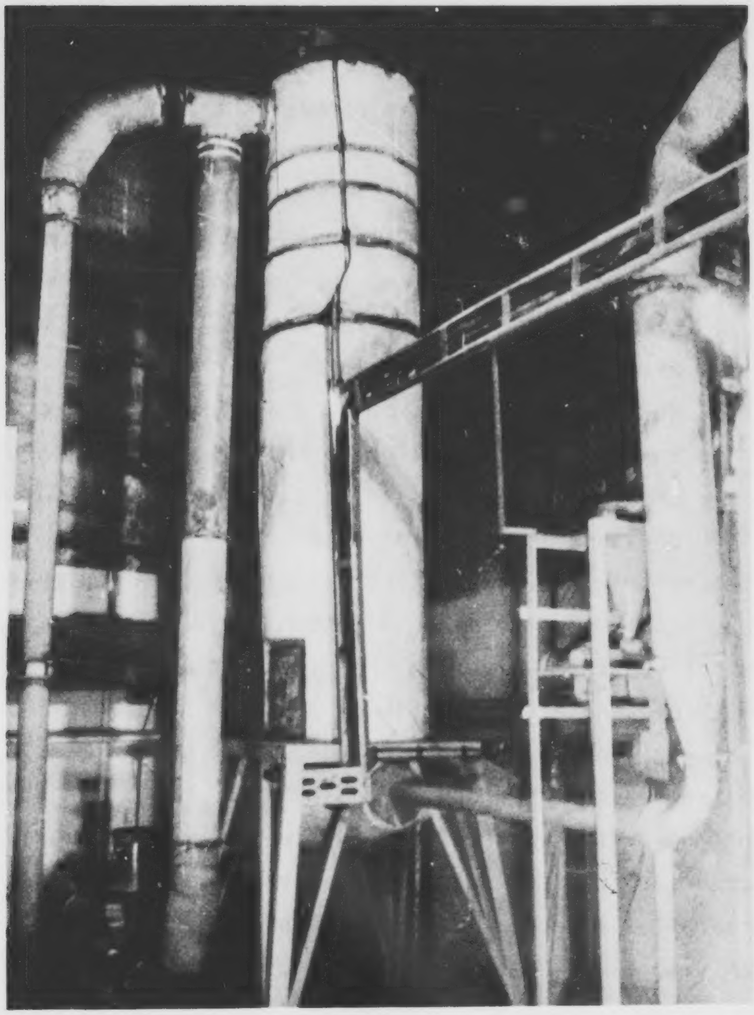

Figure 26. Illustration of large-scale stand.

and the net area, 1.884 m^2. A diagram of the single compartment baghouse with a control and measurement system is shown in Figure 27. The test dust is fed into circulation by a screw dust feeder with a capacity of 0.5 to 15 kg/hr ± 10 percent. A variable gear regulates the capacity of the screw dust feeder.

The single compartment baghouse is equipped with two fans:

1. Main fan - type MWW 14, used for keeping negative pressure in all test apparatus and for producing gas flow throughout the filter chamber. Main fan capacity is 1,200 m^3/hr and total pressure is 600 mm of water.
2. Reverse air fan - type WP 20/1, used for reverse air flow (in the opposite direction to the gas flow during the filtration process). Reverse fan capacity is 1,200 m^3/hr and total pressure is 300 mm of water.

Both the reverse and circulating gas systems are equipped with electric heaters, type NP-27, so as to maintain dry filtration conditions in the filter chamber. Control valves on the pipelines allow control of the A/C at the desired values and assure continuous load on the fans. Actuations of particular systems and instruments of the single compartment baghouse are remotely controlled from the control desk in the operational room.

The control system works either in a manual mode or an automatic mode according to one of the following three variants of filter bag regeneration: 1) reverse air flow regeneration, 2) mechanical regeneration, or 3) mechanical regeneration with simultaneous reverse air flow. It is equipped with several sensors and control-measurement devices for recording the following parameters:

- Humidity of gas,
- Temperature of gas,
- Rate of flow,
- Static pressure,
- Dust concentration before and after filter chamber,
- Time of particular filtration cycles, and
- Temperature and humidity of air in the laboratory.

General experimental conditions are:

- Maximum length of filter bag: 3,500 mm,

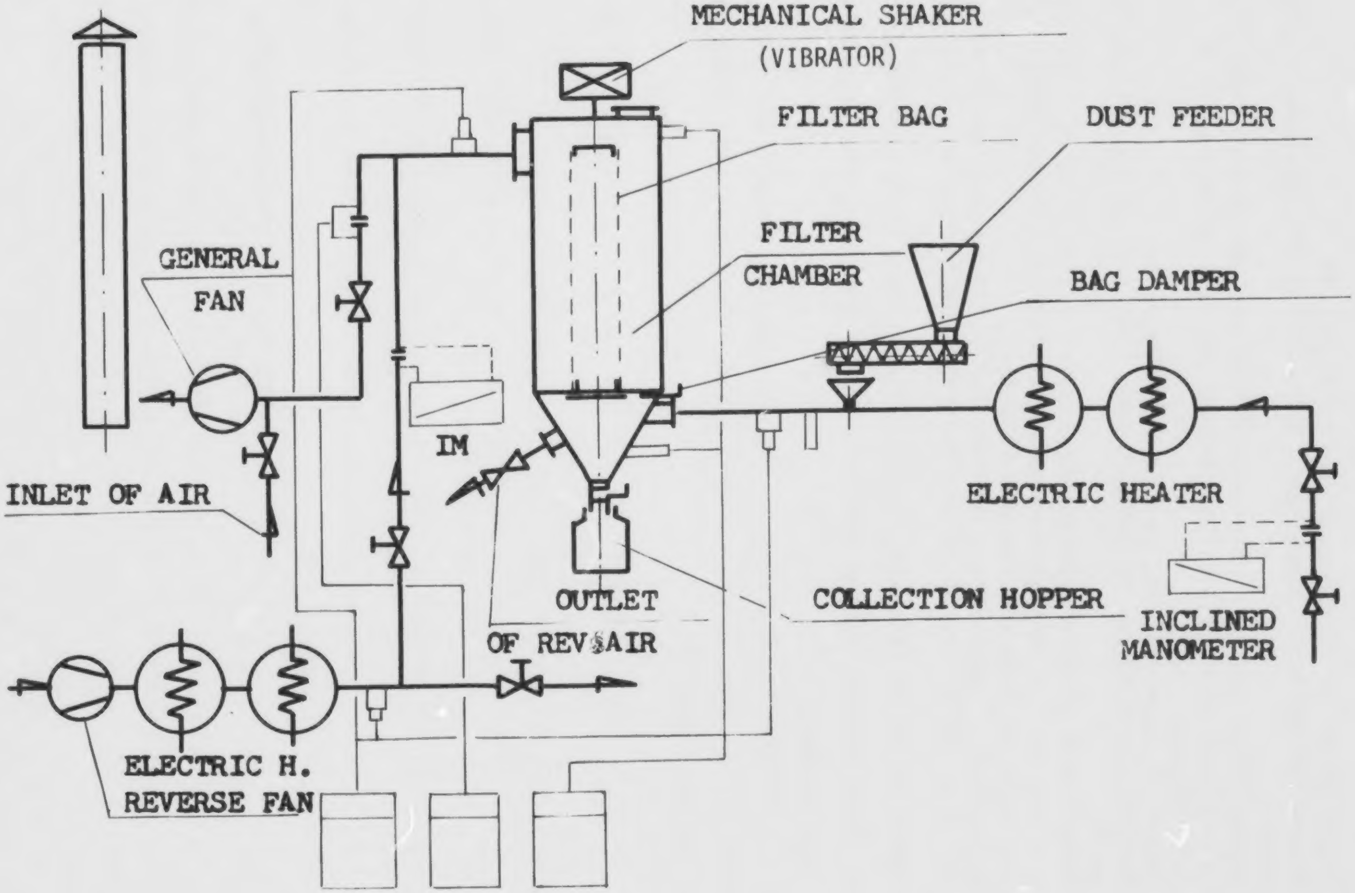
MECHANICAL SHAKER
(VIBRATOR)
FILTER BAG
DUST FEEDER
FILTER
CHAMBER
BAG DAMPER
GENERAL
FAN
INLET OF AIR
IM
ELECTRIC HEATER
OUTLET
OF REV AIR
COLLECTION HOPPER
INCLINED
MANOMETER
ELECTRIC H.
REVERSE FAN

Figure 27. Diagram of the large-scale test stand.

- Construction of filter bag: as in Figure 28,
- Dispersion medium: atmospheric air without any adjustable parameters,
- Regeneration system: reverse air flow and mechanical vibration but without reverse air flow during the last cycle before a measurement,
- Manner of regeneration: as shown in Figure 29,
- Reverse air loading: 20 percent more than A/C during filtration cycle,
- Measurement of dust concentration after filter chamber: by aspiration method (in some measurements particle size distribution was done with an Andersen cascade impactor),
- Conduction of experiments on bags fully filled with dust: by multiple repetition of filtration-regeneration cycles.

A detailed description of the preparatory and auxiliary work performed during large scale fabric testing was included in the periodical report of phase I of this project.

The dust collection efficiency of the one-bag compartment was determined by weighing the dust in the cleaned gases. The total efficiency was calculated from the relation:

$$E_{T1} = \frac{G_c - G_o}{G_c} \times 100 = \left[1 - \frac{c_o}{c_i}\right] \times 100 \qquad (11)$$

where: E_{T1} = total efficiency, in percent,

G_c = total weight of the dust introduced to the hopper of the test chamber, in grams,

G_o = weight of dust in the cleaned gases (measurement of dust emission), in grams,

c_i = initial dust concentration fed to the compartment, in g/m^3, and

c_o = outlet dust concentration from the compartment, in g/m^3.

In addition to the total efficiency of the one-bag compartment, the hopper efficiency and bag efficiency were calculated by the dust balance method (weighing method). In this method the total efficiency was calculated from the relation:

$$E_{T2} = \frac{G_H + G_B + G_R + G_N}{G_c} \times 100 \qquad (12)$$

where: E_{T2} = total efficiency, in percent,

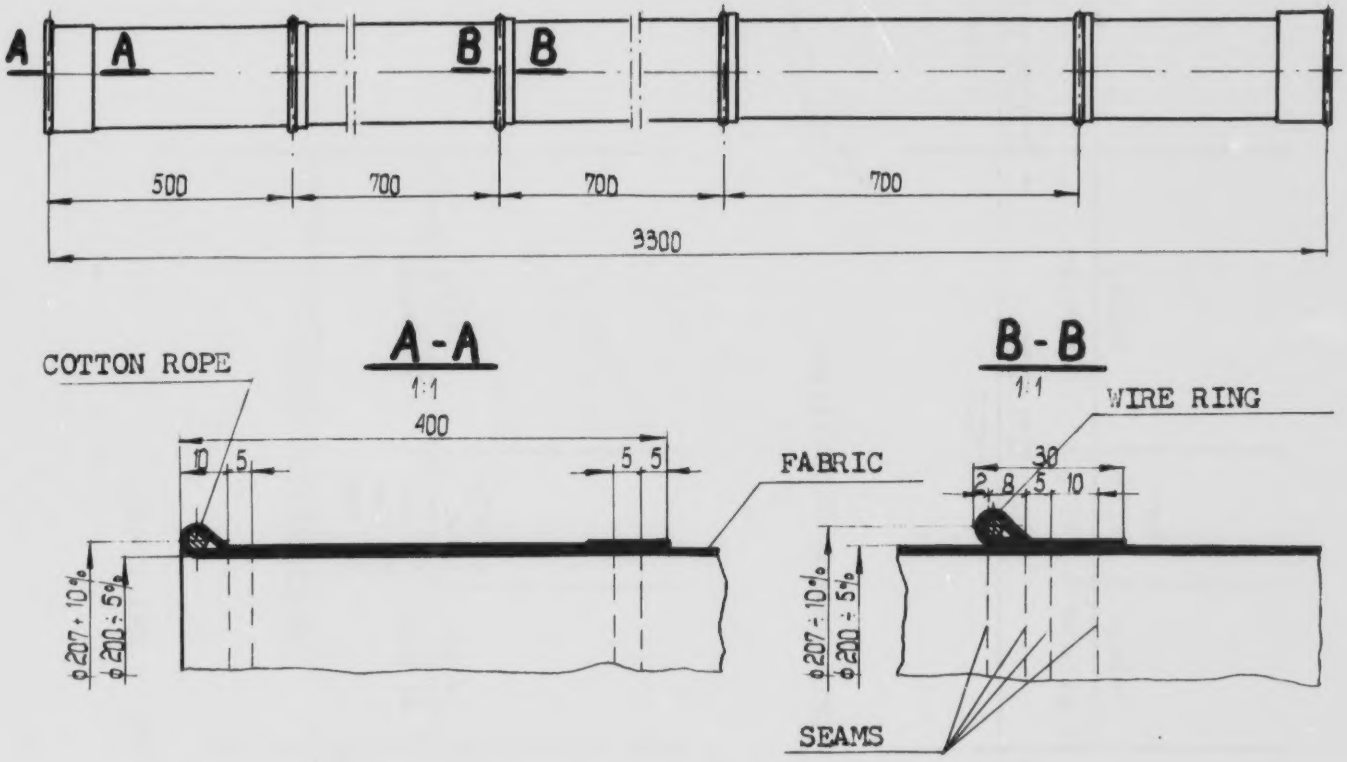
A
A
B
B
500
700
700
700
3300
A-A
1:1
COTTON ROPE
400
10
5
5
5
FABRIC
ϕ207 ÷ 10%
ϕ200 ÷ 5%
B-B
1:1
WIRE RING
30
2
8
5
10
ϕ207 ÷ 10%
ϕ200 ÷ 5%
SEAMS

Figure 28. Construction of bags.

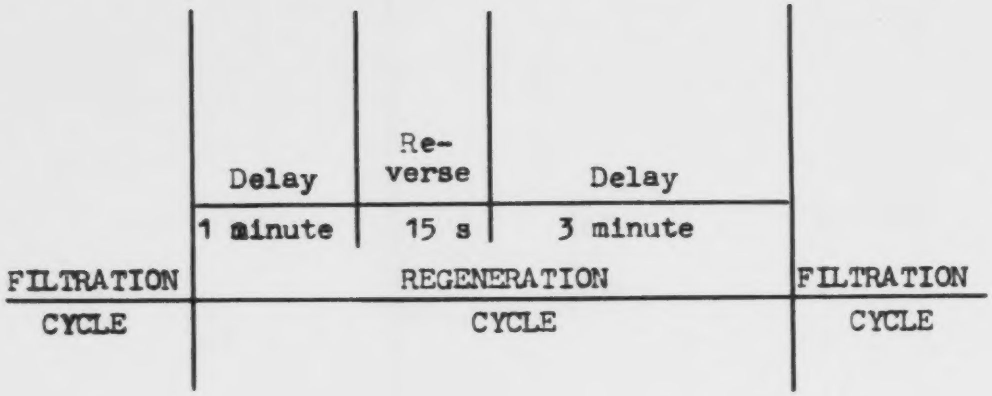
Delay
Re-
verse
Delay
1 minute
15 s
3 minute
FILTRATION
CYCLE
REGENERATION
CYCLE
FILTRATION
CYCLE

a/ For Research Objectives.

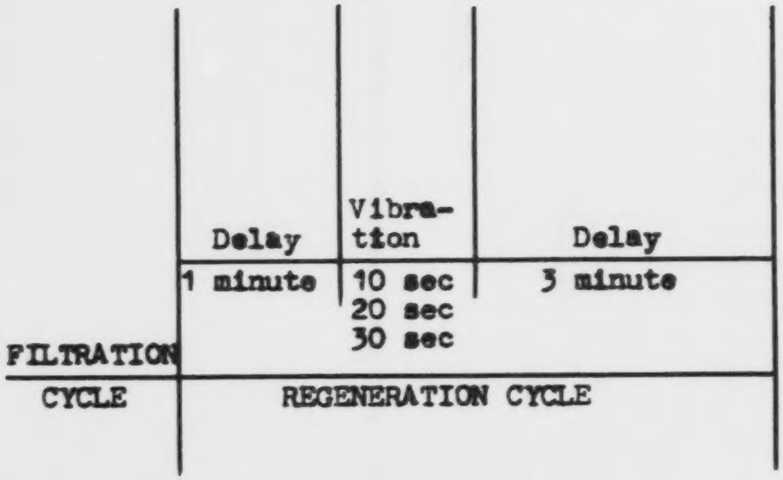
Delay
Vibra-
tion
Delay
1 minute
10 sec
20 sec
30 sec
3 minute
FILTRATION
CYCLE
REGENERATION CYCLE

b/ For Final Cycle.

Figure 29. Diagram of regeneration cycles.

G_H = weight of dust in hopper before regeneration cycle, in grams,

G_B = weight of dust from bag after regeneration, in grams,

G_R = weight of dust removed from hopper during reverse air regeneration, in grams,

G_N = dust filling of bag, in grams, and

G_C = total weight of dust introduced to the hopper during filtration, in grams.

The efficiency of the hopper was calculated according to the relation:

$$E_H = G_H/G_C \times 100 \qquad (13)$$

where E_H = hopper efficiency, in percent.

The efficiency of the tested bag, taking into consideration the dust precipitated in the hopper, was calculated from the dust balance based on the relation:

$$E_B = \frac{G_B + G_R + G_N}{G_C - G_H} \times 100 = \frac{G_C - (G_H + G_B)}{G_C - G_H} \times 100 \qquad (14)$$

where: E_B = bag efficiency, in percent.

For some experiments, measurements of the fractional composition of the dust in the cleaned gases were accomplished using a cascade impactor manufactured by 2000, Inc. and provided by EPA. The measurements were made simultaneously with the measurements of the dust concentration in the outlet gases by an aspiration method. The measurement system is shown in Figures 30 and 31, and includes a suction probe with a sampling nozzle (8 mm in diameter), an Andersen cascade impactor, a rotameter, gas meter, vacuum pump, and cutoff and control valves.

The dusty air was drawn isokinetically from a point 88 mm from the duct wall, i.e., at the point where the gas velocity reaches the mean value in the duct cross section. The velocity distribution in the duct at q_g = 60 m^3/m^2hr and q_g = 80 m^3/m^2hr is shown in Figure 32. To guarantee isokinetic suction, the suction velocity was 20 percent higher than the gas velocity in

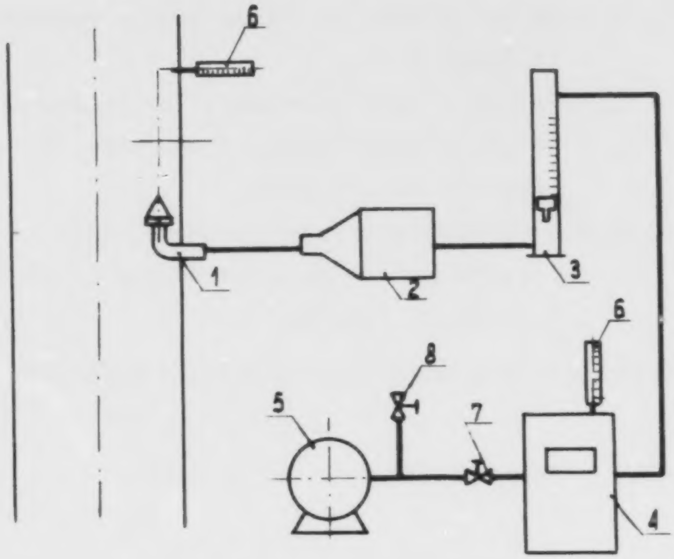

1. Suction probe
2. Andersen Cascade Impactor
3. Rotameter
4. Gas-meter
5. Vacuum pump
6. Thermometer
7, 8. Valves

Figure 30. Diagram of cascade impactor measurement system.

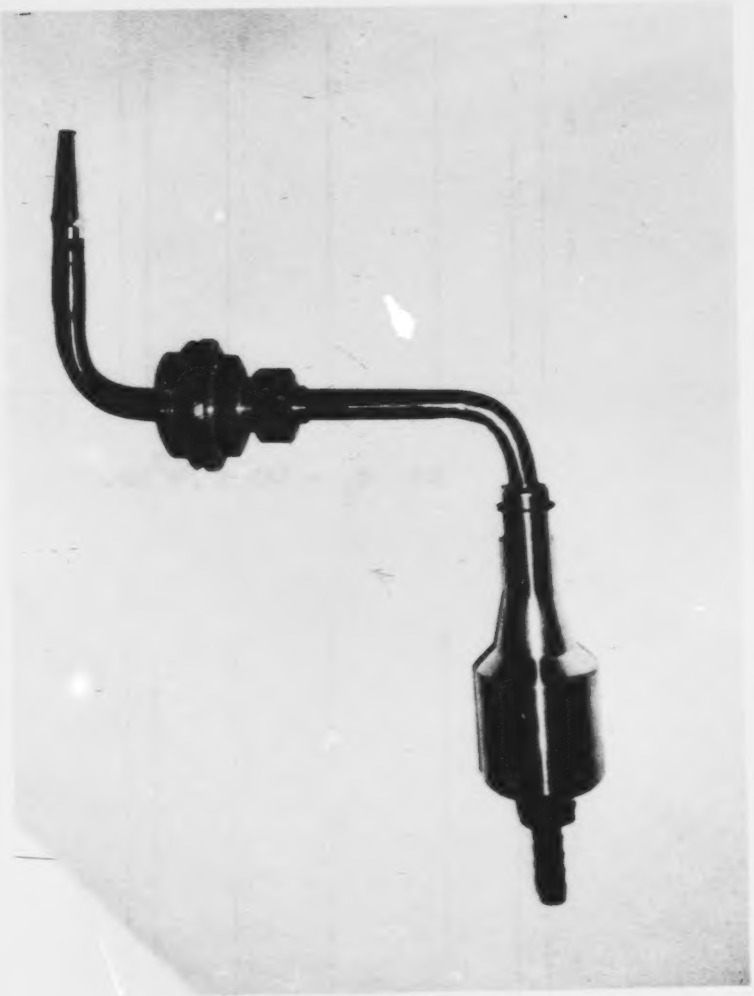

Figure 31. Photograph of cascade impactor measurement system.

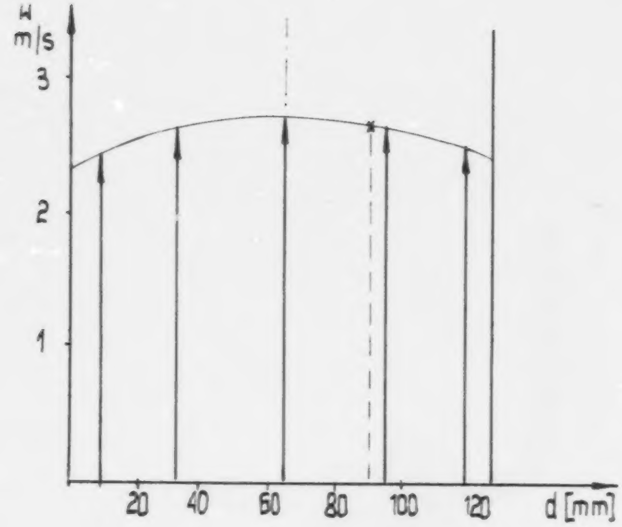

at $q_g = 60\ m^3/m^2hr.$

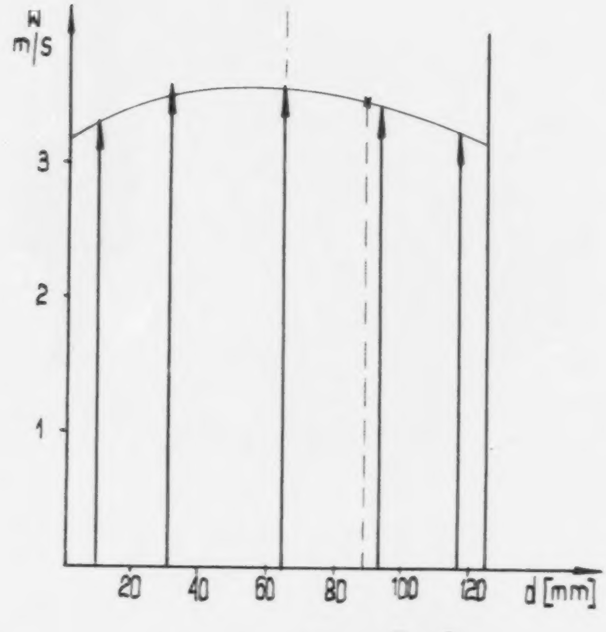

at $q_g = 80\ m^3/m^2hr.$

Figure 32. Velocity distribution in duct.

the duct (the coefficient was established experimentally). Total sampling time equalled the time of five basic measurement cycles. The dust collected on the individual impactor stages was weighed with an accuracy of 0.00005 g. All further operations concerning the true dust particle diameter were conducted according to instructions received with the impactor.

The emission behind the measurement chamber was calculated from the following relation:

$$EM = \frac{m_i \, 60}{t} \qquad (15)$$

where: EM = emission, in grams/hr,
m_i = weight of dust on i-th impactor stage, in grams, and
t = suction time, in minutes.

Dust concentration in the cleaned gases was calculated according to the relation:

$$c_o = EM/Q \qquad (16)$$

where: c_o = outlet concentration, in g/m^3,
EM = emission, in g/hr, and
Q = total gas flow through impactor, in m^3/hr.

Fractional efficiency was calculated according to the equation:

$$E_{FR} = \frac{m_w \, (1 - E_T) \, m_o}{m_w} \times 100 \qquad (17)$$

where: E_{FR} = fractional efficiency, in percent,
E_T = total efficiency of measurement chamber, in percent,
m_w = weight percent of a specific dust fraction introduced to measurement chamber, in percent, and
m_o = weight percent of same dust fraction leaving the measurement chamber, in percent.

RESULTS AND DISCUSSION

Basic Test

The initial large scale testing was conducted on separated talc. Because of the special physical properties of this dust (see Table 2) several technical difficulties were encountered in achieving the test conditions assumed in the detailed testing program. The most difficult were keeping the inlet dust concentration of the air going into the test chamber at a stable level of 10 g/m^3 ± 10 percent, and preventing dust precipitation in the lines.

For keeping the initial dust concentration in air at the required level, within the established tolerance, it was necessary to improve the dust feeder installed on the large scale test stand. Aeration of the dust was done in the dust feeder chamber before the screw conveyor. This operation gave good results, increasing the uniformity of the dust feed to the required level. This improved dust feeder was used during the entire program. The next problem, prevention of dust precipitation, was solved by using suitable vibrators and by changing the diameters of the pipelines.

These problems were eventually overcome, but some fabric tests with separated talc reflect the effects of these early problems in the form of:

- Exceeding the allowed tolerance in dust concentration (in tests at $q_g = 60$ m^3/m^{2}hr) for fabrics:
    - 853 (12.03 g/m^3)
    - 190R (11.87 g/m^3)
    - 852 (11.60 g/m^3),
- Overrunning the assumed dust loading of filtration area (L_o) during the introductory filtration cycles, i.e., during the filling of the fabric structure.

It is worthwhile to notice that the established levels of dust loading of filtration area (L_o) for the measurement cycles and tests of all other kinds of dusts were kept correctly. Figures 33 and 34 show exemplary pressure differences in filtration time for fabric C866B using separated talc and nonseparated coal dust.

The results of large scale testing calculated according to dependence (11) are shown in Table 23. Table 23 also contains mean values of filtration efficiency and outlet concentrations obtained during five measurement cycles conducted after reaching the state-of-balance with reverse air flow regeneration. The detailed reports of individual experiments are in the archives of the Dust Filtration Division of IPWMB, Opole. The results were

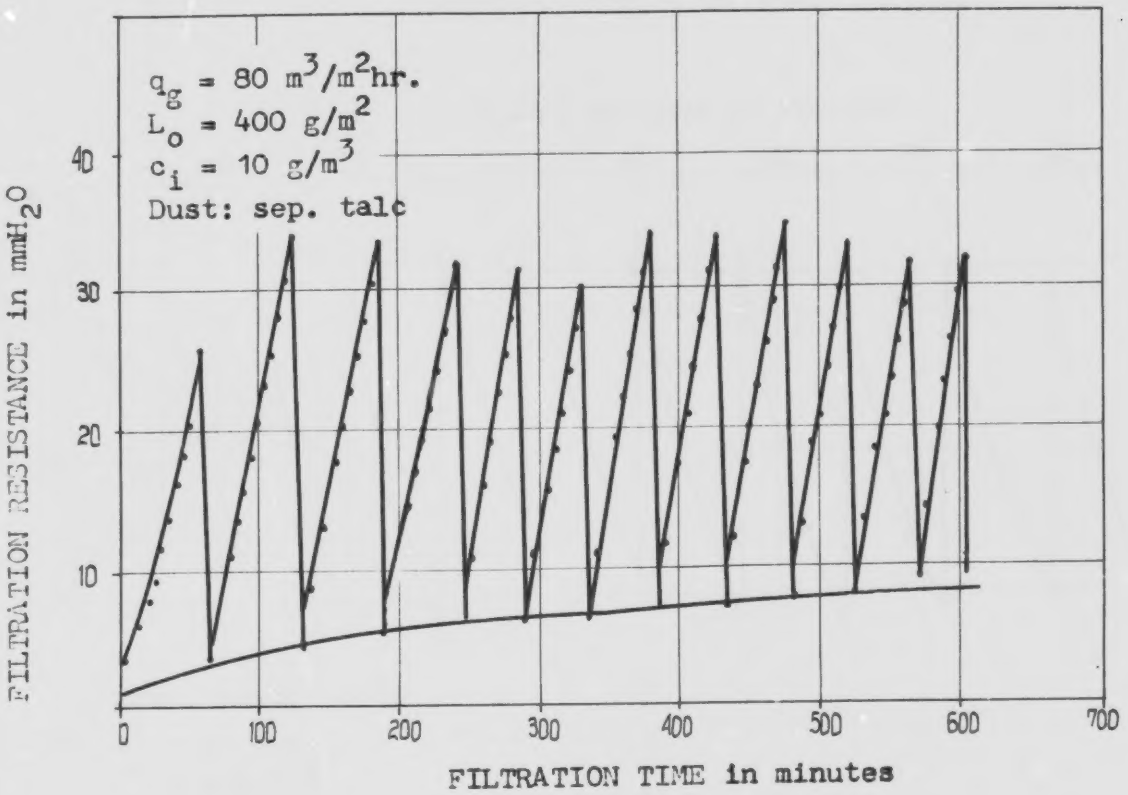

Figure 33. Time variation of filtration resistance for fabric C866B (dust: separated talc).

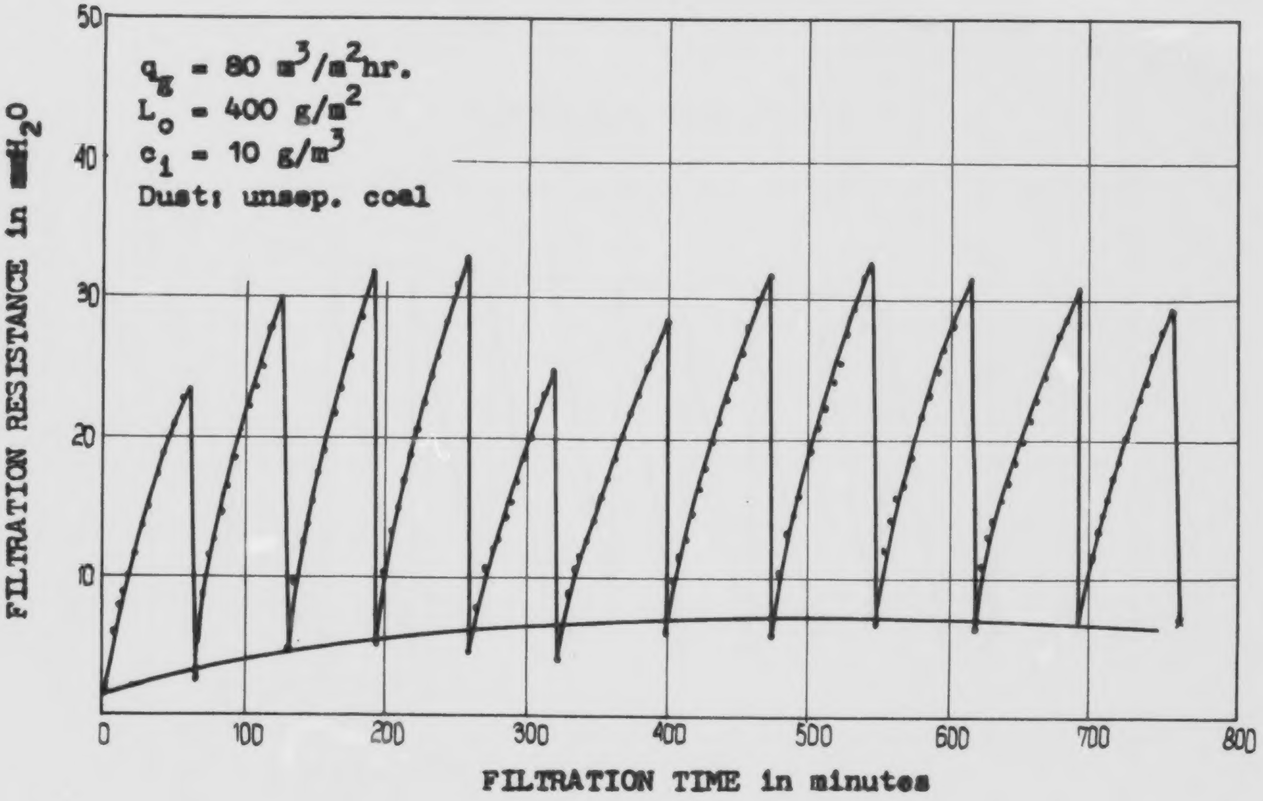

Figure 34. Time variation of filtration resistance for fabric C866B (dust: unseparated coal).

TABLE 23. LARGE-SCALE EFFICIENCY (in percent) OF TESTED FILTRATION FABRICS (c_i=10 g/m^3, L_o=400 g/m^2)

Type of filtration fabric	A/C (in m^3/m^2hr)	Efficiency (in percent)	Outlet concentration (in g/m^3)
Testing with cement			
Cotton Style No. 960	60	99.945	0.0006
	80	99.974	0.0028
Dacron® polyester Style No. 862B	60	99.966	0.0032
	80	99.912	0.0085
Style No. C866B	60	99.997	0.0003
	80	99.971	0.0029
Style No. C868B	60	99.999	0.0001
	80	99.994	0.0006
Dacron® polyester Style No. 865B	60	99.978	0.0021
	80	99.989	0.0011
Style No. C890B	60	99.985	0.0015
	80	99.979	0.0020
Style No. C892B	60	99.991	0.0009
	80	99.981	0.0018
Nomex® aromatic nylon Style No. 852	60	99.999	0.0001
	80	99.979	0.0021
Style No. 853	60	99.992	0.0007
	80	99.974	0.0026
Style No. 190R	60	99.963	0.0041
	80	99.965	0.0036
Nomex® aromatic nylon Style No. 850B	60	99.991	0.0010
	80	99.986	0.0014

(continued)

TABLE 23. (continued)

Type of filtration fabric	A/C (in m^3/m^2hr)	Efficiency (in percent)	outlet concentration (in g/m^3)
Nylon polyamide			
Style No. 802B	60	99.987	0.0013
	80	99.979	0.0021
Glass Style No. Q53-875	60	99.991	0.0010
	80	99.921	0.0074
Glass Style No. Q53-870	60	99.986	0.0014
	80	99.565	0.0444
Glass Style No. Q53-878	60	99.968	0.0032
	80	99.913	0.0082
	Testing with coal		
Cotton Style No. 960	60	99.917	0.0090
	80	99.984	0.0016
Dacron® polyester			
Style No. 862B	60	99.782	0.0226
	80	99.805	0.0181
Style No. C866B	60	99.955	0.0044
	80	99.623	0.0037
Style No. C868B	60	99.936	0.0017
	80	99.912	0.0100
Dacron® polyester			
Style No. 865B	60	99.986	0.0015
	80	99.994	0.0006
Style No. C890B	60	99.950	0.0053
	80	99.972	0.0027
Style No. C892B	60	99.957	0.0044
	80	99.976	0.0024
Nomex® aromatic nylon			
Style No. 852	60	99.989	0.0010
	80	99.974	0.0024
Style No. 853	60	99.718	0.0287
	80	99.979	0.0019

(continued)

TABLE 23. (continued)

Type of filtration fabric	A/C (in m^3/m^2hr)	Efficiency in percent)	outlet concentration (in g/m^3)
Style No. 190R	60	99.989	0.0012
	80	99.978	0.0021
Nomex® aromatic nylon Style No. 850B	60	99.959	0.0043
	80	99.989	0.0010
Nylon polyamide Style No. 802B	60	99.815	0.0174
	80	99.986	0.0015
Glass Style No. Q53-875	60	99.896	0.0128
	80	99.895	0.0099
Glass Style No. Q53-870	60	99.817	0.0193
	80	99.783	0.0223
Glass Style No. Q53-878	60	99.678	0.0323
	80	99.501	0.0495
	Testing with talc		
Cotton Style No. 960	60	99.985	0.0016
	80	99.825	0.0148
Dacron® polyester Style No. 862B	60	99.975	0.0026
	80	99.685	0.0330
Style No. C866B	60	99.989	0.0012
	80	99.958	0.0047
Style No. C868B	60	99.959	0.0038
	80	99.854	0.0131
Dacron® polyester Style No. 865B	60	99.966	0.0033
	80	99.947	0.0050
Style No. C890B	60	99.964	0.0034
	80	99.966	0.0032
Style No. C892B	60	99.911	0.0079
	80	99.307	0.0658

(continued)

TABLE 23. (continued)

Type of filtration fabric	A/C (in m^3/m^2hr)	Efficiency in percent)	outlet concentration (in g/m^3)
Nomex® aromatic nylon			
Style No. 852	60	99.963	0.0043
	80	99.864	0.0126
Style No. 853	60	99.983	0.0021
	80	99.928	0.0069
Style No. 190R	60	99.992	0.0010
	80	99.944	0.0051
Nomex® aromatic nylon			
Style No. 850B	60	99.996	0.0005
	80	99.995	0.0004
Nylon polyamide			
Style No. 802B	60	99.996	0.0004
	80	99.842	0.0155
Glass Style No. Q53-875	60	99.951	0.0048
	80	99.952	0.0046
Glass Style No. Q53-870	60	99.597	0.0406
	80	99.690	0.0304
Glass Style No. Q53-878	60	99.889	0.0108
	80	98.876	0.1123
Testing with fly ash			
Cotton Style No. 960	60	99.976	0.0025
	80	99.929	0.0072
Dacron® polyester			
Style No. 862B	60	99.864	0.0142
	80	99.863	0.0141
Style No. C866B	60	99.920	0.0084
	80	99.951	0.0049
Style No. C868B	60	99.825	0.0169
	80	99.965	0.0034
Dacron® polyester			
Style No. 865B	60	99.798	0.0198
	80	99.534	0.0462
Style No. C890B	60	99.878	0.0113
	80	99.641	0.0365
Style No. C892B	60	99.981	0.0018
	80	99.495	0.0475

(continued)

TABLE 23. (continued)

Type of filtration fabric	A/C (in m^3/m^2hr)	Efficiency (in percent)	outlet concentration (in g/m^3)
Nomex® aromatic nylon			
Style No. 852	60	99.919	0.0079
	80	99.896	0.0100
Style No. 853	60	--	--
	80	--	--
Style No. 190R	60	99.973	0.0027
	80	99.958	0.0043
Nomex® aromatic nylon			
Style No. 850B	60	99.992	0.0008
	80	99.951	0.0049
Nylon polyamide			
Style No. 802B	60	99.957	0.0041
	80	99.930	0.0066
Glass Style No. Q53-870	60	99.974	0.0025
	80	99.958	0.0040
Glass Style No. Q53-870	60	99.929	0.0074
	80	99.827	0.0171
Style No. Q53-878	60	99.975	0.0025
	80	99.951	0.0049

systematized for the purpose of carrying out the comparative analysis (similar to laboratory scale) according to the recorded values of final (outlet) dust concentration. The same ranges of dust concentration were established for fabric classification in the laboratory scale, as shown shown in Table 24.

Compared with the laboratory scale results, the filtration efficiency of fabrics examined in large scale was higher, so a larger number of the fabrics fall in classes of lower outlet dust concentration. This confirms the nonequivalence of the effects of Dust Filtration Types I and III. On structures fully filled with dust, the filtration process differs between large scale and laboratory scale.

Results given in Tables 23 and 24 indicate that all fabrics (except C892B and Q53-878 tested with talc at $q_g = 80\ m^3/m^2hr$) have satisfactory dust collection efficiency, giving final dust concentrations below 50 mg/m^3. Concerning glass fiber fabric Q53-878, it can be said that the decrease of efficiency resulted because of operation at an unsuitable A/C ratio. Concerning polyester fabric C892B, lower values of efficiency, as compared to other fabrics, probably result from structural properties. Taking into consideration the kind of dust, the best filtration effects were obtained for cement dust and the worst for fly ash.

Natural fiber fabrics, represented by cotton fabric 960, showed good filtration efficiency during testing with cement and coal dust. The efficiency of this fabric decreased during testing with talc and fly ash. A decrease in dust filtration efficiency, with increase in A/C ratio, was observed. It is possible that it is connected to electrostatic effects.

The group of polyester fabrics, represented by staple fiber fabrics 862B, C866B, and C868B and continuous filament fabrics 865B, C890B, and C892B, showed no influence of the kind of fiber on filtration effects. The fabrics of this group showed good dust collection efficiency for cement and coal dusts, but showed much worse collection efficiencies for talc and fly ash. Even worse efficiencies were observed for q_g higher than 60 m^3/m^2hr for talc and for all ranges of A/C for fly ash.

Similar efficiencies were observed for Nomex fabrics, except for continuous filament fabric 850. Among all tested fabrics, this fabric gave the best dust collection efficiencies (also the highest fly ash collection efficiencies).

TABLE 24. CLASSIFICATION OF FABRICS ACCORDING TO OUTLET CONCENTRATION

Kind of dust	A/C (in m^3/m^2hr)	Outlet concentration in g/m^3					
		below 0.0025	0.0025-0.0050	0.0050-0.01	0.01-0.05	0.05-.1	0.1-0.5
Cement	60	960 C866B C868B 865B C890B C892B 852 853 850B 802B Q53-875 Q53-870	862B 190R Q53-878				
	80	C868B 865B C890B C892B 852 850B 802B	960 C866B 853 190R	862B Q53-875 Q53-878	Q53-870		
Coal	60	C868B 865B 852 190R	C866B C892B 850B	960 C890B	862B 853 802B Q53-875 Q53-870 Q53-878		

(continued)

TABLE 24. (continued)

Kind of dust	A/C (in m^3/m^2hr)	Outlet concentration in g/m^3					
		below 0.0025	0.0025-0.0050	0.0050-0.01	0.01-0.05	0.05-.1	0.1-0.5
	80	960 865B C892B 852 853 190R 850B 802B	C866B C890B	C868B Q53-875	862B Q53-870 Q53-878		
Talc	60	960 C866B 853 190R 850B 802B	862B C868B 865B C890B 852 Q53-875	C892B	Q53-870 Q53-878		
	80	850B	C866B 865B C890B Q53-875	853 190R	960 862B C868B 852 802B Q53-878	C892B	Q53-878
Fly ash	60	C892B 850B	960 190R 802B Q53-875 Q53-878	C866B 852 Q53-870	862B C868B 865B C890B		

(continued)

TABLE 24. (continued)

Kind of dust	A/C (in m^3/m^2hr)	Outlet concentration in g/m^3					
		below 0.0025	0.0025-0.0050	0.0050-0.01	0.01-0.05	0.05-.1	0.1-0.5
	80		C866B C868B 190R 850B Q53-875 Q53-878	960 852 802B	862B 865B C890B C892B Q53-870		

Polyamide fabric 802B (staple fiber, similar to cotton fabric 960) showed interesting properties, especially during testing with coal dust.

Glass fabrics were represented by three types of fabrics of different construction. They showed better efficiencies in large scale than in laboratory scale. However, among all fabrics tested, the efficiencies of glass fabrics were the lowest. It is interesting, however, that in spite of the quite rigid testing conditions, good filtration properties for fly ash were observed. The influence of A/C on the dust collection efficiency was observed in individual tests.

The Influence of Hopper Efficiency on Conducted Experiments

To determine the influence of the separating hopper on the experiments, the dust balances for each of five measurement cycles were:

1. Weight of dust precipitated in the hopper during the filtration cycle (after shutting the hopper damper),
2. Weight of dust removed from the fabric structure during regeneration, which is a value equivalent to the dust cake,
3. Weight of dust added to the bag by the reverse air cleaning,
4. Weight of residual dust in the fabric structure after the regeneration cycle, which equals the final filling of fabric,
5. Weight of dust introduced to the 1-bag compartment by the feeder.

Based on the above amounts of dust and according to equations (12), (13), and (14), the total 1-bag compartment efficiency, hopper efficiency, and bag efficiency were calculated. The results are shown in Table 25.

During the testing, samples were taken from the following points of the system:

- From the hopper during the filtration process (before regeneration),
- From a bag, i.e., the dust covering the bag, as dust cake, and
- From the dust feeder.

The fractional compositions for these samples were determined. Based on fractional composition, MMD (d_{50}) was estimated. The results are presented in Table 26.

TABLE 25. EFFICIENCIES E_{T2}, and E_B CALCULATED BY DUST BALANCE

Type of filtration fabric	A/C (in m^3/m^2hr)	Total efficiency (in percent)	Hopper efficiency (in percent)	Bag efficiency (in percent)
		Testing with cement		
960	60	99.995	81.601	99.972
	80	99.974	75.059	99.893
862B	60	99.966	80.137	99.825
	80	99.912	70.068	99.704
C866B	60	99.997	82.542	99.983
	80	99.971	71.138	99.898
C868B	60	99.999	82.732	99.993
	80	99.994	66.769	99.981
865B	60	99.978	79.735	99.893
	80	99.989	72.613	99.958
C890B	60	99.985	83.745	99.910
	80	99.980	75.445	99.917
C892B	60	99.991	84.112	99.942
	80	99.981	78.361	99.912
852	60	99.999	76.287	99.994
	80	99.979	63.332	99.943
853	60	99.993	81.972	99.957
	80	99.974	69.092	99.915
190R	60	99.963	76.088	99.841
	80	99.965	74.978	99.855
850B	60	99.988	83.814	99.941
	80	99.986	73.759	99.946
802B	60	99.987	80.180	99.932
	80	99.979	70.743	99.930
Q53-875	60	99.991	83.590	99.944
	80	99.921	74.059	99.694
Q53-870	60	99.986	86.818	99.893
	80	99.567	75.283	98.247
Q53-878	60	99.968	83.051	99.810
	80	99.913	75.145	99.652
		Testing with coal		
960	60	99.917	75.974	99.655
	80	99.984	68.586	99.951

(continued)

TABLE 25. (continued)

Type of filtration fabric	A/C (in m^3/m^2hr)	Total efficiency (in percent)	Hopper efficiency (in percent)	Bag efficiency (in percent)
862B	60	99.782	71.991	99.223
	80	99.805	71.570	99.314
C866B	60	99.955	74.944	99.822
	80	99.963	70.957	99.871
C868B	60	99.984	71.856	99.943
	80	99.912	71.138	99.694
865B	60	99.976	77.375	99.937
	80	99.993	70.659	99.978
C890B	60	99.950	76.923	99.781
	80	99.972	72.738	99.898
C892B	60	99.959	73.789	99.843
	80	99.975	71.927	99.913
852	60	99.989	72.414	99.962
	80	99.974	69.146	99.917
853	60	99.718	71.435	99.011
	80	99.979	72.527	99.924
190R	60	99.987	72.983	99.953
	80	99.979	68.936	99.931
850B	60	99.959	75.980	99.828
	80	99.990	72.064	99.964
802B	60	99.815	76.252	99.221
	80	99.985	70.039	99.952
Q53-875	60	99.875	72.804	99.541
	80	99.895	73.752	99.600
Q53-870	60	99.817	74.513	99.281
	80	99.783	72.360	99.215
Q53-878	60	99.679	73.987	98.767
	80	99.503	72.026	98.223
		Testing with talc		
960	60	99.985	68.319	99.953
	80	99.832	60.175	99.578
862B	60	99.975	70.013	99.917
	80	99.685	57.781	99.255
C866B	60	99.989	67.128	99.966
	80	99.958	58.870	99.898
C868B	60	99.959	66.114	99.881
	80	99.854	57.604	99.656
865B	60	99.966	61.034	99.913
	80	99.947	56.761	99.877

(continued)

TABLE 25. (continued)

Type of filtration fabric	A/C (in m^3/m^2hr)	Total efficiency (in percent)	Hopper efficiency (in percent)	Bag efficiency (in percent)
C890B	60	99.964	63.848	99.901
	80	99.966	59.439	99.917
C892B	60	99.911	66.968	99.730
	80	99.311	58.551	98.340
852	60	99.963	67.044	99.887
	80	99.863	58.556	99.664
853	60	99.983	62.140	99.955
	80	99.928	55.875	99.837
190R	60	99.991	63.700	99.977
	80	99.944	54.562	99.877
850B	60	99.996	74.268	99.984
	80	99.995	62.613	99.987
802B	60	99.996	60.583	99.991
	80	99.842	54.604	99.651
Q53-875	60	99.951	66.221	99.854
	80	99.953	58.712	99.886
Q53-870	60	99.584	65.315	98.800
	80	99.681	60.478	99.337
Q53-878	60	99.889	62.708	99.702
	80	98.884	57.578	97.367
		Testing with fly ash		
960	60	99.976	69.364	99.919
	80	99.932	46.277	99.863
862B	60	99.864	49.351	99.732
	80	99.863	41.622	99.764
C866B	60	99.914	55.190	99.808
	80	99.951	42.501	99.915
C868B	60	99.823	53.080	99.619
	80	99.965	48.037	99.932
865B	60	99.798	39.116	99.667
	80	99.536	41.447	99.208
C890B	60	99.878	44.296	99.780
	80	99.643	53.184	99.237
C892B	60	99.981	59.693	99.954
	80	99.498	52.894	98.933
852	60	99.921	69.229	99.742
	80	99.896	46.785	99.804
853	60	-	-	-
	80	-	-	-

(continued

TABLE 25. (continued)

Type of filtration fabric	A/C (in m^3/m^2hr)	Total efficiency (in percent)	Hopper efficiency (in percent)	Bag efficiency (in percent)
190R	60	99.973	59.064	99.931
	80	99.957	65.823	99.868
850B	60	99.992	53.884	99.393
	80	99.951	52.263	99.897
802B	60	99.957	56.651	99.899
	80	99.934	51.357	99.860
Q53-875	60	99.974	68.201	99.918
	80	99.958	50.772	99.914
Q53-870	60	99.942	63.514	99.806
	80	99.827	53.985	99.612
Q53-878	60	99.974	55.678	99.940
	80	99.951	46.018	99.909

It appeared that the hopper efficiency is quite high and is as follows:

· Cement dust	63.3 - 86.8%
· Coal dust	68.5 - 77.4%
· Talc	54.5 - 74.2%
· Fly ash	41.4 - 69.4%

Taking A/C ratio into consideration (different velocities in the hopper), hopper efficiencies were:

- Cement dust: at $q_g = 60\ m^3/m^2hr$, $E_H = 76 - 86.8\%$
  $q_g = 80\ m^3/m^2hr$, $E_H = 63.3 - 78.3\%$
- Unseparated coal dust:
  at $q_g = 60\ m^3/m^2hr$, $E_H = 71.4 - 77.4\%$
  $q_g = 80\ m^3/m^2hr$, $E_H = 68.5 - 73.7\%$
- Talc: at $q_g = 60\ m^3/m^2hr$, $E_H = 60.5 - 74.2\%$
  $q_g = 80\ m^3/m^2hr$, $E_H = 54.5 - 62.6\%$
- Fly ash: at $q_g = 60\ m^3/m^2hr$, $E_H = 39.1 - 69.4\%$
  $q_g = 80\ m^3/m^2hr$, $E_H = 41.4 - 53.9\%$

It can be seen then that hopper efficiency depends on the A/C ratio, the dust density, and the aerodynamic coefficient of dust grain shape. This is in accordance with the theoretical base of the mechanical dust collector's operation.

The fractionating action of the hopper is clearly seen by comparing the mean grain diameter (MMD) of the feed dust probed from the bag and the hopper. In spite of the use of highly pulverized separated dusts, characterized by MMD in the range of 5.2 - 6.8 μm (coal dust is not taken into consideration), the dusts were further separated because of the fractionating properties of the hopper (its construction and geometrical proportions). The pulverized dust from the bag (see Table 26) is characterized by an MMD = 4.0 - 5.5 μm with the fraction above 20 μm, not exceeding 1% (the assumption was 10 percent).

So we come to the conclusion that the dust collection efficiencies of the tested fabrics were actually determined using dusts of higher pulverization than would be assumed from the fractional composition of the feed dust.

Comparing the du[illegible] collection efficiencies presented in Table 25 (calculated from dust bala[illegible]ith and without the hopper efficiency, it appears that the differences are considerable. Lower efficiencies were obtained for the bag itself than for the entire chamber, including the hopper efficiency (E_{T2}). Two efficiencies were calculated; one based on measurements (E_{T1}) and the other from dust balance (E_{T2}). The above total efficiencies of the chamber are very well correlated, which confirms the accuracy of the testings. Figure 35 shows the comparison of measurement and dust balance efficiencies for fabric C890B tested with cement dust. Because of the high hopper efficiency, the filtration cycles were lengthened as necessary, in order to maintain a constant L_o = 400 g/m^2.

The true concentration of dust at the bag inlet can be calculated from the equation:

$$c_{iB} = c_i\,(1-E_H) \tag{18}$$

where: c_{iB} = dust concentration at the bag inlet, in g/m^3,
c_i = initial concentration at the compartment inlet, in g/m^3, and
E_H = hopper efficiency,

TABLE 26. MMD FOR FEED DUST, BAG DUST, AND HOPPER DUST

Type of filtration fabric	A/C (in m^3/m^2hr)	Kind of dust											
		MMD of cement dust (in μm)			MMD of coal dust (in μm)			MMD of talc dust (in μm)			MMD of fly ash dust (in μm)		
		from feeder	from bag	from hopper	from feeder	from bag	from hopper	from feeder	from bag	from hopper	from feeder	from bag	from hopper
960	60	5.2	4.2	5.9	30	7.0	50	6.8	4.4	8.2	5.5	4.8	6.0
	80	5.2	4.5	7.6	30	7.5	51	6.8	5.5	7.3	5.5	5.0	6.7
862B	60	5.2	3.8	5.8	30	7.3	53	6.8	4.3	8.0	5.5	4.5	6.4
	80	5.2	-	-	30	7.4	55	6.8	4.5	8.5	5.5	4.4	5.7
C866B	60	5.2	5.0	6.2	30	6.8	46	6.8	4.3	8.0	5.5	4.5	5.3
	80	5.2	5.1	5.3	30	7.5	51	6.8	4.4	8.0	5.5	5.0	7.3
C868B	60	5.2	3.9	6.0	30	7.8	53	6.8	4.7	8.7	5.5	4.4	5.8
	80	5.2	4.5	5.0	30	7.9	58	6.8	4.5	7.8	5.5	4.8	6.5
865B	60	5.2	4.1	5.6	30	6.5	48	6.8	-	-	5.5	4.2	6.2
	80	5.2	4.5	5.6	30	-	-	6.8	-	-	5.5	4.9	8.0
C890B	60	5.2	4.2	5.3	30	6.6	55	6.8	4.2	8.2	5.5	5.7	6.0
	80	5.2	4.7	6.2	30	7.0	-	6.8	4.6	8.6	5.5	5.0	8.5
C892B	60	5.2	4.3	-	30	7.1	55	6.8	4.6	8.0	5.5	5.1	6.2
	80	5.2	4.4	5.8	30	9.0	53	6.8	4.8	8.9	5.5	5.1	6.8
852	60	5.2	3.9	6.3	30	7.0	50	6.8	4.3	8.2	5.5	4.4	5.8
	80	5.2	4.6	5.6	30	7.8	58	6.8	4.6	9.5	5.5	5.5	6.6
853	60	5.2	4.1	5.5	30	8.0	53	6.8	4.7	9.2	5.5	-	-
	80	5.2	4.4	6.2	30	7.5	53	6.8	4.8	10.5	5.5	-	-
190R	60	5.2	4.6	5.6	30	6.6	53	6.8	5.0	8.9	5.5	5.0	6.0
	80	5.2	4.2	7.8	30	7.3	56	6.8	4.8	9.5	5.5	4.4	5.3
850B	60	5.2	4.4	5.5	30	6.3	47	6.8	4.7	8.3	5.5	5.2	6.8
	80	5.2	4.5	7.0	30	8.5	53	6.8	4.7	7.9	5.5	4.7	6.0
802B	60	5.2	4.2	6.5	30	7.2	46	6.2	4.5	8.2	5.5	5.5	6.7
	80	5.2	4.2	6.0	30	8.0	52	6.8	5.0	8.3	5.5	5.0	7.8
Q53-875	60	5.2	4.0	6.4	30	7.5	56	6.8	-	-	5.5	4.5	5.8
	80	5.2	4.6	6.4	30	-	-	6.8	-	-	5.5	4.3	6.2
Q53-870	60	5.2	4.3	5.9	30	7.2	50	6.8	4.6	8.2	5.5	4.3	6.0
	80	5.2	-	-	30	7.2	56	6.2	4.4	8.3	5.5	4.5	5.8
Q53-878	60	5.2	4.0	5.8	30	8.8	54	6.8	4.5	7.3	5.5	4.5	5.3
	80	5.2	4.6	6.1	30	7.0	55	6.2	4.6	9.6	5.5	4.5	6.0

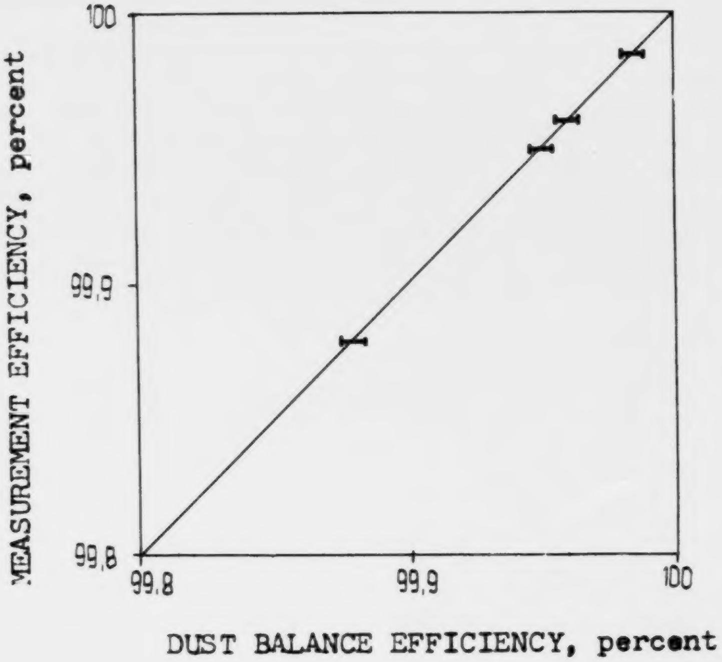

Figure 35. Correlation between measurement efficiency and dust balance efficiency for experiments for fabric C890B dusted with cement at $q_g = 60\ m^3/m^2$ hr.

Fractional Efficiency of Fabrics

The measurements of fabric fractional efficiency were made for the following dusts and values of A/C:

- Cement dust; $q_g = 80\ m^3/m^2hr$,
- Fly ash; $q_g = 60$ and $80\ m^3/m^2hr$.

TABLE 27. FRACTIONAL EFFICIENCY OF FABRICS TESTED WITH CEMENT (at $q_g = 80\ m^3/m^2hr$, $L_o = 400\ g/m^2$, and $c_i = 10\ g/m^3$)

Type of filtration fabrics	Fractional efficiency (in percent) in the ranges:				
	0-2 μm	2-3 μm	3-5 μm	5-10 μm	above 10 μm
Cotton Style No. 960	99.828	99.937	99.986	100.000	100.000
Dacron® polyester					
Style No. 862B	99.411	99.863	99.934	99.987	100.000
Style No. C866B	99.871	99.957	99.995	99.969	100.000
Style No. C868B	99.950	99.989	99.998	99.999	100.000
Dacron® polyester					
Style No. 865B	*	*	*	*	*
Style No. C890B	99.852	99.959	99.997	99.994	100.000
Style No. C892B	99.837	99.970	100.000	99.996	100.000
Nomex® aromat. nylon					
Style No. 852	*	*	*	*	*
Style No. 853	*	*	*	*	*
Style No. 190R	99.740	99.923	100.000	99.989	100.00
Nomex® aromat. nylon					
Style No. 850B	99.888	99.977	99.995	99.998	100.000
Nylon polyamide					
Style No. 802B	99.803	100.000	99.993	99.995	100.000
Glass					
Style No. Q53-875	99.374	99.876	99.968	99.991	100.000
Glass					
Style No. Q53-870	96.033†	99.571	99.794	100.000	100.000
	97.111‡	99.126	99.677	99.975	100.000
Style No. Q53-878	*	*	*	*	*

*No data--amount of dust in the impactor too small to be measured.
†For not fully filled structure.
‡After reaching state of equilibrium.

The calculated values of efficiencies are compiled in Tables 27 and 28.

Figures 36 through 40 show fractional efficiency as a function of dust grain diameter.

During the analysis of the measurements, it was observed that in many cases the outlet dust concentrations estimated by the cascade impactor were much lower than the concentrations estimated by the aspiration method (filtration sampling), even though the impactor measurement procedures were in accordance with the instructions. This discrepancy is probably caused by instantaneous duct velocity fluctuations, so that aspirated gas sample is not isokinetic. The possibility of some measurement mistakes connected with the application of the new measurement method, however, is not excluded.

The analysis of the fractional composition of the outlet dusts (in the clean air behind the test chamber) showed that the standard deviation from the mean grain diameter (MMD) is on the average about σ = 2 μm, which proves the fractionating influence of the dust-fabric system (see Table 29). An increase in the mean dust grain diameter with increasing A/C ratio was observed.

Plots of fractional efficiency as a function of grain diameter were obtained during fabric testing with separated cement dust (see Figures 36 and 37). The plots conform to our predictions. Each fabric has a definite grain diameter for which the efficiency reaches 100 percent.

The influence of the filtration structure on the formation of a definite dust cake structure can be seen. Hence the dust fabric system is characterized by the grain size, above which the efficiency is 100 percent.

The curves shown in Figures 38 through 40 have behaviors different than those presented in Figure 36 and 37. They represent the variations of fractional efficiency as a function of grain diameter during testing with separated talc.

It is interesting that in the range of fine fractions, there are some grain sizes at which the efficiencies are higher than expected by us. The characteristic decreases in efficiency were observed. They had been observed before and during research concerning fractional efficiency problems. A significant increase of dust collection efficiency was observed for fractions above 2 μm.

TABLE 28. FRACTIONAL EFFICIENCY OF FABRICS TESTED WITH FLY ASH (at q_g = 60 and 80 m^3/m^2hr, L_o = 400 g/m^2, and c_i = 10 g/m^3)

Type of filtration fabrics	A/C (in m^3/m^2hr)	Fractional efficiency (in percent) in the ranges: 0-2 μm	2-3 μm	3-5 μm	5-10 μm	above 10 μm
Cotton Style No. 960	60	99.953	99.556	99.961	100.000	100.000
	80	99.756	99.670	99.539	100.000	100.000
Dacron® polyester						
Style No. 862B	60	99.883	98.623	99.428	99.972	99.996
	80	99.665	98.866	99.691	99.972	100.000
Style No. C866B	60	99.720	100.000	99.715	100.000	99.992
	80	99.838	99.808	99.917	99.981	100.000
Style No. C868B	60	99.476	100.000	99.477	99.962	99.961
	80	99.865	100.000	99.890	99.984	100.000
Dacron® polyester						
Style No. 865B	60	99.342	100.000	99.200	99.993	99.993
	80	98.919	97.224	98.996	99.773	100.000
Style No. C890B	60	99.712	100.000	99.402	99.978	99.997
	80	98.733	97.767	99.546	99.953	100.000
Style No. C892B	60	99.931	100.000	99.927	99.998	99.999
	80	98.191	97.551	99.293	99.887	100.000
Nomex® aromat. nylon						
Style No. 852	60	99.745	100.000	99.678	99.985	100.000
	80	99.791	99.294	99.756	99.962	100.000
Style No. 853		-	-	-	-	-
Style No. 190R	60	100.000	98.056	97.981	100.000	100.000
	80	99.798	99.841	100.000	100.000	100.000
Nomex® aromat. nylon						
Style No. 850B	60	*	*	*	*	*
	80	99.856	99.583	99.915	99.995	100.000
Nylon polyamide						
Style No. 802B	60	99.830	100.000	99.893	100.000	100.000
	80	99.699	99.701	99.948	99.992	100.000

(continued)

TABLE 28. (continued)

Type of filtration fabrics	A/C (in m^3/m^2hr)	Fractional efficiency (in percent) in the ranges: 0-2 μm	2-3 μm	3-5 μm	5-10 μm	above 10 μm
Glass						
Style No. Q53-875	60	99.885	100.000	99.914	99.984	100.000
	80	99.918	99.793	99.913	99.973	100.000
Glass						
Style No. Q53-870	60	*	*	*	*	*
	80	99.563	98.986	99.682	99.928	100.000
Style No. Q53-878	60	99.877	100.000	99.944	99.995	99.995
	80	99.846	99.720	99.912	99.987	100.000

*Absent data--amount of dust in the impactor too small to be measured.

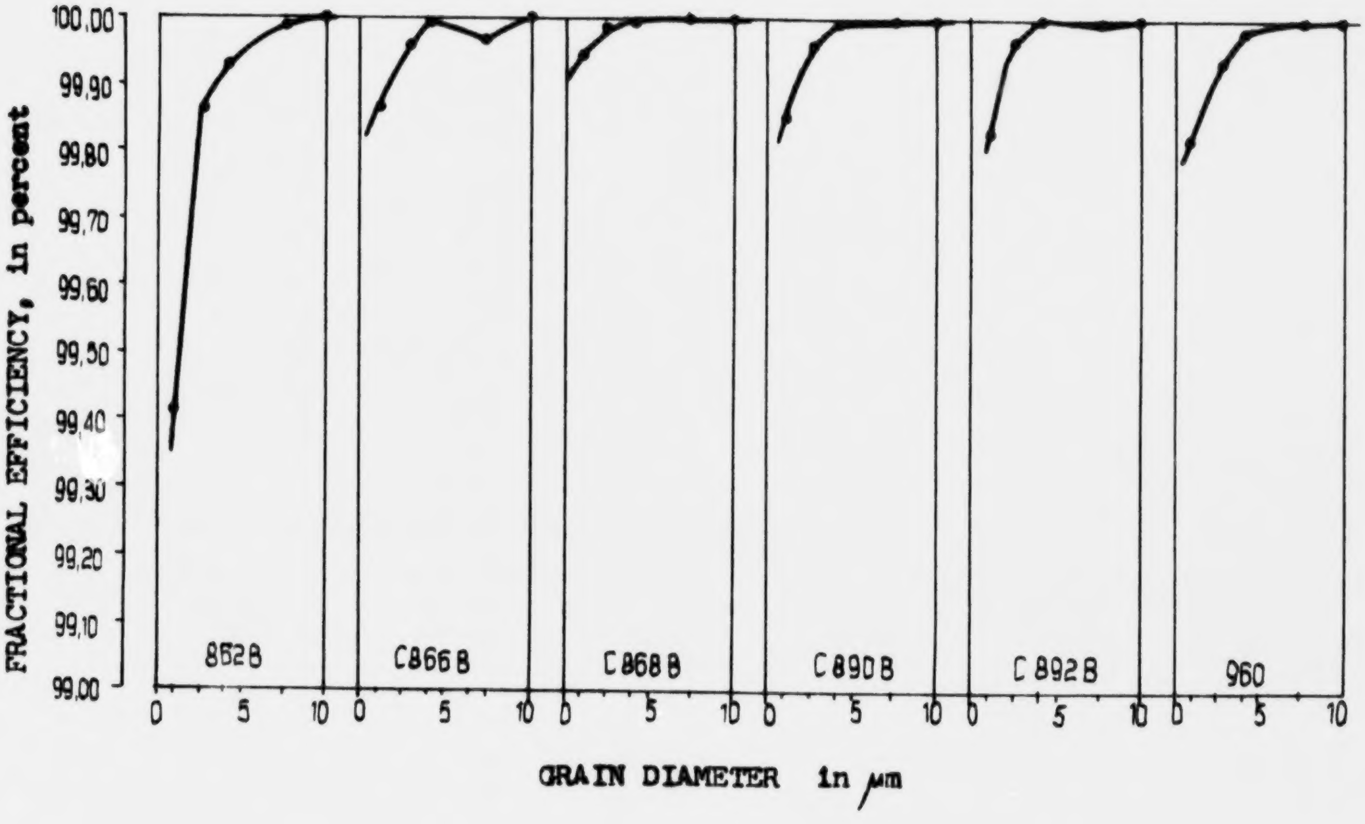

Figure 36. Fractional efficiency of polyester and cotton fabrics (cement dust at q_g = 80 m^3/m^2 hr, L_o = 400 g/m^2, and c_i = 10 g/m^3).

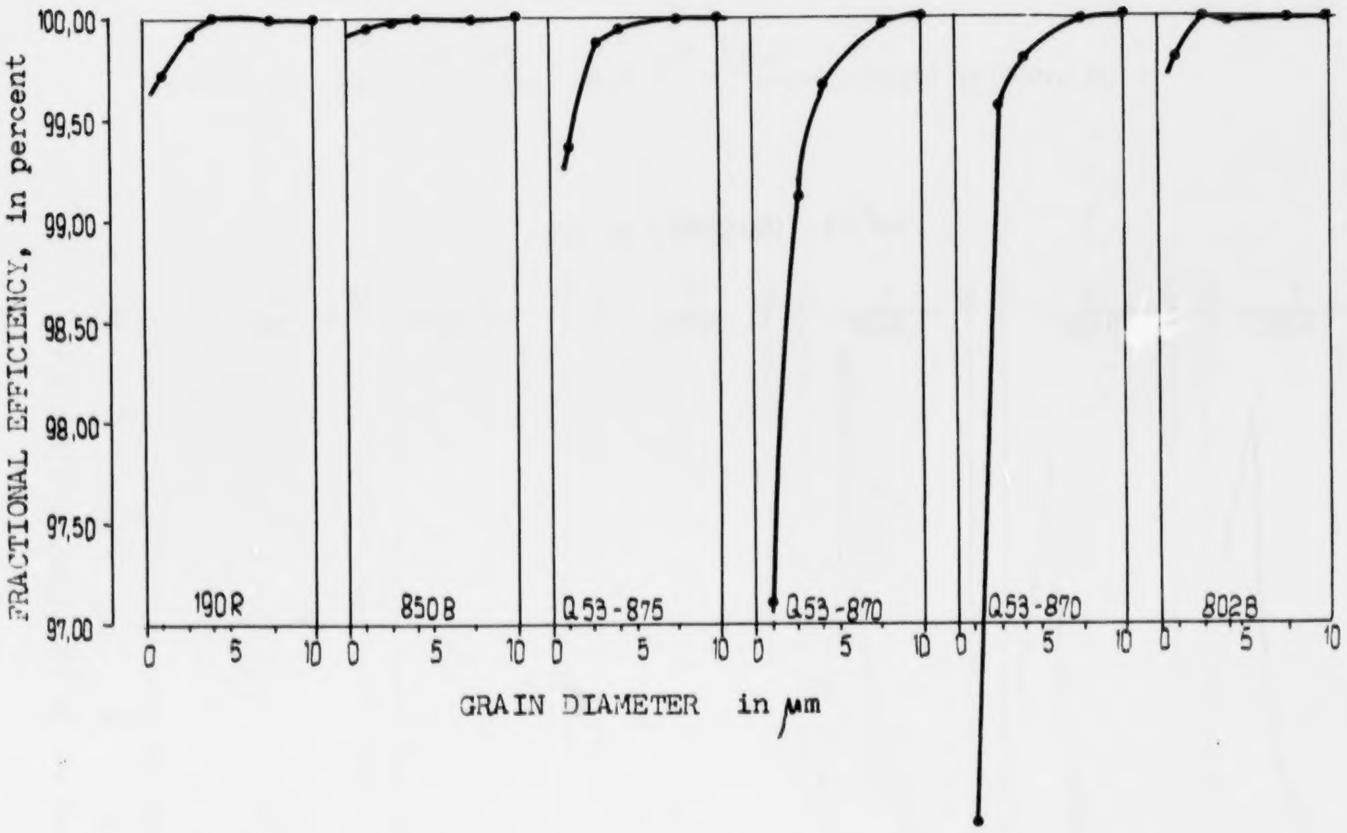

Figure 37. Fractional efficiency of Nomex, glass, and polyamide fabrics (cement dust at q_g = 80 m^3/m^2 hr, L_o = 400 g/m^2, and c_i = 10 g/m^3).

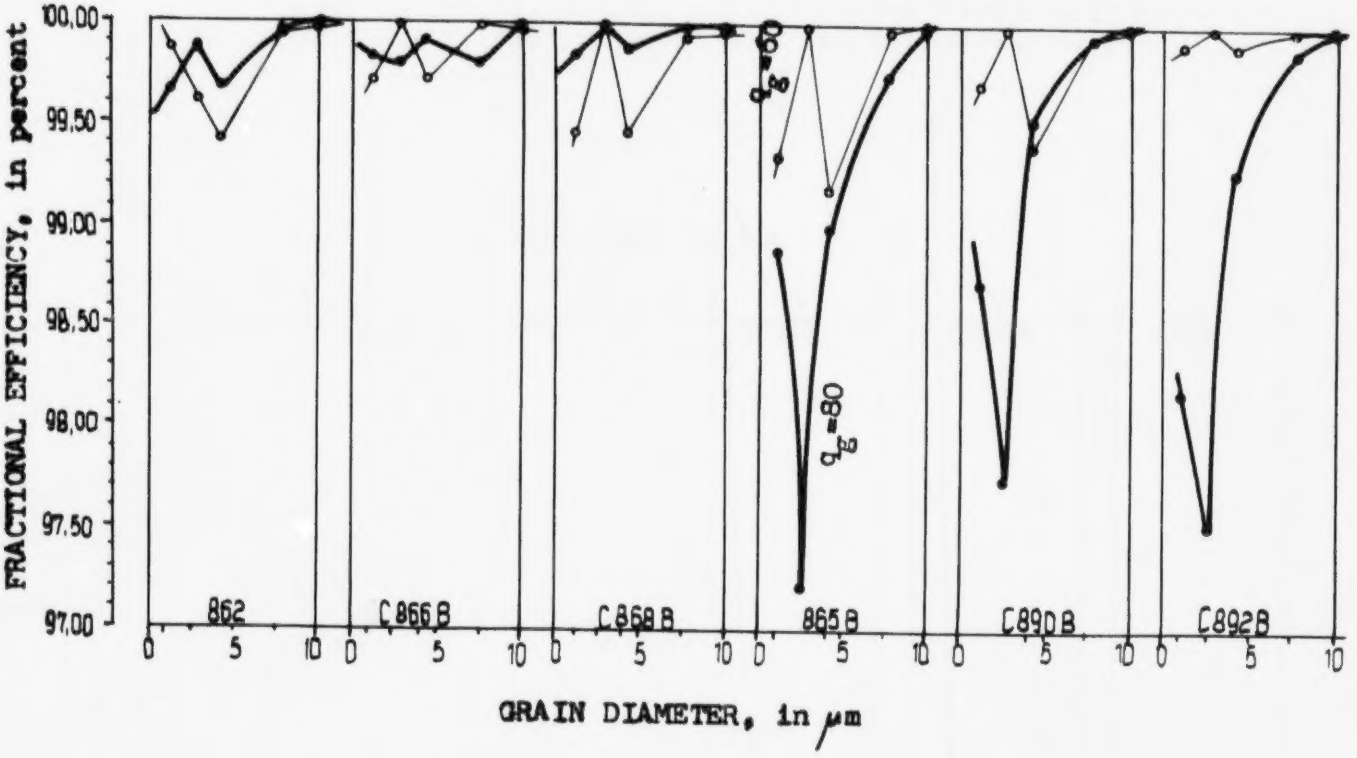

Figure 38. Fractional efficiency of polyester fabrics (fly ash at L_o = 400 g/m² and c_i = 10 g/m³).

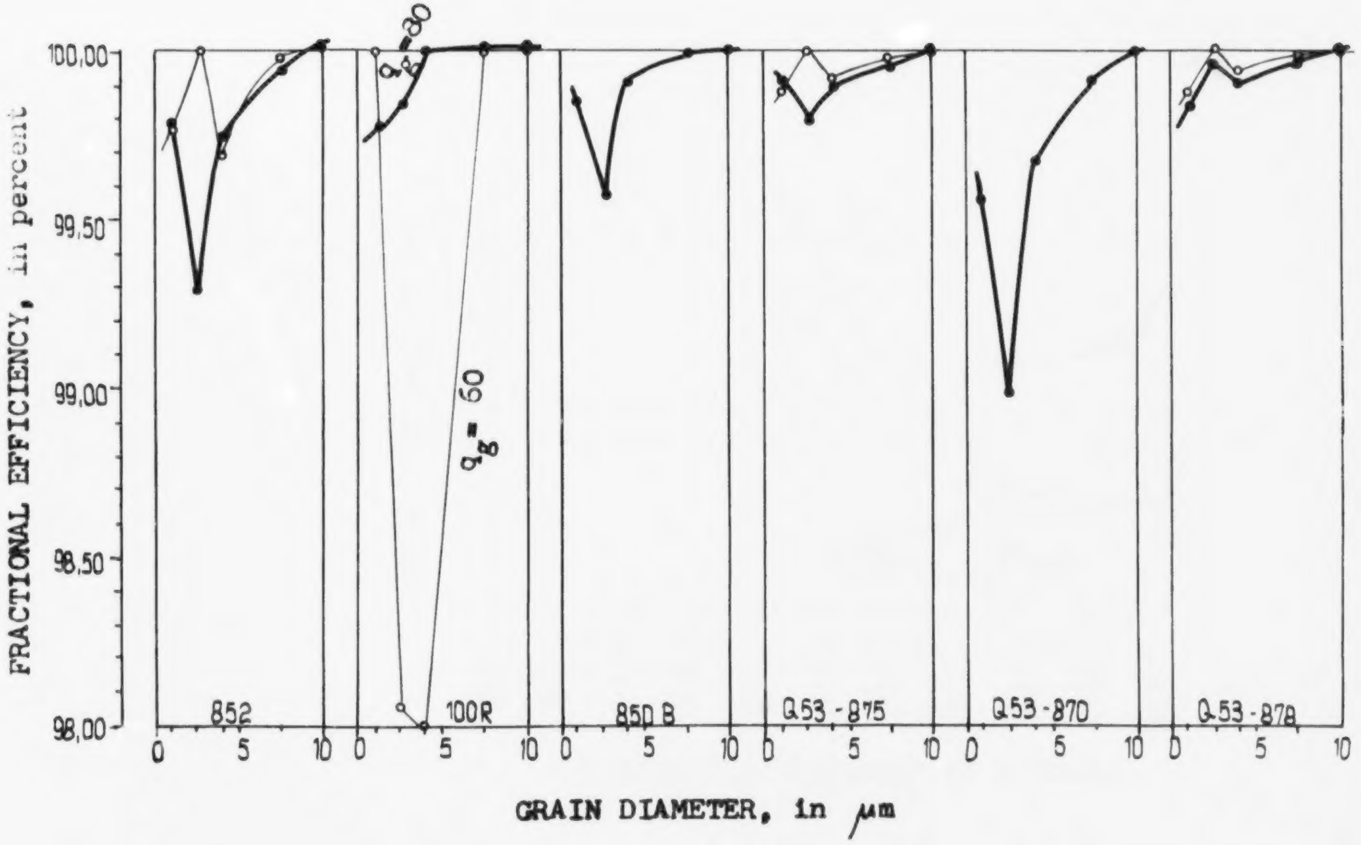

Figure 39. Fractional efficiency of Nomex and glass fabrics (fly ash at $L_o = 400$ g/m^2 and $c_i = 10$ g/m^3).

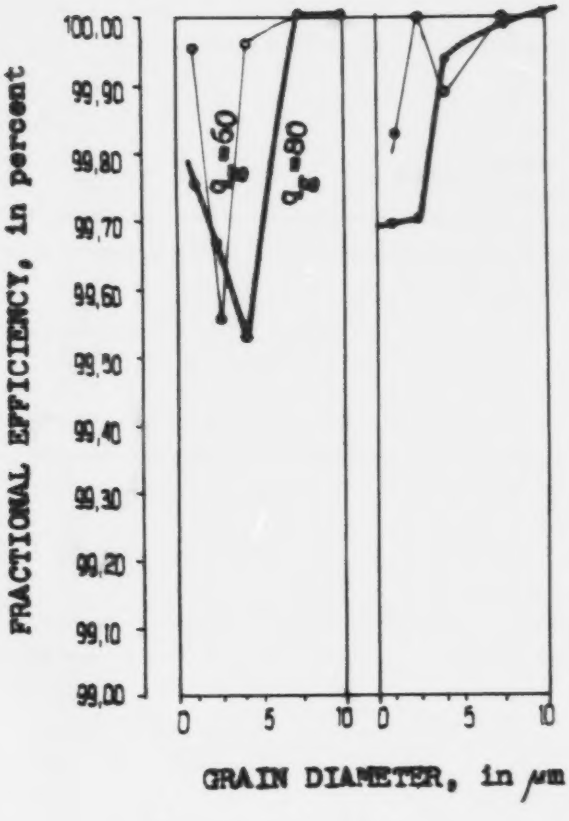

Figure 40. Fractional efficiency of cotton and polyamide fabrics (fly ash at L_o = 400 g/m^2 and c_i = 10 g/m^3).

TABLE 29. MMD OF OUTLET DUST - CASCADE IMPACTOR MEASUREMENTS

		Kind of dust			
		Cement		Fly ash	
Type of filtration fabric	A/C in m^3/m^2hr	MMD µm	σ µm	MMD µm	σ µm
Cotton					
Style No. 960	60	-	-	-	-
	80	0.95	2.57	1.70	1.89
Dacron® polyester					
Style No. 862B	60	-	-	1.90	1.81
	80	1.40	1.94	1.90	1.81
Style No. C866B	60	-	-	1.37	2.11
	80	2.30	3.65	1.65	2.36
Style No. C868B	60	-	-	1.75	2.69
	80	1.20	1.79	1.10	2.20
Dacron® polyester					
Style No. 865B	60	-	-	1.63	1.89
	80	-	-	1.76	2.32
Style No. C890B	60	-	-	1.75	1.90
	80	1.15	2.40	1.26	2.17
Style No. C892B	60	-	-	1.70	1.75
	80	0.88	2.32	1.35	2.25
Nomex®					
Style No. 852	60	-	-	1.20	2.45
	80	1.80	3.83	1.78	1.78
Style No. 853	60	-	-	-	-
	80	-	-	-	-
Style No. 190R	60	-	-	-	-
	80	1.15	2.09	-	-
Nomex®					
Style No. 850B	60	-	-	-	-
	80	1.10	2.20	1.68	1.77
Nylon polyamide					
Style No. 802B	60	-	-	1.45	1.71
	80	0.86	2.10	1.30	1.94
Glass					
Style No. Q53-875	60	-	-	1.50	2.03
	80	1.20	1.97	2.35	2.47
Glass					
Style No. Q53-870	60	-	-	1.73	2.31
	80	1.10	1.83	2.00	2.15
		0.70	2.92		
Style No. Q53-878	60	-	-	1.10	3.33
	80	0.70	6.36	1.70	2.13

Filtration Resistance

In the introduction to Section IV, the filtration resistances were discussed from two viewpoints:

1. The obtained final filtration resistance (ΔP_K) of a structure covered with dust $L_o = 400\ g/m^2$, and
2. The obtained effective drag (S_E) and resistance coefficient (K_2) of a definite dust-fabric system.

In both cases, the respective values of the two viewpoints were discussed for the same values of A/C; the regeneration system was the same during all experiments. The final resistance, ΔP_K, was presented in Tables B-4 through B-19. ΔP_K was similar within a given raw material group, but did depend upon the type (continuous vs. staple) fiber.

For the most populous group, polyester fabrics, higher filtration resistances were observed with the continuous filament fabrics. The same observation was made for Nomex and glass fabrics.

Analyzing the variation of final resistance with respect to the kind of test dust, it can be said that dusts of cement, coal, and talc show similar hydraulic effects. Much lower final resistances were observed during all tests with fly ash.

It is interesting that coal dust, which in the large scale testing was an unseparated dust of MMD = 30 μm, showed a final resistance during all tests similar to that recorded for separated cement dust and talc, even though particle size composition of the unseparted coal dust differed significantly from that of the separated dusts. This would prove that grain shape has a greater influence on the filtration resistance of a dust-fabric system than the degree of pulverization. The above observation was confirmed by laboratory scale testings (Table 16). The highest observed filtration resistances (measured by final pressure drop) were obtained for separated coal dust in all laboratory tests. It is possible that this phenomenon is connected with electrostatic effects. Coal dust has very special electrostatic properties.

From equations (4) and (5), the effective drag and resistance coefficients for the dust-fabric systems were determined for the mean values of filtration resistance as a function of time over five measurement cycles. The results of the calculations are presented in Table 30. Table 31 includes

TABLE 30. S_E (in $mmH_2O/m/hr$) AND SPECIFIC RESISTANCE COEFFICIENT K_2 (in $mmH_2O/m/hr/g/m^2$) IN LARGE SCALE TESTS

Type of fabric	q_g in m^3/m^2hr	Effective drag S_E				Specific resistance coefficient K_2			
		Sep. cement	Unsep. coal	Sep. talc	Sep. fly ash	Sep. cement	Unsep. coal	Sep. talc	Sep. fly ash
Cotton 960	60	0.48	17.20	13.46	17.95	0.31	0.06	0.06	0.04
	80	16.77	16.82	9.91	13.27	0.07	0.08	0.11	0.07
Dacron® 862B	60	11.70	10.06	7.40	10.58	0.06	0.07	0.06	0.04
	80	13.12	9.00	7.26	9.21	0.06	0.05	0.07	0.04
C866B	60	12.40	8.83	7.67	9.90	0.06	0.06	0.06	0.04
	80	10.58	10.98	6.80	11.14	0.07	0.03	0.08	0.05
C868B	60	15.55	10.52	10.05	10.51	0.06	0.07	0.05	0.04
	80	15.84	7.05	10.27	9.83	0.06	0.06	0.05	0.04
Dacron® 865B	60	16.46	10.03	11.99	14.29	0.06	0.05	0.07	0.04
	80	18.84	12.34	11.89	17.19	0.05	0.06	0.06	0.05
C890B	60	20.32	18.52	21.92	16.01	0.04	0.05	0.07	0.03
	80	26.92	25.23	23.30	21.49	0.06	0.07	0.06	0.03
C892B	60	13.93	24.37	15.27	18.92	0.05	0.08	0.05	0.04
	80	30.59	20.67	15.11	20.05	0.05	0.05	0.05	0.04
Nomex® 852	60	11.03	11.57	6.75	16.19	0.07	0.07	0.07	-0.03
	80	11.71	7.52	8.56	11.16	0.09	0.05	0.06	0.09
853	60	12.92	10.37	9.12	--	0.08	0.08	0.10	--
	80	12.36	8.87	8.91	--	0.10	0.06	0.06	--
190R	60	7.75	7.45	4.45	5.44	0.08	0.08	0.06	0.05
	80	5.65	5.47	5.00	4.23	0.10	0.05	0.05	0.09

(continued)

TABLE 30. (continued)

Type of fabric	q_g in m^3/m^2hr	Effective drag S_E				Specific resistance coefficient K_2			
		Sep. cement	Unsep. coal	Sep. talc	Sep. fly ash	Sep. cement	Unsep. coal	Sep. talc	Sep. fly ash
Nomex® 850	60	22.17	21.16	17.87	17.49	0.04	0.05	0.06	0.03
	80	24.58	22.47	19.43	20.08	0.05	0.04	0.08	0.03
Nylon 802B	60	11.59	8.24	12.45	10.37	0.06	0.05	0.07	0.05
	80	12.06	7.79	9.82	11.73	0.07	0.06	0.05	0.05
Glass Q53-875	60	20.88	23.81	22.08	18.33	0.05	0.08	0.08	0.04
	80	21.91	21.75	16.66	21.52	0.06	0.06	0.07	0.04
Glass Q53-870	60	30.38	33.35	21.66	25.43	0.06	0.08	0.06	0.04
	80	29.50	28.92	31.52	22.01	0.05	0.06	0.09	0.04
Q53-878	60	17.72	17.68	16.61	11.28	0.06	0.07	0.07	0.05
	80	19.35	16.55	16.13	15.61	0.05	0.07	0.07	0.05

TABLE 31. RATE OF INCREASE OF FILTRATION RESISTANCE

Type of fabric	Kind of dust							
	Sep. cement		Unsep. coal		Sep. talc		Sep. fly ash	
	$q_g=$ 60	$q_g=$ 80	$q_g=$ 60	$q_g=$ 80	$q_g=$ 60	$q_g=$ 80	$q_g=$ 60	$q_g=$ 80
Cotton								
960	0.58	0.31	0.14	0.45	0.18	0.77	0.11	0.65
Dacron®								
862B	0.12	0.29	0.21	0.27	0.19	0.54	0.20	0.43
C866B	0.11	0.36	0.16	0.13	0.21	0.57	0.19	0.53
C868B	0.10	0.35	0.20	0.29	0.18	0.39	0.20	0.38
Dacron®								
865B	0.11	0.25	0.12	0.30	0.26	0.46	0.24	0.50
C890B	0.07	0.24	0.10	0.32	0.26	0.41	0.19	0.28
C892B	0.09	0.17	0.20	0.25	0.18	0.35	0.14	0.30
Nomex®								
852	0.16	0.56	0.18	0.29	0.22	0.47	--	0.89
853	0.14	0.58	0.23	0.30	0.36	0.49	--	--
190R	0.20	0.47	0.22	0.28	0.22	0.44	0.22	0.57
Nomex®								
850B	0.07	0.24	0.12	0.22	0.15	0.51	0.15	0.29
Nylon								
802B	0.12	0.35	0.12	0.35	0.26	0.41	0.24	0.44
Glass								
Q53-875	0.08	0.27	0.21	0.29	0.28	0.53	0.12	0.35
Glass								
Q53-870	0.08	0.23	0.19	0.30	0.22	0.63	0.15	0.31
Q53-878	0.10	0.24	0.19	0.37	0.28	0.55	0.22	0.51

the increase of pressure drop in time calculated according to equation (6). As it can be seen from the compiled data, S_E as well as K_2 depend upon the raw material of the fabric, the kind of fiber (staple, continuous filament), and the kind of dust.

Continuous filament fabrics show a considerable increase of S_E with increasing A/C. It probably results from the very good structural filling of the spatial area with yarns of indefinite length. The spatial area of staple fiber yarns is very porous, so S_E shows only very small variations as a function of A/C ratio. A more apparent influence of A/C upon filtration resistance is observed when analyzing the rate of increase of filtration resistance (see Table 31).

In conclusion, it is worth pointing out that the calculated values, S_E and K_2, have only statistical significance because they are the secondary values of external process parameters measured during the run. They are not directly functionally dependent on physical parameters characterizing the process or structural parameters. Application of the values of S_E and K_2 has practical importance only in predicting a filtration resistance for process conditions similar to the conditions of the experiment.

The values of S_E and K_2 obtained in the laboratory tests, although similar, do not correlate with those of the large scale tests (especially for polyester fabrics). The calculation of negative values of S_E for the laboratory studies proves that the time variation of the filtration resistance has a parabolic character and cannot be assumed to be linear.

During the large scale fabric testing the influence of the superficial structure of the fabric on dust cake formation was observed. It made obtaining an assumed final resistance in time difficult. Analysis of the resistance variation in time led to the conclusion that the prolonged experimental time required to build up a predetermined pressure drop was caused by the "sliding effect" of dust cake. This effect was characteristic of the glass and polyester continuous filament fabrics tested with separated cement dust. The variation of filtration resistance in time is shown in Figures 41 through 46. [A similar influence of superficial structure on filtration resistances was described by Donovan, Daniel, and Turner (ref. 13).] The "sliding effect" of dust cake is characterized by decrease of K_2 in time. It decreases to the moment of obtaining the mean value characteristic for the specific process.

The data just discussed lead mainly to one conclusion, i.e. it is necessary to study and understand the structural parameters characteristic of woven fabric structure and its dust cake. Only in this manner will it be

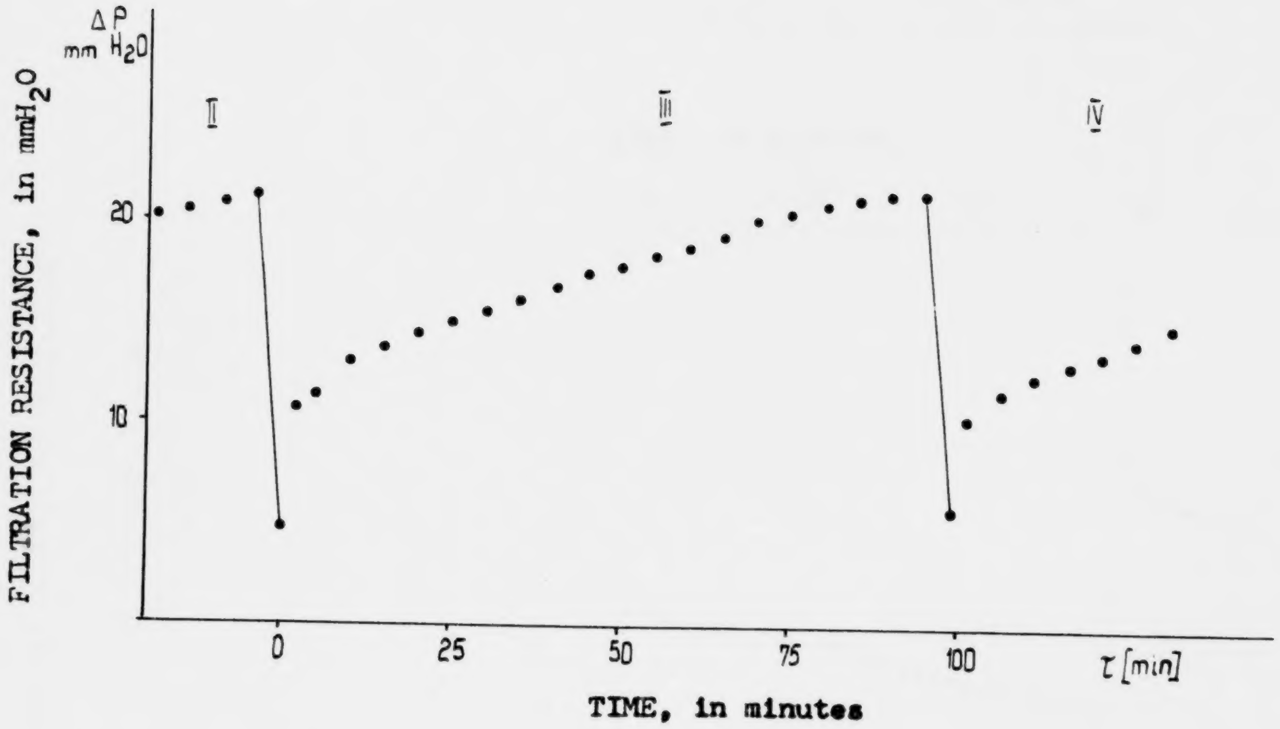

Figure 41. Variation of filtration resistance in time for fabric style no. 862B (cement dust at $q_g = 60\ m^3/m^2\ hr$).

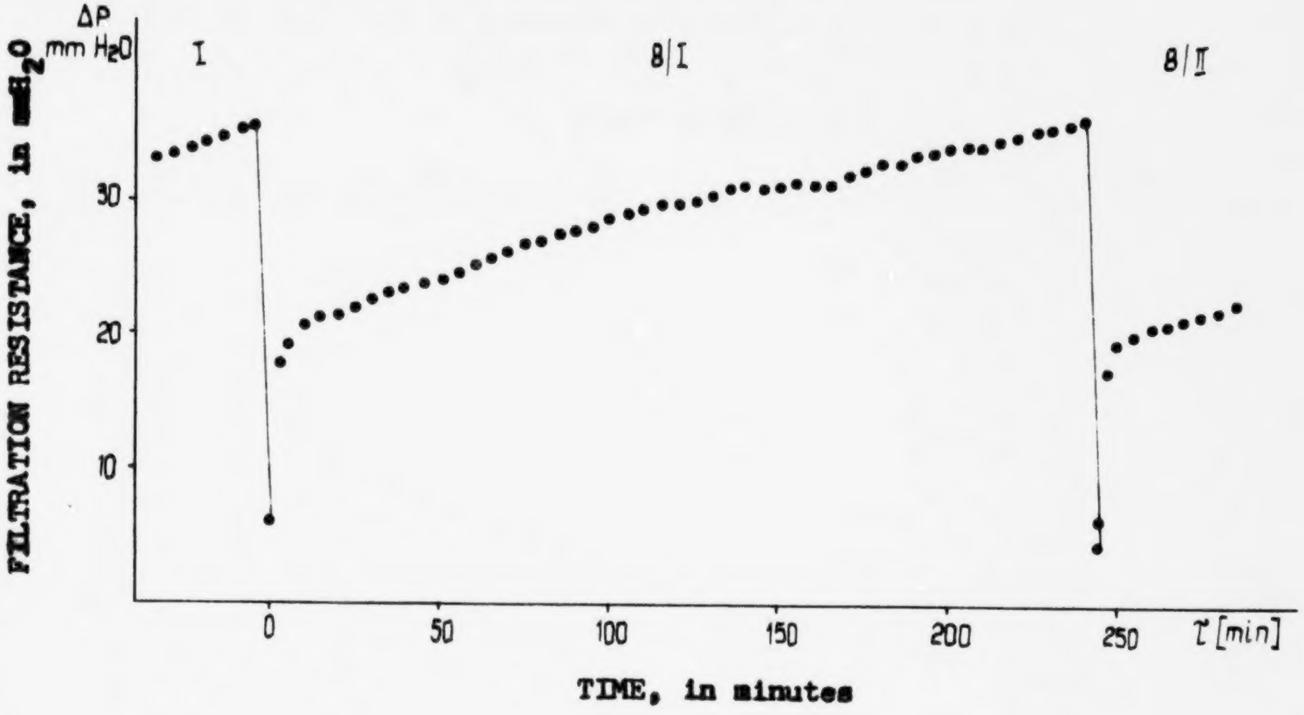

Figure 42. Variation of filtration resistance in time for fabric style no. C890B (cement dust at $q_g = 60\ m^3/m^2\ hr$).

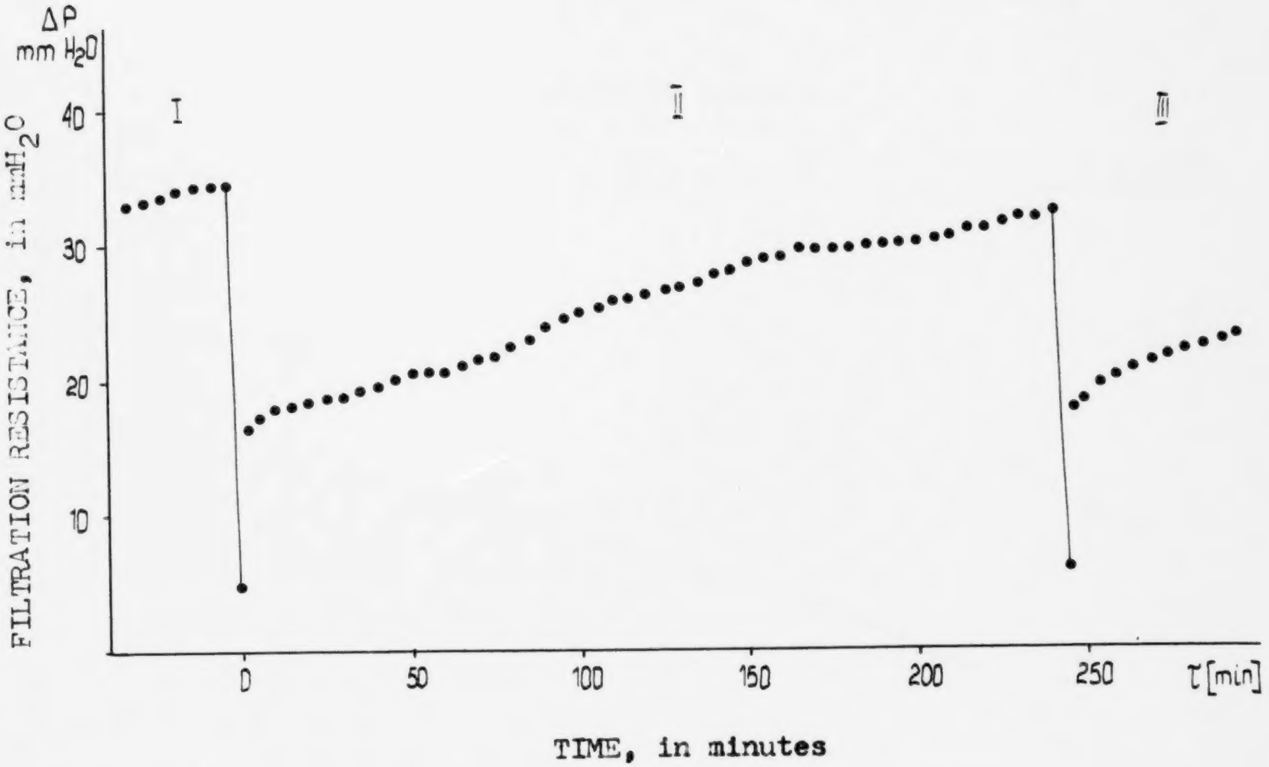

Figure 43. Variation of filtration resistance in time for fabric style no. C892B (cement dust at $q_g = 60\ m^3/m^2\ hr$).

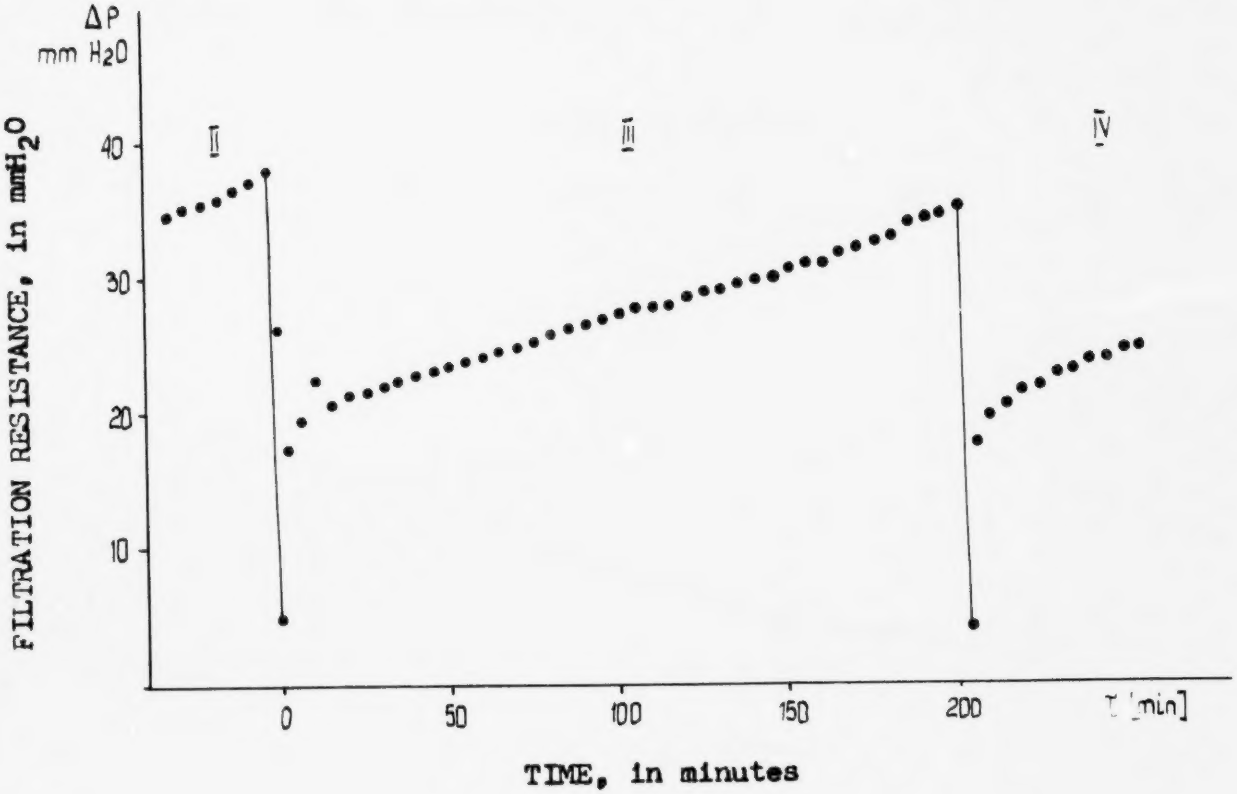

Figure 44. Variation of filtration resistance in time for fabric style no. Q53-875 (cement dust at $q_g = 60\ m^3/m^2\ hr$).

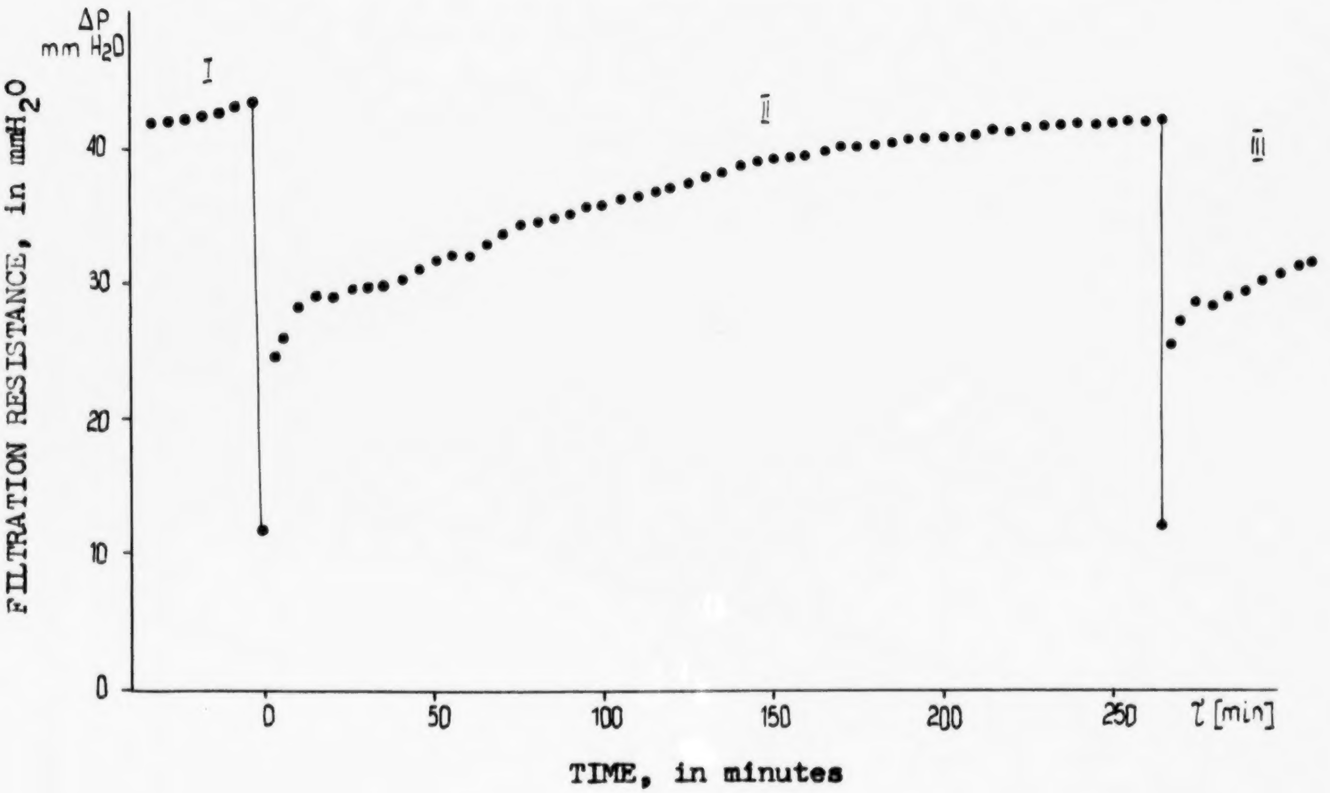

Figure 45. Variation of filtration resistance in time for fabric style no. Q53-870 (cement dust at q_g = 60 m^3/m^2 hr).

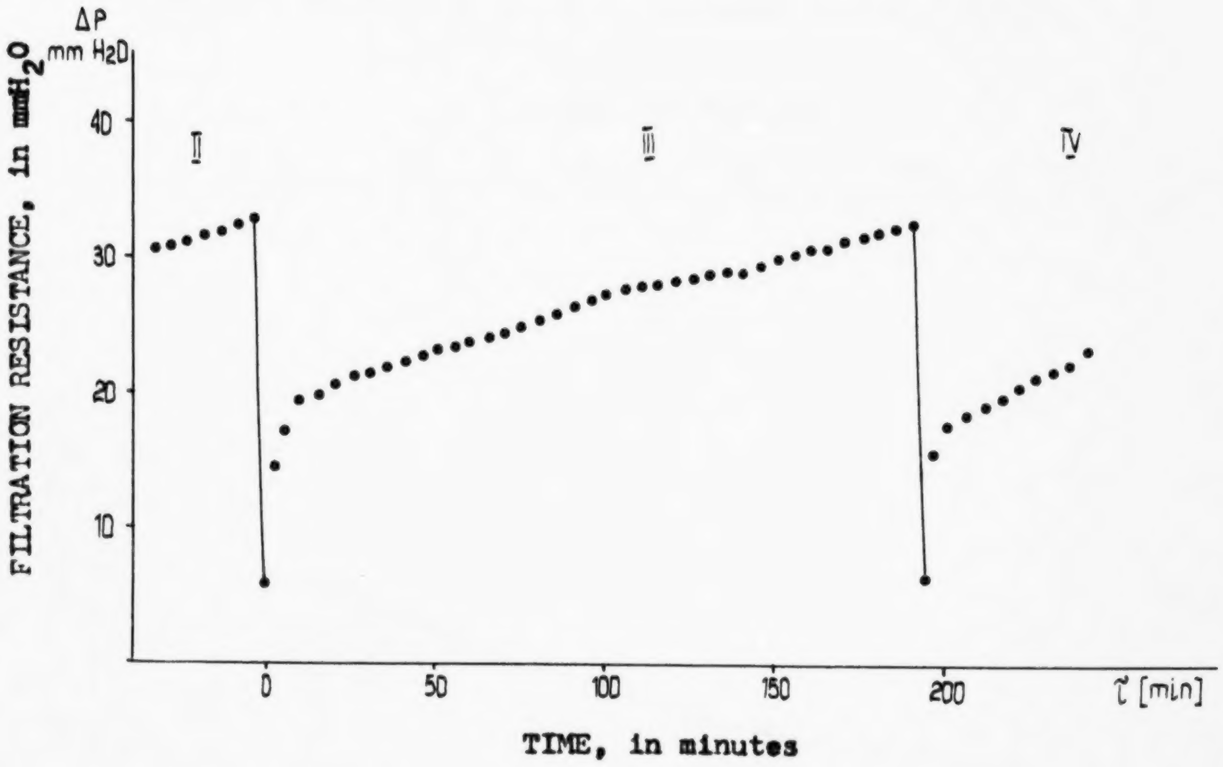

Figure 46. Variation of filtration resistance in time for fabric style no. Q53-878 (cement dust at $q_g = 60\ m^3/m^2\ hr$).

possible to control the filtration resistance, and thus the filtration process in accordance with design goals. So, the concepts developed by Stephan, Walsh, and Herrick for interpreting their results gives some indication of the differences in hydraulic effects in a dust-fabric system, but does not explain the mechanisms of the phenomena.

CONCLUSIONS

- The basic large scale tests identified the following types of fabrics as having the best filtration properties for the various test dusts:
  - Cement dust

Cotton fabric	No.	960
Polyester fabrics	Nos.	C866B C868B 865B C890B C892B
Nomex fabrics	Nos.	852 853 190R 850B
Polyamide fabric	No.	802B

  - Coal dust

Cotton fabric	No.	960
Polyester fabrics	Nos.	C866B 865B C890B C892B
Nomex fabrics	Nos.	852 190R 850B

  - Talc

Polyester fabrics	Nos.	C866B 865B C890B

Nomex fabrics	Nos. 190R 850B
Glass fabric	No. Q53-875

- Fly ash

Cotton fabric	No. 960
Polyester fabric	No. C866B
Nomex fabrics	Nos. 190R 850B
Polyamide fabric	No. 802B
Glass fabric	Nos. Q53-875 Q53-878

- Because of the hopper fractionating properties, the dust collection efficiency of the tested fabrics was actually determined for dusts of higher pulverization than the feed dust.
- The average hopper efficiencies are in the range 40 - 86 percent.
- Each dust-fabric system, depending on the kind of dust and the type of fabric, has a specific fractional efficiency (the limit grain size above which the collection efficiency is 100 percent).
- A characteristic decrease of fractional efficiencies was observed during testing of fabrics with fly ash.
- The effective drag and specific dust-fabric resistance coefficient was determined for all combinations of fabrics and dusts.
- Calculated values of S_E and K_2 have only statistical significance because they are not explicit functions of the physical parameters characterizing the process or the fabric structural parameters.

SECTION VI

STUDY OF THE REGENERATION PROPERTIES OF FABRICS

INTRODUCTION

The filtration fabric assumes the following states during its use in a fabric filter:

- Clean fabric - the fabric before initial contact with the dirty gas,
- Fully filled fabric - the used, dirty fabric after regeneration but before additional contact with the dirty gas medium. Equilibrium is assumed to have been reached in that the quantity of dust in/on the fabric is assumed to be constant from regeneration cycle to regeneration cycle. Before equilibrium is reached the fabric is simply filled with dust not fully filled.
- Covered with dust fabric - the fabric fully filled with dust and with a dust cake. Dust cake's thickness depends on time of contact with dirty gas.

These stages of filtration fabrics are determined by the resistivity (static pressure drop) of the fabric (at a constant A/C):

ΔP_o = clean fabric resistance,
ΔP_{NK} = fully filled fabric resistance, and
ΔP_K = covered with dust fabric resistance.

Employing the principle of superposition, the following relation can be assumed (at q_g = constant):

$$\Delta P_K = \Delta P_{NK} + \Delta P_W \qquad (19)$$

where ΔP_W = dust cake resistance.

This dependence is not very precise (because the real thickness of the dust cake formed on the filtration structure during the filtration process is unknown), but it is sufficient for technical purposes. Equation 19 is also of practical value in adjusting the fabric regeneration process. The covered with dust fabric resistance, the final resistance in a given filtration cycle, depends on the clean fabric resistance, the physical-chemical properties of the dust, and the A/C ratio.

Figure 47 shows a theoretical and experimental plot of filtration and regeneration processes in a bag filter, with labels identifying the characteristic values. In a theoretical plot, at a constant A/C ratio and a constant dust loading of filtration area, the filtration time of each filtration cycle is constant, which causes the final resistance in each cycle to reach the value ΔP_K = constant. However, in practice, where all values characterizing the gas and dust loads vary in time, and we can take into consideration only their means, the behavior of the hydraulic pressure drop is completely different (see Figure 48).

The duty cycle of a filtration fabric in the bag filter depends, to a great extent, on how the regeneration system is regulated. When regulation is based on constant filtration time (determined experimentally for the mean parameters of the aerosol at the dust collector inlet):

$$t'_{F1} = t'_{F2} = \ldots = t'_{Fn} \qquad (20)$$

where t'_{Fi} = filtration time of cycle i.

With this method of regulation, ΔP_K can take on arbitrary values proportional to variations of the aerosol state at the dust collector inlet (illustrated by a discontinuous line in Figure 48). In the case of periodical regulation, when the filtration time depends upon the state reached by the dust-fabric system, as characterized by the assumed and established value ΔP_K, there is:

$$t_{F1} \neq t_{F2} \neq \ldots \neq t_{Fn}. \qquad (21)$$

In this case ΔP_K is constant (illustrated by a continuous line in Figure 48). For a given concentration, the final resistance of the covered with dust fabric should be reached at a constant level of ΔP_K.

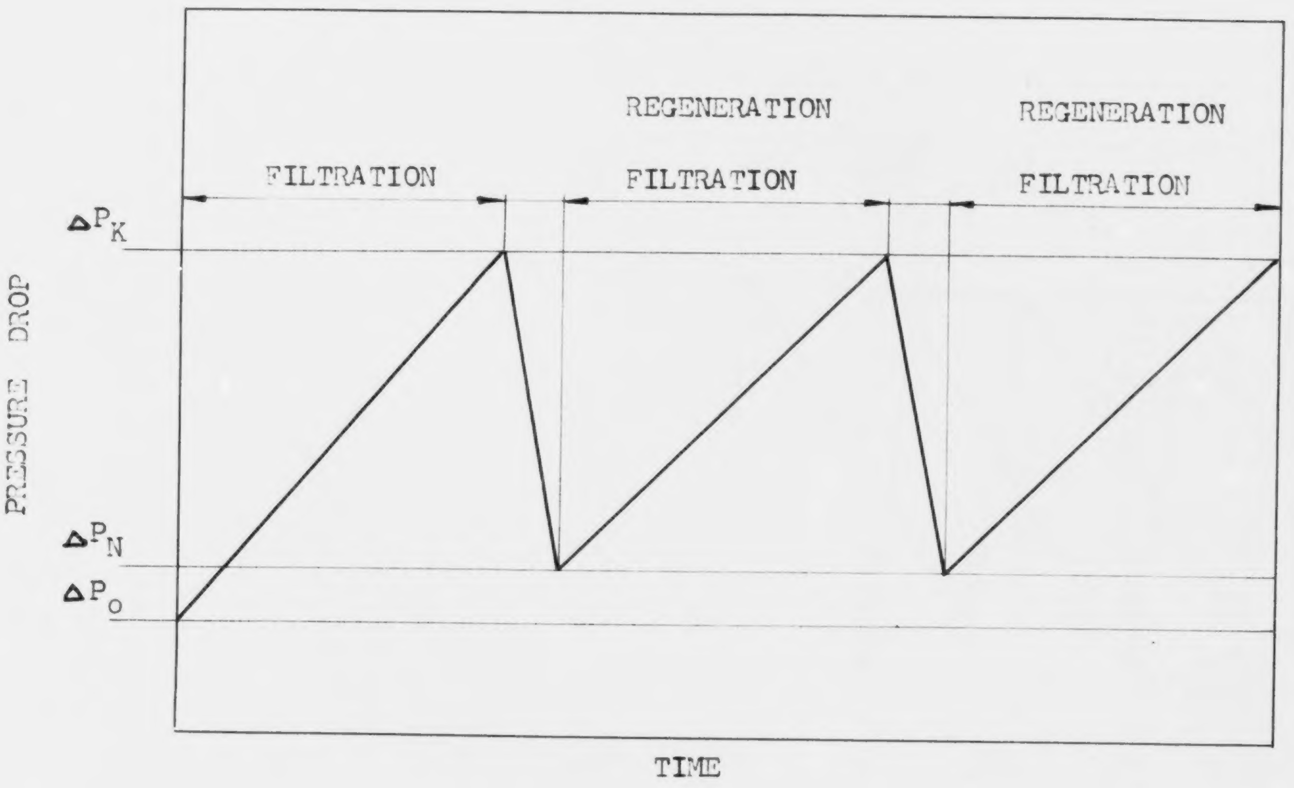

Figure 47. Theoretical plot of filtration and regeneration process.

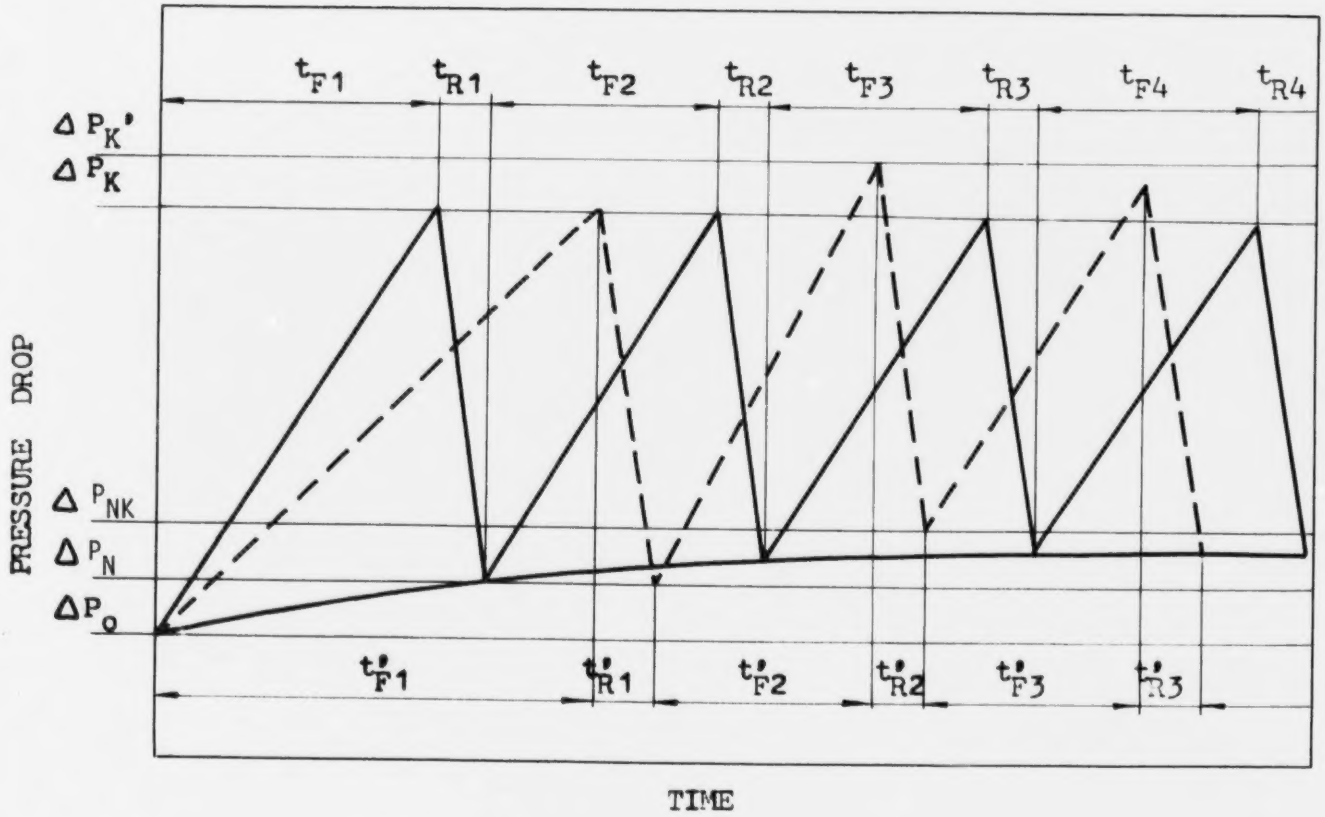

Figure 48. Realistic behavior of filtration and regeneration process.

Multiple repetition of the filtration-regeneration cycles leads to increases in the filled-fabric resistance, measured after regeneration. This increase tends towards a constant value, ΔP_{NK}, for the established methods of regeneration as a result of a fabric structure with large specific surface and thickness. It is easy to determine fabric susceptibility for regeneration by measuring the final resistance of a fully filled fabric for a specific regeneration system. To facilitate the comparison of filtration fabrics, the following formula for susceptibility for regeneration was derived (for constant q_g and q_p):

$$S_R = \left(1 - \frac{\Delta P_{NK} - \Delta P_o}{\Delta P_K - \Delta P_o}\right) \times 100 \qquad (22)$$

where ΔP_{NK} = established final fully filled fabric resistance for a definite system of regeneration, in mmH_2O,

ΔP_o = clean fabric resistance, in mmH_2O, and

ΔP_K = established final covered with dust fabric resistance, in mmH_2O.

The values of fabric susceptibility for regeneration are between 0 and 100 percent. Because the intensity of regeneration as well as the susceptibility for regeneration are complicated functions of time, as shown in Figure 49, the use of equation (22) requires standardization of the regeneration time.

RESULTS AND DISCUSSION

Estimation of the regeneration properties of the test group of fabrics was based on the susceptibility for regeneration formula (equation 22) previously noted in this section. Appropriate values of pressure drop were taken from data recorded during large scale testing as shown in Tables B-4 through B-19. The susceptibility for regeneration was calculated for four stages of the regeneration cycle as follows:

- After reverse flow regeneration, S_{RR},
- After 10 seconds mechanical shaking (vibration), S_{RM1},
- After 20 seconds mechanical shaking (vibration), S_{RM2}, and
- After 30 seconds mechanical shaking (vibration), S_{RM3}.

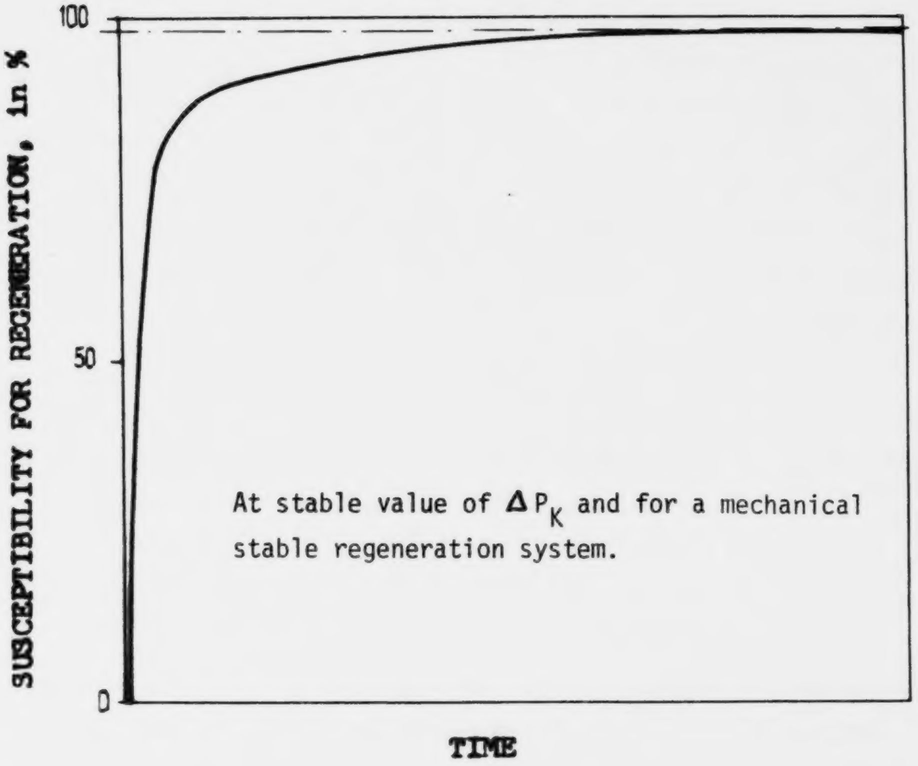

Figure 49. Theoretical plot of susceptibility for regeneration vs. time.

The test results for various test dusts and A/C's are shown in Tables 32 through 39.

Actual variations of susceptibility for regeneration as a function of time for fabrics C866B, C868B, and Q53-875, tested with cement dust at q_g = 60 m^3/m^2hr, are presented in Figure 50.

The susceptibility for regeneration, which is to a great degree a property of the filtration fabric surface, depends on adhesion effects at the fabric/dust cake interface. So it depends on fiber properties (and/or the fiber coatings), as well as dust properties. The interaction of dust

TABLE 32. SUSCEPTIBILITY FOR REGENERATION (in percent) OF FABRICS TESTED WITH CEMENT AT q_g = 60 m^3/m^2hr

Kind of fabric	Susceptibility for regeneration			
	S_{RR}*	S_{RM} †	S_{RM2}‡	S_{RM3}§
Style 960	51.14	47.03	47.03	45.21
Style 862B	78.51	82.25	85.98	89.25
Style C866B	73.42	68.92	72.97	75.68
Style C868B	61.14	62.88	65.50	65.94
Style 865B	70.50	78.93	79.69	80.84
Style C890B	89.60	92.20	91.04	91.33
Style C892B	91.00	92.60	92.60	91.96
Style 852	69.11	68.06	68.06	70.16
Style 853	58.10	49.72	50.84	51.40
Style 190R	72.07	72.07	72.07	72.07
Style 850B	79.83	92.11	93.86	93.86
Style 802B	62.29	64.00	64.00	64.00
Style Q53-875	88.74	89.01	90.38	91.21
Style Q53-870	74.54	61.93	68.24	67.54
Style Q53-878	83.41	85.25	87.40	87.40

*S_{RR} = reverse air flow regeneration.

†S_{RM1} = 10 seconds mechanical shaking.

‡S_{RM2} = 20 seconds mechanical shaking.

§S_{RM3} = 30 seconds mechanical shaking.

TABLE 33. SUSCEPTIBILITY FOR REGENERATION (in percent) OF FABRICS TESTED WITH CEMENT AT $q_g = 80$ m^3/m^{2}hr

Kind of fabric	Susceptibility for regeneration			
	S_{RR}	S_{RM1}	S_{RM2}	S_{RM3}
Style 960	59.91	50.86	48.28	48.28
Style 862B	85.93	89.52	91.62	93.41
Style C866B	76.13	73.87	76.45	79.03
Style C868B	49.21	60.20	61.18	61.84
Style 865B	84.75	67.76	77.34	80.83
Style C890B	86.79	80.75	87.93	88.74
Style C892B	86.04	76.08	85.23	85.23
Style 852	72.55	67.84	68.63	72.16
Style 853	62.40	57.85	59.09	59.09
Style 190R	82.80	81.53	78.98	78.98
Style 850B	76.98	73.48	82.32	82.51
Style 802B	75.00	66.67	68.48	68.48
Style Q53-875	86.08	88.43	95.30	95.66
Style Q53-870	71.38	63.88	75.47	73.42
Style Q53-878	88.53	85.28	91.13	91.13

TABLE 34. SUSCEPTIBILITY FOR REGENERATION (in percent) OF FABRICS TESTED WITH COAL AT $q_g = 60$ m^3/m^{2}hr

Kind of fabric	Susceptibility for regeneration			
	S_{RR}	S_{RM1}	S_{RM2}	S_{RM3}
Style 960	58.20	55.40	55.40	55.40
Style 862B	83.90	83.90	84.60	85.00
Style C866B	79.60	78.70	80.10	81.50
Style C868B	78.40	78.00	77.30	77.30
Style 865B	82.20	75.90	77.10	78.30
Style C890B	83.30	83.30	79.50	78.60
Style C892B	86.10	85.50	84.70	84.70
Style 852	75.20	73.20	72.40	73.20
Style 853	70.90	68.40	69.60	69.60
Style 190R	80.60	77.50	77.50	79.40
Style 850B	77.30	74.00	71.70	70.00
Style 802B	77.40	75.30	74.70	75.30
Style Q53-875	89.10	84.30	84.90	85.50
Style Q53-870	76.60	69.20	66.70	64.70
Style Q53-878	88.90	85.80	85.10	85.10

TABLE 35. SUSCEPTIBILITY FOR REGENERATION (in percent) OF FABRICS TESTED WITH COAL AT q_g = 80 m^3/m^2hr

Kind of fabric	Susceptibility for regeneration			
	S_{RR}	S_{RM1}	S_{RM2}	S_{RM3}
Style 960	62.80	57.70	56.50	55.00
Style 862B	84.50	82.00	82.90	83.80
Style C866B	83.10	81.40	81.60	82.40
Style C868B	80.70	78.90	80.30	81.00
Style 865B	86.60	86.90	85.90	85.90
Style C890B	85.90	76.70	75.40	74.40
Style C892B	83.10	77.50	73.90	76.90
Style 852	84.20	84.60	82.70	83.80
Style 853	76.30	69.80	68.30	67.80
Style 190R	84.10	79.30	80.90	81.90
Style 850B	77.40	60.90	64.60	67.30
Style 802B	75.70	74.50	74.50	74.50
Style Q53-875	88.40	80.40	80.40	82.00
Style Q53-870	84.80	79.50	79.50	80.40
Style Q53-878	92.20	92.40	91.80	91.80

TABLE 36. SUSCEPTIBILITY FOR REGENERATION (in percent) OF FABRICS TESTED WITH TALC AT q_g = 60 m^3/m^2hr

Kind of fabric	Susceptibility for regeneration			
	S_{RR}	S_{RM1}	S_{RM2}	S_{RM3}
Style 960	67.30	63.60	61.40	61.40
Style 862B	81.10	81.10	82.70	83.70
Style C866B	77.10	78.00	74.80	74.80
Style C868B	68.90	70.90	69.40	69.90
Style 865B	79.20	79.50	79.50	80.10
Style C890B	70.20	69.10	71.30	72.40
Style C892B	75.90	70.90	73.90	74.70
Style 852	86.30	90.60	89.80	90.00
Style 853	43.40	40.40	38.20	38.20
Style 190R	83.10	79.50	78.70	78.70
Style 850B	64.30	65.30	65.10	64.50
Style 802B	70.30	63.60	63.20	63.20
Style Q53-875	77.60	72.70	79.10	80.90
Style Q53-870	67.10	63.00	63.00	62.50
Style Q53-878	73.90	70.70	70.70	71.50

TABLE 37. SUSCEPTIBILITY FOR REGENERATION (in percent) OF FABRICS TESTED WITH TALC AT q_g = 80 m^3/m^2hr

Kind of fabric	Susceptibility for regeneration			
	S_{RR}	S_{RM1}	S_{RM2}	S_{RM3}
Style 960	63.20	61.30	60.70	60.70
Style 862B	85.90	83.80	84.40	85.00
Style C866B	78.10	73.40	75.20	77.10
Style C868B	68.70	62.20	62.60	63.70
Style 865B	83.50	77.80	78.00	78.60
Style C890B	80.10	71.70	71.20	71.90
Style C892B	84.60	85.20	90.30	91.70
Style 852	74.60	54.90	59.20	60.60
Style 853	57.50	56.30	57.30	57.30
Style 190R	80.50	78.50	77.90	78.50
Style 850B	73.10	69.50	68.60	68.90
Style 802B	68.90	64.80	63.90	64.80
Style Q53-875	86.10	80.70	79.20	80.20
Style Q53-870	75.00	71.30	69.60	69.90
Style Q53-878	77.70	74.20	73.80	74.20

TABLE 38. SUSCEPTIBILITY FOR REGENERATION (in percent) OF FABRICS TESTED WITH FLY ASH AT q_g = 60 m^3/m^2hr

Kind of fabric	Susceptibility for regeneration			
	S_{RR}	S_{RM1}	S_{RM2}	S_{RM3}
Style 960	43.48	21.74	23.37	29.35
Style 862B	68.35	75.54	77.70	79.86
Style C866B	46.81	32.62	38.30	40.43
Style C868B	58.06	57.42	58.06	60.00
Style 865B	69.80	66.83	72.77	75.25
Style C890B	73.48	62.72	70.25	75.27
Style C892B	69.83	72.20	58.98	91.52
Style 852	66.23	72.85	73.51	76.82
Style 853	--	--	--	--
Style 190R	56.58	56.58	59.21	56.58
Style 850B	65.57	58.61	63.11	63.11
Style 802B	62.34	29.22	37.66	42.21
Style Q53-875	59.76	59.36	57.54	52.99
Style Q53-870	55.59	60.61	56.17	51.95
Style Q53-878	64.00	64.00	65.33	64.00

TABLE 39. SUSCEPTIBILITY FOR REGENERATION (in percent) OF FABRICS TESTED WITH FLY ASH AT $q_g = 80\ m^3/m^2hr$

Kind of fabric	Susceptibility for regeneration S_{RR}	S_{RM1}	S_{RM2}	S_{RM3}
Style 960	56.62	47.44	45.30	45.30
Style 862B	66.89	78.15	81.46	84.11
Style C866B	60.19	43.06	46.76	49.54
Style C868B	64.10	61.54	61.54	62.56
Style 865B	63.91	62.69	69.42	71.87
Style C890B	79.57	77.40	79.09	79.09
Style C892B	77.94	74.82	78.90	77.70
Style 852	58.25	6.31	8.74	11.17
Style 853	--	--	--	--
Style 190R	70.83	15.62	15.62	17.71
Style 850B	62.09	65.35	64.19	63.95
Style 802B	51.98	47.46	48.02	48.02
Style Q53-875	79.82	73.54	76.91	77.80
Style Q53-870	74.52	85.75	86.45	88.08
Style Q53-878	73.21	66.07	68.57	68.57

particles and fibers is conditioned by different kinds of mechanisms. The main mechanisms causing adhesion effects are molecular forces, electrostatic forces, and capillary attraction. In dry filtration the role of capillary forces is much less than that of electrostatic effects. The testing conducted at our Institute confirms the great influence of electrostatic effects not only on filtration fabric efficiency, but also on susceptibility for regeneration.

For preliminary interpretation of the calculated values of susceptibility for regeneration, the following criteria (based on experimental results obtained up to now) were developed:

- Susceptibility for regeneration $S_R \geq 80$ percent is good,
- Susceptibility for regeneration $80 > S_R > 70$ percent is satisfactory,
- Susceptibility for regeneration $S_R \leq 70$ percent is bad.

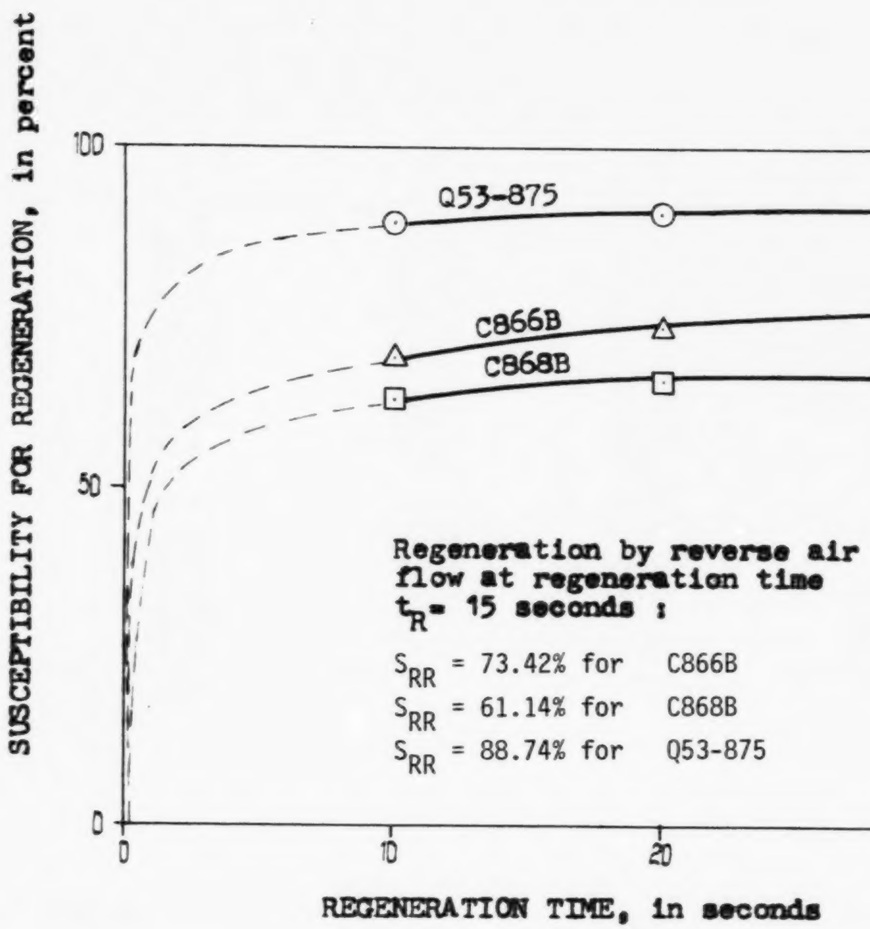

Figure 50. Empirical time dependence of susceptibility for regeneration during mechanical regeneration (cement dust, q_g = 60 m³/m² hr).

Table 40 classifies the fabrics according to their susceptibility for regeneration with various dusts at the given A/C ratio.

Because each fabric was tested over 16 experimental conditions (4 kinds of dust, 2 levels of q_g, 2 regeneration systems), the percent of experiments where the fabric could be regarded as good or satisfactory, from the regeneration viewpoint, was calculated.

The fabrics that in at least 50 percent of the 16 experiments can be regarded as having good S_R, are as follow.

Fabric	Percent of cases showing good regeneration
862B	68.7
Q53-875	56.2
Q53-878	50
C890B	50
C892B	50

The fabrics that in at least 50 percent of the 16 experiments show satisfactory regeneration properties are as follow.

Fabric	Percent of cases showing satisfactory regeneration
862B	87.5
C892B	87.5
C890B	81.3
Q53-875	75
Q53-878	75
190R	75
C866B	68.7
865B	68.7
852	56.2
Q53-870	56.2
850B	50

As can be gathered from these data, the best regeneration properties are shown by fabrics with polyester and glass fibers. Nomex fabrics have only average regeneration properties. Because the group of fabrics with good regeneration properties include both continuous filament and staple fiber fabrics, it can be presumed that the fiber style does not influence the regeneration properties as much as the applied weave and the fabric finishing.

TABLE 40. REGENERATION PROPERTIES OF TESTED FABRICS

Regeneration system	Kind of dust	A/C (in m^3/m^2hr)	Susceptibility for regeneration	
			Good	Satisfactory
Reverse air flow	cement	60	C890B C892B Q53-875 Q53-878	862B C866B 865B 190R 850B Q53-870
		80	862B 865B C890B C892B 190R Q53-875 Q53-878	C866B 852 850B 802B Q53-870
	Unsep. coal	60	862B 865B C890B C892B 190R Q53-875 Q53-878	C866B C868B 852 853 850B 802B Q53-870
		80	862B C866B C868B 865B C890B C892B 852 190R Q53-875 Q53-870 Q53-878	853 850B 802B
	Talc	60	862B 852 190R	C866B 865B C890B C892B

(continued)

TABLE 40. (continued)

Regeneration system	Kind of dust	A/C (in m^3/m^{2}hr)	Susceptibility for regeneration	
			Good	Satisfactory
				802B Q53-875 Q53-878
		80	862B 865B C890B C892B 190R Q53-875	C866B 852 850B Q53-870 Q53-878
	Fly ash	60	--	C890B
		80	--	C890B C892B 190R Q53-875 Q53-870 Q53-878
Mechanical (10 sec. vibration)	Cement	60	862B C890B C892B 850B Q53-870 Q53-878	865B 190R
		80	862B C890B 190R Q53-875 Q53-878	C866B C892B 850B
	Unsep. Coal	60	862B C890B C892B Q53-875 Q53-878	C866B C868B 865B 852 190R 850B

(continued)

TABLE 40. (continued)

Regeneration system	Kind of dust	A/C (in m^3/m^2hr)	Susceptibility for regeneration	
			Good	Satisfactory
				802B
		80	862B C866B 865B 852 Q53-875 Q53-878	C868B C890B C892B 190R 802B Q53-870
	Talc	60	862B 852	C866B C868B 865B C892B 190R Q53-875 Q53-878
		80	862B C892B Q53-875	C866B 865B C890B 190R Q53-870 Q53-878
	Fly ash	60	--	862B C892B 852
		80	Q53-870	862B C890B C892B Q53-875

Overall, mechanical regeneration exhibits lower susceptibility for regeneration than regeneration with reverse air flow, although in some cases, the opposite was observed. However, it should be pointed out that the longer mechanical regeneration time (longer than 10 seconds) generally did not increase the regeneration effects. So, the hypothesis can be made that the most important factor is the first impulse applied to the dust/cake fabric interface.

Concerning the problem of correlating regeneration susceptibility with the kind of test dust, the worst results were obtained for fly ash. There were no fabrics that could be regarded as having good susceptibility for regeneration with fly ash and there were only six fabrics that showed satisfactory regeneration properties. Both regeneration systems were investigated. It is interesting that the group of fabrics with satisfactory regeneration properties included all three glass fabrics which were designed especially for filtration of gas containing fly ash. The relationship between susceptibility for regeneration and the kind of dust should be the object for more detailed examinations.

At present it can be said that the fiber plastic, the grain shape, and the difference in fractional composition are decisive in this matter. All the cases discussed above are connected with the adhesion phenomenon (electrostatic effects) that appear at the boundary between the fiber surface and the dust grain surface. Figure 51 is a comparison of dust grain shapes and individual grain surfaces.

CONCLUSIONS

The experiments described above lead to the following conclusions concerning fabric regeneration susceptibility and regeneration systems.

- The regeneration properties depend upon the kind of dust, the kind of plastic of the filtration structure, the kind of weave, and the method of fabric finishing.
- To obtain good regeneration, mixed regeneration systems should be applied--only under certain conditions should a single regeneration system be applied, e.g., regeneration of glass fabrics with reverse air flow.

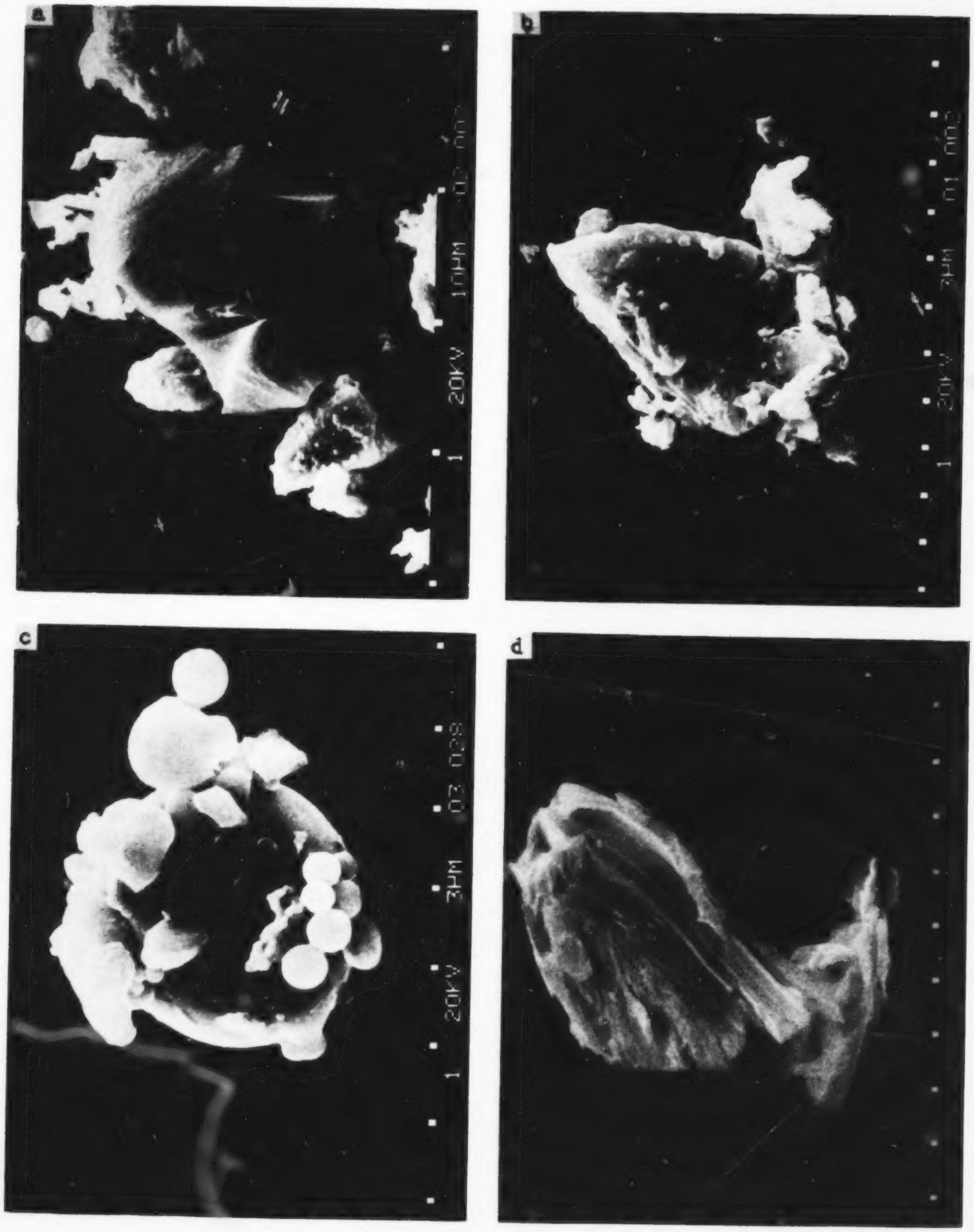

Figure 51. Microscopic pictures of testing dusts (a-cement, b-coal, c-fly ash, d-talc).

Photo credit: SEM by K. Skudlanski, Electronic Microscopy Laboratory of Wrocław Polytechnic.

- Mechanical regeneration using vibration is most effective during the initial part of the regeneration process. Hence, longer regeneration time does not increase the regeneration effects but can reduce the life of the filtration material.
- Overall fly ash showed the worst regeneration properties, being considerably lower in regeneration susceptibility than the other dusts tested.

SECTION VII

COMPARISON OF THE FILTRATION PROPERTIES OF POLISH AND U.S. FABRICS

INTRODUCTION

The analysis and comparison of the filtration properties of the Polish and U.S. fabrics presented in this section was based on results of laboratory and large scale testing conducted during this project and on previously obtained data (from Polish fabrics). Advantage was also taken of results of Polish polyester and polyamide fabric testing conducted during Project 5-533-3 (testing with initial concentration $c_i = 10\ g/m^3$). (The testing conditions for Polish fabrics conducted during the years 1969 - 1974 differed from those assumed for Projects 5-533-3 and 5-533-4).

First of all, the experiments in both the laboratory and on large scale were conducted with dusts having fractional composition as well as other physical-chemical properties the same as those of dusts sampled directly from specific points of the appropriate technological process. The basic test dusts were cement, coal, and hydrated lime. Some experiments were carried out on dusts from rotary kilns (with the dust precipitated in the dust collection systems) and from limestone grinding.

The test conditions were as follow:

- Initial concentration: 30 g/m^3.
- A/C ratio: 60, 80, and 120 m^3/m^2hr.
- Dust covering of filtration structure: 100, 400, and 700 g/m^2.
- Temperature: irregular.
- Humidity: ambient.
- Dispersing medium: atmospheric air at ambient temperature.

Because of the higher initial concentrations (U.S. fabrics were tested at $c_i = 10\ g/m^3$), the Polish fabrics were tested at higher dust loading of filtration area $q_p = 1800 - 3600\ g/m^2hr$.

Taking into consideration the above differences in the test conditions, the comparison of Polish and U.S. fabrics is general rather than complete because some parameters cannot be compared.

ANALYSIS OF FILTRATION PROPERTIES

The analysis of filtration properties concerns the definite material groups of fabrics. Figures 52 through 65 represent the qualitative properties of fabrics such as:

- Efficiency, outlet concentration, and filtration resistance obtained on laboratory scale,
- Efficiency, outlet concentration, and filtration resistance obtained on large scale, and
- Fabric filling and resistance of filled structure on laboratory and large scale.

The data show test results at an A/C ratio of $q_g = 60\ m^3/m^2hr$ and a structure covered with cement dust, $L_o = 400\ g/m^2$. The basic technical data concerning Polish fabrics were added as auxiliary material (Table B-21). As can be seen from the comparison, Polish as well as U.S. fabrics are characterized by very high dust collection efficiency.

Natural Fiber Fabrics

This group was represented by wool and cotton fabrics.

- Wool: WT-202 and WT-203
- Cotton: BT-57 and Cotton 960.

At high dust collection efficiency, the natural fiber fabrics showed different filtration resistances and quite high structure filling. U.S. cotton 960 and Polish BT-57 have similar dust collection efficiencies of 99.9 percent. The lower filtration resistances of fabric BT-57 result from its testing with dusts of lower pulverization (MMD = 36 μm).

Polyester Fabrics

The group of polyester fabrics was represented by:

- Staple fiber polyester fabrics

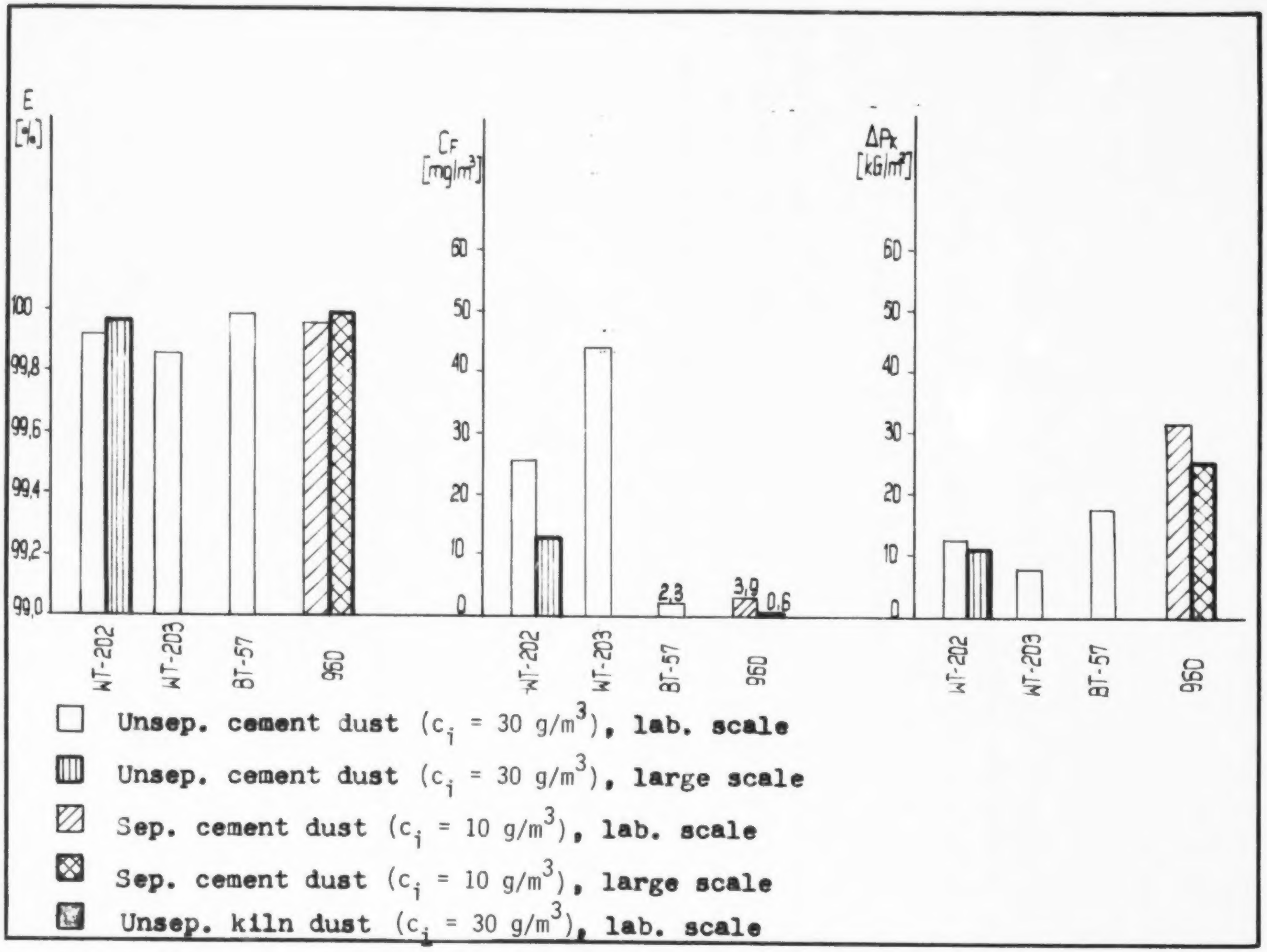

Figure 52. Comparison of filtration properties of Polish and U.S. fabrics (wool, cotton).

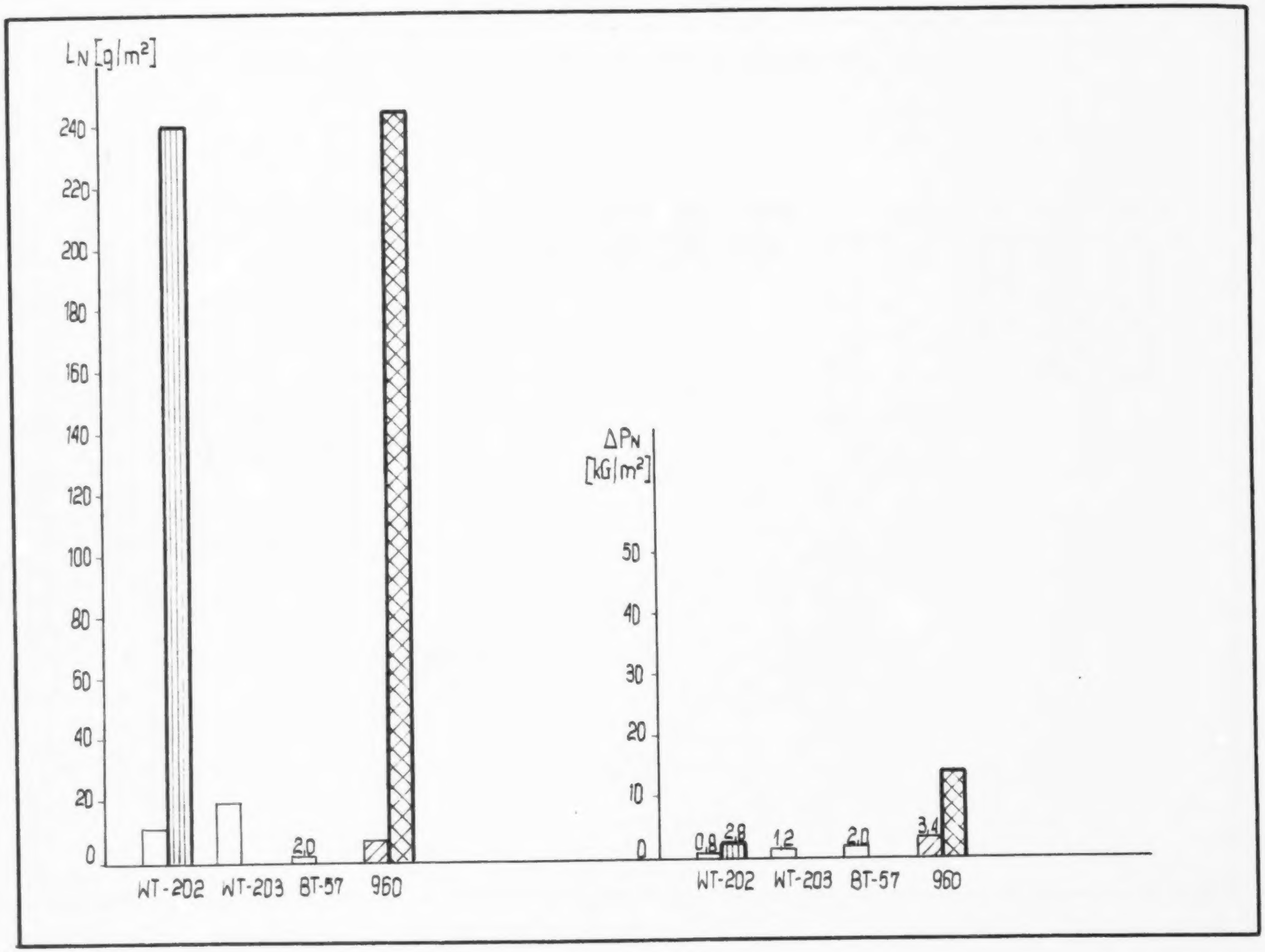

Figure 53. Comparison of regeneration properties of Polish and U.S. fabrics (wool, cotton).

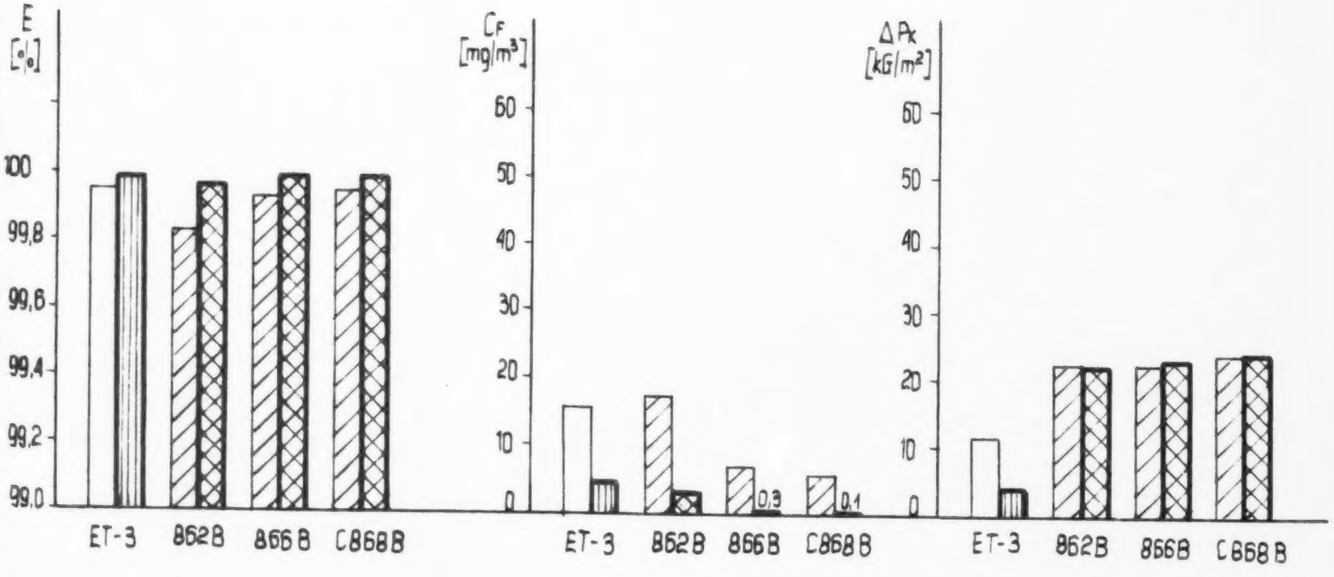

Figure 54. Comparison of filtration properties of Polish and U.S. polyester fabrics.

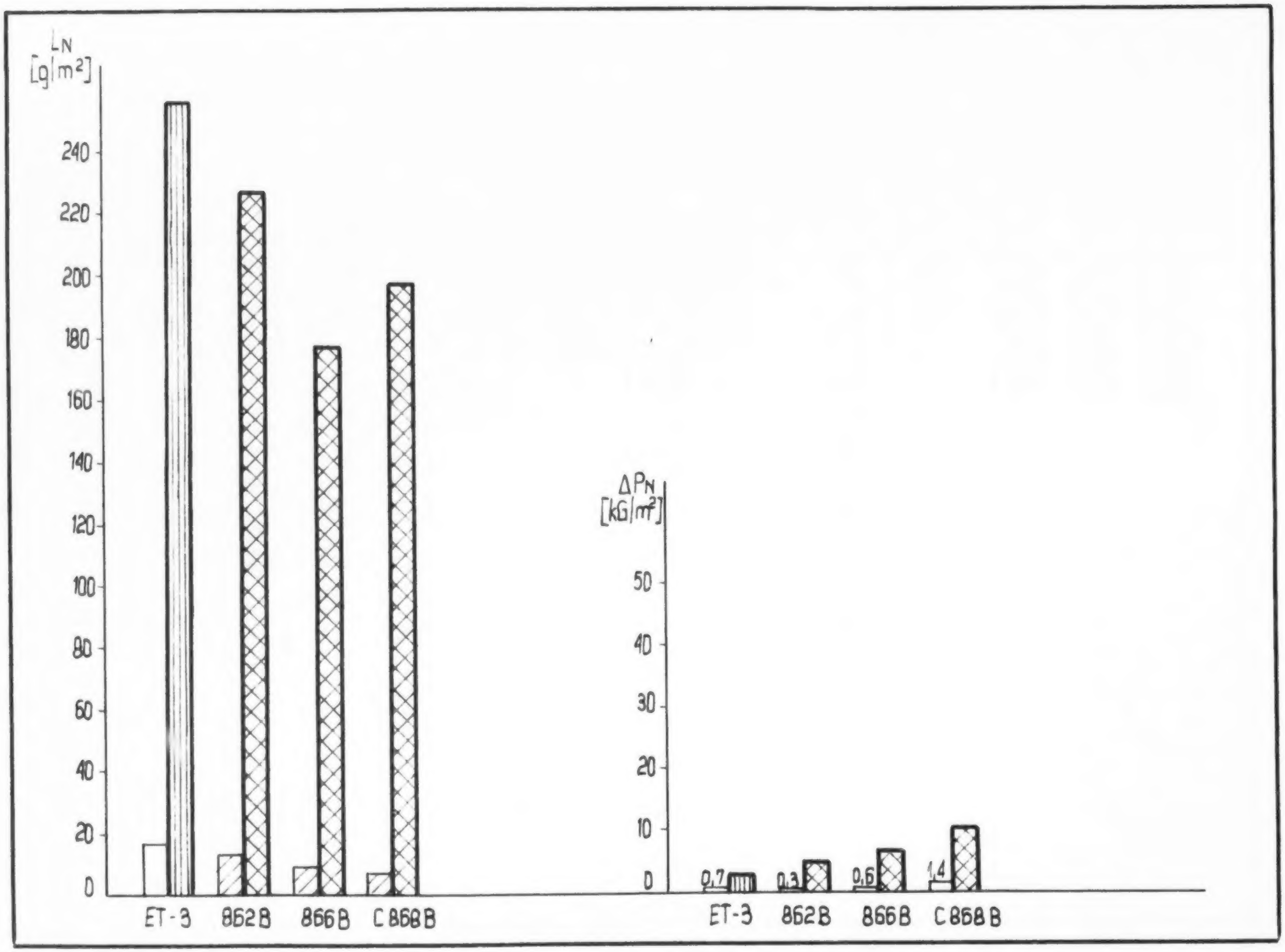

Figure 55. Comparison of regeneration properties of Polish and U.S. polyester fabrics.

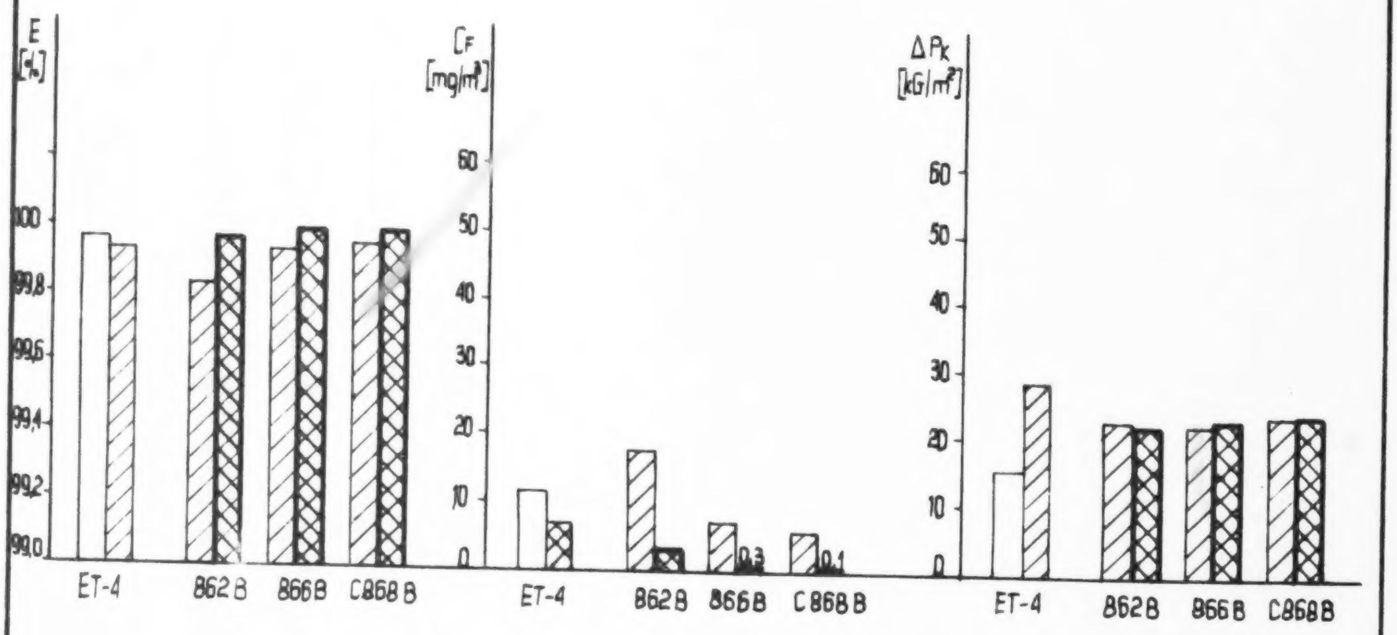

Figure 56. Comparison of filtration properties of Polish and U.S. polyester fabrics.

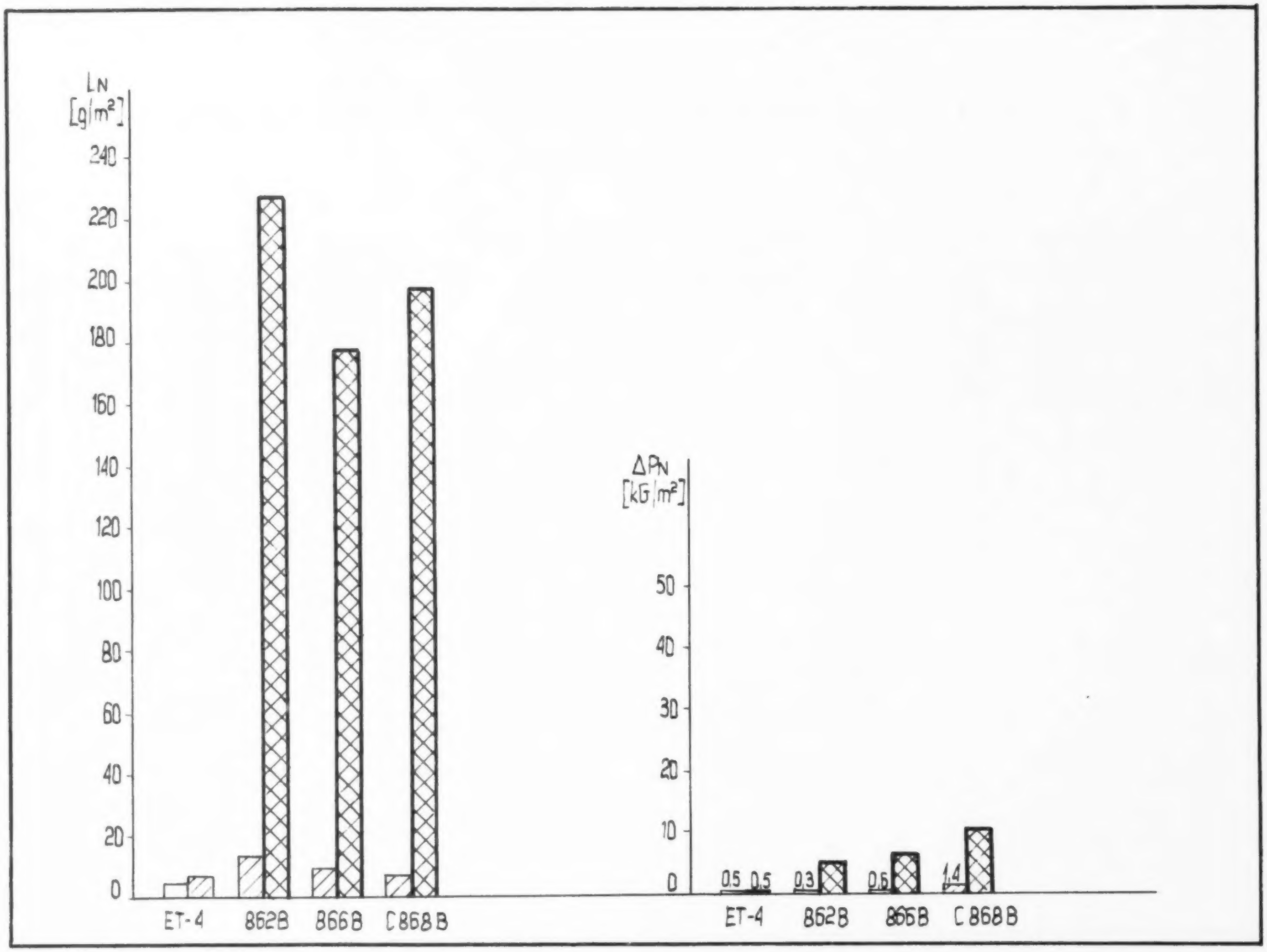

Figure 57. Comparison of regeneration properties of Polish and U.S. polyester fabrics.

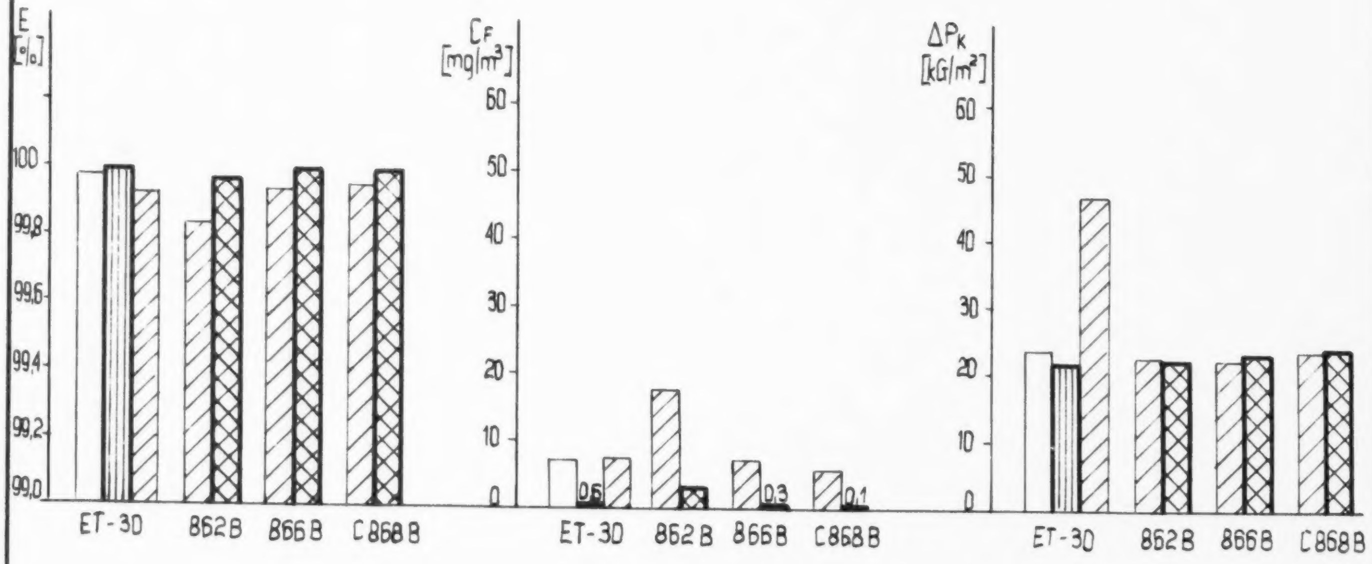

Figure 58. Comparison of filtration properties of Polish and U.S. polyester fabrics.

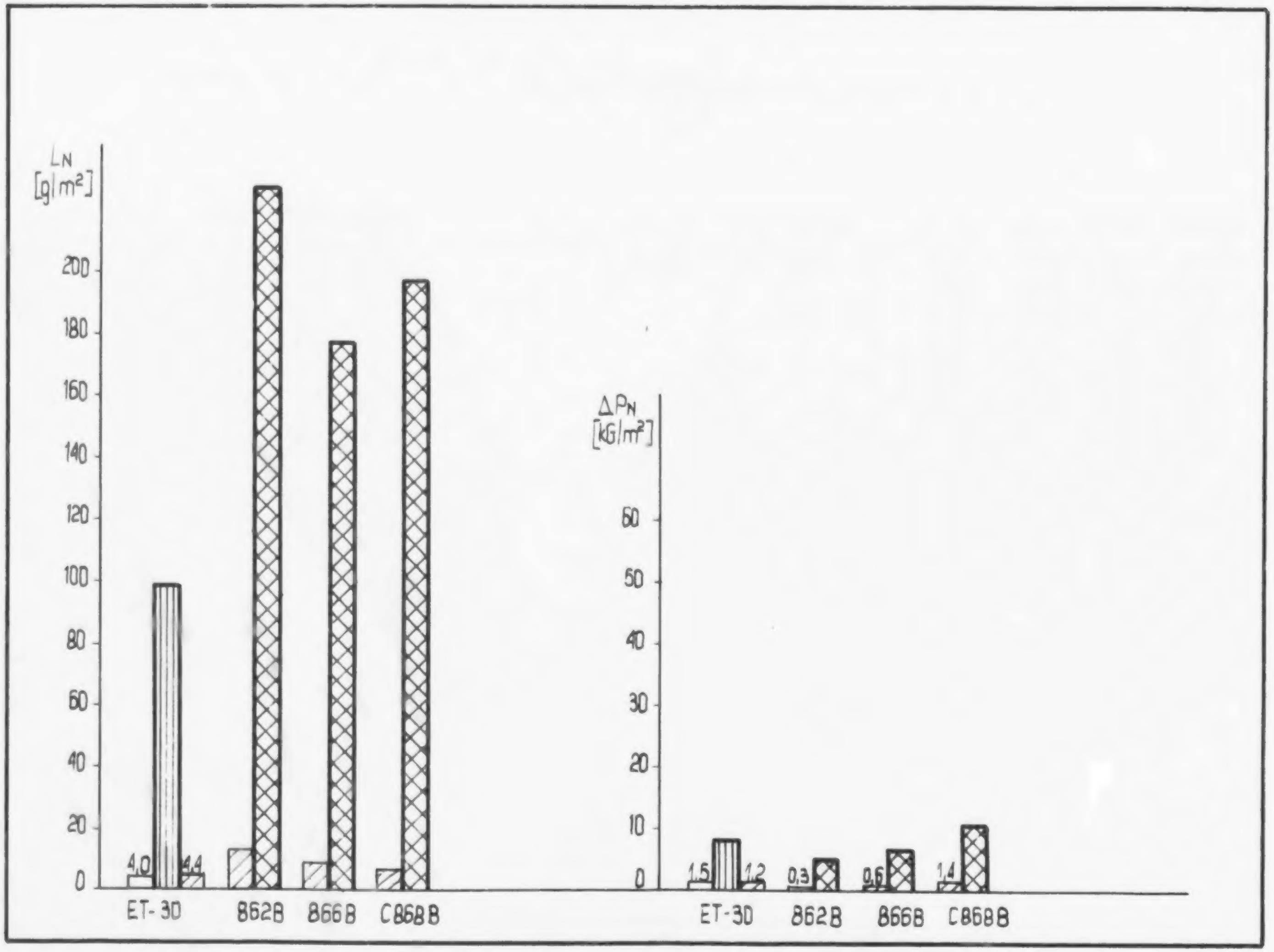

Figure 59. Comparison of regeneration properties of Polish and U.S. polyester fabrics.

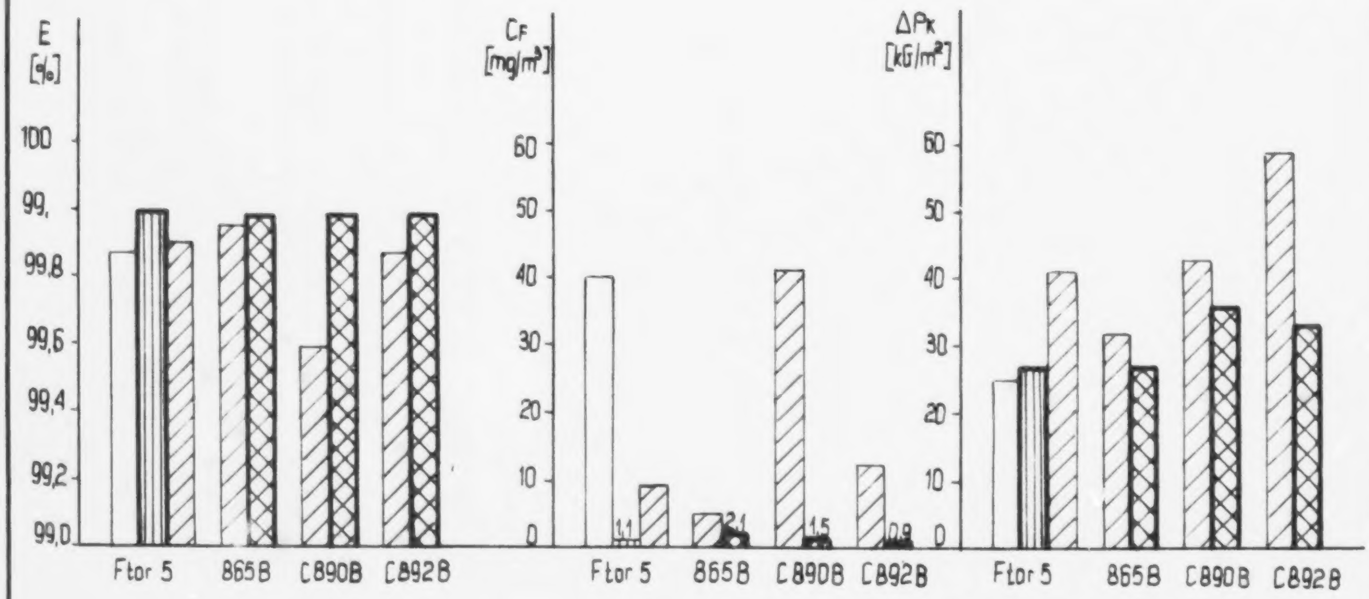

Figure 60. Comparison of filtration properties of Polish and U.S. polyester fabrics.

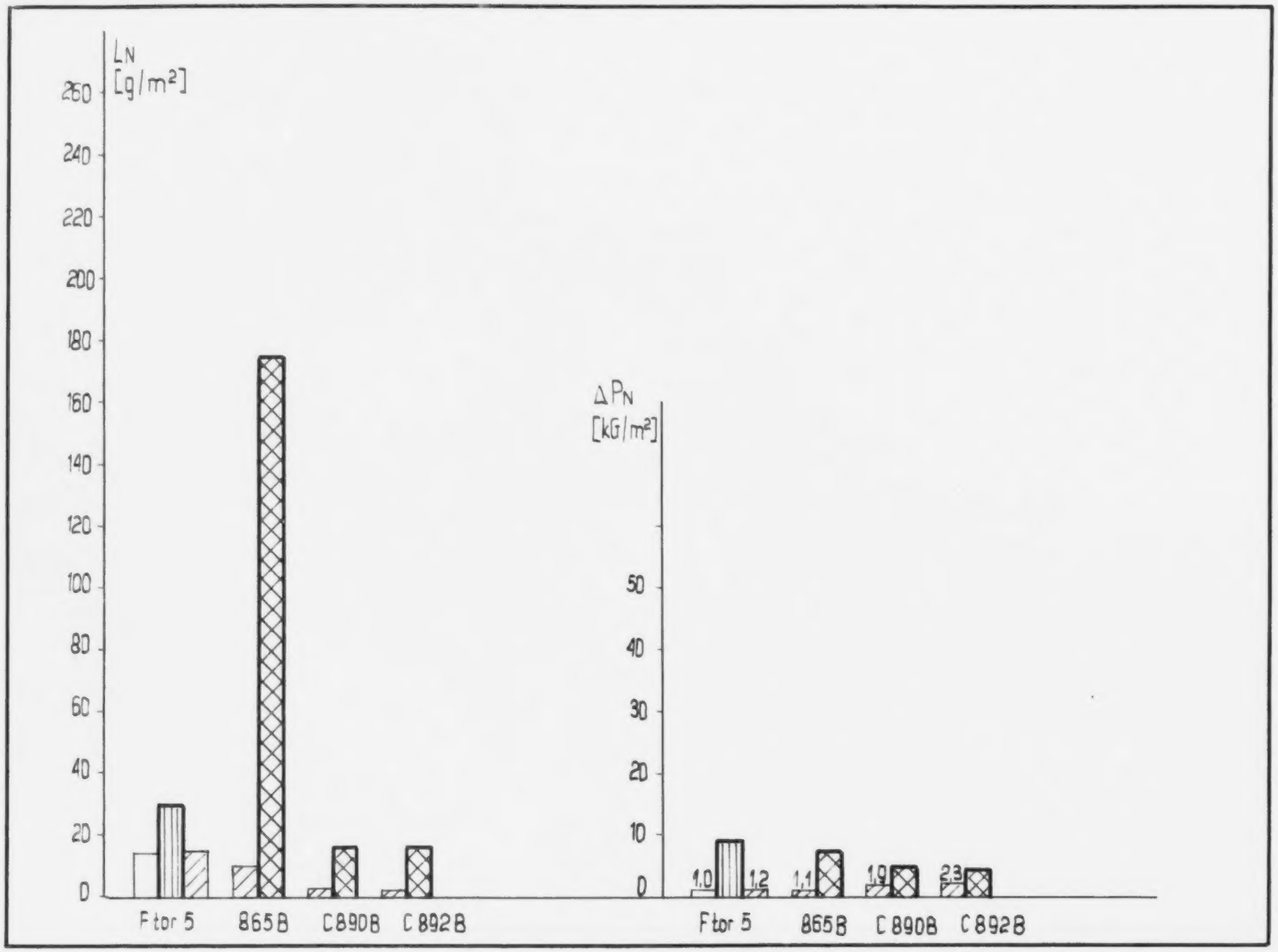

Figure 61. Comparison of regeneration properties of Polish and U.S. polyester fabrics.

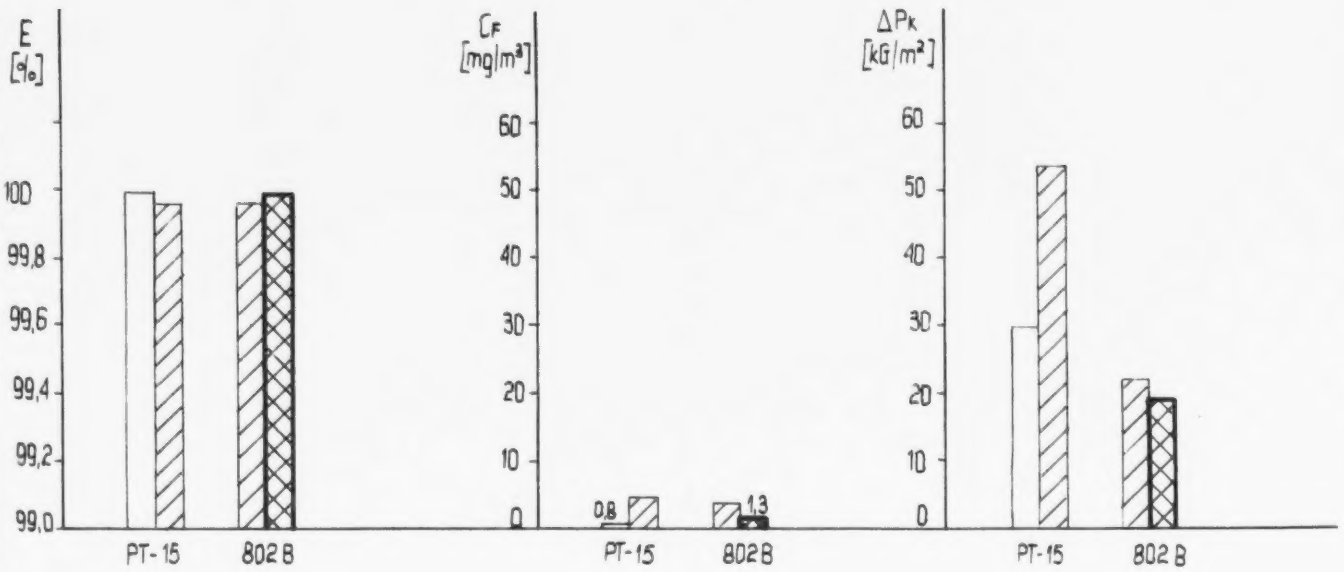

Figure 62. Comparison of filtration properties of Polish and U.S. polyamide fabrics.

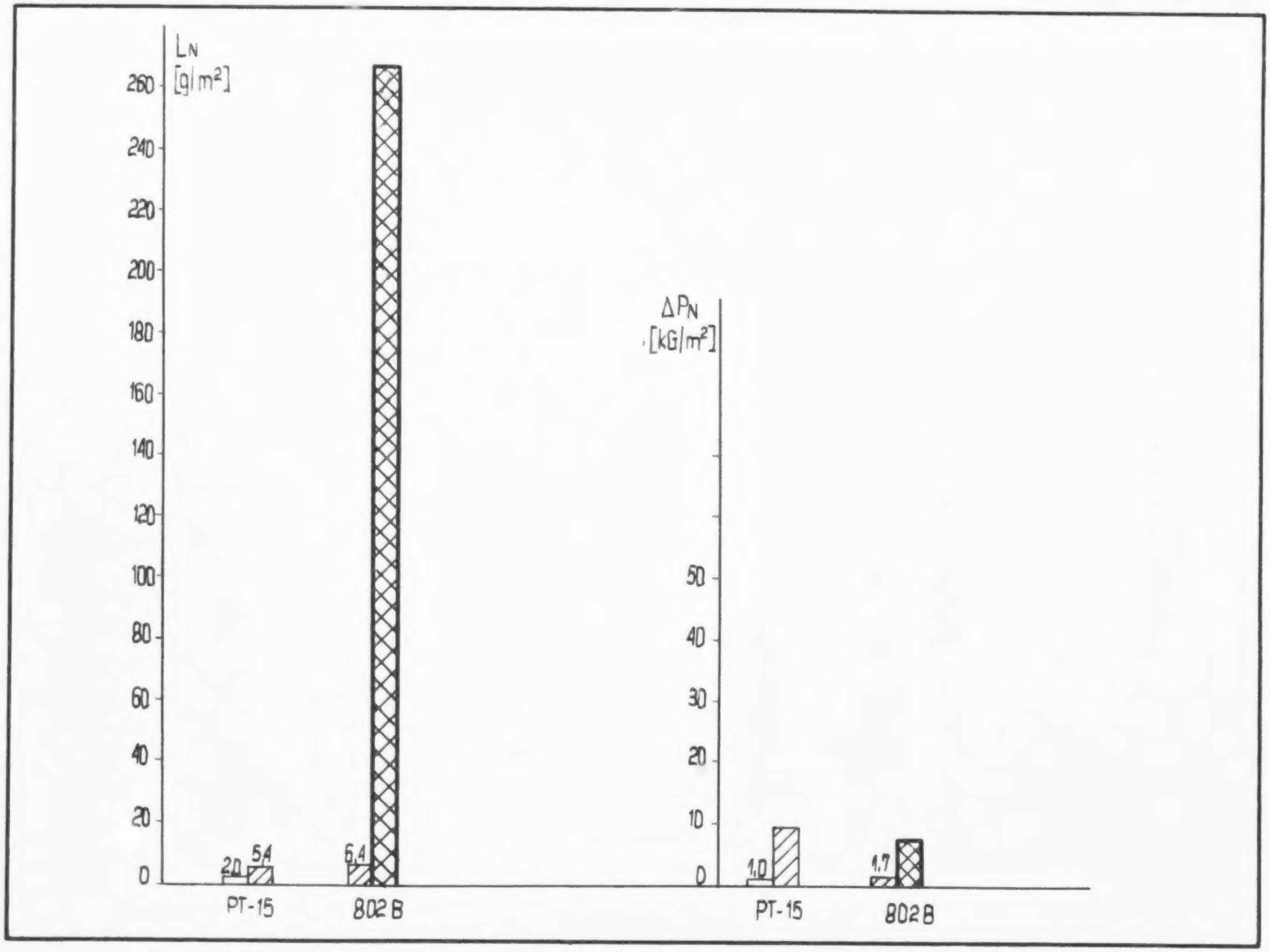

Figure 63. Comparison of regeneration properties of Polish and U.S. polyamide fabrics.

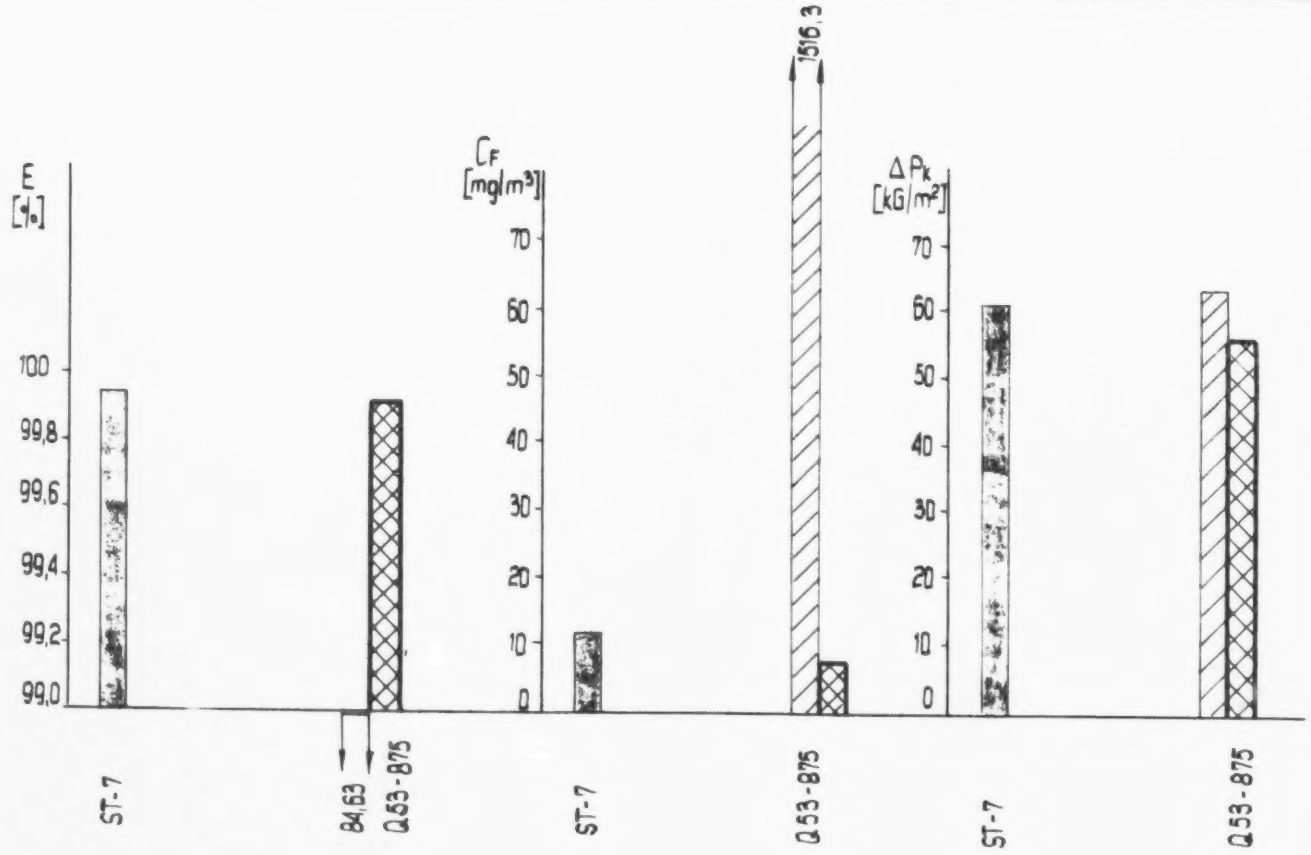

Figure 64. Comparison of filtration properties of Polish and U.S. glass fabrics.

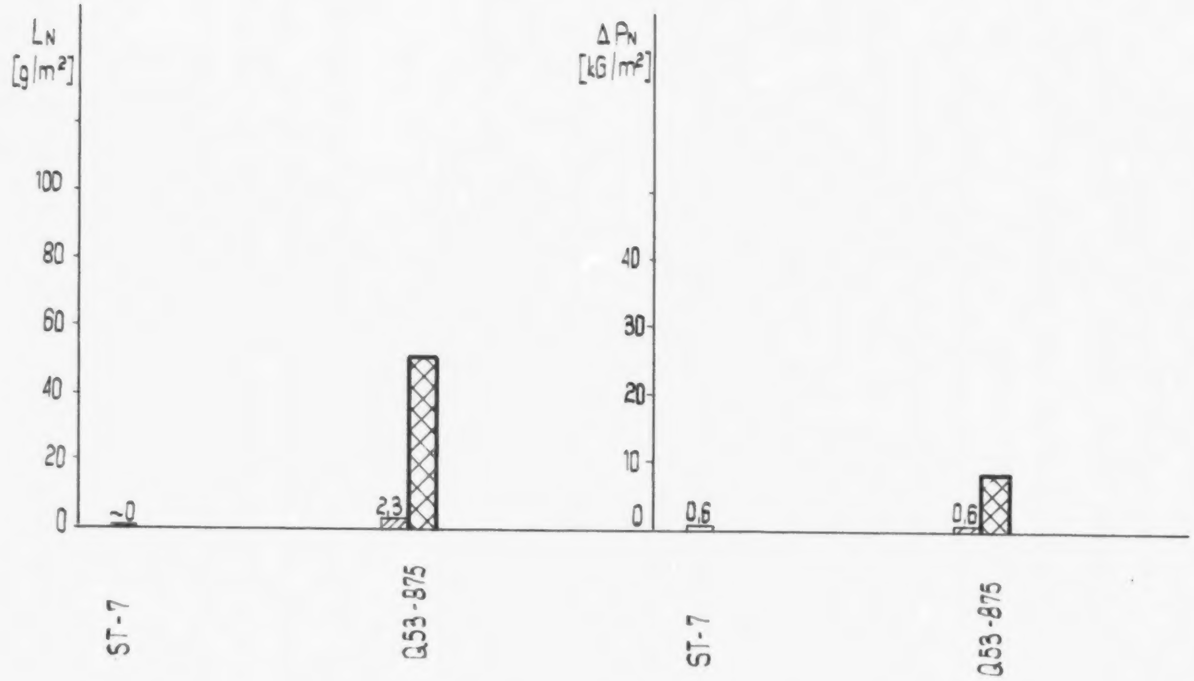

Figure 65. Comparison of regeneration properties of Polish and U.S. glass fabrics.

ET-3, ET-4, ET-30 - Polish production,
862B, C866B, C868B - U.S. production,

- Continuous filament polyester fabrics
  F-tor 6 - Polish production,
  865B, C890B, C892B - U.S. production.

Polyester fabrics are most often used in industrial dust collectors because of the advantages of polyester fiber.

Staple fiber polyester fabrics have filtration properties similar to natural fabrics, but have much higher mechanical strength. The fabric structure favors high efficiencies and low filtration resistivities. Regarding filtration properties, fabric ET-30 produced for the cement industry equals U.S. fabrics C866B and C868B. Higher filtration resistances for finer dusts, compared to those of fabrics C866B and C868B, result from its more compact structure. Compared to staple fiber fabrics, the continuous filament fabrics show lower filling of structure (L_N) and higher filtration resistances.

Dust collection efficiency, after reaching a steady state, is also very high, but to a larger degree depends upon q_g because of the "basket effect" and interyarn areas (in plain fabric). Fabric F-tor 5 showed filtration properties similar to U.S fabrics C890B and C892B.

Polyamide Fabrics

This group of fabrics is represented by two fabrics: U.S. staple fiber fabric 802B and Polish continuous filament fabric PT-15. Dust collection efficiencies are on the same level, but fabric PT-15 showed higher filtration resistance. The same reasons as stated above caused lower filling of structure (L_N) of fabric PT-15 than of fabric No. 802B.

Glass Fabrics

Figures 64 and 65 show the results of the Polish prototype glass fabric tested with dust from the rotary kiln (MMD = 16 μm) at $q_g = 80\ m^3/m^2hr$ (laboratory scale). This fabric is produced as fabric ST-7. Similar to Q53-875, this fabric is also manufactured with staple fibers. The finishing of the fabrics is different: prototype ST-7 is silicated and fabric Q53-875 is graphited.

Because of large differences in the test conditions, it is nearly impossible to compare filtration properties. Prototype ST-7 was tested in industrial conditions, yielding a dust collection efficiency of 99.95 percent at $q_g = 45\ m^3/m^2hr$ and MMD = 8 - 20 μm, at an average gas temperature of 260° C. Based on these results, it can be said that this fabric has very good filtration properties.

CONCLUSIONS

Comparison of Polish and U.S. woven filtration fabrics, made of different materials, confirms their very good filtration properties in all analyzed cases. Also, the conclusion can be made that the woven filtration fabrics are good filter media for industrial applications. Apart from good filtration properties, they have high mechanical strength, which in industrial conditions results in long periods of operation. From a costs viewpoint, the polyester fabrics are the most attractive for engineering applications.

REFERENCES

1. Davies, C. N. Aerosol Science. Academic Press, London and New York. 1966.

2. Kościanowski, J. R., and L. Kościanowska. Effect of Filtration Parameters on Dust Cleaning Fabrics, Phase I. EPA-600/2-76-074, U.S. Environmental Protection Agency, March 1976.

3. Kościanowski, J. R., and L. Kościanowska. Effect of Filtration Parameters on Dust Cleaning Fabrics, Phase II. (in press).

4. Kościanowski, J. R., L. Kościanowska, and M. Szablewicz. Test of Fabric Filtration Materials, Phase I. (in press).

5. Draemel, D. C. Relationship Between Fabric Structure and Filtration Performance in Dust Filtration. EPA-R2-73-288, U.S. Environmental Protection Agency, July 1973.

6. Billings, C. E., and J. Wilder. Handbook of Fabric Filter Technology, Vol. I. Fabric Filter Systems Study. EPA publication APTD 0690, NTIS No. PB-200 648, December 1970.

7. Billings, C. E. Fabric Filter Installations for Flue Gas Fly Ash Control, Status Report. Powder Technology, Vol. 18. 1977. pp. 79-110.

8. Dennis, R., R. W. Cass, and R. R. Hall. Observed Dust Dislodgement From Woven Fabrics and Its Measured and Predicted Effect on Filter Performance. Paper 77-32.3 presented to 70th APCA Meeting, Toronto, Ontario, June 1977.

9. Stephan, D. G., G. W. Walsh, and R. A. Herrick. Concepts in Fabric Air Filtration. Am Ind Hyg Ass J., Vol. 21. February 1960. pp. 1-14.

10. Troskolański, T. A. Hydrodynamika Techniczna, Vol. II. Hydraulika, Warszawa, PWT, 1954.

11. Holland, C. R., and E. Rothwell. Model Studies of Fabric Dust Filtration, Filtration and Separation. Vol. 14, No. 1 (January/February 1977). pp. 30-36.

12. Operating Instructions for Andersen Stack Sampling Equipment.

13. Donovan, R. P., B. E. Daniel, and J. H. Turner. EPA Fabric Filtration Studies: 3. Performance of Filter Bags Made From Expanded PTFE Laminate. EPA-600/2-76-168c, U.S. Environmental Protection Agency, December 1976.

APPENDIX A

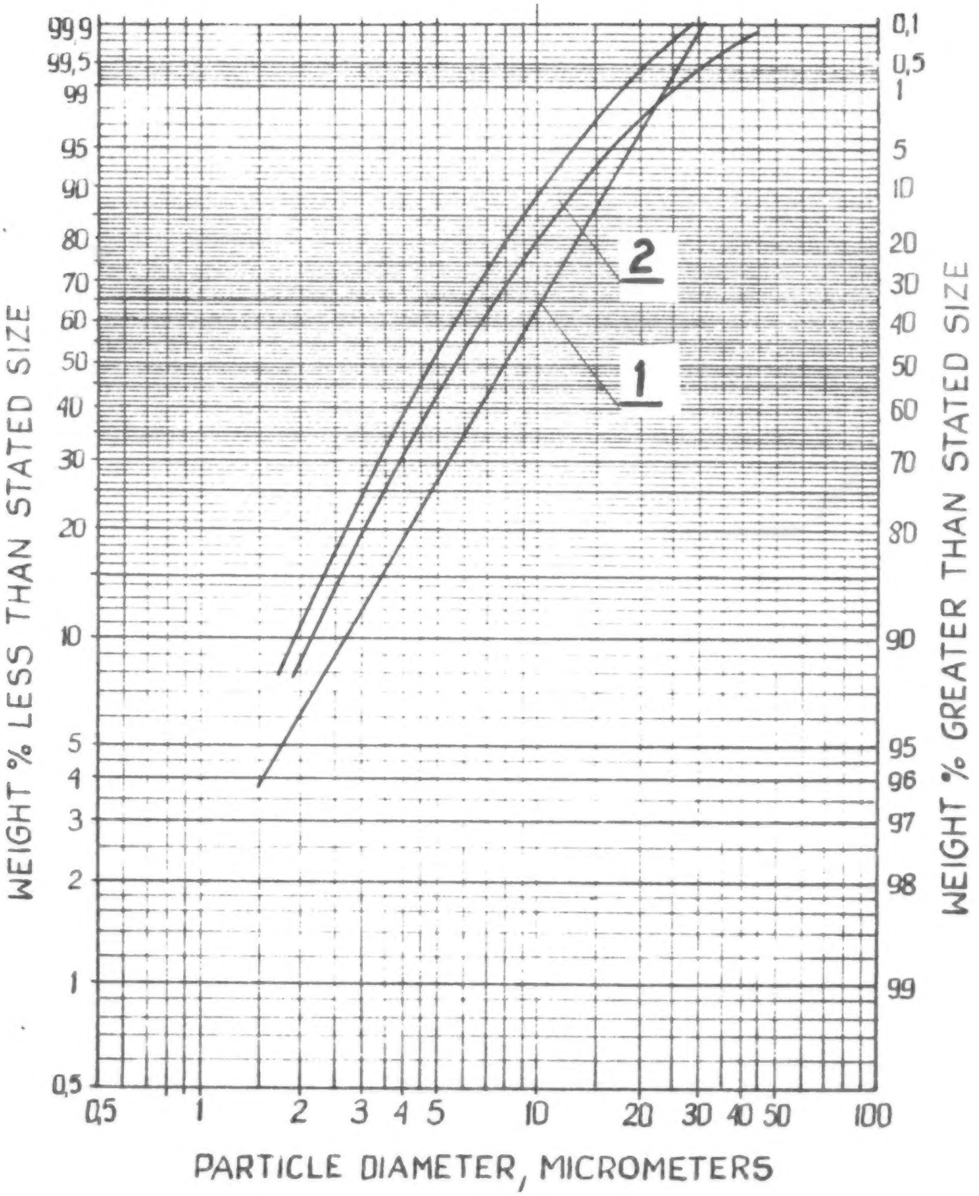

Figure A-1. Particle size distribution of cement test dusts: 1 - for laboratory testing; 2 - for large scale testing.

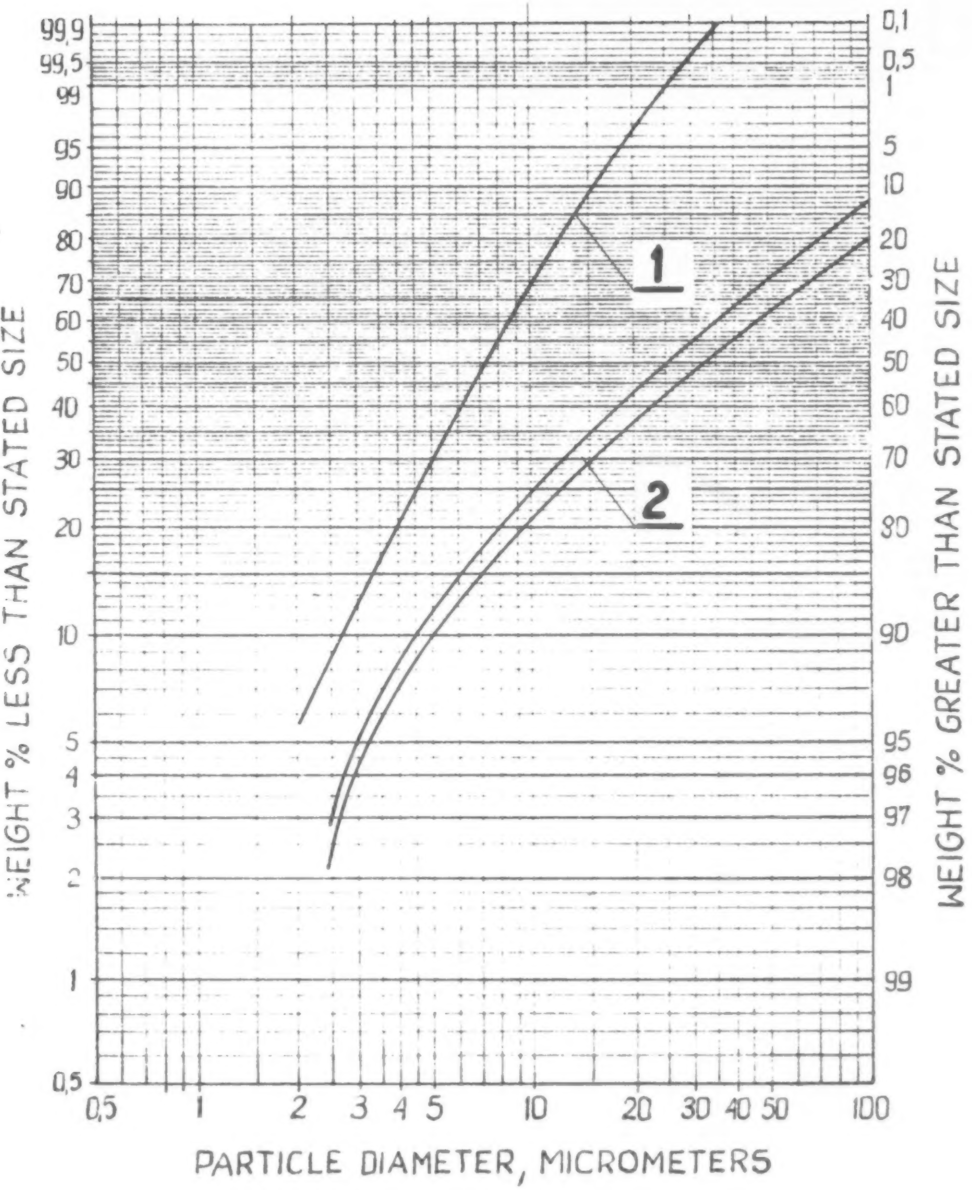

Figure A-2. Particle size distribution of coal test dusts: 1 - for laboratory testing; 2 - for large scale testing.

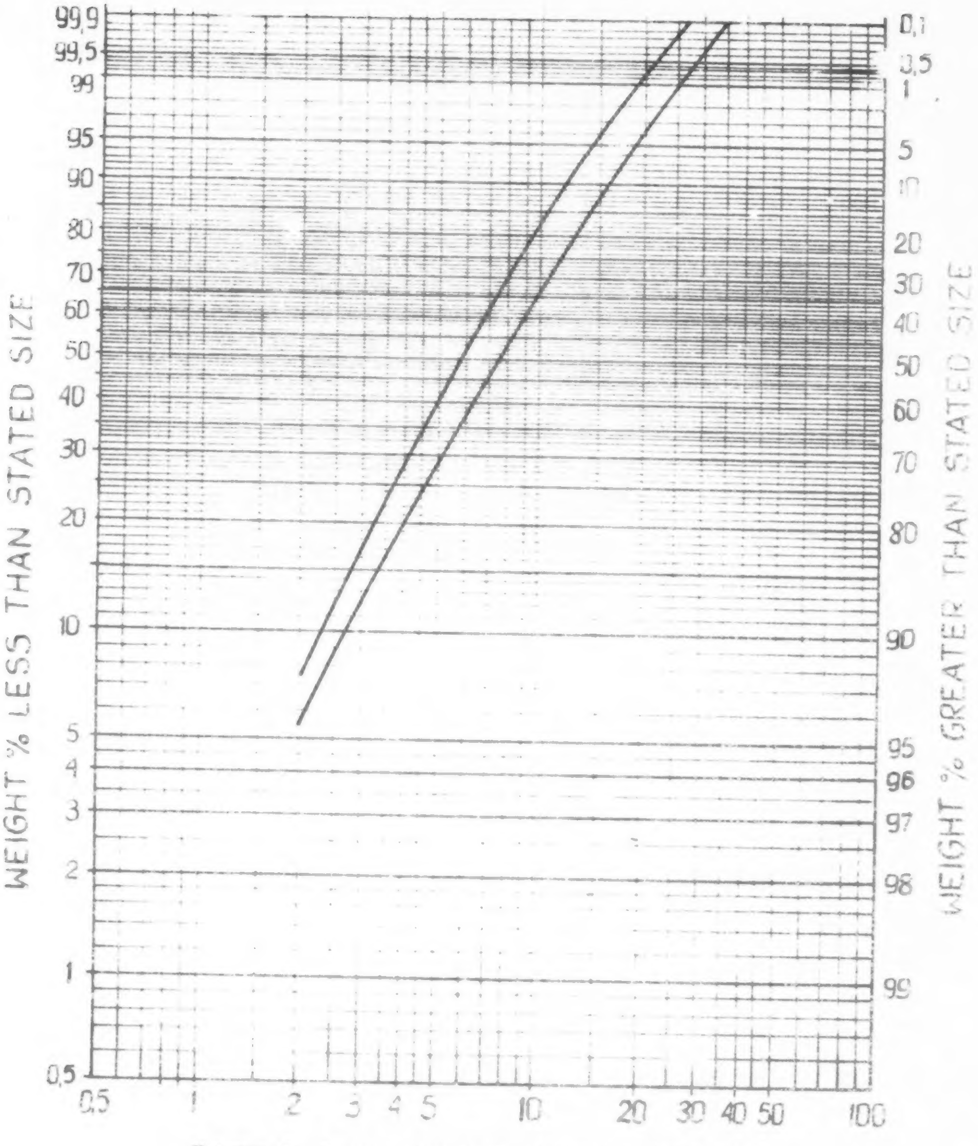

Figure A-3. Particle size distribution of talc test dust.

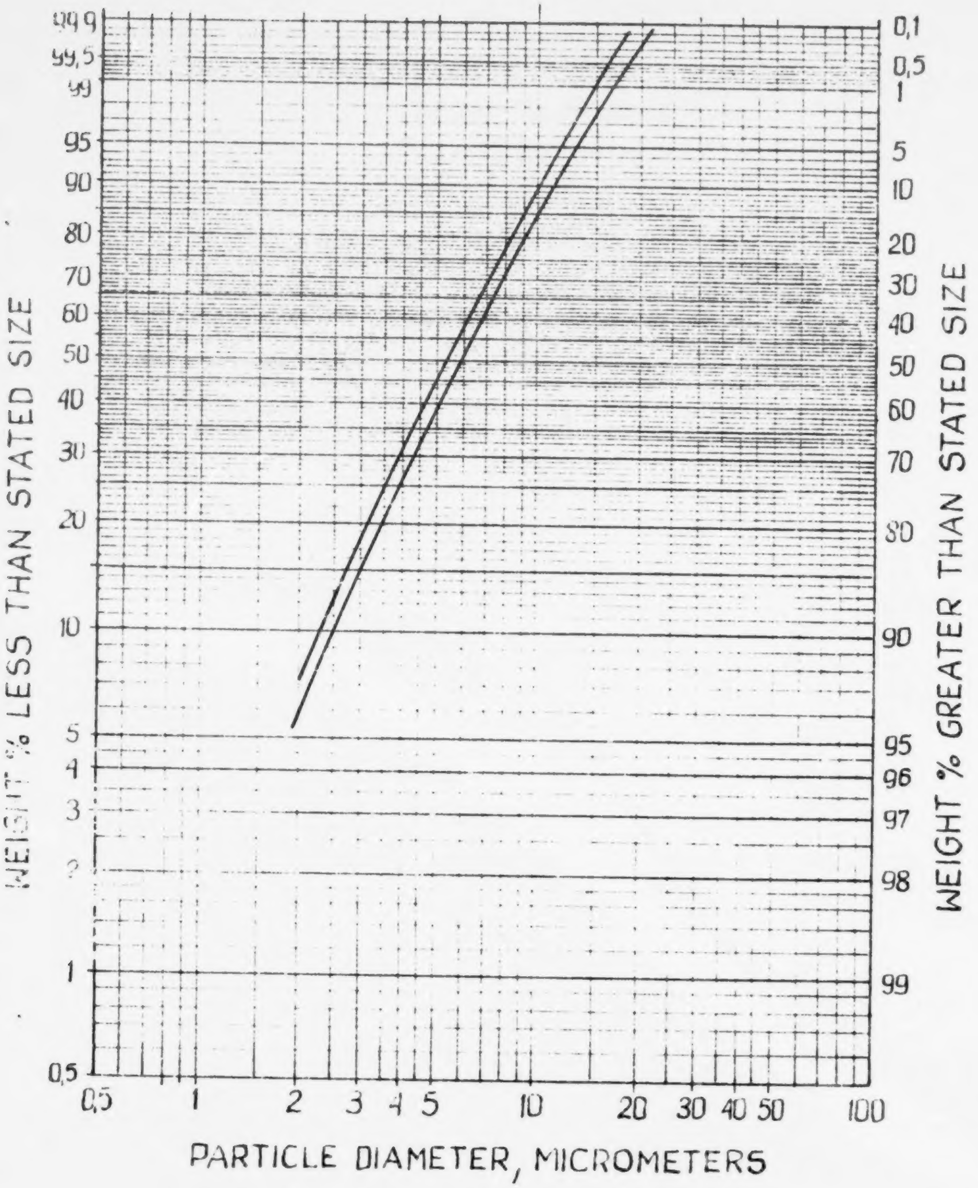

Figure A-4. Particle size distribution of fly ash test dust.

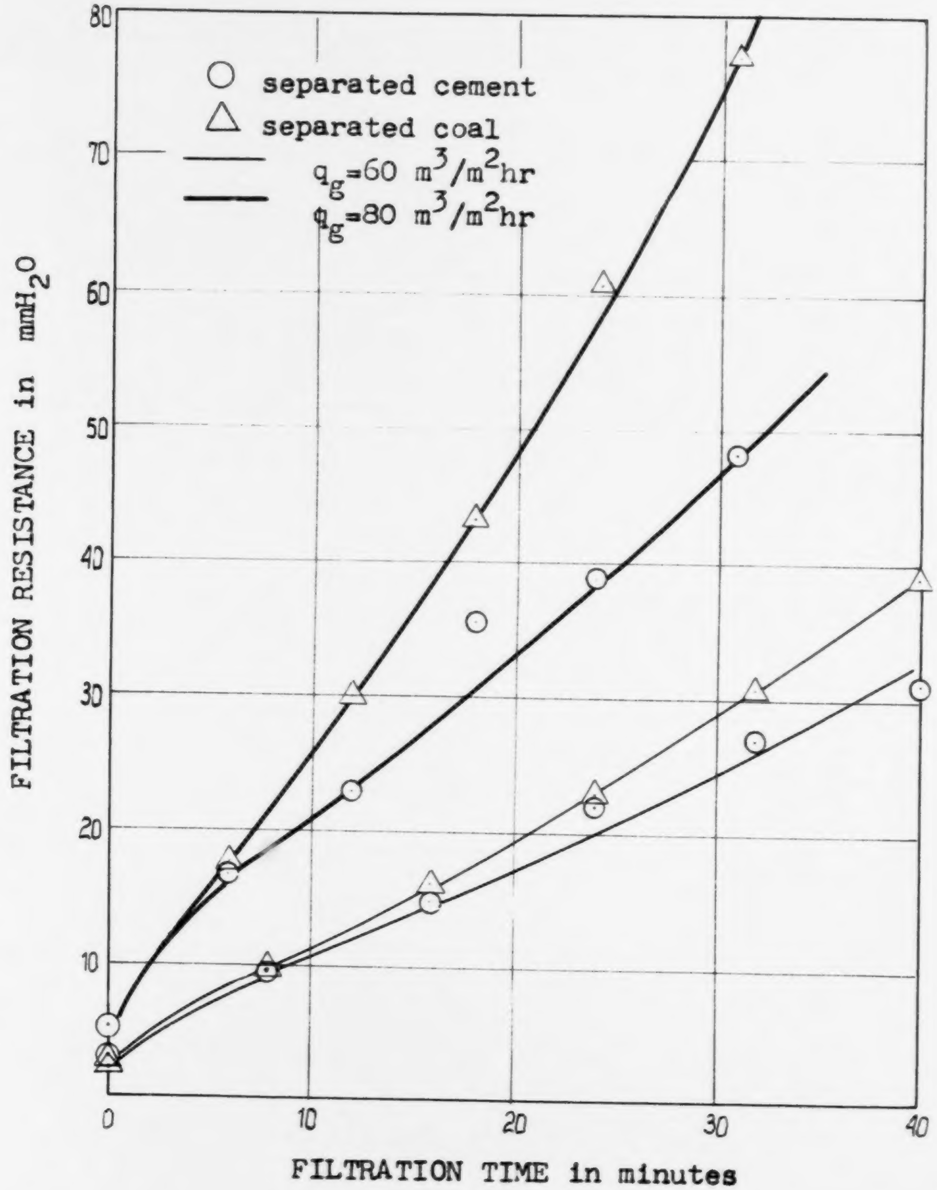

Figure A-5. Filtration resistance vs. filtration time for fabric style no. 960.

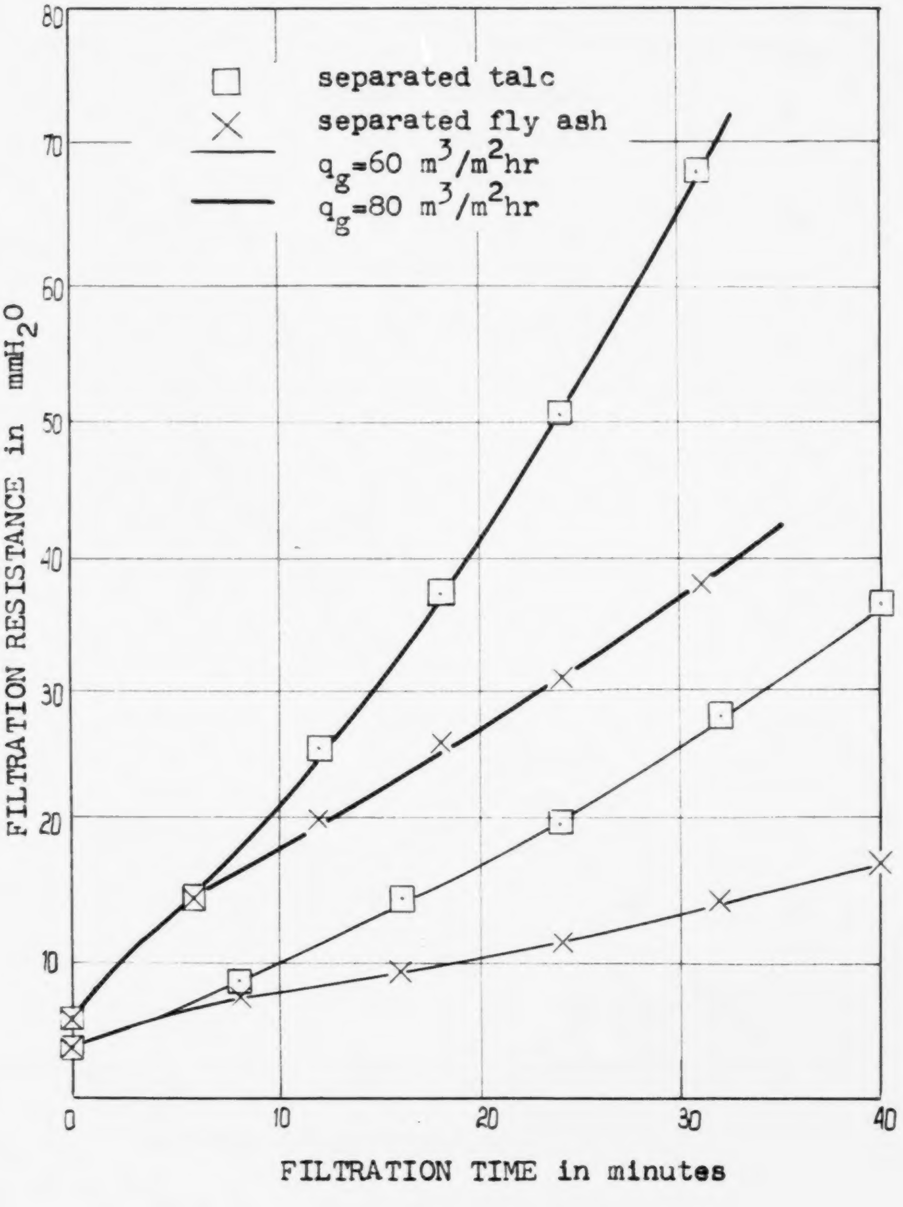

Figure A-6. Filtration resistance vs. filtration time for fabric style no. 960.

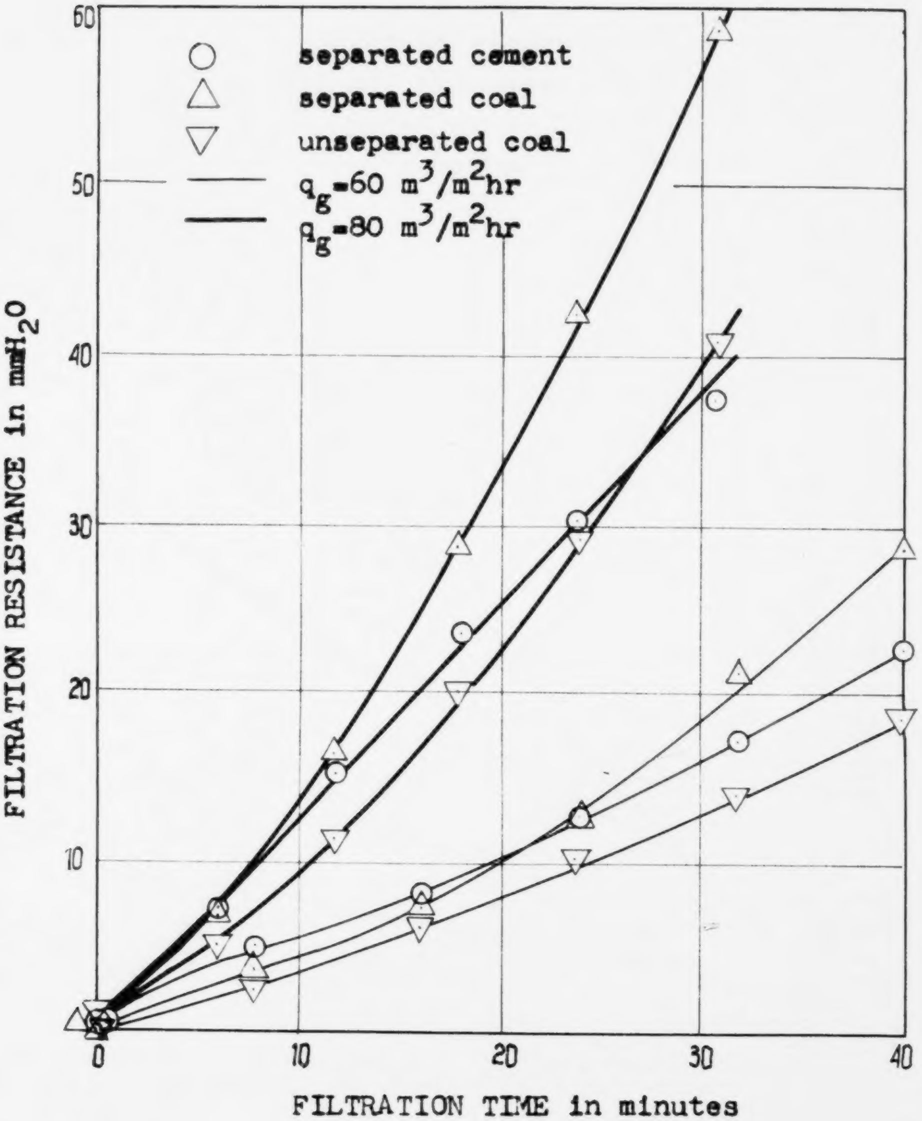

Figure A-7. Filtration resistance vs. filtration time for fabric style no. 862B.

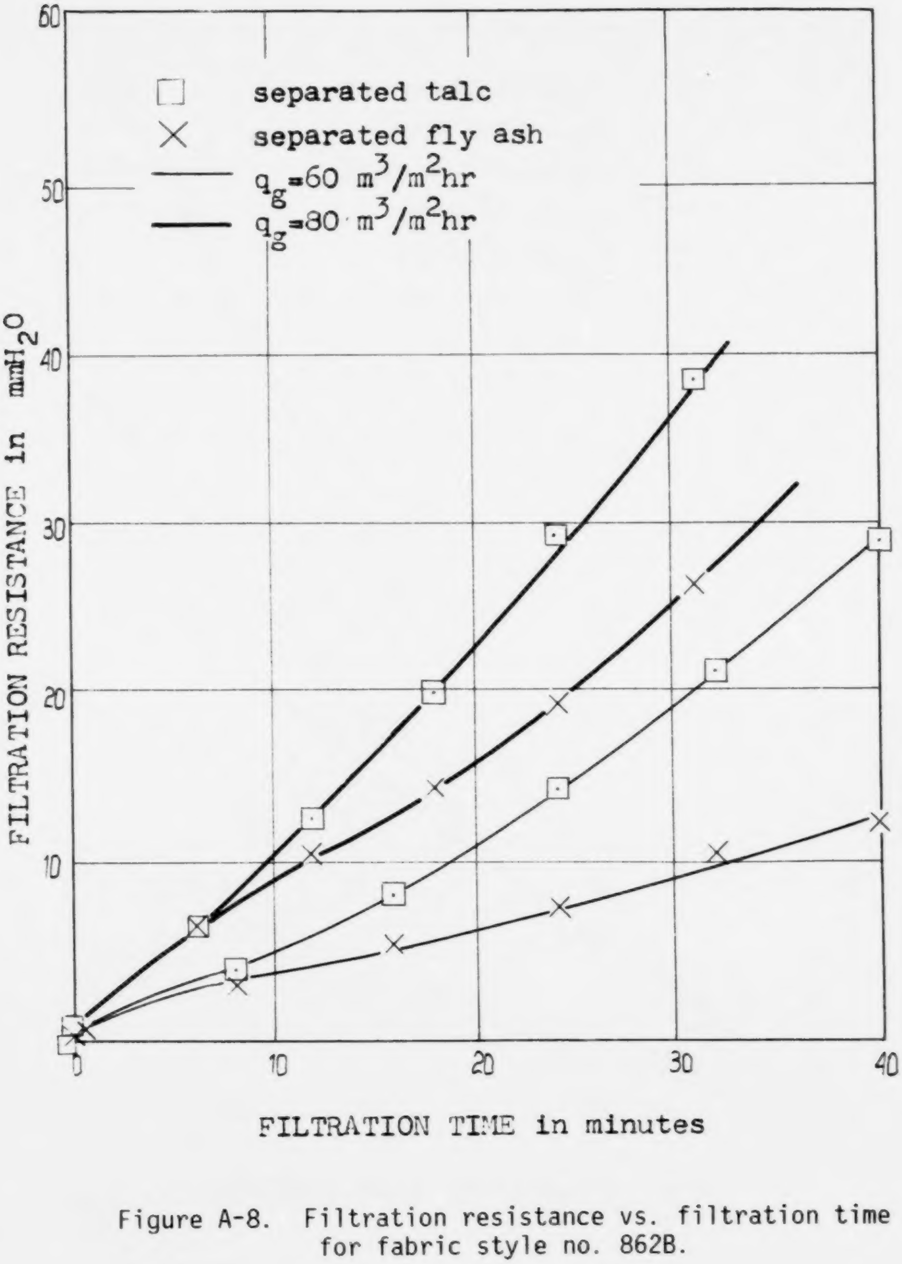

Figure A-8. Filtration resistance vs. filtration time for fabric style no. 862B.

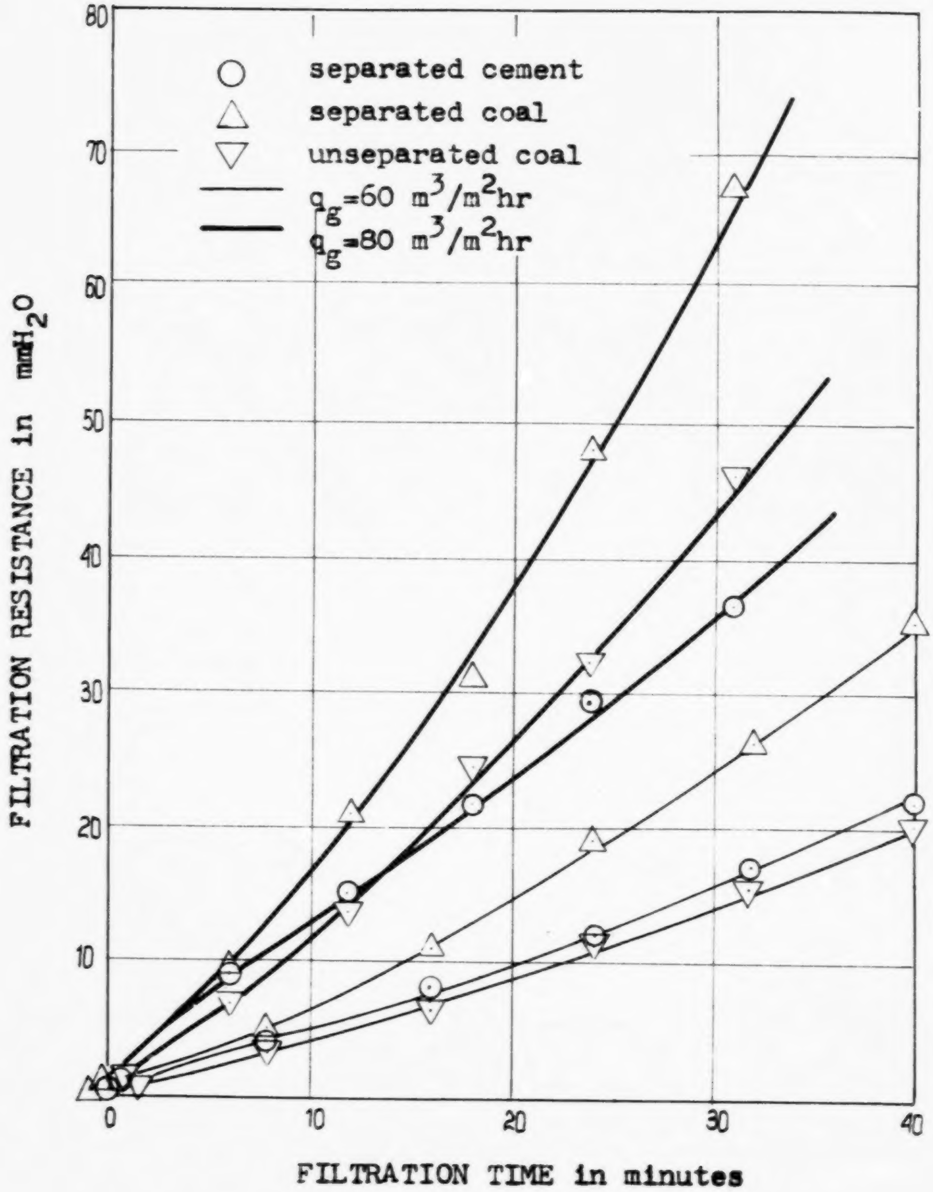

Figure A-9. Filtration resistance vs. filtration time for fabric style no. C866B.

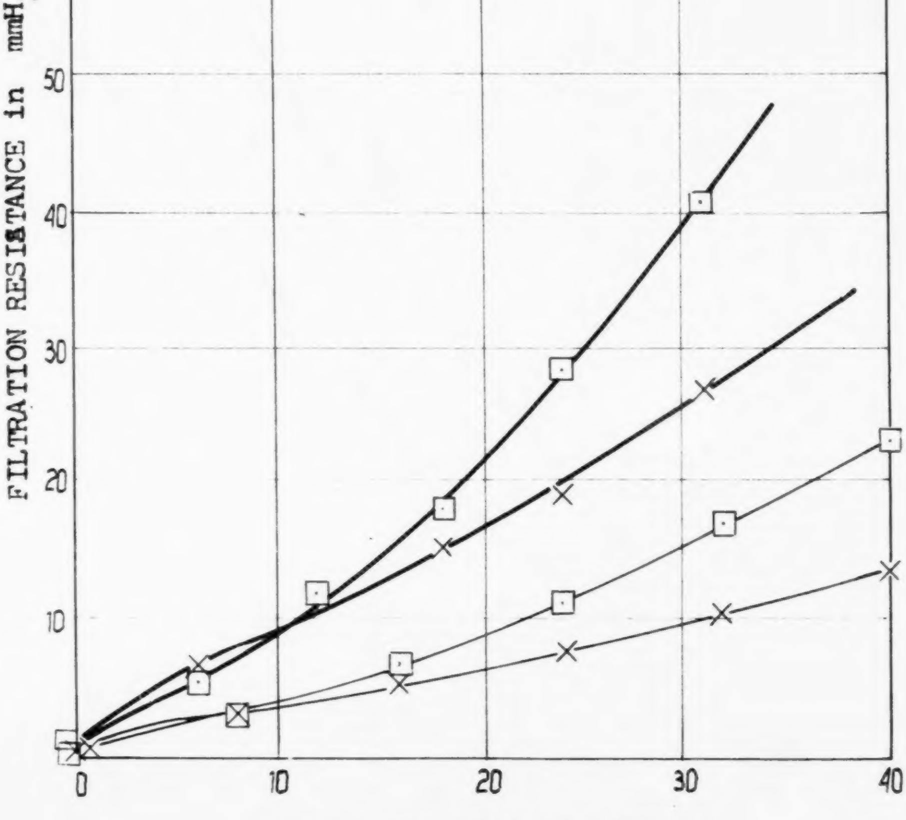

Figure A-10. Filtration resistance vs. filtration time for fabric style no. C866B.

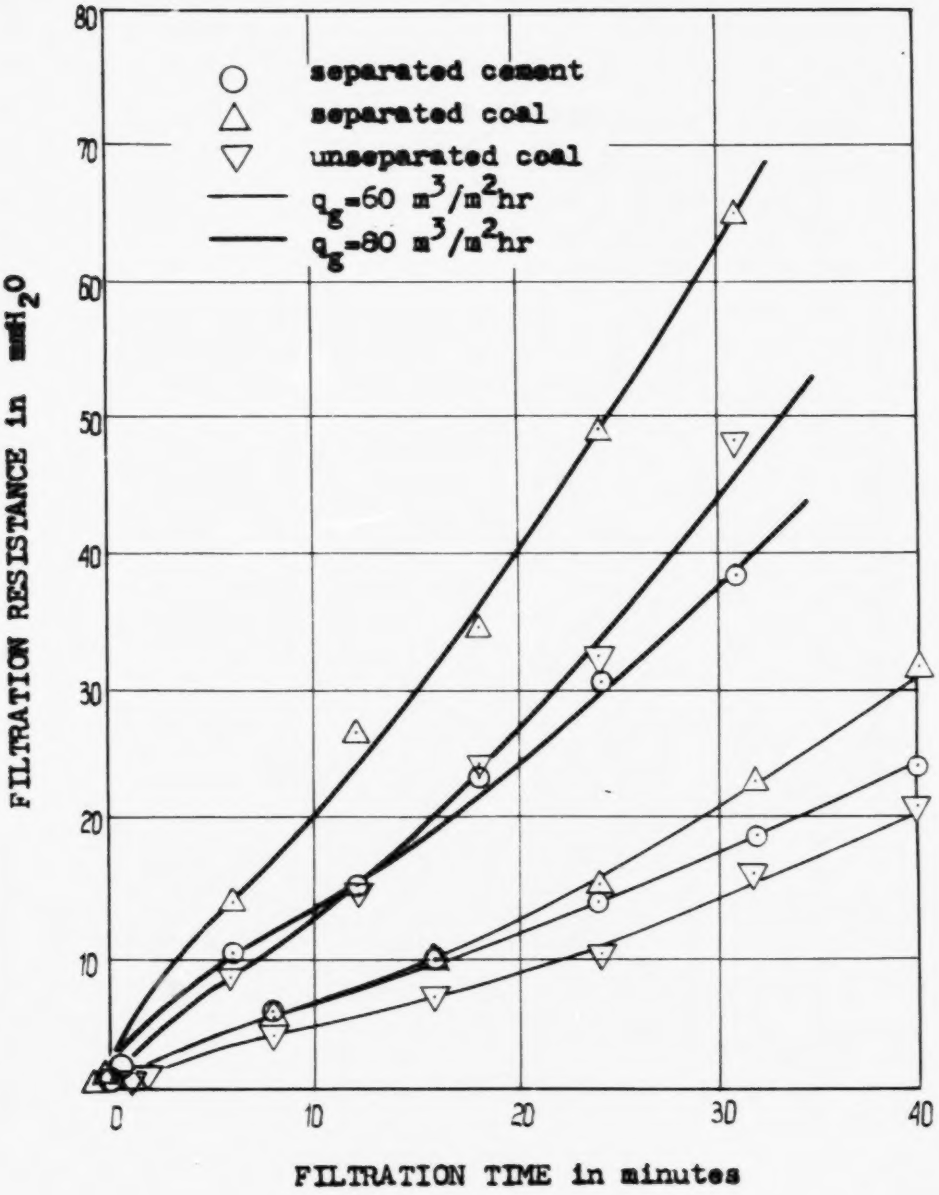

Figure A-11. Filtration resistance vs. filtration time for fabric style no. C868B.

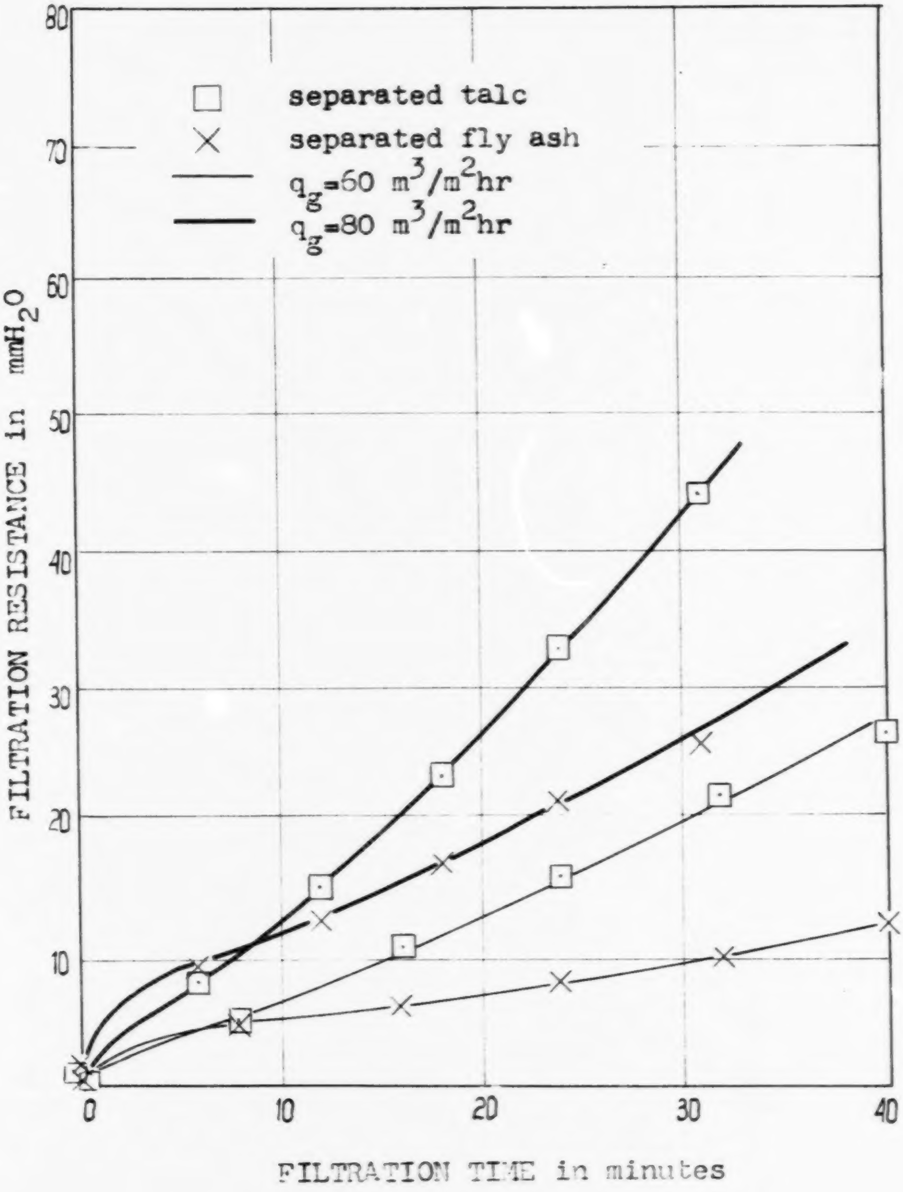

Figure A-12. Filtration resistance vs. filtration time for fabric style no. C868B.

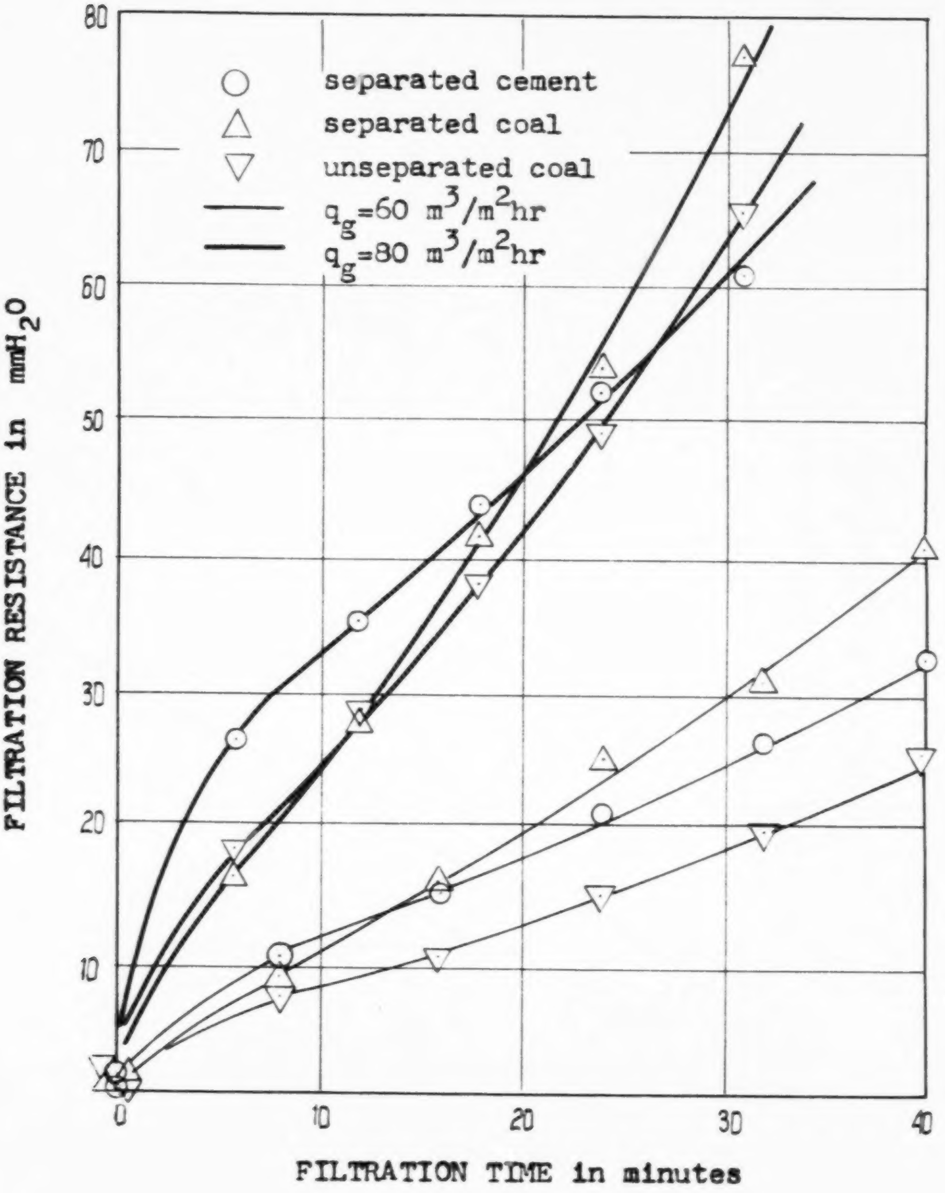

Figure A-13. Filtration resistance vs. filtration time for fabric style no. 865B.

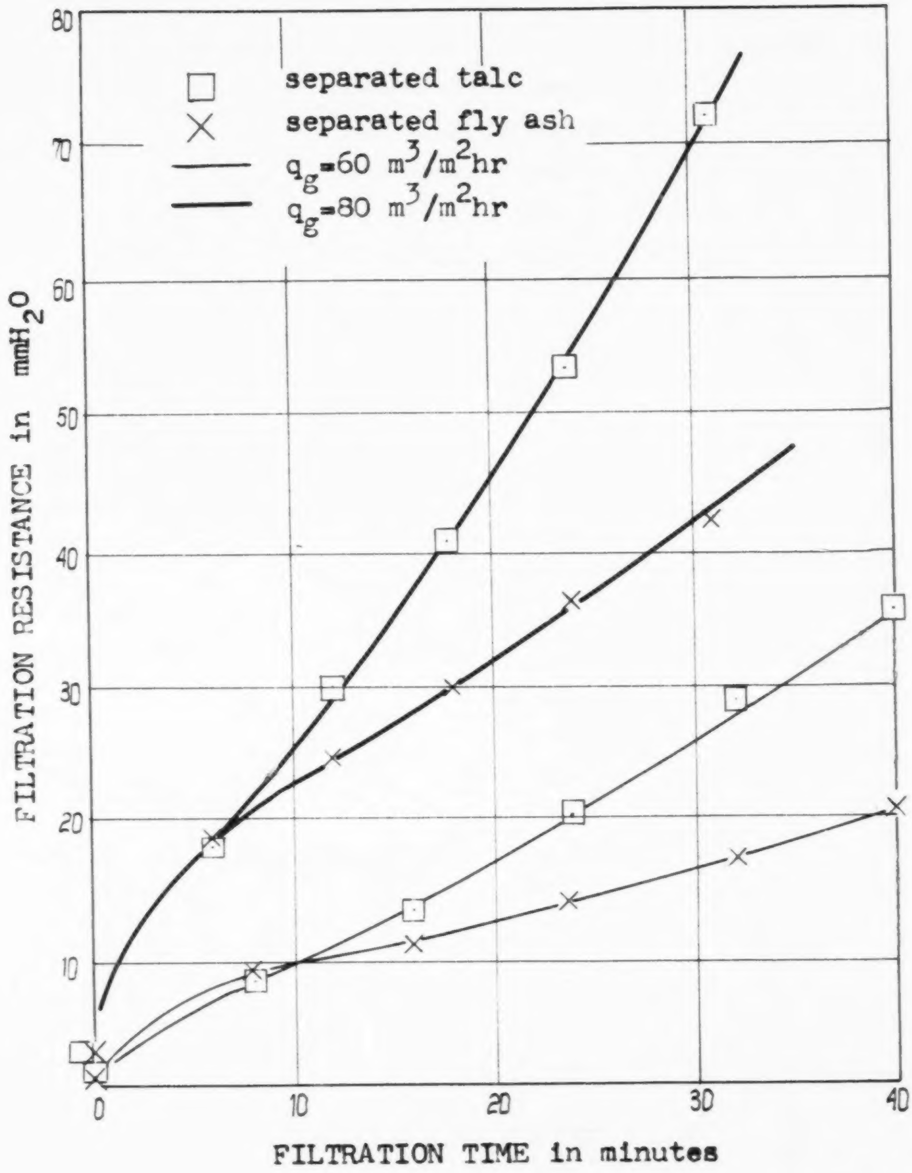

Figure A-14. Filtration resistance vs. filtration time for fabric style no. 865B.

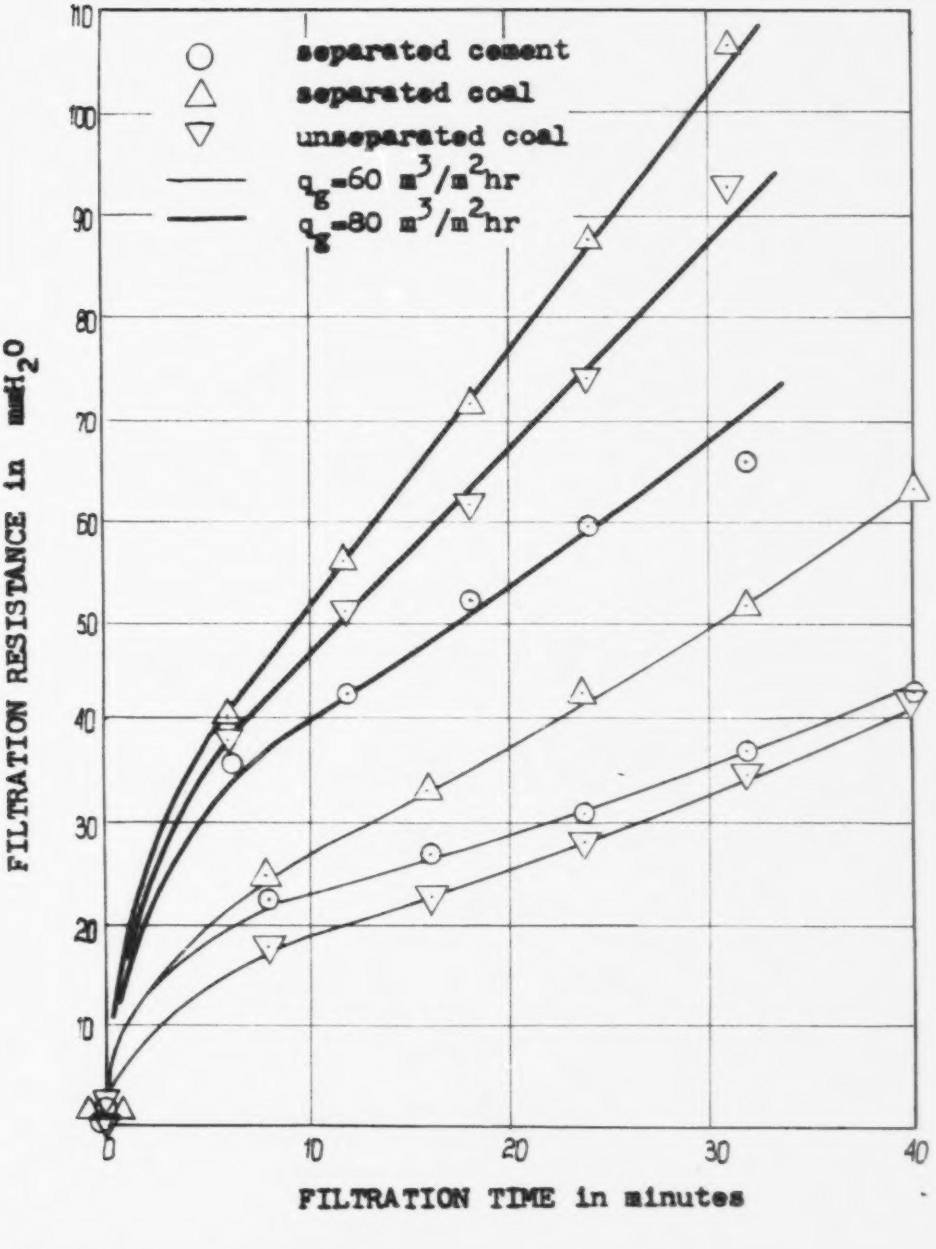

Figure A-15. Filtration resistance vs. filtration time for fabric style no. C890B.

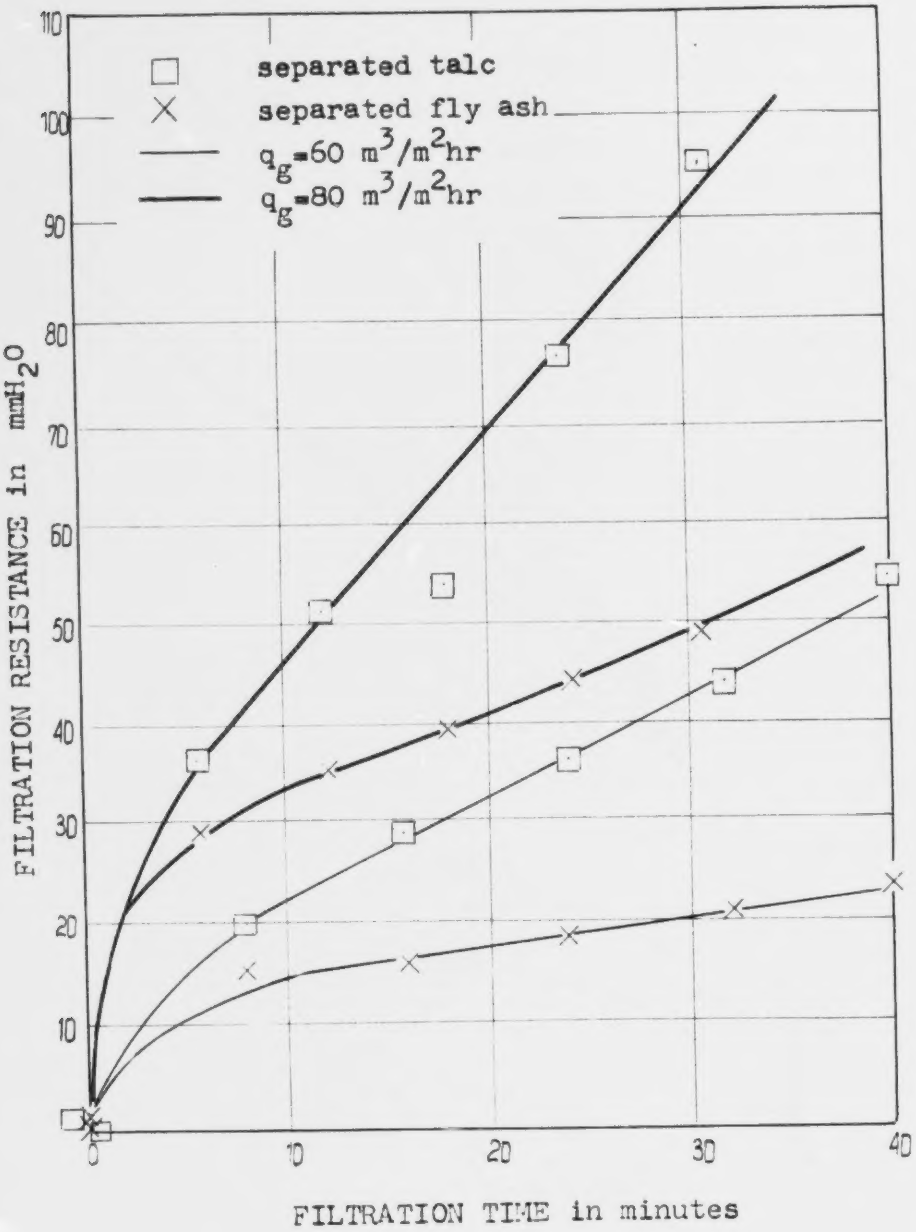

Figure A-16. Filtration resistance vs. filtration time for fabric style no. C890B.

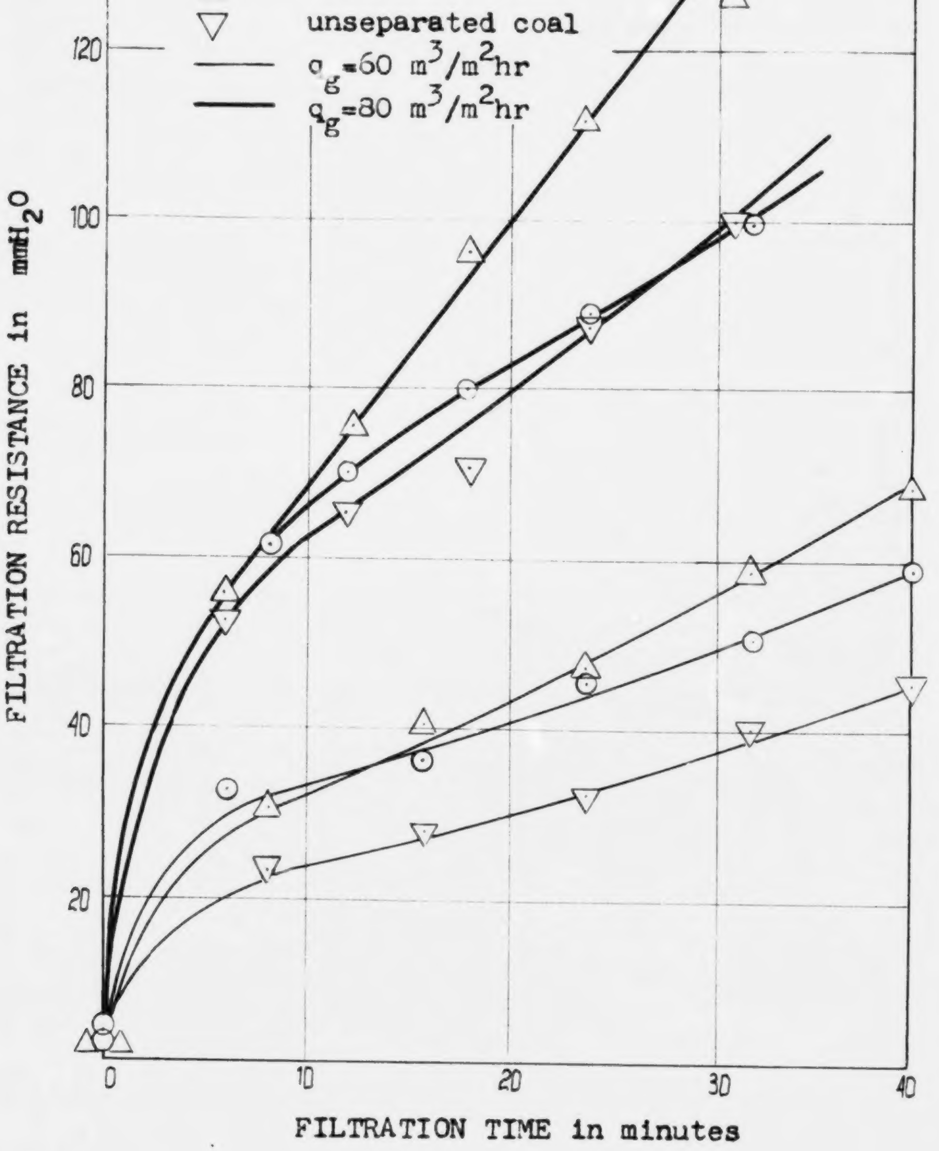

Figure A-17. Filtration resistance vs. filtration time for fabric style no. C892B.

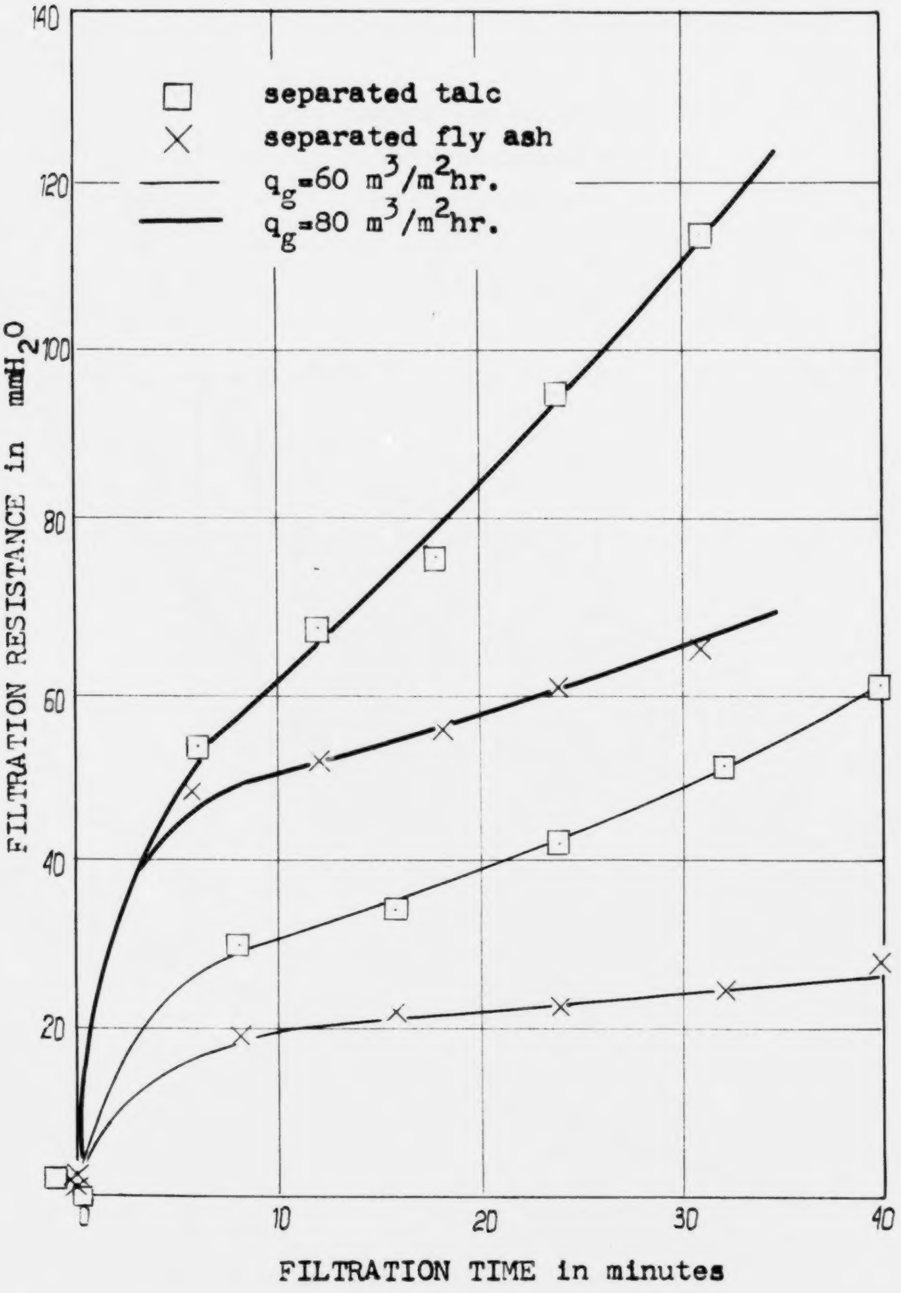

Figure A-18. Filtration resistance vs. filtration time for fabric style no. C892B.

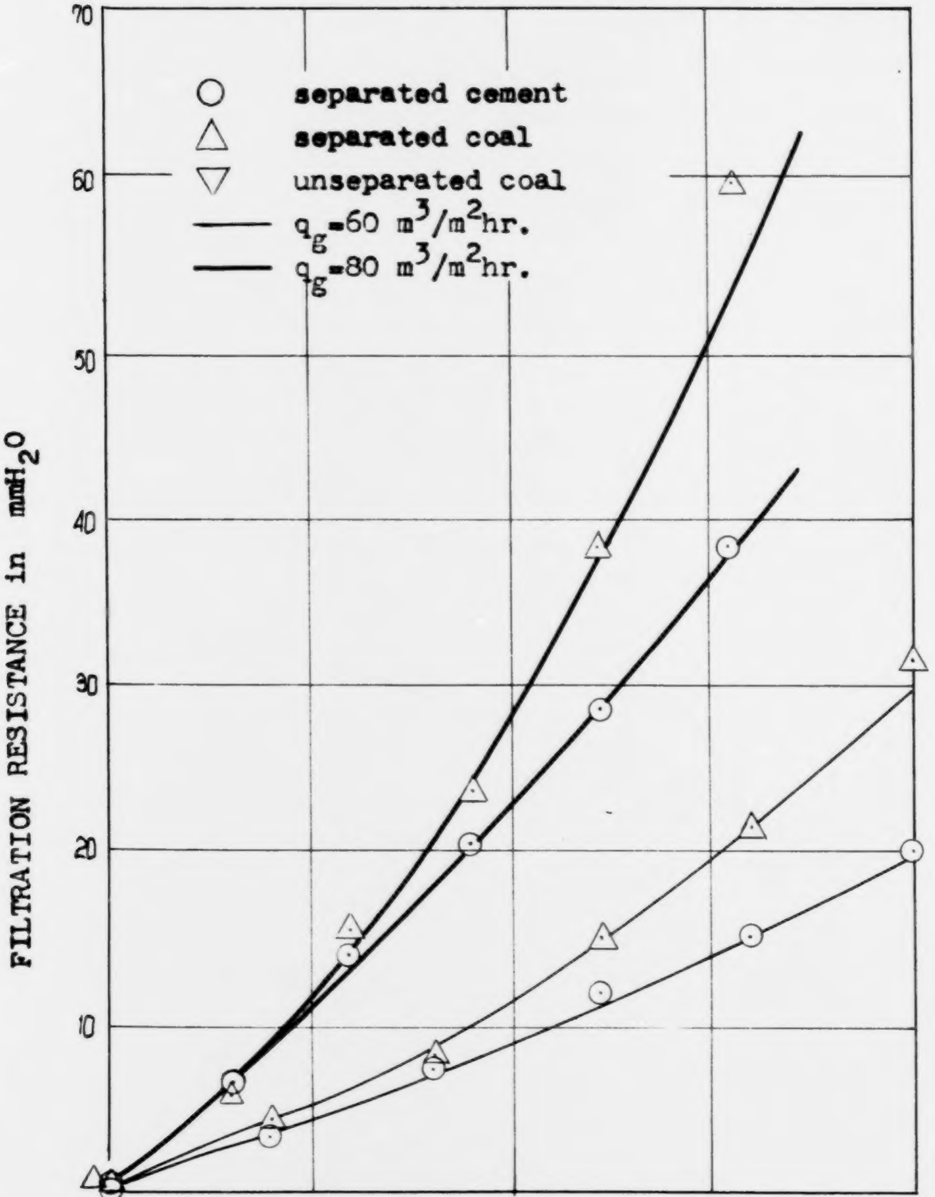

Figure A-19. Filtration resistance vs. filtration time for fabric style no. 852.

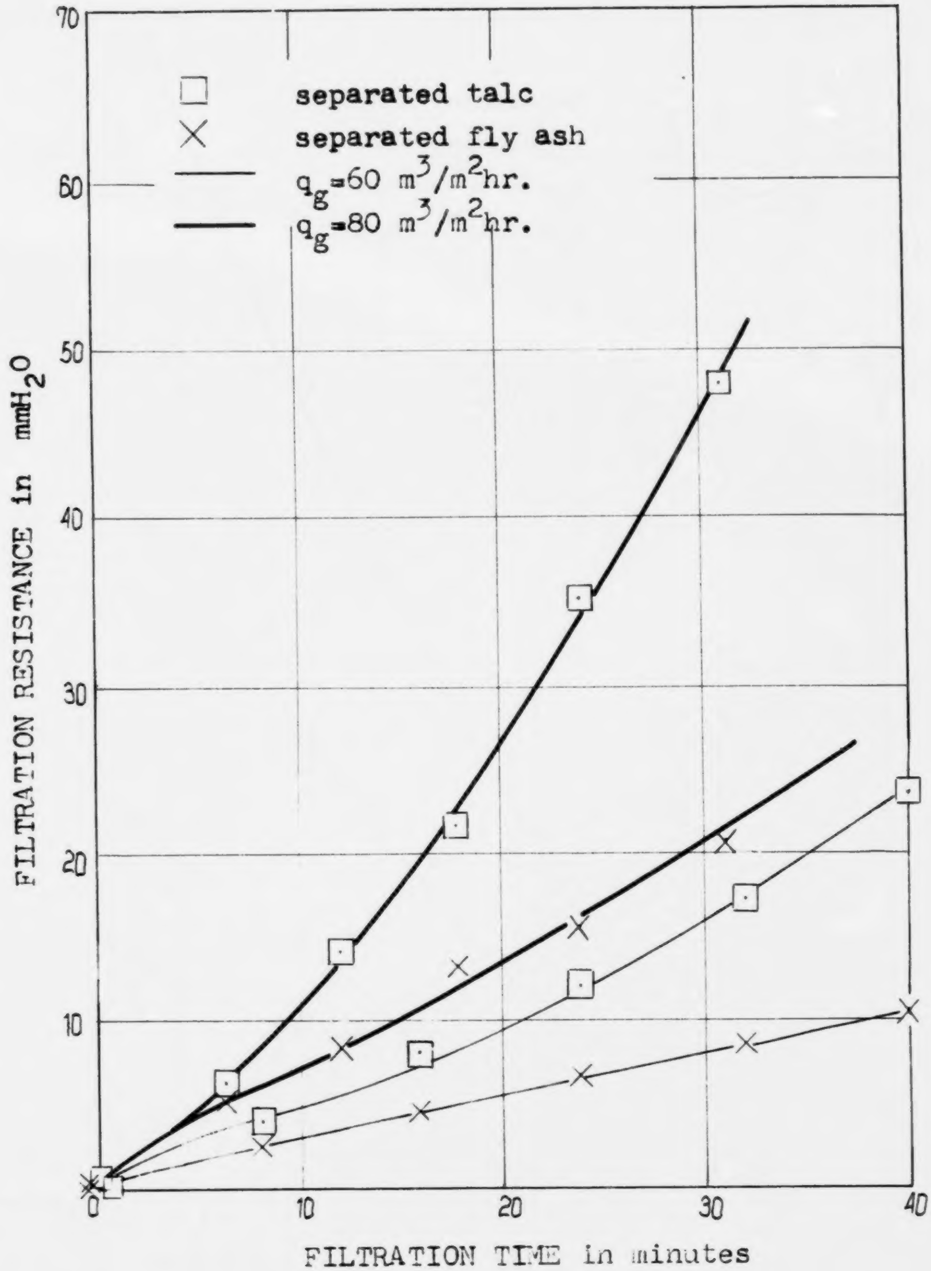

Figure A-20. Filtration resistance vs. filtration time for fabric style no. 852.

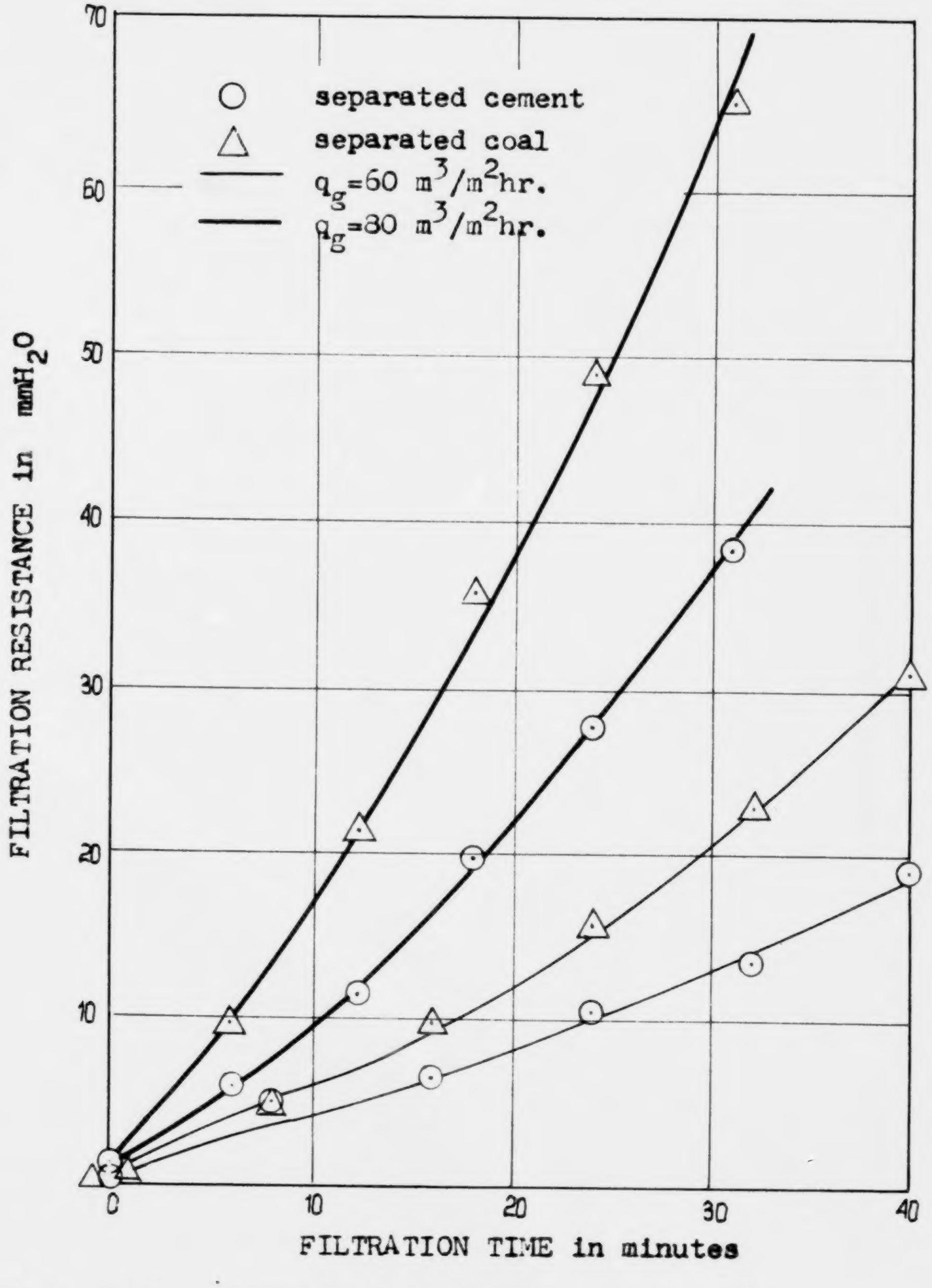

Figure A-21. Filtration resistance vs. filtration time for fabric style no. 853.

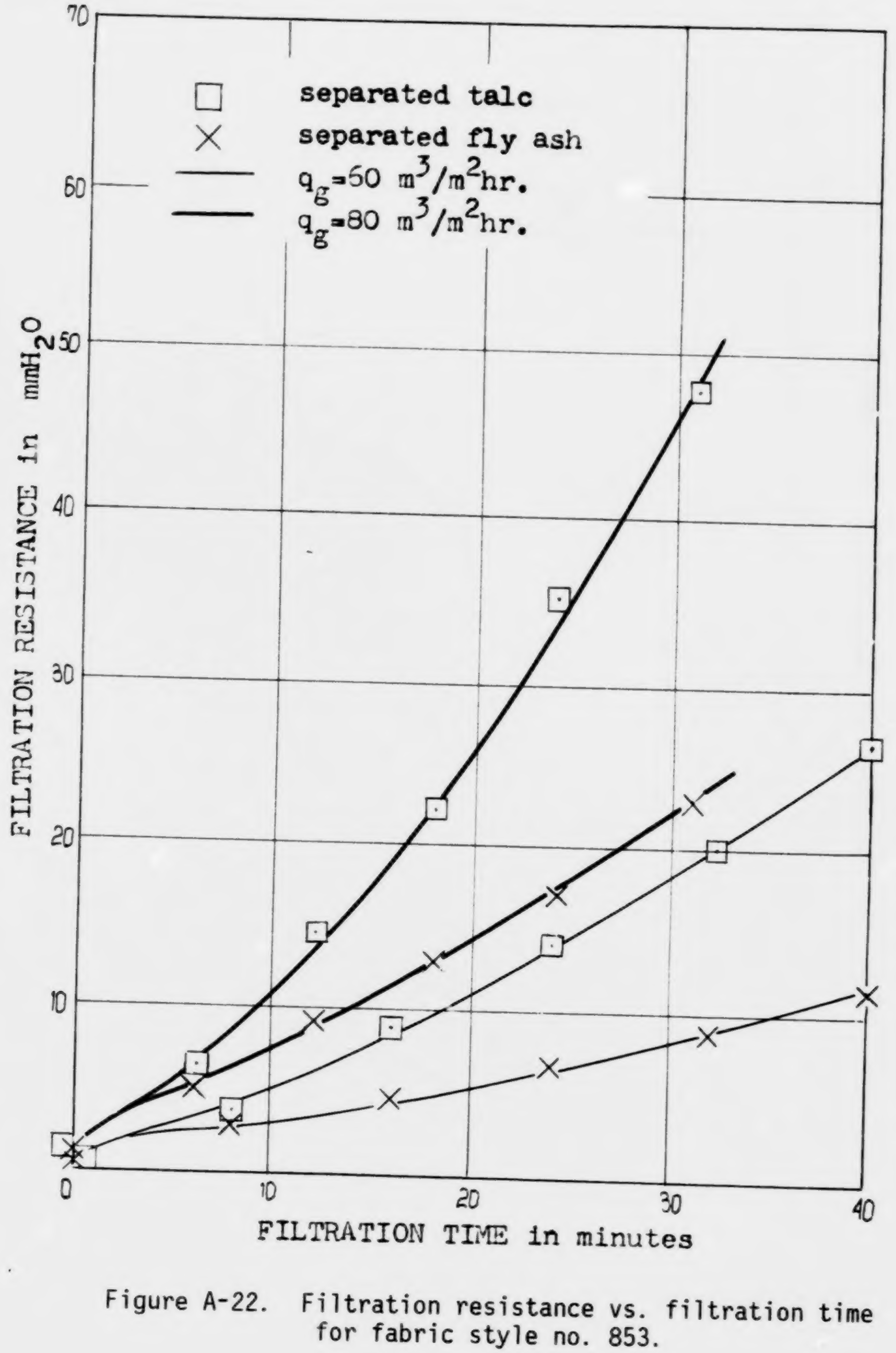

Figure A-22. Filtration resistance vs. filtration time for fabric style no. 853.

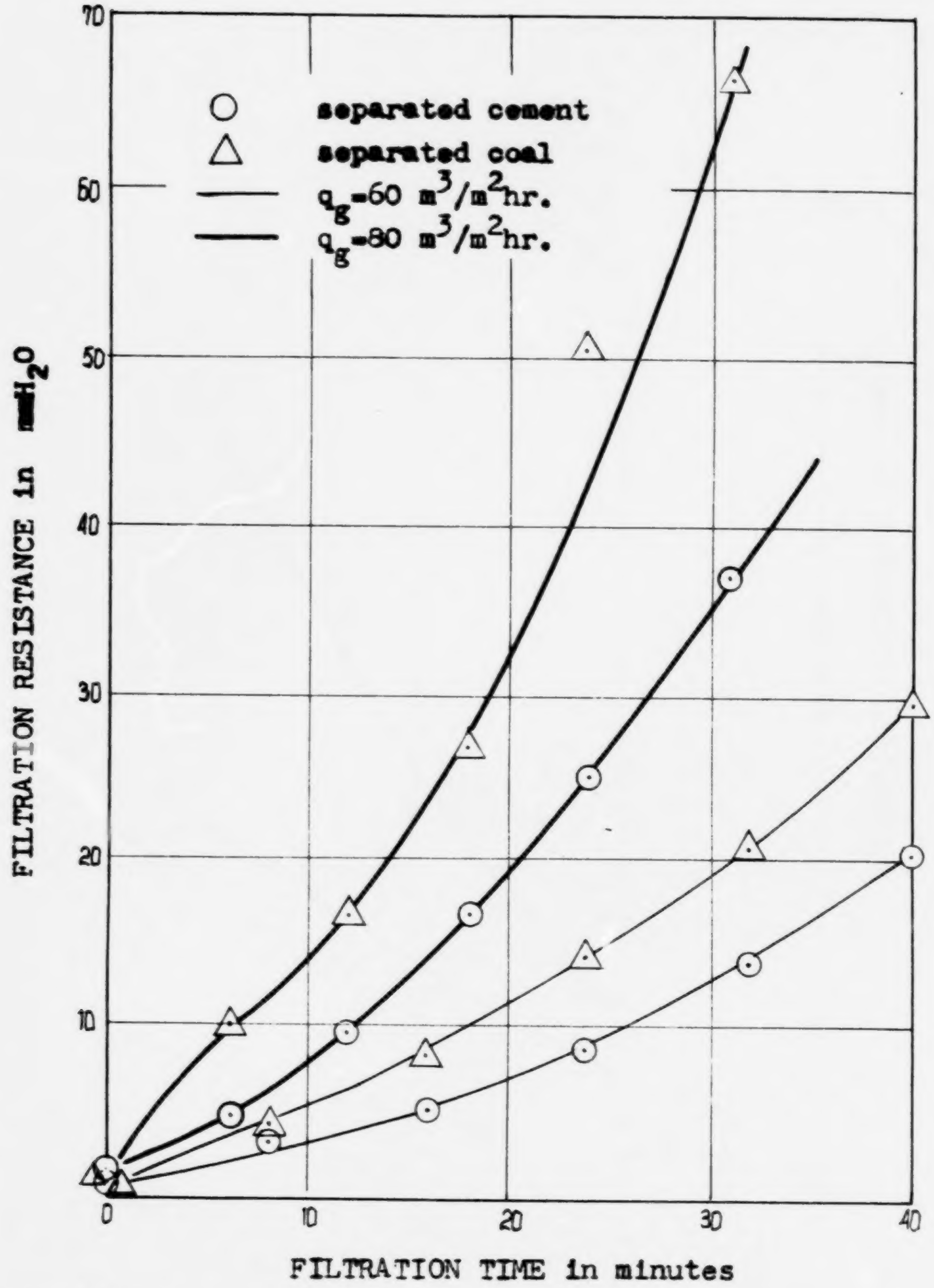

Figure A-23. Filtration resistance vs. filtration time for fabric style no. 190R.

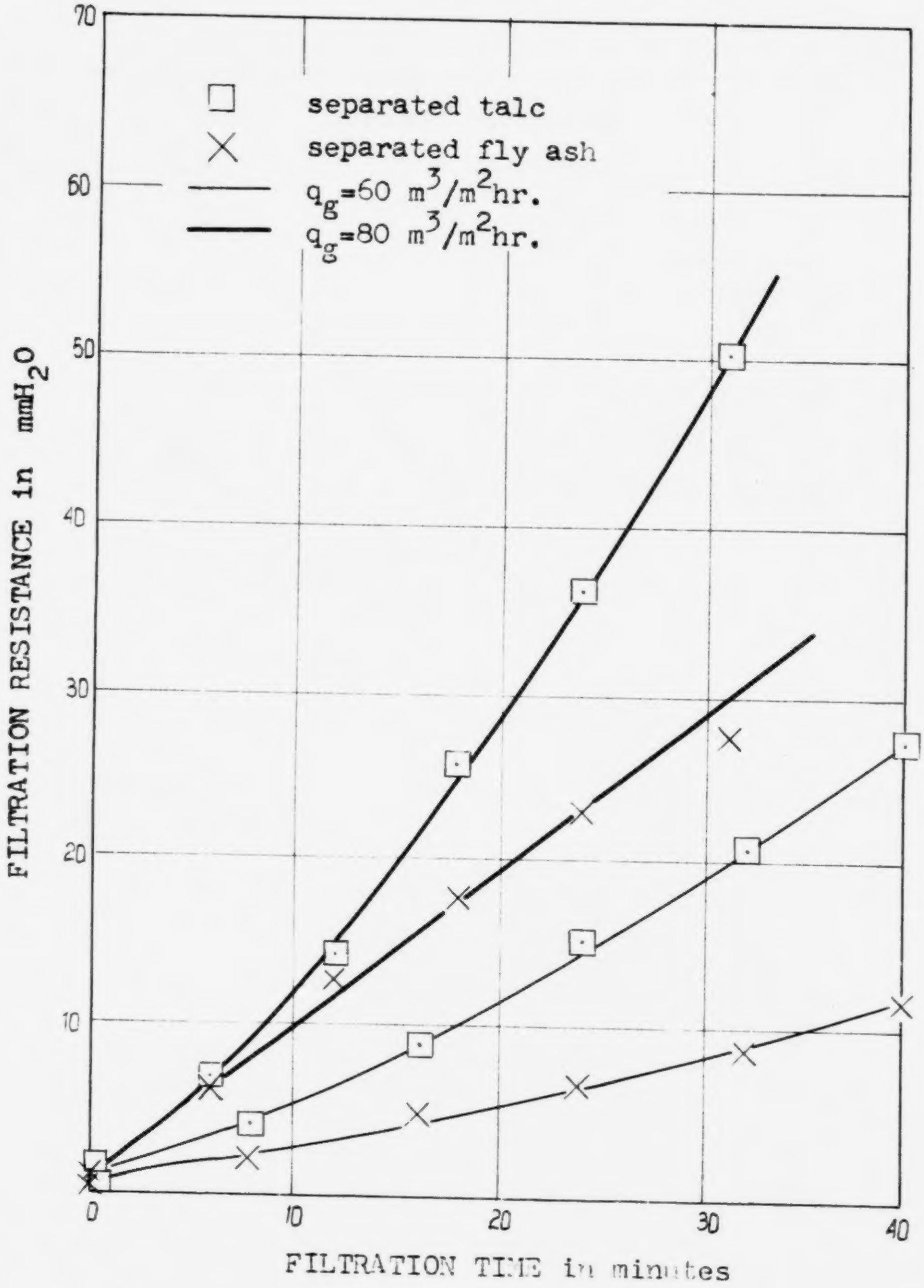

Figure A-24. Filtration resistance vs. filtration time for fabric style no. 190R.

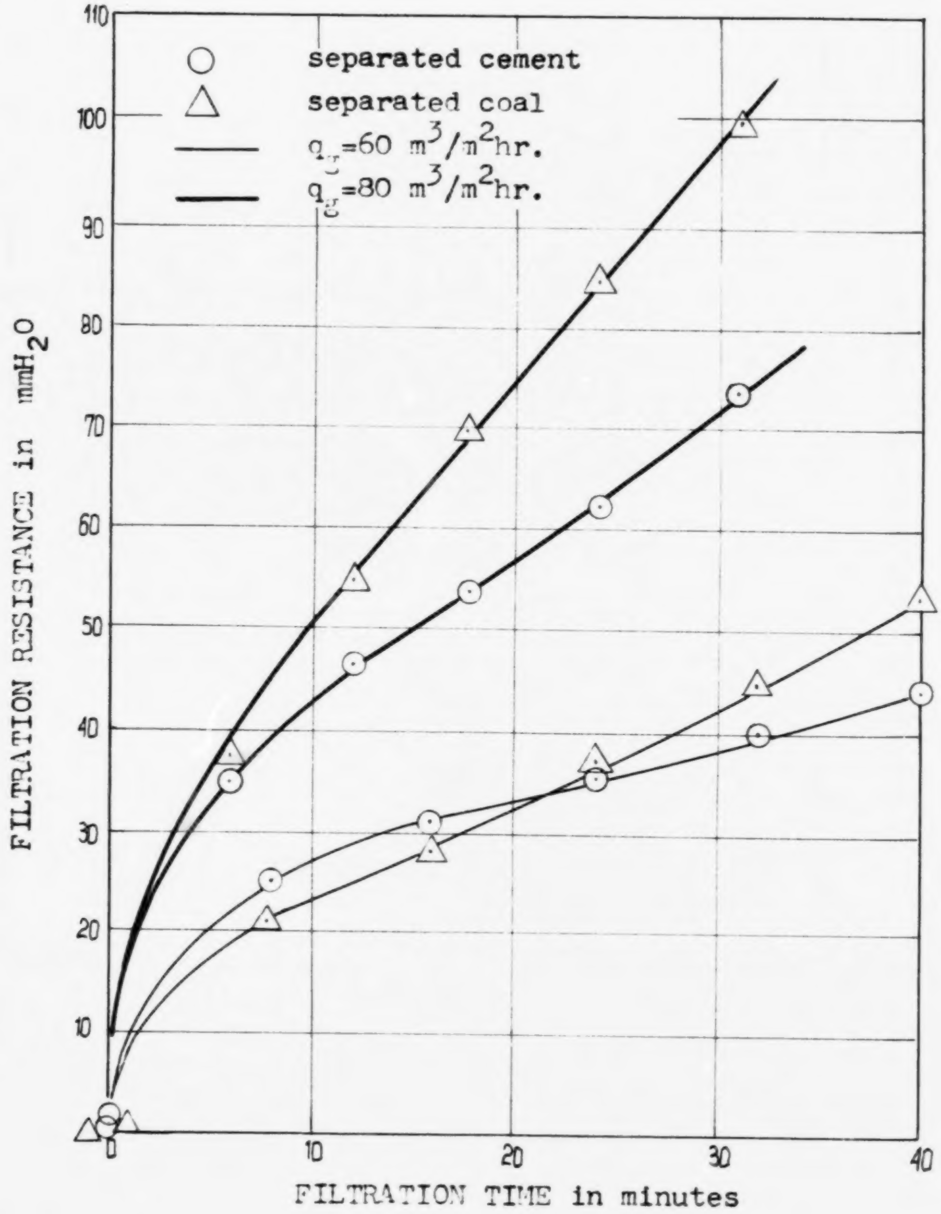

Figure A-25. Filtration resistance vs. filtration time for fabric style no. 850B.

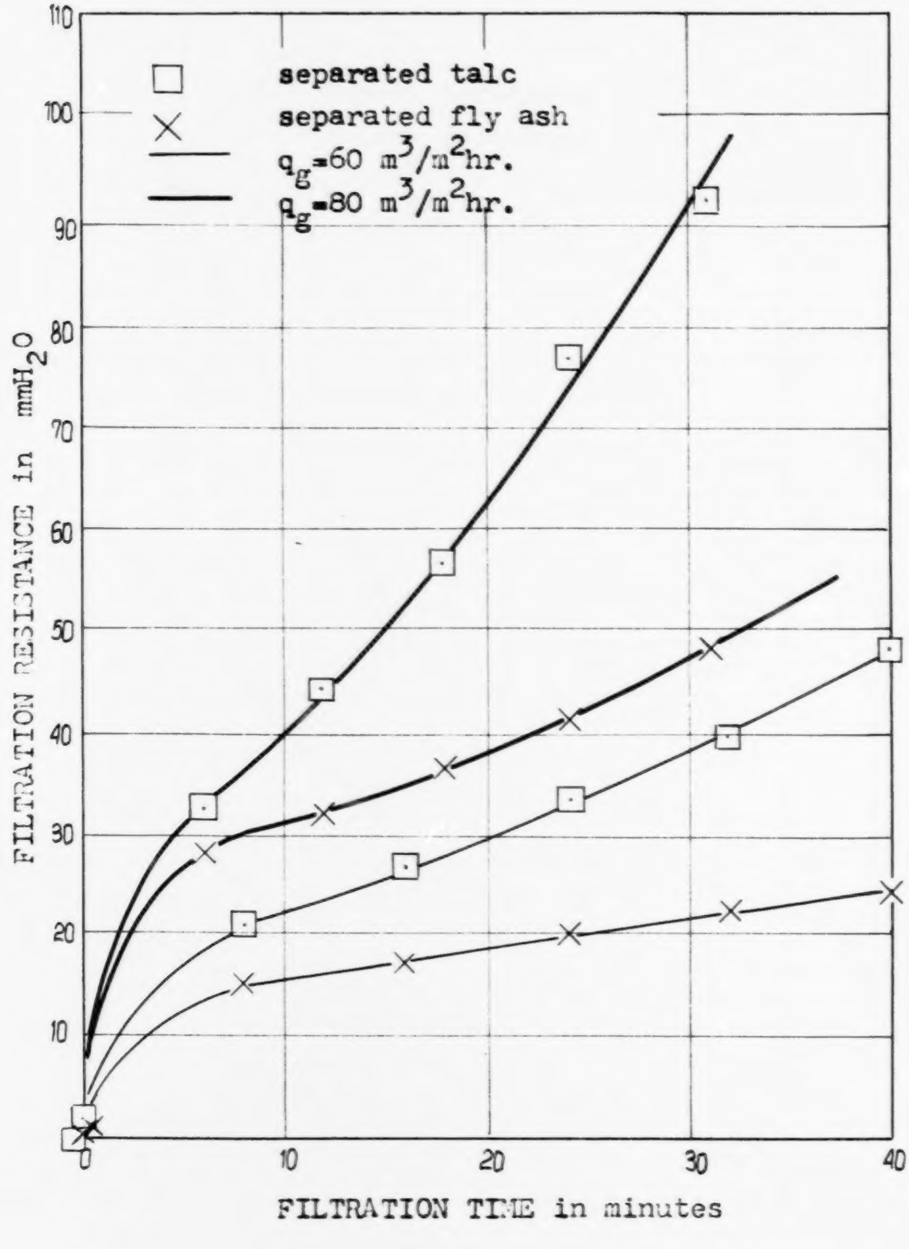

Figure A-26. Filtration resistance vs. filtration time for fabric style no. 850B.

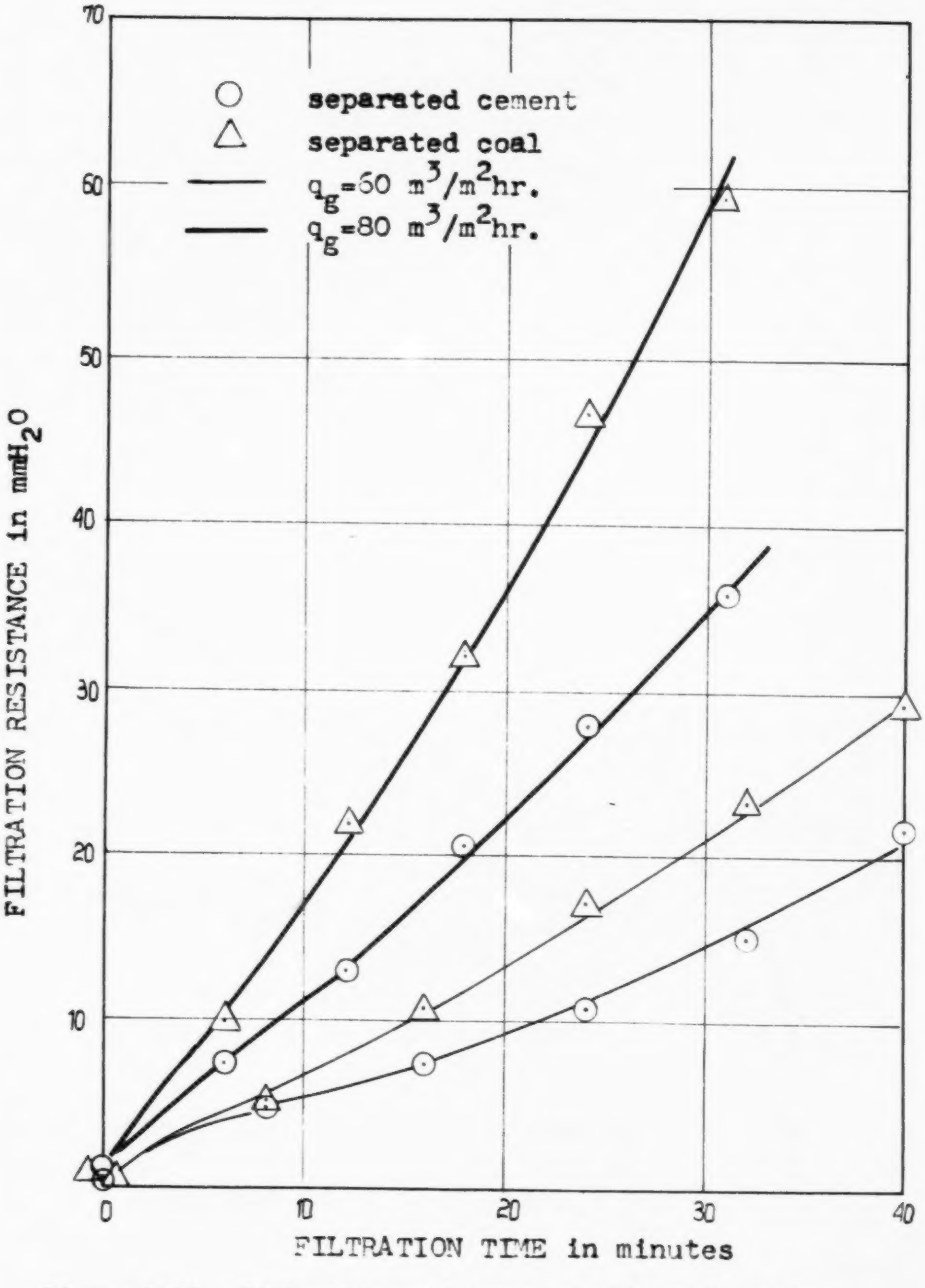

Figure A-27. Filtration resistance vs. filtration time for fabric style no. 802B.

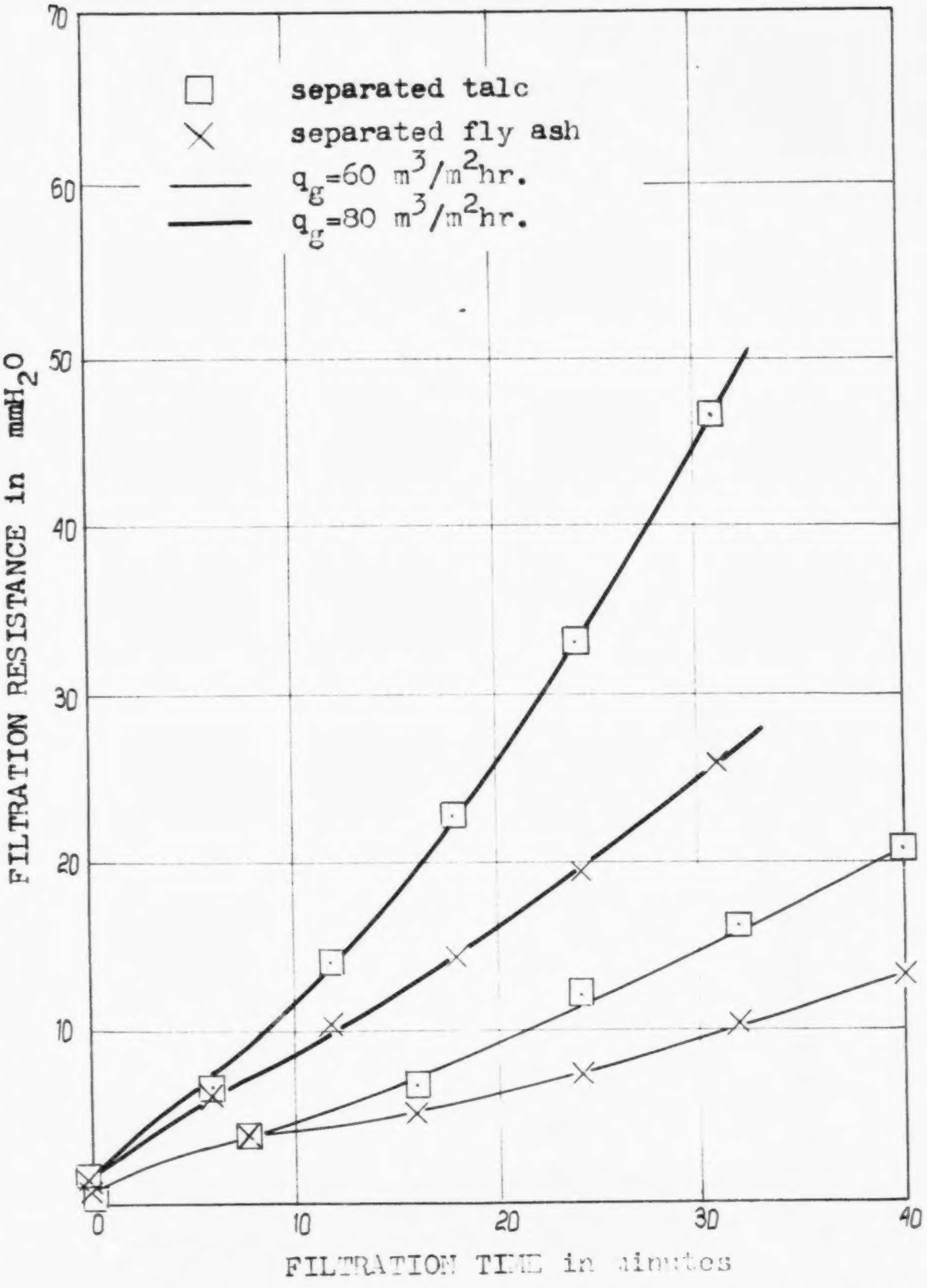

Figure A-28. Filtration resistance vs. filtration time for fabric style no. 802B.

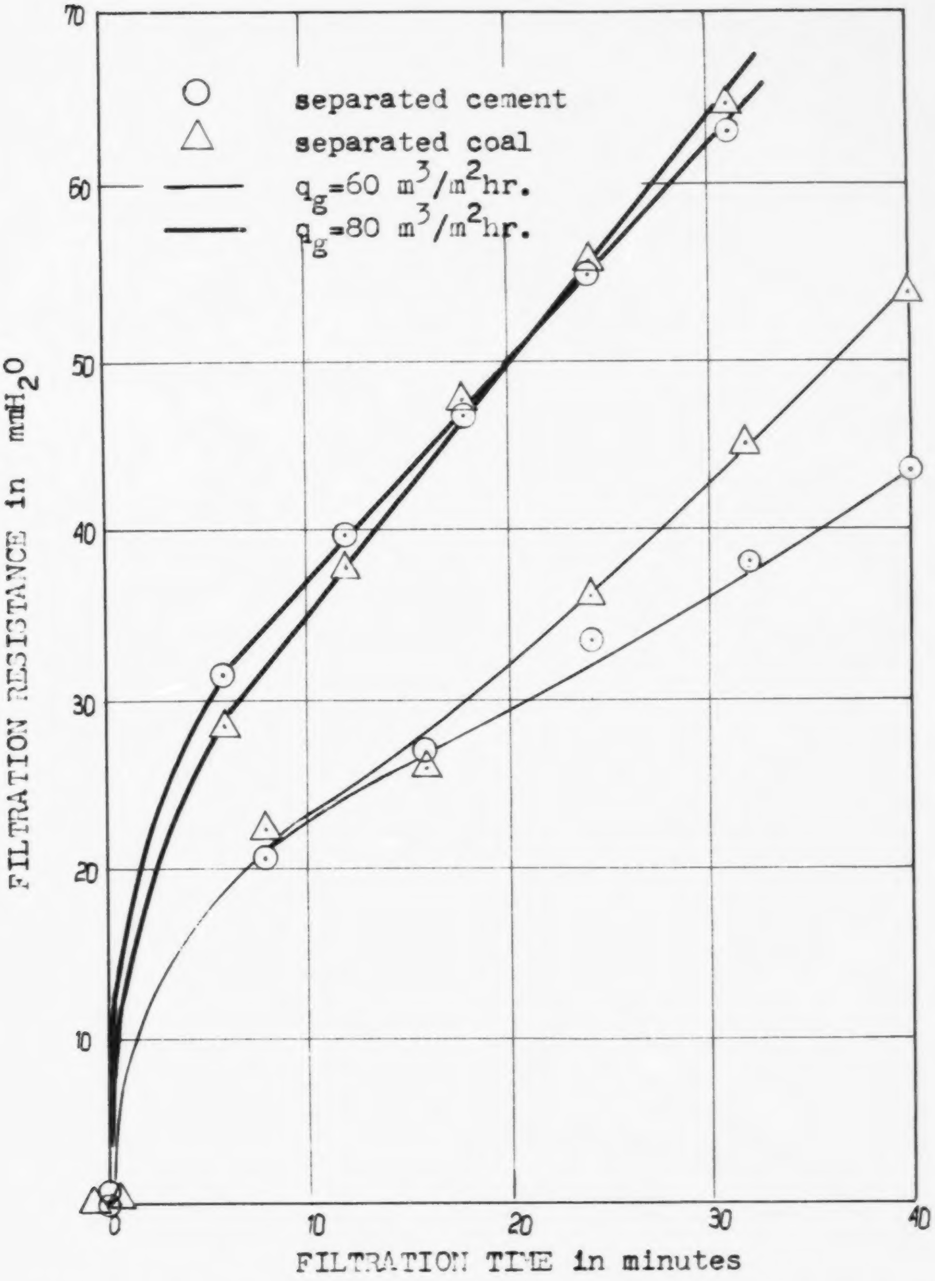

Figure A-29. Filtration resistance vs. filtration time for fabric style no. Q53-875.

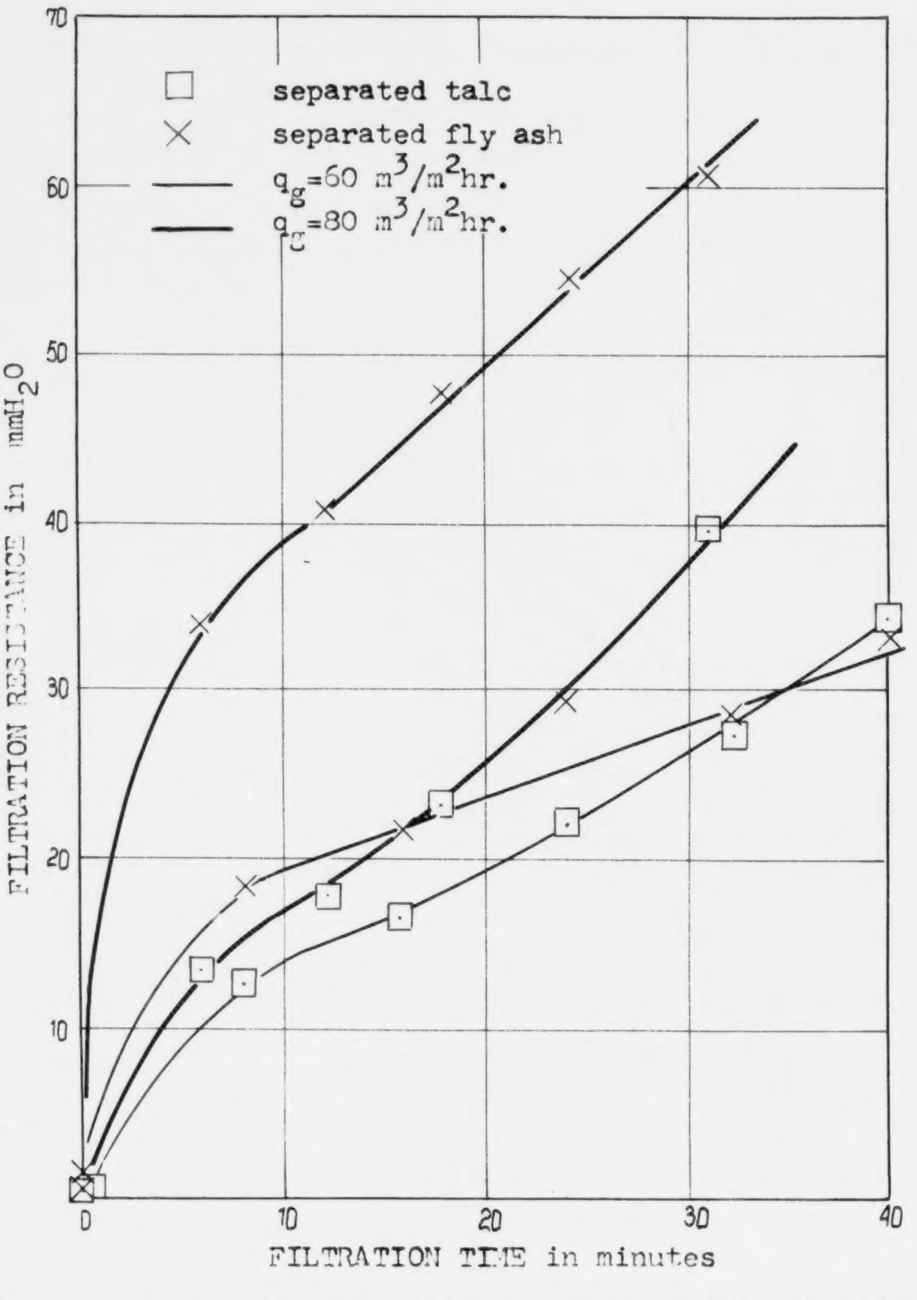

Figure A-30. Filtration resistance vs. filtration time for fabric style no. Q53-875.

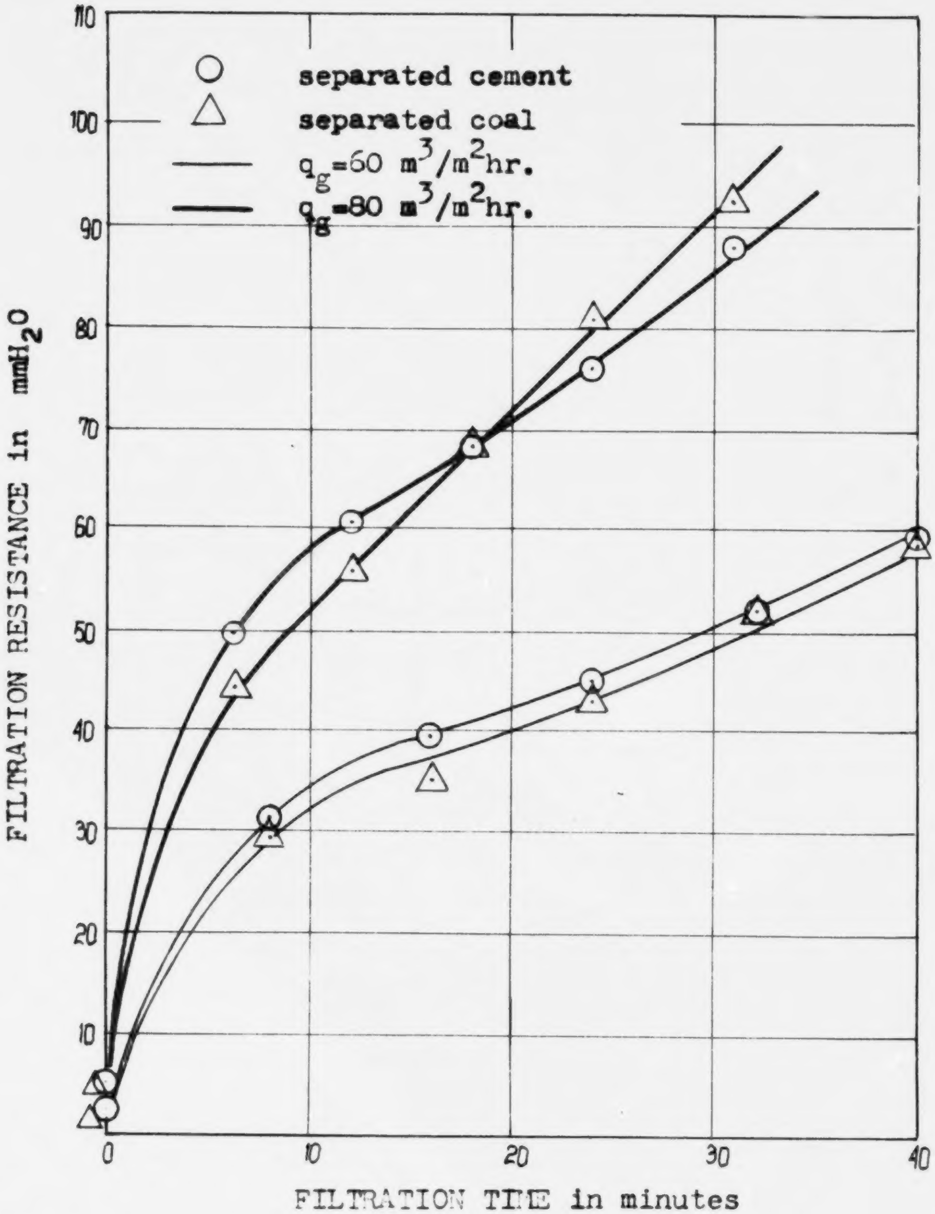

Figure A-31. Filtration resistance vs. filtration time for fabric style no. Q53-870.

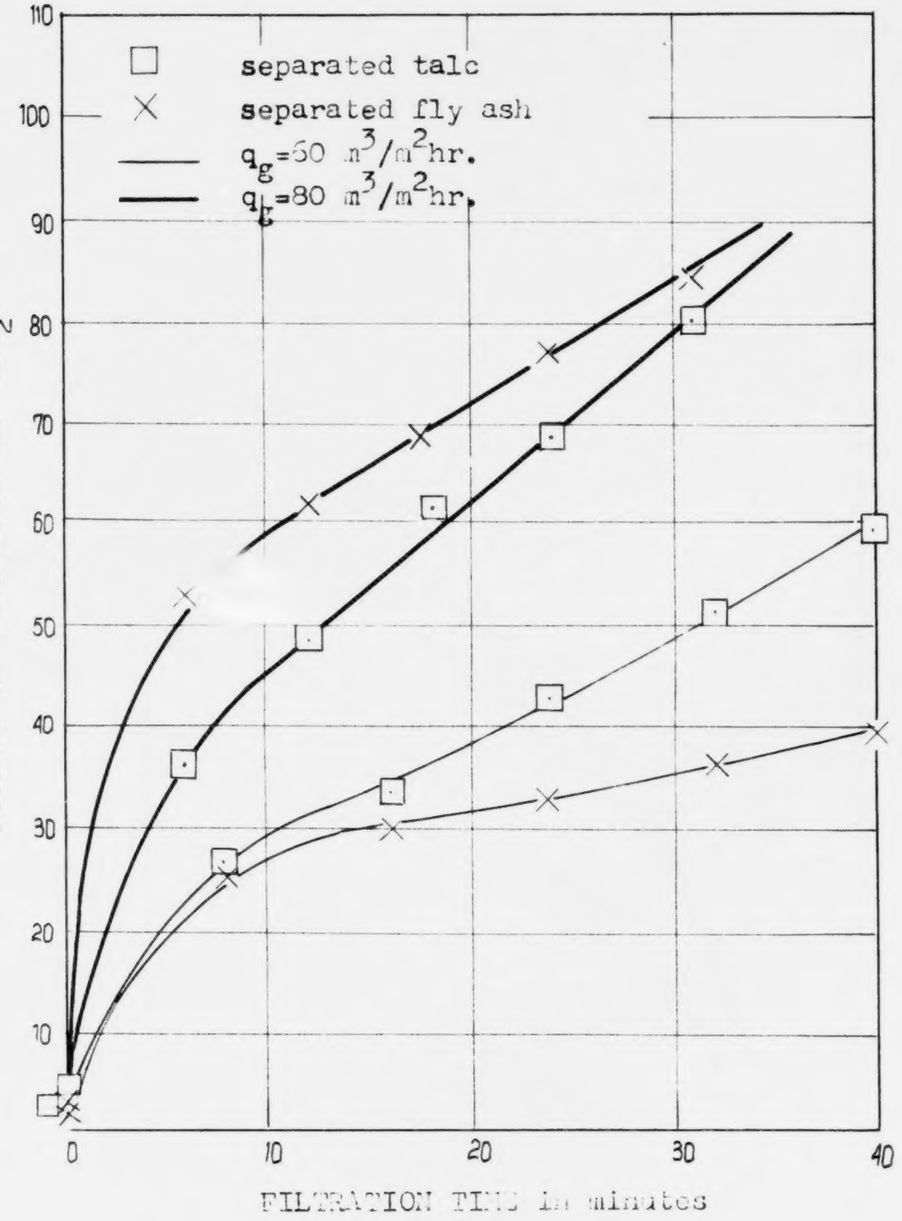

Figure A-32. Filtration resistance vs. filtration time for fabric style no. Q53-870.

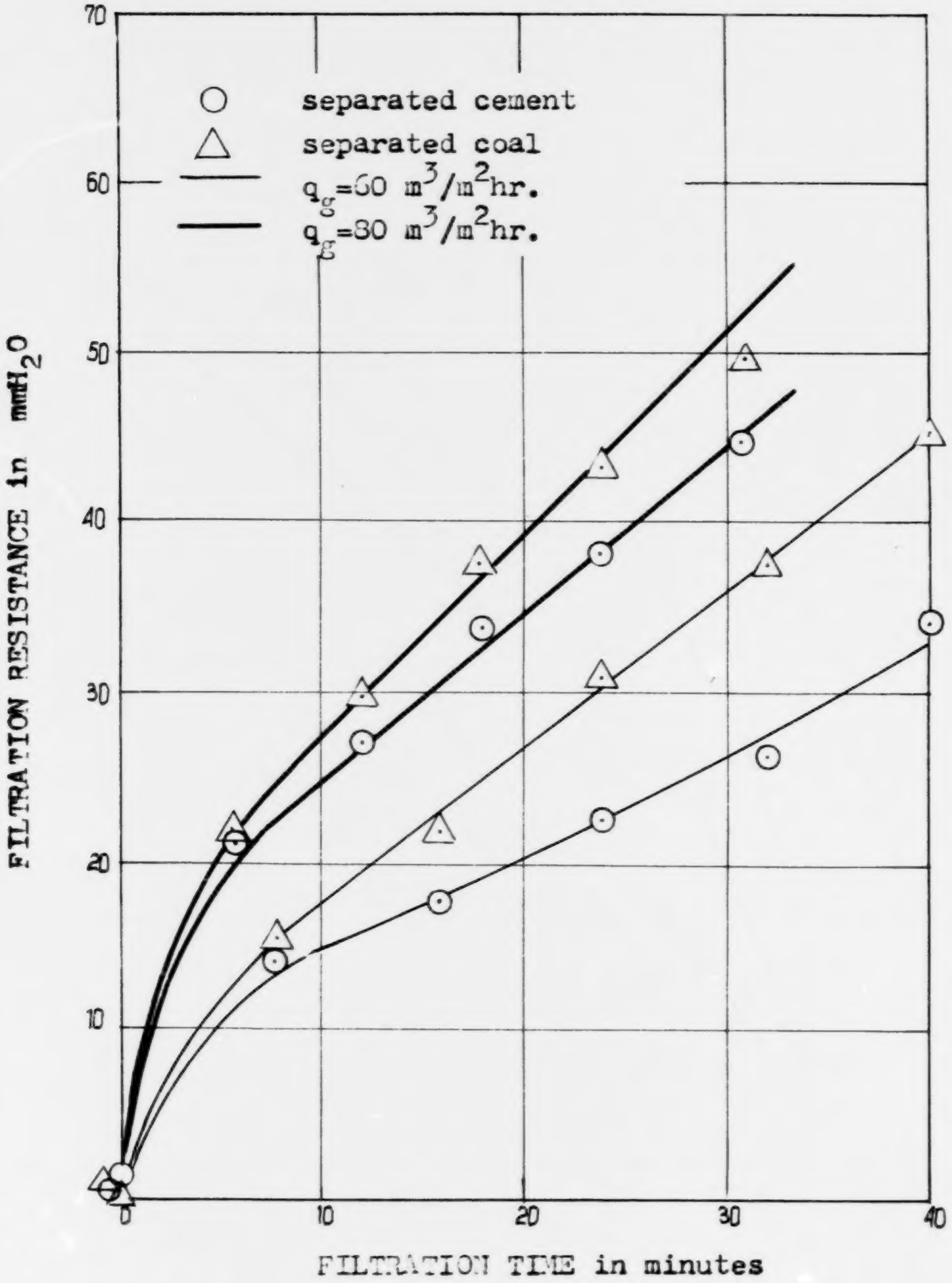

Figure A-33. Filtration resistance vs. filtration time for fabric style no. Q53-878.

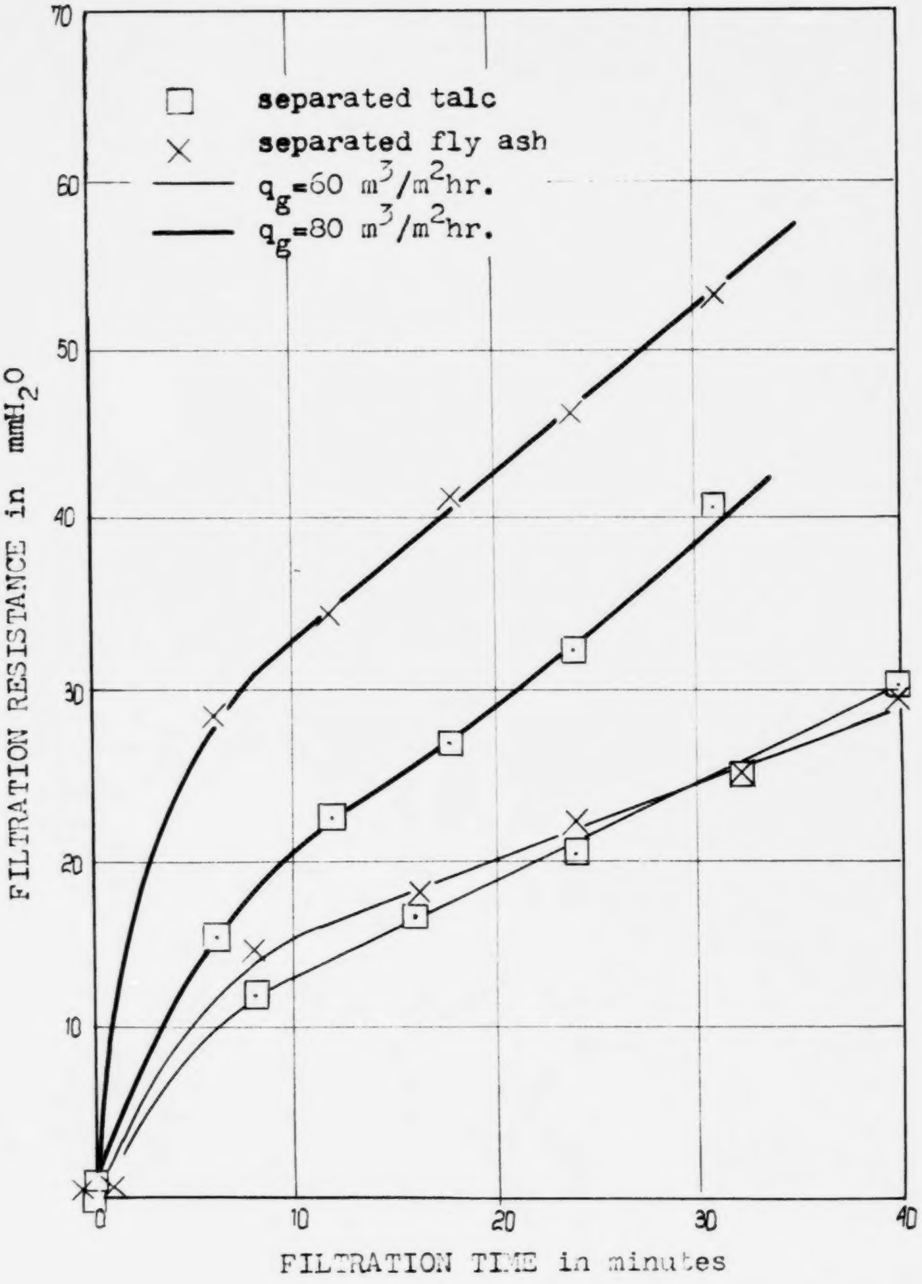

Figure A-34. Filtration resistance vs. filtration time for fabric style no. Q53-878.

APPENDIX B

TABLE B-1. PRESSURE DROP (in mmH_2O) vs. GAS LOADING OF FILTRATION AREA FOR PURE FABRICS

Kind of fabric	q_g in m^3/m^2hr								Conditions		
	50	60	80	100	120	140	160	180	Temp. °C	Rel. Hum. %	Atm. Press. mmHg
960	2.77	3.63	5.29	7.11	8.85	10.83	12.72	14.62	20	47	745
	3.08	3.79	5.29	7.27	9.64	11.77	13.98	16.04			
	3.16	3.87	5.61	7.90	10.19	12.32	14.54	16.59			
	2.84	3.40	4.98	7.03	9.09	11.14	13.04	14.85			
	2.84	3.48	5.06	7.19	9.32	11.38	13.19	15.01			
Average	2.94	3.63	5.25	7.30	9.42	11.49	13.49	15.42			
862B	0.16	0.19	0.25	0.35	0.51	0.66	0.79	0.92			
	0.16	0.19	0.25	0.38	0.51	0.66	0.82	0.95			
	0.16	0.19	0.28	0.38	0.51	0.66	0.82	0.95			
	0.19	0.22	0.32	0.44	0.60	0.79	0.95	1.11			
	0.16	0.19	0.28	0.38	0.54	0.70	0.82	0.98			
Average	0.17	0.20	0.28	0.39	0.53	0.69	0.84	0.98			
C866B	0.40	0.47	0.63	0.95	1.26	1.58	1.90	2.29	20	42	748
	0.40	0.47	0.71	0.95	1.26	1.58	1.90	2.21			
	0.47	0.55	0.79	1.11	1.50	1.98	2.29	2.69			
	0.40	0.47	0.71	0.95	1.34	1.74	2.05	2.45			
	0.32	0.40	0.55	0.71	1.03	1.34	1.58	1.82			
Average	0.40	0.47	0.68	0.93	1.28	1.64	1.94	2.29			
C868B	0.79	0.87	1.26	1.74	2.29	2.92	3.56	4.11	23	47	742
	0.71	0.87	1.26	1.66	2.21	2.84	3.40	3.95			
	0.63	0.79	1.19	1.58	2.31	2.69	3.16	3.63			
	0.63	0.79	1.11	1.50	1.98	2.45	2.92	3.40			
	0.63	0.79	1.11	1.50	2.05	2.61	3.08	3.63			
Average	0.68	0.82	1.19	1.60	2.13	2.70	3.22	3.74			

(continued)

TABLE B-1. (continued)

Kind of fabric	q_g in m^3/m^2hr								Conditions		
	50	60	80	100	120	140	160	180	Temp. °C	Rel. Hum. %	Atm. Press. mmHg
865B	0.63	0.95	1.26	1.90	2.53	3.00	3.48	3.95	20	47	745
	0.79	1.03	1.50	2.21	2.84	3.48	3.95	4.66			
	0.79	1.03	1.50	2.21	2.84	3.48	3.95	4.74			
	1.03	1.26	1.90	2.69	3.48	4.19	4.99	5.61			
	0.95	1.19	1.82	2.61	3.40	4.11	4.82	5.53			
Average	0.84	1.09	1.58	2.32	3.01	3.65	4.24	4.90			
C890B	1.19	1.42	2.05	2.69	3.48	4.19	5.06	6.00	22	35	742
	1.03	1.26	1.74	2.29	2.92	3.48	4.11	4.98			
	1.03	1.26	1.82	2.37	3.00	3.63	4.27	4.98			
	1.26	1.50	2.13	2.37	3.63	4.35	5.21	6.16			
	0.95	1.19	1.58	2.13	2.69	3.24	3.79	4.42			
Average	1.09	1.33	1.86	2.37	3.14	3.78	4.49	5.31			
C892B	1.50	1.82	2.61	3.48	4.50	5.53	6.64	7.74	22	35	742
	1.50	1.82	2.69	3.79	4.82	5.77	6.79	7.82			
	1.66	2.13	3.00	4.03	5.21	6.32	7.66	8.77			
	1.74	2.21	3.08	4.03	5.21	6.56	7.74	8.93			
	1.90	2.37	3.32	4.58	5.77	7.19	8.53	10.03			
Average	1.66	2.07	2.94	3.98	5.10	6.27	7.47	8.63			
852	0.16	0.24	0.32	0.47	0.55	0.71	0.87	1.03	23	53	746
	0.19	0.25	0.35	0.47	0.60	0.79	0.92	1.11			
	0.22	0.25	0.38	0.51	0.66	0.85	1.01	1.14			
	0.19	0.22	0.35	0.44	0.60	0.76	0.89	1.04			
	0.19	0.25	0.35	0.47	0.63	0.79	0.95	1.07			
Average	0.19	0.24	0.35	0.47	0.61	0.78	0.93	1.08			

(continued)

TABLE B-1. (continued)

Kind of fabric	q_g in m^3/m^2hr								Conditions		
	50	60	80	100	120	140	160	180	Temp. °C	Rel. Hum. %	Atm. Press. mmHg
853	0.63	0.79	1.11	1.50	1.98	2.37	2.84	3.24	23	48	750
	0.79	0.95	1.42	1.83	2.45	3.00	3.56	4.11			
	0.63	0.79	1.11	1.42	1.90	2.29	2.77	3.08			
	0.63	0.79	1.19	1.50	2.05	2.53	3.00	3.40			
	0.55	0.71	1.03	1.34	1.74	2.12	2.61	2.92			
Average	0.65	0.81	1.17	1.52	2.02	2.46	2.96	3.35			
190R	1.11	1.34	1.90	2.53	3.32	4.03	4.74	5.37	23	54	746
	1.19	1.42	2.05	2.77	3.63	4.42	5.14	5.93			
	1.03	1.26	1.82	2.45	3.24	3.95	4.58	5.29			
	1.11	1.42	1.97	2.61	3.40	4.19	4.90	5.61			
	1.11	1.34	1.98	2.61	3.40	4.19	4.90	5.61			
Average	1.11	1.36	1.94	2.59	3.40	4.16	4.85	5.56			
850B	0.63	0.79	1.11	1.50	1.98	2.53	3.00	3.63	23	48	750
	0.63	0.79	1.11	1.50	1.98	2.45	2.92	3.32			
	0.63	0.79	1.11	1.50	1.98	2.45	2.92	3.32			
	0.63	0.79	1.19	1.58	2.13	2.61	3.00	3.48			
	0.63	0.79	1.11	1.50	2.05	2.53	2.92	3.40			
Average	0.63	0.79	1.13	1.52	2.02	2.51	2.95	3.43			
802B	0.87	1.03	1.50	1.98	2.69	3.40	4.03	4.66	23	47	742
	0.79	0.95	1.34	1.74	2.29	2.92	3.48	3.95			
	0.79	0.95	1.34	1.82	2.45	3.00	3.63	4.19			
	0.87	1.03	1.50	2.05	2.69	3.40	4.03	4.66			
	0.95	1.11	1.58	2.13	2.92	3.63	4.35	4.98			
Average	0.85	1.01	1.45	1.94	2.61	3.27	3.90	4.49			

(continued)

TABLE B-1. (continued)

Kind of fabric	q_g in m^3/m^2hr								Conditions		
	50	60	80	100	120	140	160	180	Temp. °C	Rel. Hum. %	Atm. Press. mmHg
Q53-875	0.22	0.28	0.41	0.54	0.76	0.95	1.11	1.26	25	50	747
	0.22	0.32	0.44	0.57	0.79	0.98	1.14	1.33			
	0.22	0.25	0.38	0.51	0.73	0.89	1.07	1.26			
	0.22	0.25	0.38	0.54	0.76	0.92	1.11	1.30			
	0.22	0.28	0.41	0.57	0.79	1.01	1.17	1.33			
Average	0.22	0.28	0.40	0.55	0.77	0.95	1.12	1.30			
Q53-870	1.90	2.21	3.32	5.06	6.64	8.22	9.64	11.22	26	38	747
	1.90	2.21	3.48	5.06	6.64	8.06	9.48	11.06			
	1.90	2.21	3.32	4.74	6.32	7.90	9.32	10.74			
	1.90	2.21	3.32	4.90	6.48	7.90	9.48	10.90			
	1.90	2.21	3.48	5.06	6.64	8.06	9.64	11.06			
Average	1.90	2.21	3.38	4.96	6.54	8.03	9.51	11.00			
Q53-979	0.35	0.44	0.66	0.92	1.26	1.61	1.92	2.24	25	50	747
	0.35	0.44	0.63	0.89	1.20	1.55	1.83	2.17			
	0.38	0.47	0.70	0.95	1.30	1.65	1.98	2.34			
	0.35	0.44	0.60	0.95	1.26	1.61	1.96	2.28			
	0.38	0.44	0.69	0.98	1.33	1.65	1.98	2.31			
Average	0.36	0.45	0.66	0.94	1.27	1.61	1.93	2.27			

TABLE B-2. YARN PARAMETERS
(Accomplished by Textile Institute in Lódź)

	Parameter						
Kind of fabric	Diameter of fiber in μm	Number of fibers in cross-section of yarn	Tex of yarn	Diameter of fiber calculated from Tex in μm	Projecting diameter of yarn, width/thickness in μm	Degree of yarn flatten	Number of twist in n/meter
Polyester - staple fiber							
862B							
warp	19.2	230	112.7	443	616/422	0.32	279
fill	19.0	266	137.0	489	683/431	0.33	235
C866B							
warp	--	307	119.3	456	573/455	0.21	394
fill	--	276	113.6	445	645/431	0.33	268
C868B							
warp	22.0	215	135.8	487	543/430	0.21	399
fill	22.0	180	138.1	491	573/439	0.23	279
Polyester - continuous filament fiber							
865B							
warp	24.2	100	67.1	388	400/240	0.40	274
fill	18.9	209	79.2	372	527/320	0.39	399
C890B							
warp	23.2	50	29.2	256	343/173	0.50	133
fill	23.4	50	30.1	260	368/164	0.55	146
C892B							
warp	23.4	50	29.8	259	--	--	without twist
fill	23.8	50	30.9	264	--	--	21

(continued)

TABLE B-2. (continued)

	Parameter						
Kind of fabric	Diameter of fiber in µm	Number of fibers in cross-section of yarn	Tex in yarn	Diameter of fiber calculated from Tex in µm	Projecting diameter of yarn, width/thickness in µm	Degree of yarn flatten	Number of twist in n/meter
Nomex - staple fiber							
852							
warp	--	--	119.4	519	--	--	334
fill	--	--	122.7	525	--	--	331
853							
warp	--	--	110.0	497	--	--	314
fill	--	--	118.8	518	--	--	334
Nomex - continuous filament fiber							
350B							
warp	--	--	22.5	225	--	--	160
fill	--	--	22.2	224	--	--	200
Polyamide - staple fiber							
802B							
warp	--	--	119.5	519	679/533	0.22	416
fill	--	--	137.5	556	852/655	0.23	238
Natural fiber - cotton							
960							
warp	--	--	39.8	250	325/218	0.33	871
fill	--	--	66.8	323	478/360	0.25	515

(continued)

TABLE B-2. (continued)

Kind of fabric	Parameter: Diameter of fiber in μm	Number of fibers in cross-section of yarn	Tex of yarn	Diameter of fiber calculated from Tex in μm	Projecting diameter of yarn, width/thickness in μm	Degree of yarn flatten	Number of twist in n/meter
Glass - staple fiber							
Q53-875							
warp	--	--	67.6	216	443/175	0.60	145
fill	--	--	66.2	214	442/183	0.57	126
Glass - continuous filament fiber							
Q53-870							
warp	--	--	67.5	216	445/186	0.58	144
fill	--	--	68.6	217	474/167	0.65	128
Q53-878							
warp	--	--	138.8	309	558/278	0.50	146
fill	--	--	211.5	383	891/395	0.56	81

TABLE B-3. SIZE OF DUCTS/CANALS FORMED DURING TESTING OF GLASS FABRIC Q53-878 WITH SEPARATED CEMENT

q_g in m^3/m^2hr	Size of ducts/ canals a × b in µm	Equivalent diameter $d_e = 4ab / a + b$ in µm
	Series 2 experiment 1	
60	80×150	104.35
	50×100	66.67
	30×90	45.00
80	50×220	81.48
	60×150	85.71
	50×200	80.00
	90×110	99.00
	30×70	42.00
	60×220	94.28
	60×170	88.69
	20×70	31.10
	110×200	141.93
	120×240	160.00
	110×200	141.93
	10×160	18.82
	70×170	99.17
	100×110	104.76
	70×100	82.35
	60×160	87.27
	40×100	57.14
	70×180	100.80
	90×260	133.71
	60×110	77.65
	30×70	42.00
	20×130	34.67
	60×110	77.65
	30×60	40.00
	50×100	66.67
	30×60	40.00
	20×110	33.85
	50×50	50.00
	60×190	91.20
	90×120	102.86
	60×110	77.65
100	60×160	87.27
	110×180	136.55
	60×220	94.29
	50×190	79.17
	20×170	35.79
	20×150	35.29

(continued)

TABLE B-3. (continued)

q_g in m^3/m^2hr	Size of ducts/ canals a × b in μm	Equivalent diameter $d_e = 4ab / a + b$ in μm
	60×150	85.71
	30×110	47.14
	10×110	18.33
	70×160	97.39
	100×120	109.09
	80×150	104.35
	40×80	53.33
	70×150	95.45
	80×100	88.89
	100×130	113.04
	20×170	35.79
	80×200	114.29
	60×150	85.71
	100×100	100.00
120	150×150	150.00
	70×220	160.21
	110×220	146.67
	50×200	80.00
	20×180	36.00
	60×250	96.77
	30×130	48.75
	60×150	85.71
	100×180	128.57
	40×100	57.14
	120×250	133.33
	70×180	100.80
	50×230	82.14
	20×200	36.36
	60×150	85.71
	60×280	98.82
	40×200	66.67
	50×120	70.59
	50×170	77.27
	60×200	92.31
	20×170	35.79
	100×200	133.33
	50×220	81.48
	120×220	155.29
	30×150	50.00
	50×150	75.00
	50×50	50.00
	50×50	50.00

(continued)

TABLE B-3. (continued)

q_g in m^3/m^2hr	Size of ducts/ canals a × b in µm	Equivalent diameter $d_e = 4ab / a + b$ in µm
150	80×150	104.35
	10×140	18.67
	30×130	48.00
	50×70	58.33
	40×160	64.00
	100×170	125.93
	20×140	35.00
	70×170	99.17
	60×160	87.27
	30×180	51.43
	40×140	62.22
	20×150	35.29
	50×200	80.00
	30×130	48.75
	30×200	52.17
	20×150	35.29
	50×170	77.27
	70×150	95.45
	30×200	52.17
	70×170	99.17
	60×90	72.00
	40×250	68.97
	100×120	109.09
	40×140	62.22
	20×120	34.29
	60×260	97.50
	50×250	83.33
	70×150	95.45
	50×160	76.19
	50×250	83.33
	50×200	80.00
	70×220	106.21
	60×230	95.17
	50×170	77.27
	80×150	104.35
	40×210	67.20
	40×110	58.67
	90×270	135.00
	30×130	48.75
	60×180	90.00
	90×240	187.83
	60×80	68.57
	70×250	159.09

(continued)

TABLE B-3. (continued)

q_g in m^3/m^2hr	Size of ducts/ canals $a \times b$ in µm	Equivalent diameter $d_e = 4ab / a + b$ in µm
	80×220	117.33
	60×260	97.50
	90×140	109.56
	100×150	120.00
200	80×200	114.29
	50×160	76.19
	20×130	34.67
	50×120	70.59
	30×160	50.53
	20×160	35.56
	60×120	80.00
	100×150	120.00
	20×70	31.11
	40×150	63.16
	100×150	120.00
	20×250	37.04
	90×210	126.00
	90×290	137.37
	40×140	62.22
	40×120	60.00
	20×140	35.00
	30×120	48.00
	80×100	88.89
	20×70	31.11
	30×50	37.50
	60×150	85.71
	50×170	77.27
	40×200	66.67
	50×100	66.67
	60×150	85.71
	60×160	87.27
	30×70	42.00
	60×120	80.00
	70×130	91.00
	30×60	40.00
	40×80	53.33
	30×120	48.00
	70×90	78.75
	40×140	62.22
	50×110	68.75
	100×200	133.33
	30×100	46.15

(continued)

TABLE B-3. (continued)

q_g in m^3/m^2hr	Size of ducts/ canals $a \times b$ in μm	Equivalent diameter $d_e = 4ab / a + b$ in μm
	60×100	75.00
	60×120	80.00
	50×260	83.87
	50×90	64.29
	60×250	96.77
	20×100	33.33
	100×200	133.33
	60×160	87.27
	50×120	70.59
	60×200	92.31
	40×90	55.38
	80×220	117.33
	Series 2 experiment 2	
80	100×150	120.00
	60×130	82.10
	40×130	61.18
	30×120	48.00
	30×150	50.00
	40×150	63.16
	40×170	64.76
	20×240	36.92
	60×140	84.00
	20×180	36.00
	90×140	109.56
	70×210	105.00
	10×120	18.46
	50×160	76.19
	20×180	36.00
	50×150	75.00
	100×130	113.04
	80×90	84.71
	40×170	64.76
	10×130	18.57
	40×130	61.18
	50×100	66.67
	20×250	37.04
	20×200	36.36
	70×290	112.78
	80×210	115.86
	70×70	70.00
	120×130	124.80
	30×130	48.75

(continued)

TABLE B-3. (continued)

q_g in m^3/m^2hr	Size of ducts/ canals a × b in µm	Equivalent diameter $d_e = 4ab / a + b$ in µm
	50×110	68.75
	30×100	46.15
	60×190	91.20
	20×180	36.00
	80×150	104.35
	60×170	88.70
100	70×160	97.39
	50×140	73.68
	130×130	130.00
	60×130	82.10
	60×150	85.71
	10×200	19.05
	40×200	66.67
	90×250	187.50
	30×120	48.00
	60×210	93.33
	130×230	166.11
	90×220	127.74
	100×140	116.67
	60×150	85.71
	70×180	100.80
120	100×200	133.33
	70×250	109.37
	70×230	107.33
	20×200	33.33
	30×150	50.00
	50×200	80.00
	70×220	106.21
	70×130	91.00
	40×120	60.00
	60×200	92.31
	100×150	120.00
	40×140	62.22
	70×190	102.31
	50×200	80.00
	60×240	96.00
	80×160	106.67
	30×100	46.15
	120×200	150.00
	50×200	80.00
	40×180	65.45
	50×50	50.00

(continued)

TABLE B-3. (continued)

q_g in m^3/m^2hr	Size of ducts/ canals a × b in μm	Equivalent diameter $d_e = 4ab / a + b$ in μm
	70×140	93.33
	60×150	85.71
150	50×80	61.54
	30×130	48.75
	40×150	63.16
	70×200	103.70
	100×140	116.67
	70×220	106.21
	40×100	57.14
	30×200	52.17
	50×200	80.00
	100×130	113.04
	20×200	36.36
	40×80	53.33
	10×120	18.46
	30×150	50.00
	140×200	164.71
	60×120	80.00
	40×120	60.00
	90×220	127.74
	40×150	63.16
	50×130	72.22
	40×120	60.00
	30×170	51.00
	80×220	117.33
	40×180	65.45
	50×150	75.00
	70×270	111.18
	40×100	57.14
	60×170	88.70
	40×80	53.33
	70×180	100.80
	50×150	75.00
	70×120	88.42
	60×120	80.00
	70×170	99.17
	90×170	117.69
	100×250	142.86
	80×220	117.33
	80×150	104.35
	50×200	80.00
	40×120	60.00

(continued)

TABLE B-3. (continued)

q_g in m^3/m^2hr	Size of ducts/ canals a × b in µm	Equivalent diameter $d_e = 4ab / a + b$ in µm
	100×130	113.04
	50×90	64.29
200	40×150	63.16
	70×200	103.70
	70×250	109.37
	30×250	53.57
	60×220	94.29
	30×130	48.75
	100×150	120.00
	50×250	83.33
	40×150	63.16
	80×180	110.77
	30×120	48.00
	50×120	70.59
	50×120	70.59
	40×170	64.76
	30×120	48.00
	30×150	50.00
	40×200	66.67
	30×70	42.00
	50×220	81.48
	70×70	70.00
	80×110	92.63
	70×170	99.17
	90×220	127.74
	50×180	78.26
	20×200	36.36
	30×200	52.17
	70×120	88.42
	100×220	137.50
	100×100	100.00
	60×70	64.61
	60×160	87.27
	100×240	141.18
	90×190	122.14

TABLE B-4. CHARACTERISTIC PRESSURE DROP (in mmH_2O) FOR REVERSE AIR FLOW REGENERATION
(Dust: separated cement, $q_g = 60\ m^3/m^2hr$)

Kind of fabric	ΔP_K	ΔP_o	ΔP_{NK}
960	25.5	3.6	14.3
862B	21.9	0.5	5.1
C866B	23.0	0.8	6.7
C868B	24.3	1.4	10.3
865B	27.1	1.0	8.7
C890B	36.2	1.6	5.2
C892B	33.2	2.1	4.9
852	19.6	0.5	6.4
853	18.7	0.8	8.3
190R	12.7	1.6	4.7
850B	38.9	4.7	11.6
802B	18.5	1.0	7.6
Q53-875	37.0	0.6	4.7
Q53-870	44.72	1.9	12.8
Q53-878	33.14	0.6	6.0

TABLE B-5. CHARACTERISTIC PRESSURE DROP (in mmH_2O) FOR MECHANICAL REGENERATION
(Dust: separated cement, $q_g = 60\ m^3/m^2hr$)

Kind of fabric	ΔP_{RM1}	ΔP_{RM2}	ΔP_{RM3}
960	15.2	15.2	15.6
862B	4.3	3.5	2.8
C866B	7.7	6.8	6.2
C868B	9.9	9.3	9.2
865B	6.5	6.3	6.0
C890B	4.3	4.7	4.6
C892B	4.4	4.4	4.6
852	6.6	6.6	6.2
853	9.8	9.6	9.5
190R	5.5	5.5	5.5
850B	7.4	6.8	6.8
802B	7.3	7.3	7.3
Q53-875	4.6	4.1	3.8
Q53-870	18.2	15.5	15.8
Q53-878	5.4	4.7	4.7

TABLE B-6. CHARACTERISTIC PRESSURE DROP (in mmH_2O) FOR REVERSE AIR FLOW REGENERATION
(Dust: separated cement, q_g=80 m^3/m^2hr)

Kind of fabric	ΔP_K	ΔP_o	ΔP_{NK}
960	30.6	7.4	16.7
862B	34.2	0.8	5.5
C866B	32.1	1.1	8.5
C868B	32.5	2.1	14.5
865B	47.5	1.6	8.6
C890B	64.8	3.5	11.6
C892B	65.9	3.6	12.3
852	26.3	0.8	7.8
853	26.6	2.4	11.5
190R	17.9	2.2	4.9
850B	56.2	1.9	14.4
802B	29.5	1.9	8.8
Q53-875	56.2	0.9	8.6
Q53-870	61.7	3.0	19.8
Q53-878	47.3	1.1	6.4

TABLE B-7. CHARACTERISTIC PRESSURE DROP (in mmH_2O) FOR MECHANICAL REGENERATION
(Dust: separated cement, q_g = 80 m^3/m^2hr)

Kind of fabric	ΔP_{RM1}	ΔP_{RM2}	ΔP_{RM3}
960	18.8	19.4	19.4
862B	4.3	3.6	3.0
C866B	9.2	8.4	7.6
C868B	14.2	13.9	13.7
865B	16.4	12.0	10.4
C890B	15.3	10.9	10.4
C892B	18.5	12.8	12.8
852	9.0	8.8	7.9
853	12.6	12.3	12.3
190R	5.1	5.5	5.5
850B	16.3	11.5	11.4
802B	11.1	10.6	10.6
Q53-875	7.3	3.5	3.3
Q53-870	24.2	17.4	18.6
Q53-878	7.9	5.2	5.2

TABLE B-8. CHARACTERISTIC PRESSURE DROP (in mmH_2O) FOR REVERSE AIR FLOW REGENERATION
(Dust: unseparated coal, q_g = 60 m^3/m^2hr)

Kind of fabric	ΔP_K	ΔP_o	ΔP_{NK}
960	28.6	3.5	14.0
862B	28.9	0.9	5.4
C866B	22.7	1.1	5.5
C868B	28.3	1.9	7.6
865B	26.9	1.6	6.1
C890B	35.5	1.4	7.1
C892B	51.5	3.3	10.1
852	25.4	0.8	6.9
853	22.0	1.4	7.4
190R	17.6	1.6	4.9
850B	41.0	1.4	10.4
802B	20.2	1.6	5.8
Q53-875	51.1	0.8	6.3
Q53-870	58.0	2.8	15.7
Q53-878	42.4	0.9	5.5

TABLE B-9. CHARACTERISTIC PRESSURE DROP (in mmH_2O) FOR MECHANICAL REGENERATION
(Dust: unseparated coal, q_g = 60 m^3/m^2hr)

Kind of fabric	ΔP_{RM1}	ΔP_{RM2}	ΔP_{RM3}
960	14.7	14.7	14.7
862B	5.4	5.2	5.1
C866B	5.7	5.4	5.1
C868B	7.7	7.9	7.9
865B	7.7	7.4	7.1
C890B	7.1	8.4	8.7
C892B	10.3	10.7	10.7
852	7.4	7.6	7.4
853	7.9	7.7	7.7
190R	5.2	5.2	5.2
850B	11.7	12.6	13.3
802B	6.2	6.3	6.2
Q53-875	8.7	8.4	8.1
Q53-870	19.8	21.2	22.3
Q53-878	6.8	7.1	7.1

TABLE B-10. CHARACTERISTIC PRESSURE DROP (in mmH$_2$O) FOR REVERSE AIR FLOW REGENERATION
(Dust: unseparated coal, $q_g = 80$ m^3/m^{2}hr)

Kind of fabric	ΔP_K	ΔP_o	ΔP_{NK}
960	38.9	5.8	18.1
862B	29.5	1.1	5.5
C866B	31.2	1.6	6.6
C868B	29.3	1.9	7.2
865B	42.1	1.7	7.1
C890B	65.6	3.8	12.5
C892B	53.9	4.1	12.5
852	28.3	1.7	5.9
853	26.4	1.9	7.7
190R	20.9	2.1	5.1
850B	54.4	2.7	14.4
802B	26.2	1.9	7.8
Q53-875	51.9	0.9	6.8
Q53-870	66.7	3.4	13.0
Q53-878	52.4	1.3	5.3

TABLE B-11. CHARACTERISTIC PRESSURE DROP (in mmH$_2$O) FOR MECHANICAL REGENERATION
(Dust: unseparated coal, $q_g = 80$ m^3/m^{2}hr)

Kind of fabric	ΔP_{RM1}	ΔP_{RM2}	ΔP_{RM3}
960	19.8	20.2	20.7
862B	6.2	6.0	5.7
C866B	7.1	7.1	6.8
C868B	7.7	7.3	7.1
865B	7.0	7.4	7.4
C890B	18.2	19.0	19.6
C892B	15.3	17.1	15.6
852	5.8	6.3	6.0
853	9.3	9.6	9.8
190R	6.0	5.7	5.5
850B	22.9	21.0	19.6
802B	8.1	8.1	8.1
Q53-875	10.9	10.9	10.1
Q53-870	16.0	16.0	16.0
Q53-878	5.2	5.5	5.5

TABLE B-12. CHARACTERISTIC PRESSURE DROP (in mmH_2O) FOR REVERSE AIR FLOW REGENERATION

(Dust: separated talc, q_g = 60 m^3/m^2hr)

Kind of fabric	ΔP_K	ΔP_o	ΔP_{NK}
960	26.8	4.0	11.5
862B	20.2	0.6	4.3
C866B	22.2	0.8	5.7
C868B	22.0	1.4	7.8
865B	34.4	1.3	8.2
C890B	49.1	2.8	16.6
C892B	38.1	2.1	10.7
852	19.6	0.6	3.2
853	14.7	1.1	8.8
190R	14.1	1.4	3.6
850B	36.6	1.4	14.0
802B	23.6	2.7	8.9
Q53-875	50.6	0.8	12.0
Q53-870	41.4	2.5	15.3
Q53-878	38.3	1.1	10.8

TABLE B-13. CHARACTERISTIC PRESSURE DROP (in mmH_2O) FOR MECHANICAL REGENERATION

(Dust: separated talc, q_g = 60 m^3/m^2hr)

Kind of fabric	ΔP_{RM1}	ΔP_{RM2}	ΔP_{RM3}
960	12.3	12.8	12.8
862B	4.3	4.0	3.8
C866B	5.5	6.2	6.2
C868B	7.4	7.7	7.6
865B	8.1	8.1	7.9
C890B	17.1	16.1	15.6
C892B	12.3	11.2	10.9
852	5.1	5.5	5.4
853	9.2	9.5	9.5
190R	4.0	4.1	4.1
850B	13.6	13.7	13.9
802B	10.3	10.4	10.4
Q53-875	14.4	11.2	10.3
Q53-870	12.0	12.0	11.7
Q53-878	16.9	16.9	17.1

TABLE B-14. CHARACTERISTIC PRESSURE DROP (in mmH_2O) FOR REVERSE AIR FLOW REGENERATION
(Dust: separated talc, $q_g = 80\ m^3/m^2hr$)

Kind of fabric	ΔP_K	ΔP_o	ΔP_{NK}
960	37.5	5.7	17.4
862B	34.2	0.8	5.5
C866B	33.0	1.1	8.1
C868B	28.6	2.4	10.6
865B	40.8	2.1	8.5
C890B	60.5	4.3	15.5
C892B	45.6	2.9	9.5
852	22.4	1.1	6.5
853	22.5	1.9	10.6
190R	16.8	1.9	4.8
850B	63.9	2.5	19.0
802B	23.8	1.9	8.7
Q53-875	54.5	1.1	8.5
Q53-870	80.6	3.4	22.7
Q53-878	51.9	1.1	12.6

TABLE B-15. CHARACTERISTIC PRESSURE DROP (in mmH_2O) FOR MECHANICAL REGENERATION
(Dust: separated talc, $q_g = 80\ m^3/m^2hr$)

Kind of fabric	ΔP_{RM1}	ΔP_{RM2}	ΔP_{RM3}
960	18.0	18.2	18.2
862B	6.2	6.0	5.8
C866B	9.6	9.0	8.4
C868B	12.3	12.2	11.4
865B	10.7	10.6	10.4
C890B	20.2	20.5	20.1
C892B	8.8	6.6	6.0
852	9.6	9.8	9.5
853	10.9	10.7	10.7
190R	5.1	5.2	5.1
850B	21.2	21.8	21.6
802B	9.6	9.8	9.6
Q53-875	11.4	12.2	11.7
Q53-870	25.4	26.7	26.5
Q53-878	14.2	14.4	14.2

TABLE B-16. CHARACTERISTIC PRESSURE DROP (in mmH_2O) FOR REVERSE AIR FLOW REGENERATION
(Dust: separated fly ash, $q_g = 60\ m^3/m^2hr$)

Kind of fabric	ΔP_K	ΔP_o	ΔP_{NK}
960	23.1	4.7	15.1
862B	15.2	1.3	5.7
C866B	14.9	0.8	8.3
C868B	16.6	1.1	7.6
865B	22.3	2.1	8.2
C890B	29.2	1.3	8.7
C892B	31.9	2.4	11.3
852	15.7	0.6	5.7
853	--	--	--
190R	8.9	1.3	4.6
850B	26.8	2.4	10.8
802B	16.4	1.0	6.8
Q53-875	26.4	1.3	11.4
Q53-870	37.7	1.9	17.8
Q53-878	15.6	0.6	6.0

TABLE B-17. CHARACTERISTIC PRESSURE DROP (in mmH_2O) FOR MECHANICAL REGENERATION
(Dust: separated fly ash, $q_g = 60\ m^3/m^2hr$)

Kind of fabric	ΔP_{RM1}	ΔP_{RM2}	ΔP_{RM3}
960	19.1	18.8	17.7
862B	4.7	4.4	4.1
C866B	10.3	9.5	9.2
C868B	7.7	7.6	7.3
865B	8.8	7.6	7.1
C890B	11.7	9.6	8.2
C892B	10.6	14.5	4.9
852	4.7	4.6	4.1
853	--	--	--
190R	4.6	4.4	4.4
850B	12.5	11.4	11.4
802B	11.9	10.6	9.9
Q53-875	11.5	12.3	13.1
Q53-870	16.0	17.1	19.1
Q53-878	6.0	5.8	6.0

TABLE B-18. CHARACTERISTIC PRESSURE DROP (in mmH_2O) FOR REVERSE AIR FLOW REGENERATION
(Dust: separated fly ash, q_g = 80 m^3/m^2hr)

Kind of fabric	ΔP_K	ΔP_o	ΔP_{NK}
960	27.2	3.8	15.6
862B	18.1	3.0	8.0
C866B	22.9	1.3	9.9
C868B	21.2	1.7	8.7
865B	34.6	1.9	13.7
C890B	44.4	2.8	11.3
C892B	44.9	3.2	12.4
852	21.4	0.8	9.4
853	--	--	--
190R	11.3	1.7	4.5
850B	44.4	1.4	17.7
802B	19.6	1.9	10.4
Q53-875	45.4	0.8	9.8
Q53-870	46.2	3.4	14.3
Q53-878	28.8	0.8	8.3

TABLE B-19. CHARACTERISTIC PRESSURE DROP (in mmH_2O) FOR MECHANICAL REGENERATION
(Dust: separated fly ash, q_g = 80 m^3/m^2hr)

Kind of fabric	ΔP_{RM1}	ΔP_{RM2}	ΔP_{RM3}
960	16.1	16.6	16.6
862B	6.3	5.8	5.4
C866B	13.6	12.8	12.2
C868B	9.2	9.2	9.0
865B	14.1	11.9	11.1
C890B	12.2	11.5	11.5
C892B	13.7	12.0	12.5
852	20.1	19.6	19.1
853	--	--	--
190R	9.8	9.8	9.6
850B	16.3	16.8	16.9
802B	11.2	11.1	11.1
Q53-875	12.6	11.1	10.7
Q53-870	9.5	9.2	8.5
Q53-878	10.3	9.6	9.6

TABLE B-20. TABULATION OF L_o, L_W, AND L_{NK} CALCULATED FROM DUST BALANCE FOR EXPERIMENTS IN LARGE SCALE

Kind of fabric	Kind of dust	q m^3/m^2h	L_o g/m^2	L_W g/m^2	L_{NK} g/m^2	Filtration time (minutes)
960	Sep. Cement	60	403.6	159.2	244.4	78
		80	396.6	139.8	256.8	36.4
862B		60	400.6	173.4	227.2	89
		80	398.0	220.1	177.9	54
C866B		60	398.3	221.5	176.8	115
		80	395.5	199.2	196.3	51
C868B		60	398.8	201.9	196.9	109
		80	396.4	171.4	225.0	35
865B		60	400.9	225.9	175.0	108
		80	400.5	336.3	64.2	95
C890B		60	391.8	375.6	16.2	241
		80	399.0	387.0	12.0	112
C892B		60	400.7	384.6	16.1	240
		80	394.6	374.7	19.9	134
852		60	401.1	129.4	271.7	53
		80	394.8	131.0	263.8	27
853		60	400.5	100.0	300.5	55
		80	399.5	100.5	299.0	22
190R		60	402.8	98.8	304.0	34
		80	399.7	109.1	290.6	25
850B		60	403.8	375.0	28.8	243
		80	396.1	374.0	22.1	108
802B		60	404.4	137.9	266.5	68
		80	401.7	171.0	230.7	41
Q53-875		60	403.0	338.1	64.9	195
		80	405.7	355.4	50.3	104
Q53-870		60	400.4	349.6	50.8	255
		80	400.6	341.8	58.8	103
Q53-878		60	403.5	312.0	91.5	181
		80	393.2	299.7	93.5	95
960	Unsep. Coal	60	400.5	210.9	189.6	78
		80	402.7	219.7	183.0	50.6
862B		60	401.3	258.4	142.9	90
		80	397.4	224.2	173.2	67
C866B		60	397.9	256.9	141.0	101
		80	403.2	261.9	141.2	68

(continued)

TABLE B-20. (continued)

Kind of fabric	Kind of dust	q_g m^3/m^2h	L_o g/m^2	L_W g/m^2	L_{NK} g/m^2	Filtration time (minutes)
C868B		60	385.5	258.1	127.4	89
		80	400.3	267.2	133.1	67
865B		60	398.4	335.8	62.6	146
		80	397.5	325.0	72.5	88
C890B		60	403.9	382.4	21.5	161
		80	401.1	380.4	20.7	104
C892B		60	405.2	381.6	23.6	137
		80	395.1	377.1	18.0	100
852		60	391.3	193.1	198.2	75
		80	402.7	229.0	173.7	59
853		60	397.9	179.4	218.5	61
		80	401.8	200.3	201.5	56
190R		60	396.1	228.1	168.0	62
		80	413.6	192.3	221.3	47
850B		60	396.3	369.3	27.0	150
		80	394.3	371.8	22.5	98
802B		60	411.4	214.2	197.2	98
		80	403.7	205.6	198.1	52
Q53-875		60	397.8	339.9	57.9	124
		80	401.4	342.3	59.1	102
Q53-870		60	398.3	343.9	54.4	130
		80	394.6	340.3	54.3	92
Q53-878		60	401.7	330.7	71.0	129
		80	401.5	328.6	72.9	90
960	Sep. Talc	60	391.8	240.8	151.0	69.6
		80	397.4	208.0	189.4	41.4
862B		60	406.1	286.3	119.8	86
		80	398.4	264.2	134.2	46
C866B		60	386.4	252.4	134.0	75
		80	383.0	237.1	145.9	40
C868B		60	382.7	236.1	146.6	73
		80	358.9	214.3	144.6	41
865B		60	400.9	319.1	82.8	87
		80	379.3	317.4	61.9	57

(continued)

TABLE B-20. (continued)

Kind of fabric	Kind of dust	q_g m^3/m^2h	L_o g/m^2	L_W g/m^2	L_{NK} g/m^2	Filtration time (minutes)
C890B		60	376.9	365.7	11.2	112
		80	375.8	352.6	23.2	70
C892B		60	382.3	362.1	20.2	126
		80	351.0	330.2	20.8	67.6
852		60	409.4	244.5	164.9	66
		80	363.1	148.6	214.5	28
853		60	379.2	93.6	285.6	18.4
		80	385.5	119.8	265.7	19
190R		60	370.3	179.6	190.7	43.6
		80	393.0	142.4	250.6	25
850B		60	372.1	356.9	15.2	127.5
		80	394.2	379.7	14.5	80
802B		60	402.9	182.3	220.6	49
		80	372.1	178.7	193.4	30
Q53-875		60	402.2	353.4	48.8	107
		80	387.3	322.4	64.9	62
Q53-870		60	378.3	333.6	44.7	95
		80	385.2	335.7	49.5	68
Q53-878		60	384.1	309.5	74.6	80
		80	372.9	279.9	93.0	54
960	Sep. Fly Ash	60	403.0	106.7	296.3	39.2
		80	400.0	86.6	313.4	11
862B		60	399.9	153.8	246.1	28
		80	392.6	129.1	263.5	15
C866B		60	411.0	86.0	325.0	18,8
		80	397.9	121.8	276.1	14.4
C868B		60	403.3	113.8	289.5	24
		80	400.1	147.4	252.7	20
865B		60	397.2	205.4	191.8	31
		80	397.5	206.4	191.1	25
C890B		60	396.4	347.0	49.4	65
		80	394.8	377.0	17.8	60
C892B		60	391.2	358.4	32.8	90
		80	399.2	377.0	22.2	64

(continued)

TABLE B-20. (continued)

Kind of fabric	Kind of dust	q_g m^3/m^2h	L_o g/m^2	L_W g/m^2	L_{NK} g/m^2	Filtration time (minutes)
852		60	408.8	116.4	292.4	37
		80	409.6	64.0	345.6	10.5
853		60	--	--	--	--
		80	--	--	--	--
190R		60	404.3	78.3	326.0	15
		80	412.6	146.8	265.8	11
850B		60	401.2	374.4	26.8	82
		80	412.0	394.4	17.6	63
802B		60	403.5	98.2	305.3	25
		80	397.5	91.2	306.3	13
Q53-875		60	398.4	301.3	97.1	99
		80	400.5	327.7	72.8	53
Q53-870		60	394.0	302.7	91.3	79
		80	399.0	330.0	69.0	55
Q53-878		60	401.6	119.0	282.6	25
		80	404.4	132.0	272.4	17

Note: All values are means from five measurement cycles.

TABLE E-21. PARAMETERS OF POLISH FABRICS

Parameter	Unit	Kind of fabric						
		BT-57	ET-3	ET-4	ET-30	F-tor5	PT-15	ST-7
Kind of fiber	--	Cotton	Polyester	Polyester	Polyester	Polyester	Polyamide	Glass
Fabric weight	g/m^2	429	510±36	450±31	365±25	271±13	272±14	307±16
Thread count in 10 cm: warp		122	204±6	180±5	477±10	540±12	564±12	215
fill		118	124±5	126±5	276±6	376±12	360±11	215
Tensile strength: warp	kg/5cm	121	270	240	250	346	300	250
fill	kg/5cm	110	220	370	130	276	200	250
Elongation during tension: warp	%	25	70	75	60	30	60	6
fill	%	20	55	56	50	20	40	6
Permeability at P = 20 mm	m^3/m^2. minute	13	15-22	12-18	12-18	13	5	14
Weave		$\frac{2}{2}Z$	$\frac{1}{3}Z$	$\frac{1}{3}Z$	$\frac{2}{1}Z$	$\frac{2}{2}Z$	$\frac{3}{3}Z$	$\frac{3}{1}Z$
Finishing		--	One side scraping	--	Stabilizing, washing	--	Stabilizing	Siliconizing or graphiting

APPENDIX C

APPENDIX C-1

APPARATUS FOR AIR PERMEABILITY TESTING
Type ATL-2 /FF-12/

Producer: METEFEM - Budapest - Hungary

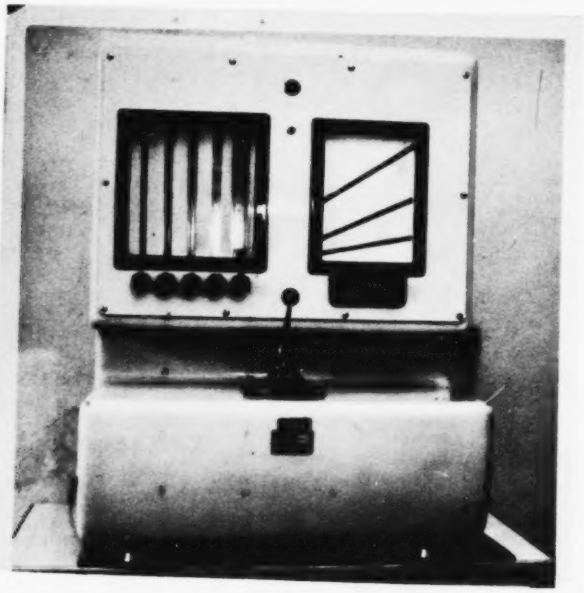

TECHNICAL DATA

Testing area	20,50, and 100 cm^2
Measurement range of manometer	0 - 30 mm of water
	30 - 100 mm of water
	100 - 200 mm of water
Measurement range of rotameter (tolerance ±5 percent according to extreme swing)	10 - 50 liter/hr
	40 - 200 liter/hr
	150 - 750 liter/hr
	600 - 3,000 liter/hr
	2,500 - 15,000 liter/hr
Max. capacity of fan	8,000 liter/hr

OPERATIONAL PRINCIPLE

The fabric sample is placed on two rings and after stretching is fastened. The rings can be regulated and enable regulation of the fabric sample size to 20, 50, and 100 cm^2. The ambient air is sucked through the fabric by a suction nozzle. The air volume is measured by rotameters supplied with individual needle valves. The pressure difference before and behind the fabric sample, during the flow of a definite volume of air, is measured by a manometer. The air permeability is defined as the volume of air flowing through unit area of acclimatized flat textile material during time unit, at a constant difference of pressure before and behind the sample, (expressed as cm^3/m^2s or m^3/m^2min). For technical materials, the pressure difference is assumed to be 20 mmH_2O.

CALCULATION OF RESULTS

The air permeability measured by the ATL-2 apparatus is calculated from the following formula:

$$Q = q/6f \qquad (m^3/m^2min)$$

where q = air volume measured by rotameter in l/hr, and
f = examined area of sample in cm^2.

The measurement is made at various points of the examined fabric (depending upon its uniformity). The number of measurements must obey the condition that the relative random error does not exceed 5 percent. Permeability of the testing fabric is the arithmetic mean of the measured permeabilities of the individual points. The relative random error of air permeability should be calculated according to the equation:

$$\Delta = \frac{t\sigma}{\bar{x}n}$$

where σ = mean quadratic deviation of air flow velocity,
$\bar{x}$ = mean air flow velocity,
n = number of measurements, and
t = confidence coefficient at 95 percent probability and n-1 number of degrees of freedom read from the Student t-distribution table.

APPENDIX C-2

CENTRIFUGAL DUST CLASSIFIER - BAHCO

Producer: ETABLISSEMENTS NEU, Lille - France

PRINCIPLE OF OPERATION

The determination of dust grain size using the Bahco centrifugal dust classifier is based on the following principle.

The dust is introduced into a spiral-shaped air current flowing towards the center with suitable values of the tangential and radial velocity. It is divided into two parts so a certain quantity of dust is accelerated by the centrifugal force against the periphery of the whirl while the other part of the dust is carried by the air current towards the center of the whirl by means of the friction between the air and the dust particles. The Stokes' and Archimedes' laws can be applied.

The sifting chamber, in which the separation takes place, is driven by an electric motor operating at stable peripheral speed. Air is sucked into the sifting space by the fan and goes through the slots. Due to the slots, the air has rotational motion determined by the motion of the apparatus, so the relative peripheral speed of the air amounts to zero. Thus, in the sifting chamber there is only the radial velocity. The centrifugal force and the friction between the air and the dust particles result in grains larger than the limit being thrown out and collected on the ring. Smaller grains are taken by the air stream.

The grain sizes are determined from the loss of dust mass after each separation, with the mass being the residue collected after each previous separation. The known different air flow velocities in the sifting space determine, according to Stokes' law, the limiting dynamic dust grain sizes of the successive ranges.

PREPARATION OF THE SAMPLE

The sample has to be dried at a temperature below 105° C, but above the temperature of ambient air, for 1 hr. Then it should be cooled in an exsiccator and left in contact with air for at least 24 hr. The sample will reach thermodynamic equilibrium with the ambient air. The laboratory temperature should not be lower than 10° C and not higher than 35° C, and the relative air humdity should not be higher than 60 percent.

CALCULATION OF THE WEIGHT-PERCENTAGE OF PARTICLES IN INDIVIDUAL RANGES

The percentage, by particle weight, can be determined using the following formula:

$$k_i = \left[\frac{m_{i-1} - m_i}{m_o}\right] 100$$

where m_{i-1} = the weight of dust introduced each time to the feeder, in grams,

m_i = the weight of dust collected after each separation, in grams, and

m_o = the weight of the analytical sample, in grams.

Dynamic dust particle sizes a_i, which are the upper grain size limits in individual ranges "i", correspond to the k_i. The dynamic grain sizes of dust a_i, expressed in m, are determined from the following equation:

$$a_i = a_{oi} \sqrt{\frac{\rho_o}{\rho_t}}$$

where a_{oi} = dynamic dust particle size, in µm, corresponding to particle density $\rho_o = 1$ g/cm^3, and

ρ_t = density of tested dust, in g/cm^3.

APPENDIX C-3

ALPINE MULTI - PLEX
FABOR - ZICKZACKSICHTER 100 MZR

Producer: ALPINE Aktiengesellschaft Maschinenfabrik und Eisengiesserei,
Augsburg - West Germany

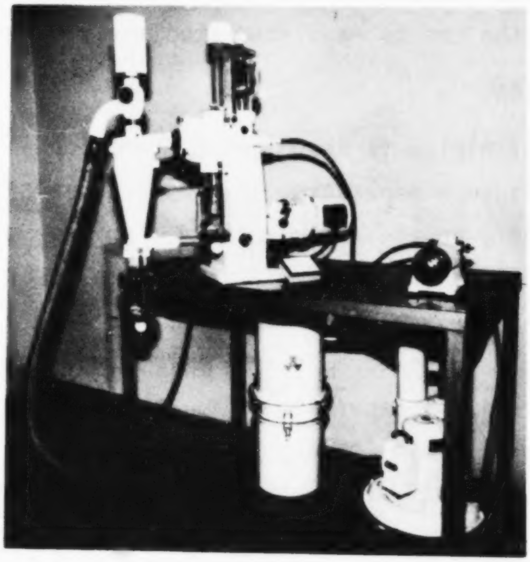

TECHNICAL DATA

Separator:	Rotation	2,400 - 20,000	rpm
	Air flow	15 - 53	Sm^3/hr
Blower:	Static negative pressure	1,500 - 1,600	mmH_2O
	Air flow	100	m^3/hr
Alpine Filter:	Filtration area	1	m^2
Feeder:	Maximum capacity (ground limestone)	10	kg/hr

APPLICATION

- Determination of particle size distribution of samples above 50 grams,
- Laboratory separation for individual grain fractions, capacity of a few kilograms,
- Industrial separation into two fractions, with a capacity of a few kg/hour, depending upon the kind of material.

Concerning ground limestone, the range of separation is 1 - 75 microns. The range of separation can be regulated steplessly.

PRINCIPLE OF OPERATION

The operation of Alpine is based on the centrifugal force principle. The material is fed into a separating zone by a screw feeder. The rotor blades, placed radially on the rotor surface, increase the velocity of the material up to the circumferential velocity of the rotor. Thus the material is being suspended in the air stream entering the separating zone from two sides. Then the dust-air mixture is introduced under negative pressure to zigzag passages where it is separated. The separating air and the fines enter the rotor center, travel through the outlet duct, and are delivered to the cyclone. Here the fines are separated from the air and they are collected in the fines' glass hopper. Under the centrifugal force the tailings are thrown from zigzag blade passages to the outside circumference of the separating zone and they leave the separating zone through the slot on the separating zone circumference, entering the tailings glass hopper.

The necessary air volume is supplied by a high-pressure blower and is indicated by a rotameter.

The range of separation is regulated by two independent factors: the number of revolutions and the volume of air. The range of separation can be adjusted to 1-70 μm. The calibration curve for limestone of specific gravity 2.6 - 2.7 g/cm^3 was presented in the servicing instructions. The range of separation d_T in μm for a definite number of revolutions can be read out from the diagram. The range of separation is obtained for the volume of air calculated from the following formula:

$$V' = 55 - \frac{n}{1,000}$$

where n = number of revolutions of the separator.

For the materials that have specific gravity different than standard limestone, the range of separation can be calculated based on the following formula:

$$d_1 = d \sqrt{\frac{\gamma}{\gamma_1}}$$

where d_1 = the range of separation of material, in μm,
d = the range of separation of limestone, in μm,
γ_1 = specific gravity of testing material, in g/cm^3, and
γ = specific gravity of limestone, in g/cm^3.

For the calculated range of separation of testing material, the number of revolutions is read out from the calibrating curve and then the volume of air V' is calculated.

APPENDIX C-4

TENSILE TESTING MACHINE TYPE FMGw 500

Producer: VEB Thuringer Industriewerk, Ranenstein - DDR

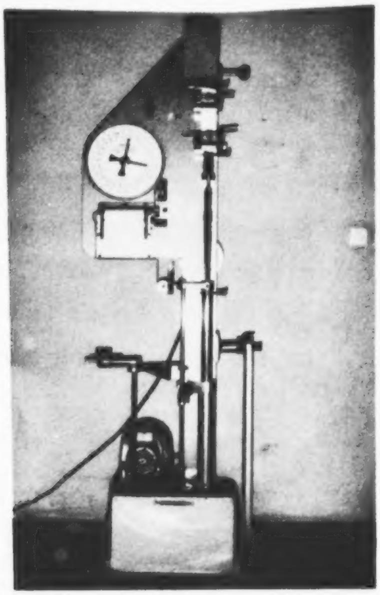

TECHNICAL DATA

Velocity of strokes	20 - 250	mm/min
Active length of sample	200,300,360,400,500	mm
Elongation	0 - 200	mm
Maximum force	500	kPa
Measurement ranges	0 - 100	kPa
	0 - 250	kPa
	0 - 500	kPa

The apparatus is equipped with a recorder.

APPLICATION

The testing of tension and elongation of fabrics--sailcloth, transmission belts, board, etc.

PRINCIPLE OF OPERATION

The testing of tensile strength is carried out in the following manner. The fabric sample is stretched between two alligator clips. The clips are placed in parallel one over the other. Then the sample is extended by continuous forces until rupture. Simultaneously the elongation, i.e. the increase of length between clips during the sample extension, is determined. According to Polish standards the testing is accomplished with the fabric samples cut out along the fill and warp. Sample sizes: width greater than about 50 ±5 mm; length greater by about 150 mm than the attached clip spacing. The clip spacing of the tensile testing machine should be 200 mm for fabrics with elongation at rupture below 150 percent and 100 mm for fabrics with elongation of rupture greater than 150 percent. The frequency of strokes of the lower clip is determined by the time between starting the testing to the moment of rupture which should be 30 ±10 seconds.

The tensile strength criterion is the maximum force at which the rupture appears, with the exact elongation read out from the elongation scale (or from the recorder).

APPENDIX D

APPENDIX D

GLOSSARY OF TERMS

Because of the different terms used in the literature concerning dust filtration through filtration media and because of the many parameters, stages, etc. that are characteristic of dust filtration processes, we list the terms and their definitions as used in this project. The proposed terms have physical meaning according to the processes and phenomena occurring during the dust filtration process, which is quite different from other filtration processes.

Aerosol - A 2-phase system, composed of a gas dispersion phase and a solid dispersed phase, which under certain conditions can be treated as stable or quasi-stable (dry filtration).

Filtration - Removal of solid particles from an aerosol stream by deposition in or on the structure of a porous medium.

Air Filtration - Filtration of atmospheric aerosols.

Dust Filtration - Filtration of industrial aerosols.

Dust Filtration Type I - The initial phase of the complete dust filtration process when the fabric first begins operation as a filter medium. This phase ends when the pressure drop reaches a predetermined level.

Dust Filtration Type II - The second phase continues until the fabric is fully filled with dust. This phase ends when the structure reaches a steady state.

Dust Filtration Type III - This phase occurs when a stable level of filling of the fabric, by dust, has been reached and when the pressure drop returns to a constant level after regeneration. This is a typical process for industrial dust collectors.

Gas Loading of Filtration Area - Mean calculated value of gas quantity, in cubic meters, passing through a square meter of filtration medium per hour (air-to-cloth [A/C] ratio).

Dust Loading of Filtration Area - Mean calculated value of dust quantity, in grams, deposited on a square meter of filtration medium per hour.

Filtration Velocity - The actual local velocity of an aerosol, in meters per second, passing through a filter medium (measured in true conditions).

Filled With Dust Structure - The areal mass density of the dirty filter including all dust retained after regeneration but without dust cake in (g/m^2).

Fully Filled With Dust Structure - Filled with dust structure after reaching steady-state operation.

Covered With Dust Structure - The areal mass density of dust accumulated on the filter including the dust cake prior to regeneration (g/m^2).

Dust Cake - The porous dust layer built up on the fabric surface during dust filtration. Its characteristics depend on the kind of fabric, the kind of dust, and the parameters of the process.

Free Area Effect - Decrease of dust filtration efficiency caused by interyarn free area viewed in plane of fabric.

Basket Effect - Decrease of dust filtration efficiency caused by interyarn free area viewed askew to plane of fabric.

APPENDIX E

APPENDIX E

NOMENCLATURE

b = 1.) thickness of the porous layer; 2.)a coefficient

c_i = initial concentration

c_o = outlet concentration

d_o = diameter of the warp yarn

d_w = diameter of the fill yarn

d_{50} = MMD (mass median diameter)

B = ambient pressure

E = efficiency

E_B = bag efficiency

E_{FR} = fractional efficiency

E_H = hopper efficiency

E_T = total efficiency

EM = emission

FA = free area

G_B = weight of dust from bag after regeneration

G_c = weight of dust fed into the testing chamber or into the hopper of testing chamber

G_H = weight of dust in hopper before regeneration cycle

G_N = dust filling of bag

G_o = weight of dust collected on the control filter or weight of dust in cleaned gases

G_R = weight of dust removed during regeneration from hopper

G_z = weight of dust collected on the fabric

K_1, K_1' = resistance coefficient of Darcy equation for pure fabric

K_2 = specific dust-fabric resistance

L = quantity of dust per unit area of filtration fabric

L_N = dust filling of structure

L_{NK} = full dust filling of structure

L_o = dust covering of structure

L_p = areal mass density of the dust cake

L_W = quantity of dust on square unit of dust cake

m_i = weight of dust on i-th impactor stage

m_o = weight percent of definite dust fraction leaving the measurement chamber

m_w = weight percent of definite dust fraction introduced to measurement chamber

n_o = number of warp threads in 10 cm

n_w = number of fill threads in 10 cm

ΔP = pressure drop

ΔP_i = specific hydraulic resistance of porous layer

ΔP_K = covered with dust fabric resistance (the before regeneration pressure drop)

ΔP_N = filled with dust fabric resistance

ΔP_{NK} = fully filled with dust fabric resistance

ΔP_o = clean fabric resistance

ΔP_W = dust cake resistance

Q = gas flow intensity through impactor

q_g = gas loading of filtration area (A/C ratio)

q_p = dust loading of filtration area

S_E = effective drag

S_R = susceptibility for regeneration

t = time

t_F = filtration time

t_R = regeneration time

$V_{\Delta P}$ = rate of increase of filtration resistance

ε = porosity

$(1-\varepsilon)/\varepsilon$ = porosity function

σ = standard deviation

a, b,
b_o,b_1 = coefficients